Developing a toolbox of Affimer reagents targeting SH2 domains to study protein-protein interactions in disease

Sophie Jane Heseltine

Submitted in accordance with the requirements for the degree of

Doctor of Philosophy

The University of Leeds
Faculty of Biological Sciences
School of Molecular and Cellular Biology

January 2019

The candidate confirms that the work submitted is his/her own, except where work which has formed part of jointly-authored publications has been included. The contribution of the candidate and the other authors to this work has been explicitly indicated below. The candidate confirms that appropriate credit has been given within the thesis where reference has been made to the work of others.

Jointly-authored publications:

Tiede et al. (2017). Affimer proteins are versatile and renewable affinity reagents. eLife, 6.

Work included from this publication in the thesis; the Grb family SH2 domain phage display screens and phage ELISAs, results from which are shown in Chapters 3 and 4.

In Chapter 3; The screening of the Grb2 SH2 domain was previously carried out by the Tomlinson group. Phage ELISA results are shown in Figure 3.2A.

In Chapter 4; The screening of the BAP-tagged Grb7, Grb10 and Grb14 proteins was carried out by Naomi Gibson. Screening and phage ELISA results are shown in section 4.2.4.2 and 4.2.6.

Acknowledgements

My greatest thanks go to Dr Darren Tomlinson; for his expertise and guidance throughout the project, and for giving me this opportunity. Also to my co-supervisor Professor Mike McPherson, for all his insight and support. I'd like to thank both of you for the advice and encouragement you've given me over the years, and for the time you've spent reading through this thesis.

Thank you to all the members of the Tomlinson and McPherson groups, without whom this project would not have been possible. Particular thanks to Dr Christian Tiede, for all your help with those many phage display screens! Also to Tom, for your help with the Affimer subcloning (I've actually missed your singing a bit). I'm so grateful to everyone, not just for your advice and support in the lab, but also for your friendships; for the messy Christmas parties, the skiing conference, the after-work drinks, the daily laughter. To my fellow PhD students who started this journey with me; Lia, Rob and Danah. What can I say, except that I really couldn't have done this without you. Having friends like you to come into work with is what got me through the tough days. I'm very glad I had other people at the same stage as me to despair/panic/ complain with.

I'd also like to thank the three students that I supervised, for your hard work and contributions to this thesis; Eleanor Foy, Grace Reddy and Naomi Gibson.

I'm very grateful to Avacta Life Sciences for the funding of this project and for access to the facilities there. Particular thanks go to Dr Matt Johnson, and to Dr Kit-Yee Tan who helped me with my work on site.

To my family and my friends outside the lab; thank you for your encouragement, care and understanding of my lack of free time. Thank you to the most supportive parents and sisters one could wish for, and the best housemates to come home to after a bad day.

And finally to Keir; for always being there for me, for keeping me grounded and for making it all worthwhile. Thanks for putting me up for the past 6 months!

Abstract

Src Homology 2 (SH2) domains are phosphotyrosine-binding modules that mediate a range of protein-protein interactions. These domains are found in over 120 human proteins and are involved in several signalling pathways that can become deregulated in diseases such as cancer. Research into the role of individual SH2s in disease has been hampered by a lack of protein-specific reagents available for intracellular functional assays. Specificity of reagents is difficult to achieve, due to the high sequence and structural homology of the domains.

Research presented in this thesis investigates the use of a novel non-immunoglobulin binding protein, the Affimer, as an SH2 domain research reagent. The project aimed to isolate Affimer reagents that bound to SH2 domains in a protein-specific manner, and to explore their ability to inhibit their target in several *in vitro* assays. Affimer binders were raised against 38 SH2 domains and tested in protein microarrays to determine specificity; revealing the isolation of 62 protein-specific reagents. A subset of Grb2 SH2-binding Affimer reagents were used in *in vitro* characterisation studies, demonstrating high binding affinities for their target and competitive inhibition of the domain. Selected binders used in mammalian cell-based assays also showed disruption of Grb2-mediated signalling, evidenced by reduced phosphorylation of a downstream target.

The SH2-binding Affimer reagents tested in this study showed comparable qualities to other previously SH2-targeting binding proteins, with many displaying higher specificity for their target. The Affimer therefore has good potential for use in the study of SH2 domain-mediated signalling. In particular, utilising SH2-binding Affimer proteins as a screening tool in functional cell-based assays is an exciting future prospect.

Table of contents

List of Tables

List of Figures

Abbreviations

Abbreviations for SH2 domain targets used in this project can be viewed in Appendix B.

A_{280}	Absorbance at 280 nm
A_{260}	Absorbance at 260 nm
BAP	Biotin acceptor peptide
BCA	Bicinchoninic acid
BSA	Bovine serum albumin
CML	Chronic myelogenous leukaemia
DD	Destabilisation domain
DMSO	Dimethyl sulfoxide
DNA	Deoxyribonucleic acid
E.coli	Escherichia coli
EC_{50}	Half maximal effective concentration
EDTA	Ethylenediaminetetraacetic acid
EGF	Epidermal growth factor
EGFR	Epidermal growth factor receptor
ELISA	Enzyme-linked immunosorbent assay
ERα	Oestrogen receptor α
Erk	Extracellular signal-regulated kinase
FGF1	Fibroblast growth factor 1
FP	Fluorescence polarisation
FYp	Fluorescent Grb2 SH2-binding phosphopeptide
Grb2	Growth factor receptor-bound protein 2
HA	Hemagglutinin
HGF	Hepatocyte growth factor

HRP	Horseradish peroxidase
IC_{50}	Half maximal inhibitory concentration
IL6	Interleukin-6 receptor
IL-2Rα	Interleukin-2 receptor α-chain
IPTG	Isopropyl-β-D-thio-galactoside
K_D	Equilibrium dissociation constant
kDa	Kilodaltons
KGF	Keratinocyte growth factor
MAPK	Mitogen-activated protein kinase
MW	Molecular weight
nABP	Non-antibody binding protein
NEB	New England Biolabs
Ni-NTA	Nickel-nitrilotriacetic acid
OD	Optical density
PBD	Protein data bank
PBS	Phosphate buffered saline
PBST	PBS-Tween (0.1%)
PCR	Polymerase chain reaction
PEG	Polyethylene glycol
PI3K	Phosphatidylinositol-4,5-bisphosphate 3-kinase
PPI	Protein-protein interaction
pY	Phosphotyrosine
RNA	Ribonucleic acid
RU	Response units
ScFv	Single-chain variable fragment
SDS-PAGE	Sodium dodecyl sulphate polyacrylamide gel electrophoresis

SEC	Size exclusion chromatography
SH2	Src Homology 2 domain
SiRNA	Short interfering RNAs
SPR	Surface plasmon resonance
SUMO	Small ubiquitin-like modifier
TB	Terrific broth
TBS	Tris buffered saline
TBST	TBS-Tween (0.1%)
TCEP	Tris(2-carboxyethyl)phosphine
TMB	3,3',5,5'-Tetramethylbenzidine
VEGF	Vascular endothelial growth factor
VEGFR	Vascular endothelial growth factor receptor
VR	Variable region
ySUMO	Yeast Small ubiquitin-like modifier

Amino acid abbreviations:

Single letter code	Amino acid
A	Alanine
D	Aspartic acid
E	Glutamic acid
F	Phenylalanine
G	Glycine
H	Histidine
I	Isoleucine
K	Lysine
L	Leucine
M	Methionine
N	Asparagine
P	Proline
Q	Glutamine
R	Arginine
S	Serine
T	Threonine
V	Valine
W	Tryptophan
Y	Tyrosine

Abbreviation	Meaning
Ac	Acidic group; E or D
Am	Amide group; N or Q
Ar	Aromatic group; F, W or Y
B	Basic group; H, K or R
Hy	Hydrophobic group; A, G, I, L or V
Hx	Hydroxyl group; S or T
X	Any amino acid

Chapter 1

Introduction

Chapter 1

Introduction

1.1 Protein-protein interactions

Proteins are fundamental to most molecular functions needed by living organisms and they rarely act alone; they often interact with each other to perform their biological functions (Garcia-Garcia et al., 2012). Protein-protein interactions are therefore intrinsic to virtually every cellular process (Rivas and Fontanillo, 2010). Each protein in an interaction network has been shown to associate on average with 3.6 partners and some proteins with more than six (Han et al., 2004). With this level of interconnectivity, proteins can form highly complex signalling networks to maintain cellular functions (Yeh et al., 2013). Mapping of these protein-protein interaction networks has become a main topic in current biological research and is critical to understanding cellular biology and how it becomes aberrant in disease (Rivas and Fontanillo, 2010, Yeh et al., 2013).

Modular protein domains regulate these interactions by recognition of short peptide sequences within their target protein. These recognition domains play a key role in regulating the specificity of signal transduction, through the selective recognition and binding of their targets (Pawson et al., 2002). Examples of such modules include: phosphotyrosine-binding (PTB) domains, Src homology 2 and 3 (SH2 and SH3) domains, Pleckstrin homology (PH) domains, PDZ domains and LIM domains (Pawson et al., 2002; Kadrmas and Beckerle, 2004).

1.2 The SH2 domain; structure and function

One of these modules mediating protein-protein interactions is the Src homology 2 (SH2) domain. The SH2 domain is a phosphotyrosine (pY) binding module found in over 110 human proteins (Kraskouskaya et al., 2013). The SH2 was first discovered through identification of a conserved sequence in the N-terminal catalytic regions of Src-related protein tyrosine kinases, which when mutated, appeared to regulate the adjacent kinase domain (Sadowski et al., 1986). Subsequent studies determined that SH2 domains bound specifically to phosphorylated tyrosine residues (Waksman et al., 2004).

Approximately 100 amino acids in length (Liu et al., 2006), the general structure of the SH2 domain consists of a central anti-parallel β-sheet flanked on both sides by an α-helix (Campbell and Jackson, 2003) (see Figure 1.1A). On the same plane of the β-sheet, two separate binding sites are formed; a conserved pY-binding site and a variable pocket that binds residues C-terminal to the pY (Figure 1.1B). The region between the first α-helix and the β-sheet forms the deep positively-charged pocket that binds the pY. Many interactions between this binding site and the pY have been observed, including; a salt bridge between the phosphate molecule and an arginine residue (ArgβB5); an interaction between the guanidinium group of another arginine (ArgαA2) and the aromatic ring of the pY; and several hydrogen bonds contributed by residues in the BC loop between the βB and βC strands (Waksman et al., 2004). The arginine at position βB5 that makes contact with the pY is highly conserved, being found in the Src SH2 and many others (Kasembeli et al., 2009).

It has been reported that more than half of the free energy of the interaction between the Src kinase SH2 and its cognate phosphopeptide (pY-E-E-I) is contributed by the pY, with other studies confirming that no other residue in a phosphopeptide ligand is nearly as important for binding (Bradshaw and Waksman, 1999). One exception to the pY being an essential requirement for SH2 binding is the signalling lymphocyte activation molecule-associated protein (SAP) SH2 domain, which is less dependent upon phosphorylation of its ligands (Waksman et al., 2004).

The region between the β-sheet and the C-terminal helix forms the variable binding pocket; this is the specificity-determining region, interacting with the residues C-terminal to the pY which provide discrimination between phosphorylation sites (Songyang et al., 1993). Many studies on SH2 specificity have deduced preferred binding motifs for different classes of SH2s. For example, the Src family kinase SH2s preferentially bind the motif pY-E-E-I, whilst the growth factor receptor-bound protein 2 (Grb2) SH2 binds the pY-X-N-X motif (where X is any amino acid) (Songyang et al., 1994).

Unlike the pY-binding site, the variable pocket is not conserved across the SH2 domain family; in Src family kinases a deep hydrophobic pocket is formed, with the I residue at position pY + 3 of the pYEEI motif fitting into this pocket

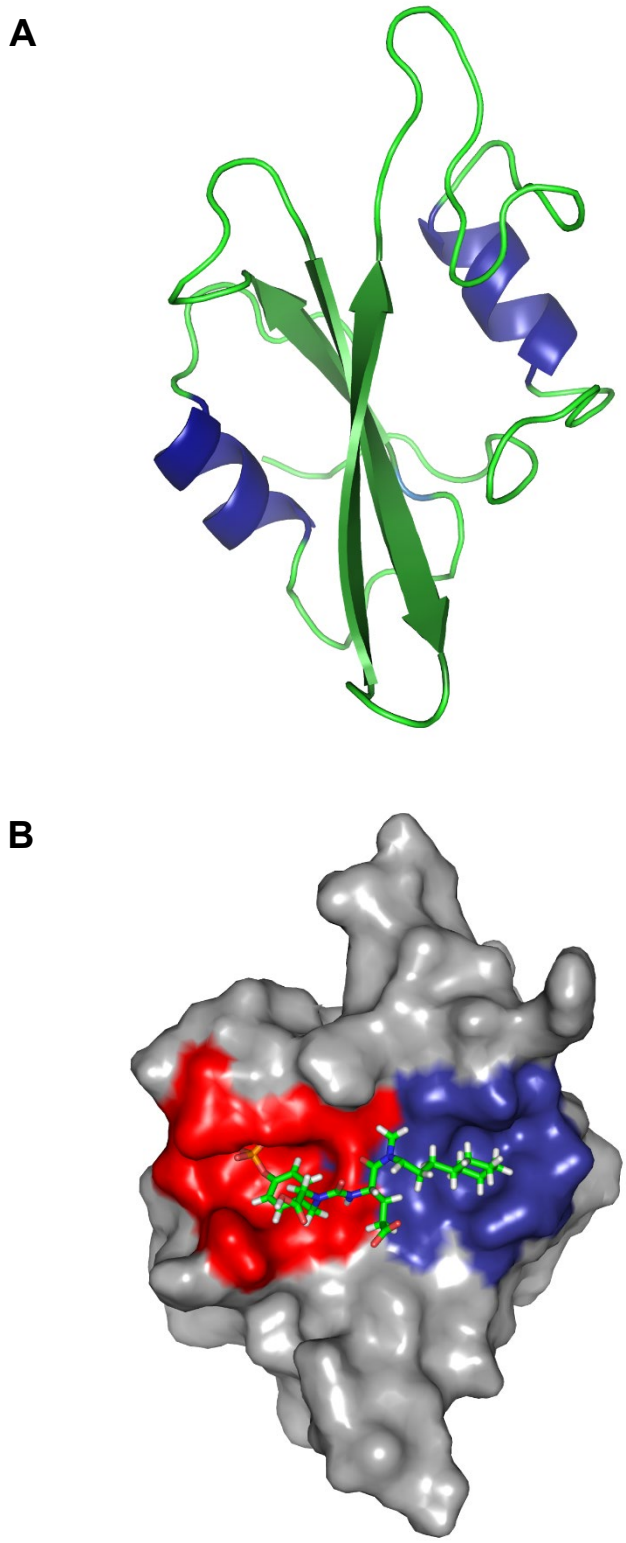

Figure 1.1. Canonical structure and ligand binding of SH2 domains. ***(A)*** *Cartoon representation of the Src SH2 domain (PDB ID: 1SKJ). The α-helices and β-sheets are coloured blue and green, respectively.* ***(B)*** *The Src SH2 domain in complex with a peptidomimetic inhibitor, 4-[3-(carboxymethyl)-3-[4-(phosphonooxy)benzyl]ureido]-4-[(3-cyclo hexylpropyl)methylcarbamoyl] butyric acid (PDB ID: 1SKJ). The pY and variable binding pockets are coloured red and blue, respectively. The SH2 domain is in the same orientation as shown in (A). (Plummer et al. 1997). Images were produced using PyMOL 2.0.*

(Waksman et al., 1993, Eck et al., 1993). In contrast, the C-terminal SH2 of phospholipase-Cγ 1 (PLCγ1-C) displays a binding interface that is extended to the pY + 5 position (Pascal et al., 1994). In total, a 4 – 7 amino acid motif is bound by SH2 domains (Liu et al., 2006).

1.3 SH2 domain signalling in normal and disease states

Phosphotyrosine signalling is dependent upon three essential molecules; protein tyrosine kinases which add a phosphate onto substrate tyrosines; protein tyrosine phosphatases which remove the phosphate from substrates; and modular protein domains which recognise the phosphorylated ligands and specify downstream signalling events (Liu and Nash, 2012). SH2 domains form the largest family of pY-recognition domains and are evolutionarily conserved in many eukaryotes, making them central to phosphotyrosine signalling (Machida and Mayer, 2005).

Through the selective binding of phosphorylated ligands, SH2 domains propagate downstream signalling by recruiting the SH2 domain-containing protein to signalling complexes, or even by altering its enzymatic activity; SH2s have been shown to auto-regulate kinase domains within the same protein, playing a critical role in the stability of the inactive and active states of many tyrosine kinases (Filippakopoulos et al., 2009). The function of each SH2 domain depends upon the nature of adjacent protein components; they are usually found in conjunction with either catalytic domains or other binding domains, such as SH3 modules (Machida and Mayer, 2005). SH2 domains are found in proteins with a wide variety of functions, including adaptor proteins; kinases; transcription factors; phosphatases; cytoskeletal regulators and nucleotide exchange factors (Kraskouskaya et al., 2013) (see Figure 1.2).

SH2 domains play an important role in propagating signals from receptor tyrosine kinases. In general, tyrosine autophosphorylation of a receptor in response to ligand binding generates docking sites for SH2-containing signalling proteins (Machida and Mayer, 2005). These SH2-containing proteins are then activated; sometimes this is achieved through their binding to the receptor alone, by their juxtaposition to membrane-associated substrates. Or alternatively, receptor-binding can relieve autoinhibition by the SH2 on the catalytic domain within the same protein. In addition, once bound to the receptor the SH2-containing protein

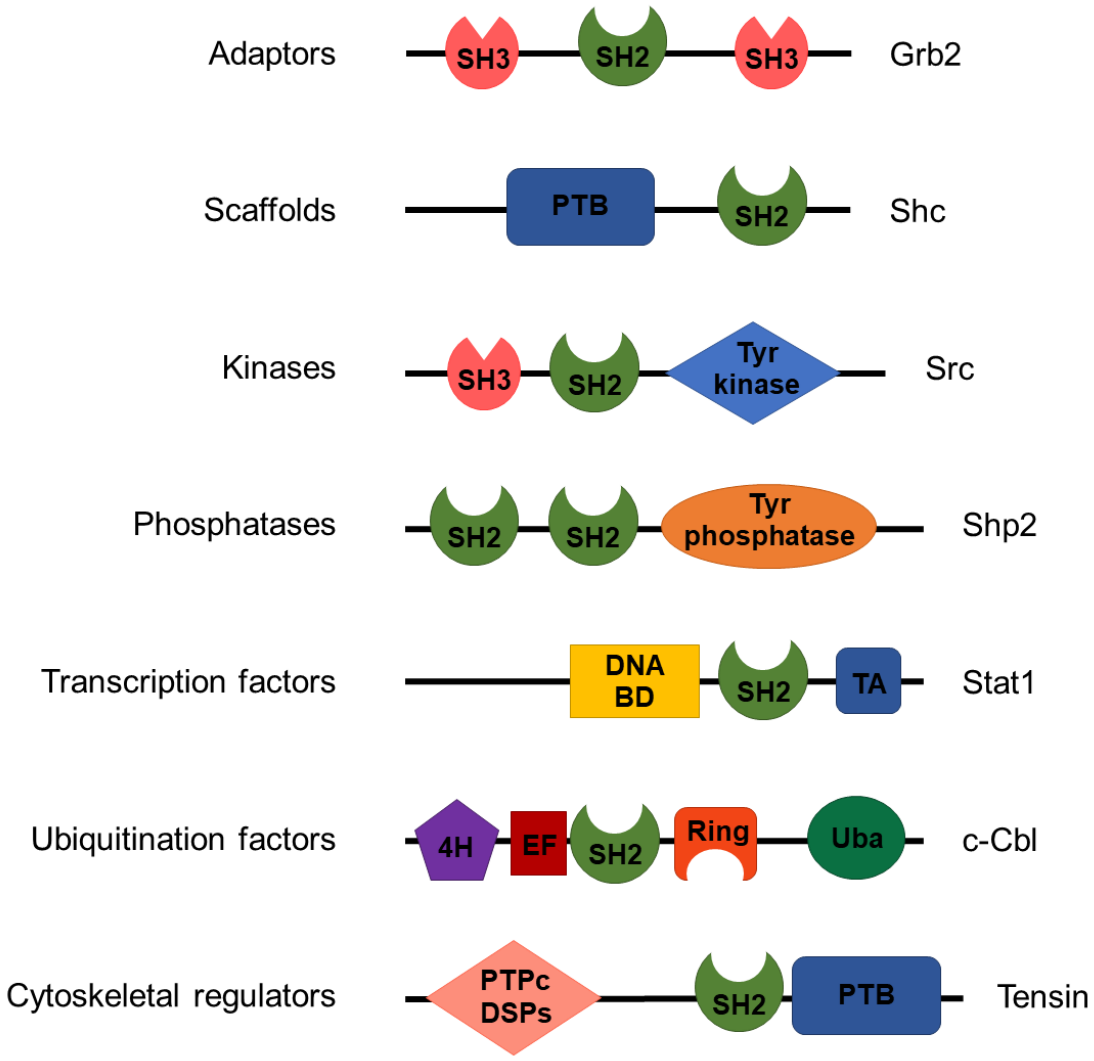

Figure 1.2. The functional variety of SH2 domain-containing proteins. *Examples of SH2 domain-containing proteins, and their modular structure. The biological functions of the proteins are listed on the left, with specific examples named on the right. The homology domains found in each protein are shown in between. Abbreviations: SH3, Src homology 3 domain; PTB, phosphotyrosine-binding domain; Tyr kinase, tyrosine kinase domain; Tyr phosphatase, tyrosine phosphatase domain; DNA BD, DNA-binding domain; TA, transcriptional activation domain; 4H, four-helix bundle; EF, EF-hand; Uba, ubiquitin association domain; PTPc DSPs, protein tyrosine phosphatase. Grb2, growth factor receptor-binding protein 2; Shc, Src homologous and collagen protein; Shp2, SH2 domain-containing protein tyrosine phosphatase 2; Stat1, signal transducer and activator of transcription 1. Abbreviations for Cbl and Src are derived from encoding viral oncogene names.*

can become a preferred substrate for phosphorylation itself (Pawson et al., 2001).

As different SH2-containing proteins bind preferentially to specific phosphorylated sites on the activated receptor, this step determines which downstream signalling pathways are initiated (Mayer, 2015). SH2-mediated interactions are not only limited to receptors; signalling proteins such as Grb2 and Src can also associate with tyrosine-phosphorylated cytoplasmic molecules via their SH2 domains (Moran et al., 1990, Lowenstein et al., 1992, Cobb et al., 1994). The binding and activation of SH2-containing proteins by a receptor therefore leads to a cascade of protein-protein interactions, including other cytoplasmic SH2-containing proteins, resulting in a series of events that eventually lead to altered patterns of gene expression or other cellular responses (Kraskouskaya et al., 2013, Pawson et al., 2001). Indeed, SH2 domain-containing proteins regulate processes such as cytoskeletal rearrangement, homeostasis, immune responses, cell cycling and angiogenesis (Waksman et al., 2004, Kraskouskaya et al., 2013). As a result of this, SH2-mediated interactions are involved in several pathways that become deregulated in disease. The inhibition of SH2 domains in a variety of signalling proteins has therefore been highlighted as a potential therapeutic strategy in the treatment of diseases such as cancer, autoimmune diseases and other conditions (Kraskouskaya et al., 2013).

Mutations in 18 SH2 domains themselves have been linked to various diseases, including cancers and leukaemias, developmental disorders, diabetes and immunodeficiencies (Liu et al., 2006). Examples include the SH2 domain of SAP, in which inactivating mutations cause X-linked lymphoproliferative disease (Coffey et al., 1998, Nichols et al., 1998). This disorder results in an extreme sensitivity to the Epstein–Barr virus, with infection resulting in uncontrolled B-cell proliferation (Sayos et al., 1998). A point mutation in the Bruton tyrosine kinase (Btk) SH2 domain has also been shown to cause X-linked agammaglobulinaemia, which is an immunodeficiency characterised by a lack of circulating B cells and a reduction in the serum concentration of antibodies (Saffran et al., 1994). Additionally, mutations in the N-terminal SH2 domain of the Src homology region 2 domain-containing phosphatase-2 (SHP-2, also known as Ptpn11) cause an autosomal dominant disorder called Noonan’s

syndrome (Tartaglia et al., 2001).This disease results in symptoms such as dysmorphic facial features, short stature and heart disease. Webbed neck, chest deformity and mental retardation also frequently occur. The N-terminal SH2 domain is involved in downregulating phosphatase activity, and therefore the disease state is thought to result from excessive phosphatase activity (Waksman et al., 2004).

SH2 domains, as well as being directly mutated in certain disorders, are also potential drugs targets in numerous other instances due to their involvement in pathways altered by disease-causing mutations (Waksman et al., 2004). Proteins highlighted as potential targets in human disease through their SH2 domain interactions include; Lck in HIV (Dutartre et al., 1998), Lyn in asthma and leukaemia (Ingley, 2012), SHP-1 in anaemia and cancer (Waksman et al., 2004, Wu et al., 2003), Grb2 and Shc in various cancers (Waksman et al., 2004), ZAP-70 in autoimmune disease (Zanotti et al., 2010), and numerous others.

1.4 SH2 domain inhibition in research & therapeutics

Though recognised as potential therapeutic targets, there is still a lack of research reagents for SH2 domains (Sjoberg et al., 2012) and the scarcity of SH2 inhibitors that are effective in intracellular assays has hampered study of SH2-mediated cellular mechanisms (Wojcik et al., 2010; Kraskouskaya et al., 2013). Due to the highly conserved sequence and structure of SH2 domains between different proteins, there are currently no inhibitors with strong selectivity for the majority of the domains (Kasembeli et al., 2009). It is therefore widely acknowledged that protein-specific SH2 inhibitors would be highly valuable research tools (Kraskouskaya et al., 2013) that would enable the discovery of novel biology and new pharmaceutical targets in various disorders (Lawrence, 2005).

1.4.1 Targeting individual protein domains for functional studies

The analysis of intracellular protein function can be achieved through techniques such as gene knockout or RNA interference. However, these methods are impractical for studying domain-specific interactions as they result in the deletion of the entire protein (Gay et al., 1999). Instead, incorporation of loss-of-function mutations can be used to study the function of individual domains; however these

suffer from limitations, such as the effects being compromised by compensating changes in the regulation of other genes (Amstutz et al., 2005). In order to observe the cellular functions of SH2 domains, binding molecules acting at the protein level are therefore preferable (Kasembeli et al., 2009). Protein inhibitors can streamline the research pipeline, as the same compound can be used in both cellular and *in vitro* target studies (Morlacchi et al., 2014), and could then even be used as first lead compounds in the drug discovery process. At the least, they simulate the effect of a future small molecule drug in cell-based assays, which genomic techniques do not (Amstutz et al., 2005; Gupta et al. 2018).

1.4.2 SH2 phosphopeptide mimetic and small molecule inhibitors

Efforts have been made since the early 1990s to generate inhibitors to impede SH2-mediated interactions, with earlier work focusing on Src kinase and the adaptor protein Grb2, and more recent studies targeting the signal transducer and activator of transcription (Stat) family (Kasembeli et al., 2009, Morlacchi et al., 2014). However, a number of problems have rendered development of these SH2 inhibitors a slow process. This is partly due to the highly conserved sequences and binding mechanisms of SH2s across proteins. ‘Hot spot’ regions responsible for phosphopeptide recognition, that would usually be suitable targets for small molecule inhibitors, are very similar in their physical-chemical properties between numerous SH2 domains (Kasembeli et al., 2009).

This therefore makes development of a selective inhibitor difficult to achieve. Furthermore, the negative charge of the phosphate group considerably reduces cell penetration, impeding the intracellular efficacy of any SH2 phosphopeptide inhibitors (Kraskouskaya et al., 2013, Morlacchi et al., 2014). In addition, these peptides are susceptible to proteolytic cleavage by peptidases and phosphatases, and as a rule, exhibit poor bioavailability (Morlacchi et al., 2014). As a result of this, phosphopeptide inhibitors were converted to peptidomimetics. This came with another obstacle; as the pY residue provides half of the binding affinity of phosphopeptide ligands for SH2 domains (Filippakopoulos et al., 2009) omitting the phosphate in inhibitors often resulted in abolition of SH2 binding (Nam et al., 2004). Indeed, overcoming the negative charge requirement was so problematic that SH2s were abandoned as ‘undruggable’ targets for some time (Morlacchi et al., 2014).

However, more recent studies have had success with developing inhibitors that also display intracellular activity. For example, several groups have developed phosphopeptide-based compounds targeting the SH2 domain of Stat3. Stat3 is an oncogenic transcription factor involved in cell cycling, metastasis and angiogenesis. Numerous studies have shown Stat3 to be hyperactivated in multiple human cancers including breast, prostate, ovarian, leukaemia and lymphoma (Buettner et al., 2002, Yue and Turkson, 2009). The most well-characterised mechanism of Stat3-regulated oncogenesis is the up-regulation of anti-apoptotic and cell proliferative genes including Bcl-XL, survivin and cyclin D1; all which lead to increased cell survival (Kraskouskaya et al., 2013).

Peptidomimetic inhibitors to the Stat3 SH2 were derived from a high-affinity binding peptide, Ac-pYLPQTV-NH_2 (Coleman et al., 2005, Mandal et al., 2009a). However, these analogues did not inhibit Stat3 phosphorylation in whole cells, due to poor cell penetration (Mandal et al., 2009b). After masking of the anionic phosphonate group present in the compounds, inhibition of Stat3 phosphorylation was then observed at low μM drug concentrations in MD-MBA-468 breast cancer cells (Mandal et al., 2009b).

Another group prepared peptidomimetic inhibitors of the Stat3 SH2 through macrocyclization of a peptide derived from a native ligand, Ac-pYLKTKF-NH_2 (Chen et al., 2007). Introduction of a lipid chain at the N-terminus, a bicyclic lactam and replacement of glutamine with histidine yielded a cell-permeable inhibitor, CJ-1383 (Gomez et al., 2009, Chen et al., 2010). This constrained inhibitor was shown to block Stat3 signalling and cancer cell growth, as well as inducing apoptosis in the breast cancer cell line MDA-MB-468 (Chen et al., 2010).

Recently, a novel small molecule Stat3 SH2 domain inhibitor (OPB-51602) effectively blocked Stat3 phosphorylation and cell proliferation in a prostate cancer cell line (Genini et al., 2017). Upon binding to Stat3, OPB-51602 triggered a complex cascade of events that resulted in disruption of mitochondrial function and protein homeostasis, leading to cell death. This inhibitor is currently being studied in clinical trials, in patients with refractory solid tumours (Genini et al. 2017).

Divalent and multivalent inhibitors for the tandem SH2 domains of Syk have also been produced; derived from native SH2-binding sequences within the motif Ac-

pYTGLNTRSQETpYETL-NH_2 (Dekker et al., 2003b, Kuil et al., 2009). Activity of Syk has been shown to be necessary for the progression of autoimmune arthritis and non-Hodgkin lymphomas-like tumours (Young et al., 2009, Coffey et al., 2013). However despite their high affinity *in vitro*, these inhibitors of the tandem Syk SH2 domains showed limited application *in vivo* (Kraskouskaya et al., 2013). A few other SH2 domains have also been targeted with peptidomimetic and small molecule inhibitors; such as the Lck, Grb7 and Grb2 SH2 domains (Dekker et al., 2003a, Wei et al., 2003, Pero et al., 2002).

However, evidence of their cellular efficacy is lacking and for the majority of the SH2 domain family, inhibitors remain to be developed (Morlacchi et al., 2014). Novel binding reagents are consequently needed for examining the role and interactions of individual SH2s in disease, and ultimately aiding in drug discovery. As mentioned previously, the main obstacle in the dissection of SH2 domain function is the lack of reagents that effectively bind or inhibit specific SH2s in the intracellular environment (Gay et al., 1999).

1.4.3 Antibodies as SH2 domain reagents

Antibodies are invaluable research reagents in the study of protein function. The recognition of antigens by antibodies is mediated through six hypervariable loop regions within the antibody variable domains, termed complementarity determining region (Sela-Culang et al., 2013). The specificity of the antibody for its cognate antigen has been exploited for the development of several *in vitro* assays, as well as therapeutics (Sela-Culang et al., 2013). These binding reagents have been well-established in numerous research applications such as immunoblotting, fluorescent imaging techniques, immunohistochemistry and affinity purification (Goldman, 2000).

Although antibodies are currently the most widely used binding molecules in research, it has become increasingly apparent that they have a number of short-comings (Hey et al., 2005). Immunoglobulins are large molecules (~150 kDa) and contain multiple domains; this size limits tissue penetration and results in them being relatively unstable, thus shortening their shelf-life (Skerra, 2007). Furthermore, antibody production is costly and time-consuming due to the requirement of animals or eukaryotic cell culture (Gebauer and Skerra, 2009, Skerra, 2007). They are difficult to express in high-throughput bacterial systems, and often suffer from batch-to-batch variability (Stadler et al., 2011); antibodies

are made from two different peptide chains, light and heavy, which causes problems with recombinant expression (Skerra, 2007, Raina et al., 2014). Their binding site is also difficult to manipulate in one step, as it is a complex structure formed by the six variable loops which are not easily engineered simultaneously. This poses a problem in synthetic library synthesis, as multiple steps are required (Skerra, 2007). Additionally, the Fc region mediates immunological functions which often result in unwanted interactions, particularly in *in vivo* diagnostics (Richter et al., 2014).

The main limitation in using antibodies for studying protein-protein interactions (such as those mediated by SH2s) is their generally poor stability and activity in the intracellular milieu. The structure of antibodies and their fragments depends upon intra-domain disulphide bonds, which do not form in the reducing intracellular environment (Amstutz et al., 2005). In addition, they are frequently incapable of folding correctly in the cytoplasm without the presence of chaperones (Kasembeli et al., 2009). For these reasons, they are often inadequate for use in functional cellular assays due to poor activity, which would limit their utility for investigating SH2-mediated signalling in a native environment (Stocks, 2004; Liu et al., 2006).

Nevertheless, recent developments in antibody engineering have enabled the successful intracellular expression of antibody fragments (termed intrabodies) which have been used as a tool to disrupt, modulate and investigate the functions of numerous targets within the cell (Lo et al., 2008; Ali et al., 2011). Intrabodies have been engineered to target antigens in various subcellular locations, including the cytoplasm; although this does entail more work than simply targeting proteins passing the endoplasmic reticulum, due to the requirement of correct folding (Marschall et al. 2015). The use of intracellular antibodies to knock out protein function at the post-translational level has demonstrated advantages over genomic techniques for determining target function, including high specificity (Cao and Heng, 2005).

The largest isolation of SH2-binding antibodies and their fragments has been the multicentre effort by the Renewable Protein Binder Working Group and colleagues, which has successfully isolated antibody reagents to a set of 20 SH2 domains (Uhlen et al., 2005, Colwill et al., 2011). These binders showed high rates of specificity for their targets in an SH2 protein microarray and low

nanomolar K_Ds as determined by surface plasmon resonance (SPR) (Sjoberg et al., 2012, Colwill et al., 2011). However, many of the Crk, Grb2 and Shc1 reagents tested in immunoprecipitation assays failed to capture endogenous or ectopically expressed target from mammalian cell lysate (Colwill et al., 2011). Additionally, these binders were not tested in intracellular applications. The results from these studies are discussed in more detail in later chapters.

1.5 Non-immunoglobulin scaffolds as novel research reagents

1.5.1 Non-antibody binding reagents

Due to the restrictions of antibodies outlined above, the development of non-immunoglobulin protein scaffolds has arisen to provide alternative binding molecules for use in research (Amstutz et al., 2005). Several protein families can be engineered to contain novel binding sites, using techniques such as site-directed mutagenesis (Gebauer and Skerra, 2009). These non-antibody binding proteins (nABPs) are reagents with strong binding affinity properties previously thought unique to antibodies, and have delivered insights into molecular recognition (Skerra, 2007). Not only are they promising as research reagents, but they are also potential biopharmaceuticals (Hey et al., 2005).

The principle idea behind the construction of nABPs is to use a robust, naturally occurring protein scaffold, and include at least one variable binding site that will bind to a specific target (Gebauer and Skerra, 2009). They are usually produced by creating a random library, using mutagenesis of a loop region or other accessible surface, followed by selection of specific reagents against a target by phage display or similar methods (Skerra, 2007). Over 50 different nABPs have been developed in the last two decades, including Affibodies, Engineered Kunitz domains, DARPins, Repebodies, monobodies and Anticalins. Targets of these engineered binding scaffolds include the interleukin-6 receptor (IL6); vascular endothelial growth factor (VEGF); kallikrein; plasmin; epidermal growth factor receptor (EGFR) and the interleukin-2 receptor α-chain (IL-2Rα) (Gebauer and Skerra, 2009). Although the number of disease proteins that have been targeted so far is relatively small, the field is rapidly expanding and commercialising (Skrlec et al., 2015). The number of viable targets for nABPs is considerably larger than those that are currently targeted by approved biopharmaceuticals,

and thus the potential for these alternative scaffolds is huge (Gebauer and Skerra, 2009).

The benefits of nABPs over antibodies include increased stability, a high production yield and the ability to express them in bacterial systems, which significantly lowers production costs (Amstutz et al., 2005). They have also shown efficient folding and retention of function in intracellular applications, attributed to their high stability and lack of di-sulphide bonds. This allows them to effectively bind targets within a cellular environment, thus potentially surpassing antibodies for use in cell-based functional assays (Stocks, 2004).

Antibodies are currently used in a number of research applications, including enzyme-linked immunosorbent assays (ELISAs), western blot analysis, flow cytometry and immunohistochemistry (Binz et al., 2005). The addition of fluorophores, enzymes or other detection molecules to nABPs can be easily achieved, making this an area in which they have already been validated as an alternative to antibodies (Lofblom et al., 2010). This is possible as long as the scaffold has sufficient specificity and binding affinity for the target (Skerra, 2007). Indeed, engineered binding proteins were deemed to surpass antibodies as recognition molecules on a label-free electrochemical biosensor, through their increased thermal stability, sensitivity and molecular recognition properties, especially when immobilised (Raina et al., 2014).

Non-immunoglobulin scaffolds also offer improved properties that could be beneficial for *in vivo* diagnostic reagents, such as a long storage life (Binz and Pluckthun, 2005), better tissue penetration due to their smaller size, lack of Fc-directed non-specific binding and faster excretion, which improves clarity of target staining (Skerra, 2007). Cysteine-free scaffolds allow the addition of a unique cysteine residue which can be bound to labelling molecules; enabling site-directed labelling of the reagent. This free cysteine also facilitates site-directed surface immobilisation of the scaffold, which is promising for protein microarrays and other applications (Hey et al., 2005).

Scaffolds such as Lipocalins, Adnectins and Affibodies have been used successfully as biotechnology reagents in several applications; such as capture molecules in affinity chromatography columns (Nord et al., 2000), in the depletion of human proteins from complex body samples (Gronwall et al., 2007) and in colorimetric assays including ELISAs, dot blots and immunohistochemistry

(Lofblom et al., 2010). Non-immunoglobulin scaffolds have also been used as crystallisation chaperones for structure determination of challenging targets (Skrlec et al., 2015). The successful crystallisation of various membrane proteins, multiprotein complexes and transient conformational states has now been achieved, using the scaffolds to reduce the conformational freedom of the target (Bukowska and Grutter, 2013). DARPins have been most applied to this purpose, attaining crystal structures of targets such as the inner membrane component of the *E. coli* AcrAB–TolC multidrug exporter; a system that contributes to drug resistance of *E. coli* (Sennhauser et al., 2007).

Studies have also demonstrated the benefits of engineered scaffolds over antibodies for intracellular applications, with efficient folding and a lack of disulphide bonds allowing nABPs to remain fully functional and effectively bind target proteins in cellular environments (Binz et al., 2005). Two DARPins selected using ribosome display were both shown to bind the protein kinase extracellular signal-regulated kinase 2 (Erk2), with one binder selective for the active (phosphorylated) form, the other for the inactive (non-phosphorylated) form (Kummer et al., 2012).

These DARPins were proven to be useful tools in selective precipitation of the different phosphorylation forms of Erk2 from cell lysates. They were also able to distinguish between phosphorylated Erk2 (p-Erk2) and Erk2 in an intracellular environment and the Erk2-binding DARPin also inhibited Erk2 phosphorylation inside the cell (Kummer et al., 2012). The p-Erk2 specific DARPin was then developed into an Erk activity biosensor by coupling to a solvatochromatic merocyanine dye (Kummer et al., 2013). The fluorescence of this dye increases in a more hydrophobic environment, such as upon binding of p-Erk. This DARPin binder was used to visualise endogenous Erk activation in mouse embryo fibroblasts, exhibiting specificity for p-Erk2 over Erk2 and other mitogen-activated protein kinases (MAPKs); thus showing its effectiveness as a tool for studying Erk function in intracellular applications (Kummer et al., 2013).

Engineered binding proteins based on the fibronectin type III (Fn3) domain, termed ‘monobodies’, were likewise shown to bind to the ligand-binding domain (LBD) of the oestrogen receptor α (ERα) (Koide et al., 2002). These monobodies were then used to probe different ligand-induced conformational changes of ERα in the nucleus. This not only validated their use in cellular experiments, but also

showed their ability to selectively bind a single domain within a protein and explore domain-specific interactions (Koide et al., 2002). These nABPs have shown functionality in cellular assays, possess resistance to proteases and do not include pY residues; overcoming some of the difficulties previously faced in finding SH2 inhibitors (Morlacchi et al., 2014). As they retain the ability to specifically target one domain of a protein while leaving the functions of other domains intact, engineered protein scaffolds would allow researchers to determine SH2-specific events (Stocks, 2004).

1.5.2 SH2-targeting monobodies

Monobodies have been previously used to target the SH2 domains of 9 different targets. A phage library of monobodies was developed and used phage display to screen against the Abelson (Abl1) kinase SH2 domain (Wojcik et al., 2010). Binders were identified with low nano-molar affinities for Abl1-SH2 and one of these, HA4, was characterised further. HA4 bound the Abl SH2 with a K_D of 7 nM, as determined by SPR; a binding affinity similar to antibodies and 500 – 1000x more potent than natural ligands of the Abl1 SH2. HA4 was also shown to displace a fluorescently-labelled phosphopeptide ligand bound to the Abl1 SH2 in a dose-dependent manner, indicating competitive inhibition of the SH2 domain by the monobody (Wojcik et al., 2010).

An SH2 domain protein microarray also demonstrated selectivity of HA4 for the Abl SH2 over other SH2 domains; although significant interactions with other SH2s including Syk were detected (Wojcik et al., 2010). Additionally, HA4 could not discriminate between the SH2s of Abl1 and Abl2 isoforms. The crystal structure of HA4 in complex with Abl-SH2 was resolved at a resolution of 1.75 Å, revealing the binding interface to include almost all of the phosphopeptide binding site, with one third of the interface outside this area. The amino acids in the binding interface that lay outside the phosphopeptide binding site are less conserved between the Abl SH2 and the Src family SH2s, providing an explanation for the binding selectivity of HA4 (Wojcik et al., 2010). This study demonstrated the ability of nABPs to detect residues outside of the canonical binding interface that can be exploited to confer specificity of SH2 reagents.

Due to the role of the Abl SH2 domain in auto-inhibition of the kinase domain, HA4 was shown to increase Abl kinase activity *in vitro* through a blockade of this SH2-kinase interaction. In addition, HA4 provided the first demonstration of

intracellular inhibition of processive phosphorylation, by reducing the phosphorylation of an Abl substrate, paxillin, in HEK 293 cells (Wojcik et al., 2010). HA4 was also shown to decrease phosphorylation and consequent activation of Stat5 in K562 cells, an event that is critical in chronic myelogenous leukaemia (CML); displaying the potential for Abl SH2 inhibition in blocking therapeutically important pathways mediated by the oncogenic fusion protein Bcr-Abl (Wojcik et al., 2010).

The same group then demonstrated that the HA4 monobody in tandem with another Abl-SH2 binding monobody, 7c12, caused disruption of the Bcr-Abl SH2-kinase interface, leading to inhibition of cellular Bcr-Abl activity and induction of apoptosis in the CML cell line K562 (Grebien et al., 2011). It also stimulated apoptosis in bone marrow and blood cells from CML patients. This work validated the SH2-kinase interface as an allosteric target for treatment of CML, which would be particularly beneficial for patients displaying resistance to current therapies (Grebien et al., 2011).

Both SHP2 SH2 domains have also been targeted using monobodies (Sha et al., 2013). Analysis of their binding partners in cells using liquid chromatography coupled with tandem mass spectrometry revealed high specificity of 3 of the 4 monobodies for SHP2, with no reproducible cross-reactions to other SH2s. Two crystal structures revealed that both C-terminal and N-terminal SH2 monobodies bound in the phosphopeptide-binding sites of the domains and could therefore act as inhibitors of SH2-mediated signalling (Sha et al., 2013). Monobodies targeting the N-SH2 domain disrupted the interaction of SHP2 with its upstream activator, the Grb2-associated binder 2 adaptor protein (Gab2), as determined by immunoprecipitation of the SHP2-Gab2 complex from monobody-expressing and control cells. Expression of monobodies also significantly altered the phosphorylation of downstream effectors paxillin, Stat5 and extracellular signal–regulated kinases (Erk1/2); signifying that SHP2 signalling was sufficiently disrupted by the monobodies (Sha et al., 2013).

More recently, targeting of SH2s by monobodies has been extended to the Src family kinases (Kukenshoner et al., 2017). Binders were isolated to 6 of the 8 domains targeted, and were shown to compete with a phosphopeptide ligand in a fluorescence polarisation assay. Clones were also revealed to be selective for either the SrcA (Yes, Src1, Src2) or SrcB subgroup (Hck, Lck, Lyn, Blk) in a yeast

binding assay. Stable expression of Lck SH2-monobodies decreased the Lck-mediated phosphorylation of Zap70, a known Lck interactor, in stimulated Jurkat T-cell acute lymphoblstic leukaemia cells (Kukenshoner et al., 2017). These reports demonstrate that nABPs are a valid novel strategy for targeting SH2 domains, serving as improved binding molecules in the use of research and also for guiding the design of SH2 domain inhibitors for therapeutic use.

1.6 The Affimer; a novel non-antibody binding reagent

1.6.1 Structure and design of the Affimer scaffolds

Recently a novel engineered protein scaffold, called the Affimer, has been developed (Tiede et al., 2014; Tiede et al., 2017). Two types of Affimer scaffold have been generated, which are described in further detail below.

1.6.1.1 Type I Affimer scaffold

The Type I scaffold was derived from the protease inhibitor stefin A, a human cystatin (Stadler et al., 2011). This protein was chosen because protease inhibitor proteins are highly stable and use exposed peptide loops to bind their targets, making them promising candidate scaffolds (Dennis and Lazarus, 1994). Stefin A is 98 amino acids in length, comprised of a single-chain, and interacts with its targets via the amino terminus and two hairpin loop regions. Binding of stefin A to its natural substrates (cathespins) was abolished by substitution of specific residues (G4W and V48D), and site-directed mutagenesis of the scaffold open reading frame allowed the use of engineered restriction sites for insertion of randomised peptide-encoding oligonucleotides into the loop regions (herein termed variable regions). This new scaffold variant was termed Stefin A Quadruple Mutant—Tracy (Stadler et al., 2011). The constraint of the random peptides in the variable regions by the scaffold was aimed to increase binding specificity and affinity; as the peptide would be restricted to a limited number of conformations and the entropic cost of binding would be decreased (Ladner, 1995). The X-ray crystal structure of stefin A, demonstrating the fold of the Type I scaffold, can be observed in Figure 1.3A.

Yeast two-hybrid libraries of this scaffold were created initially, with insertions of randomised peptides either 10 amino acids in length in variable region 1, 12 amino acids in variable region 2, or a combination of 6 residues in region 1 and

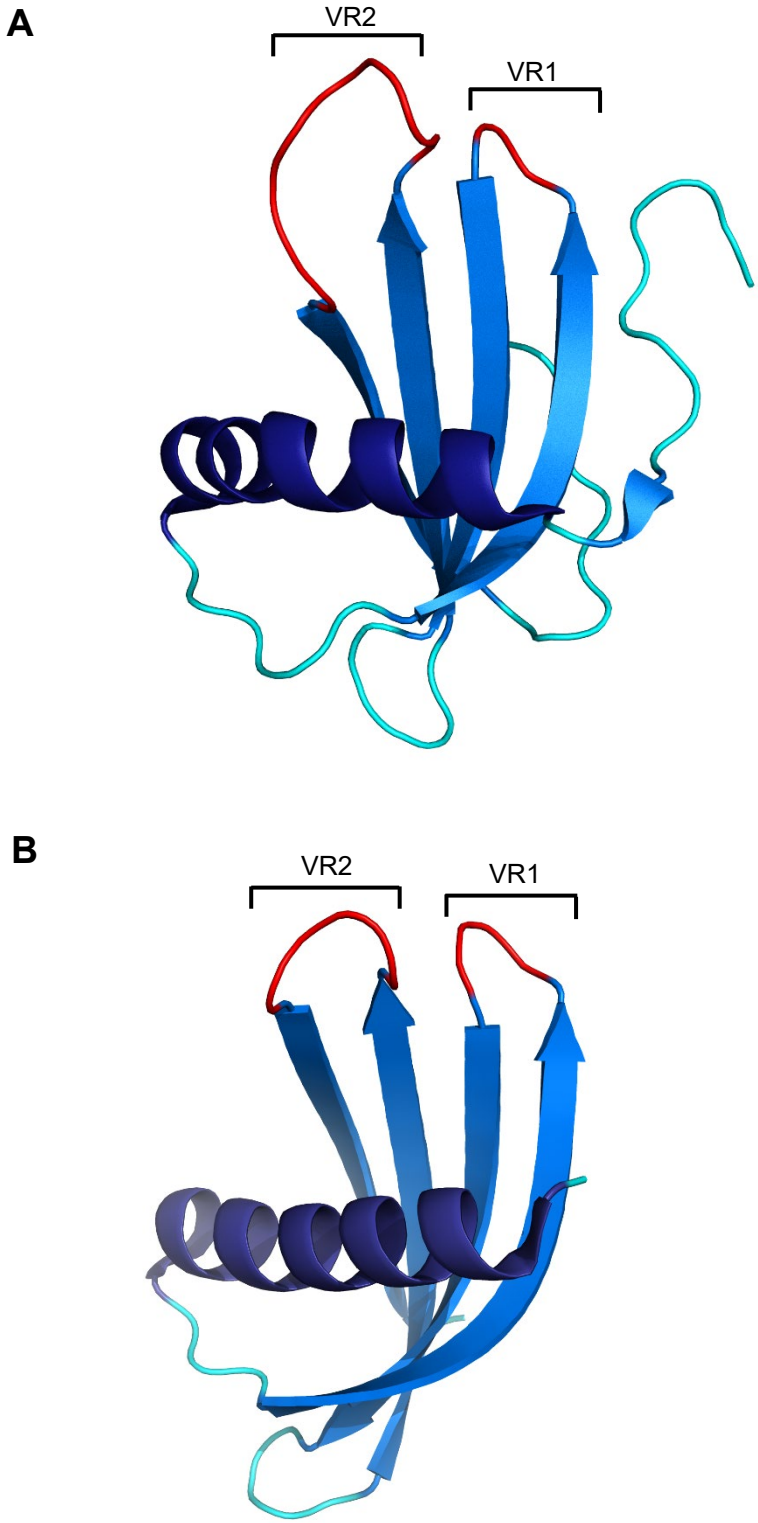

Figure 1.3. Structures of the Affimer Type I and II scaffolds. ***(A)*** *Crystal structure of stefin A (PDB ID: 1NB5). The α-helices and β-sheets are coloured blue, whilst the regions that are randomised in the Affimer Type I library are shown in red (Jenko et al. 2003).* ***(B)*** *Crystal structure of the Affimer Type II scaffold shown as cartoon representation (PDB ID: 4N6T). The α-helices and β-sheets are coloured blue, whilst the variable loop regions (VR) are shown in red (Tiede et al. 2014). Images were produced using PyMOL 2.0.*

12 residues in region 2. Each library comprised ~ 10^7 clones and showed successful screening of the POZ domain of B-cell lymphoma 6 protein (BCL-6; 130 amino acids in length) and to a peptide derived from the penicillin binding protein 2' (18 amino acids in length) (Stadler et al., 2011). Phage display libraries of this scaffold have since been created for screening.

1.6.1.2 Type II Affimer scaffold

The Type II scaffold design, originally termed 'Adhiron', was related in structure to the Type I scaffold (Tiede et al., 2014). Based on a consensus sequence of 57 phytocystatins, it was also chosen for its small size, high solubility and stability; all important properties for a successful alternative binding protein (Carter, 2011). This scaffold presents two constrained variable loop regions of 9 amino acid residues each. Scaffold variants of 92 – 81 amino acids in length have been produced.

An Affimer Type II phage library of 1.3 x 10^{10} clones has been created by insertion of random amino acid codons into the two variable regions (Tiede et al., 2014). This was achieved through splice overlap extension (SOE) of two polymerase chain reaction (PCR) products; the second of which was used to introduce the two randomised loop sequences into the Affimer scaffold, using degenerated primers synthesised by Ella Biotech. No cysteine residues or stop codons were included in these variable regions; cysteine-free scaffolds have the advantage that unique cysteine residues can be incorporated for site-directed coupling to labelling molecules (Binz et al., 2005). PCR products were used for 10 SOE cycles, then digested and cloned into a phagemid vector.

Both Affimer scaffold types are monomeric and lack disulphide bonds and glycosylation sites, resulting in high stability. X-ray crystallography of the Type II scaffold revealed the structure to be typical of cystatins, consisting of a four stranded anti-parallel β-sheet core and a central α-helix (see Figure 1.3B).

1.6.2 Affimer proteins as affinity reagents in research

The Affimer libraries have now been used in phage display to successfully screen over 350 targets (Tiede et al., 2017). These targets cover a broad range of molecules, including a receptor tyrosine kinase (VEGFR2), an ion channel (TRPV1), a viral protein (UL49) and a small organic compound (TNT) (Tiede et al., 2017). Proof-of-principle studies on yeast Small Ubiquitin-like Modifier

(ySUMO), fibroblast growth factor 1 (FGF1) and platelet endothelial cell adhesion molecule (CD31), have shown phage display to be a successful method for identifying Affimer reagents that bind with high affinity to the protein of interest.

Selected Affimer clones can be easily and rapidly amplified, extracted and purified from *E.coli* cells (Tiede et al., 2014). Due to its compact structure the Affimer scaffold shows high thermal stability, with a melting temperature of 101°C for the Type II scaffold, and a $T_{50\%}$ (temperature at which half the protein is unfolded) of 79.8°C for the Type I scaffold (Tiede et al., 2014; Stadler et al., 2011). This is superior to other nABPs such as Fibronectins and Repebodies (Jacobs et al., 2012, Lee et al., 2012) and has allowed an additional heat-denature step during purification to be used.

From the screen against ySUMO, 24 Affimer clones (out of potentially thousands) were isolated for phage ELISA. Twenty two of these were taken forward for further characterisation, helping to identify a commonly occurring binding motif that was present in 12 of the binders. These Affimer binders were then purified, biotinylated and used in western blot and ELISA analysis, to demonstrate their viability as research tools. They were found to be selective for ySUMO, as they showed no binding to human SUMO 1 or 2. They also demonstrated strong binding affinities, with K_D values in the nano-molar range. This is similar to affinities reported for other engineered protein scaffolds such as DARPins and monobodies (Schweizer et al., 2007, Gilbreth et al., 2011), making them a competitive product.

More recently, they have been shown to inhibit the function of vascular endothelial growth factor receptor 2 (VEGFR2) (Tiede et al., 2017). Signalling by VEFR2 regulates processes such as vasculogenesis, angiogenesis and arteriogenesis, making it an important research target for understanding mechanisms in metastatic cancers (Kofler and Simons, 2015). Two Affimer binders raised against VEGFR showed low nanomolar binding affinities against the receptor. Affimer B8 showed an inhibitory effect on VEGFR2 in human vascular endothelial cells (HUVECs) within 30 minutes of treatment. This was measured by a significant decrease in VEGF-induced vascular tubule formation and length in a tubulogenesis assay. Affimer B8 also blocked VEGF-dependent phosphorylation of VEGFR2 and consequent activation of downstream effectors PLCγ1, Akt, Erk, p38 and eNOS, as determined by western blot analysis (Tiede

et al., 2017). This exhibited the ability of Affimers to effectively disrupt signalling pathways.

Affimer reagents have also been used to target protein-protein interactions, using Affimer clones raised against human SUMO proteins (Hughes et al., 2017). SUMOylation is the posttranslational covalent attachment of SUMO proteins (1, 2, or 3) which regulates several cellular pathways. SUMOylated proteins are recognized by other proteins containing SUMO-interaction motifs (SIMs). Human embryonic kidney cells (HEK293) transfected with SUMO-binding Affimer reagents targeting either SUMO1/2 showed a decrease in formation of promyelocytic leukaemia protein nuclear bodies (PML-NBs) in response to arsenic-induced stress, compared with controls. As PML-NB formation is dependent upon SUMO:SIM interactions, this demonstrated inhibition of the protein-protein interactions between SIMs and SUMO1 or 2 by the Affimer proteins (Hughes et al., 2017).

The applications of Affimer proteins in research to date encompass western blotting; pull-downs; ELISAs; *in vivo* imaging; biosensors; histochemistry; super resolution microscopy; and modulators of protein function, although this list is not exhaustive (Tiede et al., 2017).

1.6.3 Affimer binders as SH2 domain reagents

Prior to the work detailed in this thesis, the Affimer libraries had also been successfully screened against the SH2 domains of Grb2 and phosphatidylinositol-4,5-bisphosphate 3-kinase (PI3K) (Tiede et al., 2017, Tiede et al., 2014). The hit rate for the Grb2 screen was 92%, with over 30 unique Affimers identified. The purification success rate of these binders was over 95% with protein yields between 50 – 100 mg/l. Compared to antibody fragment (ScFv and Fab) libraries targeting SH2 domains (Colwill et al., 2011), which had hit rates of 4 – 43% and between 2 – 6 unique clones identified, the Affimer scaffold offers a more diverse library with improved detection of binding molecules. Additionally, the purification success rate of these binders from the ScFv and Fab libraries was 80% with yields of 0.6 – 10 mg/l, highlighting the improved ease of purification provided by Affimer proteins (Tiede et al., 2014). This screen, although preliminary, validated the Affimer as an alternative binding protein that could be used in the development of novel research tools for SH2 domains.

Affimer binders were also isolated against SH2 domains of PI3K; a heterodimeric protein comprising a p110 catalytic subunit and a p85/p55 regulatory subunit (Tiede et al., 2017). The PI3K/Akt pathway is a key signal transduction system that regulates processes such as cell proliferation and survival, and is one of the most commonly activated pathways in cancer (Liu et al., 2009). Affimer reagents raised against the N-terminal SH2 domain of the p85α subunit were tested for specificity against both N- and C-terminal SH2s of p85α, p85β and p55γ subunits in an ELISA. A number of clones exhibited specificity to p85α-N, despite the high sequence homology between domains (pairwise 83 – 90%). These clones were shown to block PI3K SH2 domain function in transiently transfected murine fibroblast (NIH3T3) cells, shown by an increase in phosphorylation of downstream target protein kinase B (Akt). Importantly the reagents did not disrupt the formation of the p85:p110 subunit complex within PI3K itself (Tiede et al., 2017). These initial screens demonstrated the promise of successfully isolating SH2-binding Affimer reagents, that could bind highly specifically to their target and effect SH2-mediated intracellular signalling.

1.7 Objectives of the project

The overall aim of this project was to isolate and characterise Affimer binders against multiple SH2 domains, to evaluate their potential as SH2-targeting reagents in research. The Affimer Type II library has already been screened against the Grb2 and PI3K SH2 domains with promising results (Tiede et al., 2014; Tiede et al., 2017), suggesting this scaffold could be a competitor of established antibody fragment libraries and other nABPs (Colwill et al., 2011). Affimer reagents could therefore be a useful tool in the dissection of SH2 signalling and in the discovery of novel biology in a range of diseases. Additionally, use of the highly diverse Affimer phage libraries could enable identification of binding sequences to exploit for protein-specific SH2 inhibitor drug design (Wojcik et al., 2010).

Isolation of Affimer reagents to multiple SH2 domains would be accomplished through phage display; utilising this high-throughput method would allow a large number of targets to be screened within the project timescale. It was a high priority to then establish the specificities of the isolated reagents, because

protein-specific SH2 binding would be crucial to their success and has proven a challenging task (Kraskouskaya et al., 2013).

This project also aimed to characterise a small selection of Affimer binders *in vitro*, assessing their ability to bind and inhibit their target in a range of assays. Optimisation of functional cell-based assays testing SH2 domain inhibition by Affimer proteins was integral, as this would arguably be the most useful application for SH2 domain-binding reagents. Affimer clones previously isolated against the Grb2 SH2 domain were chosen for these proof-of-principle studies. Through these investigations, it would be determined whether Affimer binders are a valuable reagent for the study of SH2 domain function in disease.

Chapter 2

Materials and methods

Chapter 2

Materials and Methods

2.1 Materials

2.1.1 General Reagents

Reagents and equipment were manufactured by Thermo Fisher Scientific, unless otherwise stated.

2.1.2 Cell lines

Phoenix-AMPHO cells (ATCC® CRL-3213™) were acquired from St James' teaching Hospital in Leeds as a kind gift from Dr Julie Burns. U-2 OS human osteosarcoma cells (ATCC® HTB-96™), MCF-7 human breast cancer cells (ATCC® HTB-22™) and HEK-293 human embryonic kidney cells (ATCC® CRL-1573™) were also kindly provided by Dr Heather Martin and Danah Al-Qallaf.

2.1.3 Bacterial strain genotypes

Rosetta™ 2 (DE3) *Escherichia coli* (*E. coli*) cells were purchased from Novagen (Merk Millipore), BL21 Star™ (DE3) *E. coli* cells from Invitrogen (Life Technologies), and XL1-Blue Supercompetent *E. coli* cells from Stratagene (Agilent Technologies). ER2738 electrocompetent *E. coli* cells were used in phage display and purchased from Lucigen.

The choice of strain was dependent on the experiment; different strains have been optimised with mutations to perform certain functions, such as replication of plasmid DNA or protein expression. Table 2.1 below lists the genotypes of each strain.

Table 2.1. Genotypes of competent bacterial strains used in this study.

***E.coli* strain**	**Genotype**
Rosetta™ 2 (DE3)	F$^-$ *omp*T *hsdS*$_B$ ($r_B^-m_B^-$) *gal dcm* (DE3) pRARE2 (Cam^R)
BL21 Star™ (DE3)	F$^-$ *omp*T *hsdS*$_B$ (r_B^-, m_B^-) *gal dcm rne*131 (DE3)

XL1-Blue Supercompetent	*recA1 endA1 gyrA96 thi-1 hsdR17 supE44 relA1 lac* [F´ *proAB lacI^q ZΔM15 Tn10* (Tet^r)].
ER2738	[F' *proA$^+$B$^+$ lacI^q Δ(lacZ)*M15 *zzf::Tn10* (Tet^r)] *fhuA2 glnVΔ(lac-proAB) thi-1Δ(hsdS-mcrB)5*

2.1.4 Primers used for subcloning Affimer DNA

Primers were used in the amplification of Affimer DNA from parent vectors by polymerase chain reaction (PCR), for subcloning into destination vectors. Primers were used for the addition of suitable restriction sites into the amplified Affimer DNA fragments (see Table 2.2 below). Vector maps can be viewed in Appendix A.

Table 2.2. Primers used for subcloning of Affimer sequences. *List of primers, restriction enzymes, recipient and parent vectors used in the subcloning of Affimer DNA into various expression plasmids.*

Recipient vector	Parent vector	Primers name	Forward primer sequence (5' – 3')	Reverse primer sequence (5' – 3')	Restriction enzymes
pET11a	pBSTG (Tiede et al. 2014)	Affimer pET11a	ATGGCTAGCA ACTCCCTGGA AATCGAAG	TTACTAATGCG GCCGCACAAG CGTCACCAAC CGGTT TG	*NheI* / *NotI*
pET-lectra (Type I scaffold)	pBSTG	Affimer T1 pET-lectra	TACACGTACT TAGTCGCTGA AGCTCTTCTAT GATCCCGCGT GGCC	TAGGTACGAA CTCGATTGAC GGCTCTTCTA CCGAAACCCG TCAGCTCGTC	*SapI*
pET-lectra (Type II scaffold)	pBSTG	Affimer T2 pET-lectra	TACACGTACT TAGTCGCTGA AGCTCTTCTAT GAGCGCCGCT ACCG	TAGGTACGAA CTCGATTGAC GGCTCTTCTA CCGTCACCAA CCGGTTTGAA CTC	*SapI*
pRetro-X PTuner	pBSTG	Affimer pRetroX	GAACTGAGAT CTCTGCTAGC AACTCCCTGG AAATC	GTCATCCCAT GGCTAAGCGT CACCAACCGG TTTGAA C	*BglII* / *NcoI*

pBABE-puro	pET11a	Affimer pBABE	TAGGATCCGC CACCATGGCT AGCAACTCCC TGG	ATAGTCGACT CAGTGGTGAT GATGGTGGTG GCTCCCGCCA CCGCCCGCAT AGTCTGGCAC ATCGTACGGA TAACCGTCAC CAACCGGTTT GAACTCCTG	*BamHI* / *SalI*
pcDNA5	pBSTG	Affimer pcDNA	ATGGATCCGC CACCATGGCC GCTACCGGTG TTCGTG	GCATTAGCGG CCGCTTACCC TAATGATGAT GATGATGATG CTTGTCATCG TCATCTTTATA ATCAGCGTCA CCAACCGGTT TG	*BamHI* / *NotI*

2.1.5 Antibody dilutions

Table 2.3. Antibodies used during this study. *Details of antibody working dilutions for each assay. WB = western blotting; IF = immunofluorescence; MA = microarray and ELISA = enzyme linked immunosorbent assay.*

Antigen	Species	Concentration (mg/ml)	Dilution	Manufacturer & catalogue number
Grb2	Rabbit	0.032	WB: 1:5000 IF: 1:100	Abcam (ab32037)
phospho-Erk1/2 (Tyr204/Tyr185)	Mouse	0.2	WB: 1:1000	Santa Cruz (sc-7383)
Erk	Rabbit	1.0	WB: 1:50,000	Abcam (ab184699)
phospho-Akt (Ser473)	Rabbit	1.0	WB: 1:2000	Cell Signaling Technology (4060S)
Akt	Rabbit	1.0	WB: 1: 1000	Cell Signaling Technology (4691S)
PLCγ1	Mouse	1.0	WB: 1:1000	Abcam (ab41433)
Tubulin	Rat	1.0	WB: 1:3000	Bio-Rad (MCA77G)
6X His-tag	Rabbit	1.0	WB: 1:10,000 IF: 1:5000	Abcam (ab18184)

HA tag	Mouse	1.0	ELISA: 1:10,000	Abcam (ab119703)
DD tag	Mouse	0.125	WB: 1:1000	ClonTech (631073)
Fd-Bacterio-phage	Sheep	1.0	ELISA: 1:1000	Seramun Diagnostica GmbH (A-020-1-HRP)
Rabbit IgG (HRP-linked)	Goat	1.0	WB: 1:1000	Cell Signaling Technology (7074S)
Mouse IgG (HRP-linked)	Goat	2.0	WB: 1:5000 – 1:10,000	Abcam (ab6789)
Rat IgG (HRP-linked)	Goat	1.0	WB: 1:5000	Abcam (ab97057)
Rabbit IgG (AlexaFluor® 594-linked)	Goat	2.0	IF: 1:1000	Invitrogen (A11037),
Mouse IgG (AlexaFluor® 488-linked)	Goat	2.0	IF: 1:1000	Invitrogen (A11001)
HA tag (AlexaFluor® 347-linked)	Mouse	1.0	MA: 1:1000	Thermo Fisher Scientific (26183-A647)

2.1.6 Common buffers and solutions

Phosphate Buffered Saline (1X PBS): 137 mM NaCl; 2.7 mM KCl; 10 mM Na_2HPO_4; 2 mM KH_2PO_4; pH 7.4. 20X stock autoclaved before use.

PBS-Tween (PBST): 1X PBS + 0.1% Tween-20.

Tris Buffered Saline (1X TBS): 50 mM Tris-Cl; 150 mM NaCl; pH 7.6.

TBS-Tween (TBST): 1X TBS + 0.1% Tween-20.

Mammalian Lysis Buffer: 50 mM Tris; 150 mM NaCl; 1% (v/v) Nonidet P-40 (Sigma-Aldrich); pH 7.4. 1X Halt™ Protease Inhibitor Cocktail, EDTA-free and 1:100 Phosphatase Inhibitor Cocktail 2 (Sigma-Aldrich) added before use, Filter sterilised before use.

SPR Tris Buffer: 50 mM Tris; 100 mM NaCl; pH 7.4. Filter sterilised before use.

Lysis Buffer for *E. coli* cells**:** 50 mM NaH_2PO_4; 300 mM NaCl; 20 mM imidazole; 10% glycerol; pH 7.4. Autoclaved before use.

Wash Buffer: 50 mM NaH_2PO_4; 500 mM NaCl; 20 mM imidazole; pH 7.4. Autoclaved before use.

Elution Buffer: 50 mM NaH_2PO_4; 500 mM NaCl; 300 mM imidazole; 10% glycerol; pH 7.4. Autoclaved before use.

Blocking Buffer (phage display and ELISAs)**:** Casein Blocking Buffer 10X (Sigma-Aldrich), diluted to 2X in PBST.

TE Buffer: 10 mM Tris; 1 mM EDTA; pH 8.0.

Pull-down (PD) Binding Buffer: 3.25 mM NaH_2PO_4 pH 7.4; 70 mM NaCl; 0.01% Tween-20.

PD Wash Buffer: 50 mM NaH_2PO_4 pH 8.0; 150 mM NaCl; 0.01% Tween-20.

PD His Elution Buffer: 300 mM imidazole; 50 mM NaH_2PO_4 pH 8.0; 300 mM NaCl; 0.01% Tween-20.

2.1.7 Bacterial cell culture reagents

LB medium (Lennox L Broth Base) (Invitrogen® Life Technologies): 86.2 mM NaCl; 10 g/L SELECT peptone 140; 5 g/L SELECT yeast extract.

2TY medium: 10 g/L yeast extract; 16 g/L tryptone; 5 g/L NaCl.

TB medium: 24 g/L yeast extract; 20 g/L tryptone; 4 ml/L glycerol; 0.017 M KH_2PO_4; 0.072 M K_2HPO_4.

LB Agar (Lennox L agar) (Invitrogen® Life Technologies): 10 g/L SELECT peptone 140; 5 g/L SELECT yeast extract; 5 g/L sodium chloride; 12 g/L SELECT agar.

SOC medium: 0.4% (w/v) glucose, 20 g/L tryptone; 5g/L yeast extract; 0.5g/L NaCl.

2.1.8 Mammalian cell culture reagents

Dulbecco's Modified Eagle Medium (DMEM) (Sigma-Aldrich): 0.584 mg/ml L-Glutamine; 0.11 mg/ml sodium pyruvate; 4.5 mg/ml D-Glucose.

RPMI-1640 medium (Sigma-Aldrich): 0.3 mg/ml L-Glutamine; 2.0 mg/ml D-Glucose.

Opti-MEM™ (Gibco™): Reduced serum medium; 2.4 g/L sodium bicarbonate; L-Glutamine.

Trypsin-EDTA (Gibco™): 0.05% trypsin-EDTA (1X).

5X siRNA Buffer (Dharmacon): 300 mM KCl; 30 mM HEPES-pH 7.5; 1.0 mM $MgCl_2$.

1X siRNA Buffer: 60 mM KCl; 6 mM HEPES-pH 7.5; 0.2 mM $MgCl_2$; in RNase-free water (GE Healthcare).

Dulbecco's Phosphate-Buffered Saline (DPBS) (Corning): 0.2 mg/ml KCl; 0.2 KH_2PO_4 ; 8 mg/ml NaCl; 1.15 mg/ml Na_2HPO_4.

2.1.9 Sodium dodecyl sulphate polyacrylamide gel electrophoresis (SDS-PAGE) and western blotting reagents

Separating Gel Buffer: 1.5 M Tris; 0.4% (w/v) SDS; pH 8.9. Filter sterilised through 0.22µm filter.

Stacking Gel Buffer: 0.4M Tris; 0.4% (w/v) SDS; pH 6.7. Filter sterilised through 0.22µm filter.

SDS-PAGE Running Buffer: 25 mM Tris; 0.19 M glycine; 0.1% (w/v) SDS; pH 8.3.

SDS-PAGE Sample Buffer (4X): 8% (w/v) SDS; 0.2 M Tris-HCl (pH 7); 20% glycerol; 1% bromophenol blue (BDH laboratories); 20% β-mercaptoethanol added before use.

Coomassie Blue stain: 45% methanol; 7% acetic acid; 0.25% Coomassie Brilliant Blue R-250 (Sigma-Aldrich).

De-stain solution: 25% methanol; 7.5% acetic acid.

Transfer Buffer: 25 mM Tris; 0.19 M glycine; 20% methanol; pH 8.3.

Stripping Buffer: 0.2 M glycine; 0,1% SDS; 1% Tween-20; pH 2.2.

2.2 Methods

2.2.1 Preparation of chemically competent bacterial cells

Preparations of chemically competent bacterial cells were made from stock supplies using rubidium chloride. A glycerol stock of the appropriate strain was streaked onto an LB agar plate and incubated overnight at 37 °C. a single colony was used to inoculate 5 ml LB broth and incubated overnight at 37 °C, 230 rpm. A 0.5 ml aliquot of this culture was used to inoculate 50 ml pre-warmed LB broth and incubated at 37 °C, 230 rpm until an OD_{600} of ca. 0.4 was reached.

The culture was then transferred to a 50 ml tube and chilled on ice for 5 min. Cells were pelleted by centrifugation at 3000 rpm for 10 min at 4 °C. The pellet was re-suspended in 20 ml ice-cold Tfb1 Buffer (3 mM KAc; 100 mM $RbCl_2$; 10 mM $CaCl_2$; 50 mM MnCl; 15% glycerol; pH 5.8; filter sterilised through 0.22 µm filter) and incubated on ice for 5 min. Cells were centrifuged at 3000 rpm for 10 min at 4 °C, and the pellet re-suspended in 2 ml ice-cold Tfb2 Buffer (10 mM MOPS; 10 mM $RbCl_2$; 75 mM $CaCl_2$; 15% glycerol; pH 6.5; filter sterilised through 0.22 µm filter). Cells were incubated on ice for a further 15 min and aliquoted into 250 µl samples in pre-chilled 1.5 ml tubes. Samples were frozen on dry ice and stored at -80 °C.

2.2.2 DNA protocols and molecular subcloning

2.2.2.1 Polymerase Chain Reaction

The polymerase chain reaction (PCR) was used for amplification of Affimer DNA sequences during subcloning into various expression vectors. The primers used in each reaction were dependent upon the parent and recipient vectors (see Table 2.2), and are detailed in the relevant method sections describing protein production and mammalian cell line production. PCRs were performed in 200 µl PCR tubes, using a G-Storm™ GS2 thermal cycler. Reactions were carried out with either Phusion® High-Fidelity DNA polymerase (New England Biolabs; NEB) or KOD Hot Start DNA polymerase (Merck Millipore), using the components supplied with the polymerase. Reaction components and thermocycling conditions are detailed for each polymerase below.

Table 2.4. Reaction components of PCR with KOD DNA polymerase.

Component	Volume in 25 µl reaction	Final Concentration
Nuclease-free water	15.5 µl	
10X KOD Buffer	2.5 µl	1X
dNTP Mix, 2 mM	2.5 µl	200 µM each
$MgSO_4$, 25 mM	1.5 µl	1.5 mM
Forward primer (10 µM)	0.75 µl	0.3 µM
Reverse primer (10 µM)	0.75 µl	0.3 µM
KOD DNA Polymerase	0.5 µl	0.02 units/µl
Template DNA	1 µl (from DNA miniprep)	

Table 2.5. Thermocycling conditions of PCR with KOD DNA polymerase.

Cycle Step	Temperature	Time	Cycles
Initial Denaturation	95 °C	2 min	1
Denaturation Annealing Extension	95 °C 55 °C 70 °C	20 sec 20 sec 20 sec	30
Final Extension Hold	70 °C 4 °C	5 min Hold	1

Table 2.6. Reaction components of PCR with Phusion DNA polymerase.

Component	Volume in 25 µl reaction	Final Concentration
Nuclease-free Water	13.8 µl	
5X Phusion HF Buffer	5 µl	1X
dNTP Mix (25 mM)	0.2 µl	200 µM each
DMSO	0.75 µl	3%
Forward primer (10 µM)	2 µl	0.8 µM
Reverse primer (10 µM)	2 µl	0.8 µM
Phusion DNA Polymerase	0.25 µl	0.02 units/µl
Template DNA	1 µl (from DNA miniprep)	

Table 2.7. Thermocycling conditions of PCR with Phusion DNA polymerase.

Cycle Step	Temperature	Time	Cycles
Initial Denaturation	98 °C	30 sec	1
Denaturation Annealing Extension	98 °C 54 °C 72 °C	20 sec 20 sec 20 sec	30
Final Extension Hold	72 °C 4 °C	10 min Hold	1

Following thermocycling, methylated DNA was digested by 10U *DpnI* (NEB) for 1 h at 37 °C and the enzyme inactivated at 80 °C for 10 min. The product was purified using a NucleoSpin® Gel and PCR Clean-up kit (Macherey-Nagel), according to the manufacturer's instructions.

2.2.2.2 QuikChange-style linear amplification reaction

For introduction of various linker and tag sequences into plasmid DNA, two complementary oligonucleotide primers containing the insertion sequence, designed to bind to opposite strands of the plasmid, were synthesised. Using the plasmid as the template, linear amplification thermocycling was carried out with KOD Hot Start DNA polymerase (Merck Millipore) as below, to extend the two primers. The primers used in this reaction are detailed in the relevant protein production and cell line production sections (see 2.2.4 and 2.2.15).

Table 2.8. Reaction components of linear amplification with KOD DNA polymerase.

Component	Volume in 25 µl reaction	Final Concentration
Nuclease-free water	11 µl	
10X KOD Buffer	2.5 µl	1X
dNTP Mix, 2 mM	2.5 µl	200 µM each
$MgSO_4$, 25 mM	1.5 µl	1.5 mM
Forward primer (25 ng/µl)	2.5 µl	62.5 ng
Reverse primer (25 ng/µl)	2.5 µl	62.5 ng
KOD DNA Polymerase	0.5 µl	0.02 units/µl
Template DNA (5 ng/µl)	2 µl	10 ng

Table 2.9. Thermocycling conditions of linear amplification with KOD DNA polymerase.

Cycle Step	Temperature	Time	Cycles
Initial Denaturation	95 °C	2 min	1
Denaturation Annealing Extension	95 °C 65 °C 70 °C	1 min 1 min 6 min	30
Final Extension Hold	70 °C 4 °C	10 min Hold	1

Following thermocycling, the methylated template DNA which did not contain the inserted sequence was digested by 10U *DpnI* (NEB) for 1 h at 37 °C and the enzyme inactivated at 80 °C for 10 min. The product was purified using a NucleoSpin® Gel and PCR Clean-up kit (Macherey-Nagel), according to the manufacturer's instructions. DNA was eluted using 50 µl nuclease-free water and transformation of XL1-Blue Supercompetent cells was performed (section 2.2.2.6).

2.2.2.3 Agarose gel electrophoresis

DNA samples were mixed with the appropriate volume of 10x DNA loading dye (30 % glycerol; 0.2 % Orange G; H_2O) and 5 µl of samples were loaded onto a 0.7 % (w/v) agarose gel in Tris-acetate-EDTA (TAE) buffer (40 mM Tris; 20 mM acetic acid; 1 mM EDTA; pH 8.0), containing 1X SYBR® Safe DNA Gel Stain. Quick-Load® Purple 2-log DNA Ladder was also loaded (NEB). Electrophoresis was carried out in Mini-Sub® Cell GT apparatus (Bio-Rad) in TAE buffer at 100 V. DNA bands were visualised under UV light and imaged using an Amersham™ Imager 600 (GE Healthcare); or if the DNA was to be purified and used in downstream applications, bands were visualised using a Safe Imager™ Blue Light Transilluminator.

If extraction and purification of DNA from agarose gels was needed, after electrophoresis bands were excised from the gel using a scalpel. Extraction of the DNA was performed using a NucleoSpin® Gel and PCR Clean-up kit (Macherey-Nagel), according to the manufacturer's instructions. DNA was eluted using 50 µl nuclease-free water.

2.2.2.4 Restriction digestion

Restriction digests were performed in a total reaction volume of 50 µl, containing 10 U restriction enzyme(s); 1 – 5 µg DNA; 1X CutSmart® Buffer (NEB); in nuclease-free water. Reactions were incubated for 3 h at 37 °C, and the resulting fragments analysed on a 0.7 % (w/v) agarose gel and purified from the gel (section 2.2.2.3). Restriction enzymes used for cloning into each vector are displayed in Table 2.2 (section 2.1.4) and were purchased from NEB.

2.2.2.5 DNA Ligation

Affimer insert and vector DNA were ligated after restriction digestion with the same enzymes. Vector DNA was dephosphorylated after restriction digestion and before agarose gel purification, to remove the 5' phosphate and prevent self-ligation. Dephosphorylation was carried out using Antarctic Phosphatase in a total reaction volume of 60 µl, containing 5 U Antarctic Phosphatase (NEB); 5 µg vector DNA; 1X Antarctic Phosphatase Reaction Buffer (NEB), in nuclease-free water. After incubation for 15 min at 37 °C, Antarctic Phosphatase was heat inactivated by incubation at 65 °C for 5 mins.

Ligations were performed in 20 µl reactions, containing 25 ng vector DNA; 75 ng insert DNA; 1 U T4 DNA Ligase (Roche); 1X T4 DNA Ligase Buffer (Roche), in nuclease-free water. Ligation reactions were incubated at 4 °C overnight, before transformation of XL-1 Blue Supercompetent cells was performed.

2.2.2.6 Transformation of *E.coli* bacterial cells with DNA

Chemically competent *E.coli* cells were transformed with plasmid DNA by heat shock. Aliquots of 10 µl cells (per transformation) were thawed on ice, and 1 µl DNA added. After 30 min incubation on ice, cells were heat shocked at 42 °C for 45 sec in a water bath, and returned to ice for 2 min. After addition of 190 µl of antibiotic-free SOC medium, transformation reactions were incubated at 37 °C for 1 h, 230 rpm. Cells were then plated onto LB agar plates containing the relevant antibiotic (100 µg/ml carbenicillin or 50 µg/ml kanamycin) and incubated overnight at 37 °C.

2.2.2.7 Purification of plasmid DNA from *E.coli*

Purification of plasmid DNA was performed using a QIAprep® Spin Miniprep or HiSpeed® Plasmid Maxi Kit (Qiagen), depending on the yield required. A single

bacterial colony containing the plasmid DNA was used to inoculate 5 ml 2TY medium containing the appropriate antibiotic(s) and incubated overnight at 37 °C, 230 rpm. For minipreps, this culture was centrifuged at 4816 *xg* for 10 min at 4 °C and plasmid DNA purified using the QIAprep Spin Miniprep kit, according to the manufacturer's instructions. For maxipreps, the culture was used to inoculate 150 ml 2TY medium containing the relevant antibiotic(s) and incubated overnight at 25 °C, 230 rpm. Cells were pelleted at 4816 *xg* for 20 min at 4 °C and plasmid DNA purified using the HiSpeed® Plasmid Maxi Kit, according to the manufacturer's instructions. DNA was eluted from both kits in nuclease-free H_2O and stored at -20 °C.

2.2.2.8 Determination of DNA concentration

DNA concentration was measured using a NanoDrop™ Lite spectrophotometer. Nuclease-free water was used to take a blank measurement before sample reading. Concentration was determined from the absorbance at 260 nm (A_{260}) using the Beer-Lambert law; $A_{260} = \varepsilon cl$, where ε is the extinction coefficient, c is the DNA concentration in ng/µl and l is the path length in cm.

2.2.2.9 DNA sequencing

Purified DNA was diluted to 100 ng/µl and sequencing was performed by Genewiz (previously Beckman Coulter), using the primers detailed in Table 2.10 below.

Table 2.10. Primers used for DNA sequencing of plasmids. *All are universal primers provided by Genewiz unless stated otherwise (denoted by 'custom').*

Plasmid	**Primer name**	**Primer sequence (5' – 3')**
pET11a	T7	TAATACGACTCACTATAGGG
pET28 SacB AP	T7	TAATACGACTCACTATAGGG
pET-lectra	T7	TAATACGACTCACTATAGGG
pBSTG	M13R	CAGGAAACAGCTATGAC
pcDNA5	BGHR	TAGAAGGCACAGTCGAGG
pRetroX-PTuner	pRetroX sequencing (custom)	CTGACTATATCTCCAGATTATG

pBABE	pBABE sequencing (custom)	CCCTTGAACCTCCTCGTTCGACC

2.2.3 Protein analysis methods

2.2.3.1 Protein concentration determination

Protein concentration was measured using a NanoDrop™ Lite spectrophotometer. The appropriate sample buffer was used to take a blank measurement before sample reading. Concentration was determined from the absorbance at 280 nm (A_{280}) using the Beer-Lambert law; $A_{280} = \varepsilon cl$, where ε is the extinction coefficient, c is the protein concentration in mg/ml and l is the path length in cm. Extinction coefficients for each protein were calculated using ExPASy ProtParam software.

Total protein concentration of cell lysate was determined by the bicinchoninic acid (BCA) assay. A Pierce™ BCA Protein Assay Kit was used, according to the manufacturer's instructions for 10 µl samples in a microplate format.

2.2.3.2 SDS-PAGE analysis

Protein samples were re-suspended in a 1:4 volume of 4X SDS-PAGE Sample Buffer and incubated at 95 °C for 10 min. Samples were loaded onto a 15% SDS-polyacrylamide resolving gel with a 5% stacking gel and electrophoresed at 170 V in 1X Running Buffer for ca. 1 h. Unless otherwise stated, molecular weight marker used was PageRuler™ Prestained Protein Ladder, 10 – 180 kDa. Gels were stained for 45 min in Coomassie Blue and de-stained overnight. Coomassie-stained gels were imaged using an Amersham™ Imager 600 (GE Healthcare)

2.2.3.3 Western blotting

After SDS-PAGE (without gel staining), protein samples were transferred onto a PVDF membrane with 0.2 µm pore size at 25 V, 1300 mA for 7 min using the Trans-Blot® Turbo™ Transfer System (Bio-Rad). Membranes were blocked for 1 h at room temperature in TBST + 5% milk (for detection of biotinylated proteins, all steps were performed with 3% BSA in place of milk). Membranes were then incubated with primary antibodies in TBST + 1% milk overnight at 4 °C and secondary antibodies in TBST + 1% milk for 1 h at room temperature (see Table

2.3 for antibody dilutions). Membranes were washed for 3 x 5 min in TBST between each step. HRP was visualised using Luminata Forte Western HRP Substrate (Merck Millipore), according to the manufacturer's instructions. Images were taken using an Amersham™ Imager 600 (GE Healthcare). For stripping, membranes were incubated with Stripping Buffer for 2 x 5 min, followed by 1X PBS for 10 min and 1X TBST for 10 min. Membranes were then re-blocked for 1 h at room temperature before re-probing with antibody solution.

Quantification of proteins was performed using densitometry on ImageQuant TL 8.1 analysis software (GE Healthcare) and quantities were corrected against tubulin for loading errors. Paired t-tests between Affimer-expressing mammalian cell samples and the positive control sample were performed on data using GraphPad Prism 7, to determine any significant differences in protein levels between samples.

2.2.4 SH2 domain protein production

SH2 domain sequences were encoded in kanamycin-resistant pET28 SacB AP vectors with an N-terminal 6x histidine tag (His-tag) which were purchased from the Pawson Lab (Samuel Lunenfeld Research Institute, Canada).

For biotin acceptor peptide (BAP)-tagged SH2 domains, a sequence was cloned onto the N-terminus of the SH2 sequence, before the His-tag, encoding amino acids M-G-S-S-**G-L-N-D-I-F-E-A-Q-K-I-E-W-H-E**-G-S-S (BAP is highlighted in bold). The insertion was performed using the following primers in a Quikchange-style linear amplification reaction (section 2.2.2.2):

Forward primer sequence (5' – 3')	CGATATCTTCGAAGCCCAAAAAATCGAATGGCACGAAGG CAGCAGCCATCATCATC
Reverse primer sequence (5' – 3')	CATTCGATTTTTTGGGCTTCGAAGATATCGTTCAGACCG GAGCTGCCCATGGTATATCTCC

BL21 Star™ (DE3) or Rosetta™ 2 (DE3) *E.coli* cells were transformed with plasmid DNA by heat shock. The Rosetta™ 2 strains are BL21 derivatives, designed to enhance the expression of eukaryotic proteins in *E. coli*. These strains supply tRNAs for 7 codons rarely used in *E. coli* (AGA, AGG, AUA, CUA, GGA, CCC, and CGG) on a chloramphenicol-resistant plasmid. The tRNA genes

are driven by their native promoters. Cells were plated onto LB agar + kanamycin (50 µg/ml) and incubated at 37 °C overnight.

For production in BL21 Star™ (DE3) cells, 5 ml starter cultures were grown at 37 °C, 230 rpm overnight in LB broth kanamycin (50 µg/ml) + 1% glucose and used to inoculate 400 ml of LB broth kanamycin. Cells were grown at 37 °C, 230 rpm until OD_{600} reached ca. 0.6 and protein expression was induced by 0.5 mM isopropyl-β-D-thiogalactoside (IPTG). Cultures were left overnight at 20 °C, 150 rpm.

For production in Rosetta™ 2 (DE3) cells, 5 ml starter cultures were grown at 37 °C, 230 rpm overnight in TB medium supplemented with kanamycin (50 µg/ml); chloramphenicol (34 µg/ml); and 1% glucose. These were used to inoculate 400 ml or 50 ml of TB kanamycin. Cells were grown at 37 °C, 230 rpm until OD_{600} reached ca. 1.5 and temperature was reduced to 18 °C for 1 h before addition of 0.5 mM IPTG. Cultures were left overnight at 18 °C, 230 rpm.

2.2.4.1 SH2 domain manual purification

SH2 domain proteins were purified using nickel affinity chromatography. All purification steps were carried out at 4 °C. Induced cells were pelleted at 4816 *xg* for 20 min, before incubation for 40 min with lysis solution [0.1 mg/ml lysozyme; 1% Triton™ X-100 (Sigma-Aldrich); 10 U/ml Benzonase® Nuclease, Purity > 99% (Novagen®, Merck Millipore); 1X Halt™ Protease Inhibitor Cocktail, EDTA-free in Lysis Buffer], using 1 ml lysis solution per 20 ml of culture. After addition of 20% (v/v) glycerol, cell debris was pelleted and clarified lysate incubated with Amintra Nickel-nitrilotriacetic acid (Ni-NTA) resin (Expedeon) for 1-2 h. A volume of 150 µl resin was used for 50 ml cultures and 600 µl for 400 ml cultures, based on expected protein yields and resin binding capacity. Resin was washed with Wash Buffer until the A_{280} consistently read <0.09 on a Nanodrop™ Lite spectrophotometer. Protein was then eluted using 200 µl volumes of Elution Buffer + 1 mM TCEP until concentration was < 0.1 mg/ml.

2.2.4.2 SH2 domain automated purification

In the automated purification method, SH2 proteins were purified from clarified cell lysate (after cell lysis and centrifugation to remove cell debris), using His Mag Sepharose™ Ni beads (GE Healthcare) on a KingFisher Flex™ robotic platform. Beads (150 µl/well) were washed x3 and resuspended with Lysis Buffer, before

incubation with 850 µl SH2-containing lysate for 90 min. Beads were washed x5 with 1 ml Wash Buffer for 10 min and proteins eluted by incubation with 130 µl Elution Buffer + 1 mM TCEP for 10 min.

After either purification method, elution sample concentrations were measured and the purity of samples and successful *in vivo* biotinylation of BAP-tagged SH2s was confirmed by SDS-PAGE and western blotting (section 2.2.3). Samples were flash frozen in liquid nitrogen and stored in aliquots at -80 °C.

2.2.4.3 Grb2 protein purification using size exclusion chromatography

Grb2 proteins used in fluorescence anisotropy and binding affinity assays were further purified using size exclusion chromatography (SEC), to isolate the monomeric Grb2 from the dimeric species. Elution samples (section 2.2.4.1) were pooled and concentrated into a volume of 1 ml using an Amicon® Ultra-4 Centrifugal Filter Unit (Merck Millipore) and run through a Superdex® 75 gel filtration column into filter-sterilised SPR Tris Buffer. The A_{280} and A_{260} of the samples were recorded throughout. Fractions of 3 ml volume were collected and analysed by SDS-PAGE for purity. Samples were flash frozen in liquid nitrogen and stored in aliquots at -80 °C.

2.2.5 Affimer protein production

2.2.5.1 His-tagged Affimer protein production for *in vitro* assays

Affimer sequences were subcloned from the pBSTG phagemid vector into carbenicillin-resistant pET11a vectors with a C-terminal 8xHis-tag sequence. Affimer DNA was amplified from the pBSTG vector using the Affimer pET11a primers (Table 2.2) in a Phusion polymerase PCR (section 2.2.2.1) and digested with *NheI*-HF™ and *NotI*-HF™ (NEB). The Affimer DNA fragment was ligated into the similarly digested pET11a vector (Merck Millipore catalog no. 69436-3). BL21 Star™ (DE3) *E.coli* cells were transformed with plasmid DNA by heat shock and 5 ml starter cultures were grown at 37 °C, 230 rpm overnight in LB broth carbenicillin (100 µg/ml) + 1% glucose. Cultures were used to inoculate 50 or 400 ml of LB broth carbenicillin and grown at 37 °C, 230 rpm until OD_{600} reached ca. 0.6 - 0.8. Protein expression was induced with 0.5 mM IPTG and cultures were left overnight at 30 °C, 230 rpm.

Affimer proteins were purified from cell lysate using nickel affinity chromatography. All purification steps were carried out at room temperature.

Induced cells were pelleted by centrifugation at 4816 *xg* for 20 min and incubated for 20 min with lysis solution [0.1 mg/ml lysozyme; 1% Triton™ X-100 (Sigma-Aldrich); 10 U/ml Benzonase® Nuclease, Purity > 99% (Novagen®, Merck Millipore); 1X Halt™ Protease Inhibitor Cocktail, EDTA-free; in Lysis Buffer], using 1 ml lysis solution per 50 ml of culture. After heating to 50 °C for 20 min to denature non-specific proteins, cell debris was pelleted and clarified lysate incubated with 150 µl of Amintra Nickel-nitrilotriacetic acid (Ni-NTA) resin (Expedeon) for 1-2 h. Resin was washed with 1 ml Wash Buffer until the A_{280} consistently read <0.09 on a Nanodrop™ Lite spectrophotometer. Protein was then eluted using 200 µl volumes of Elution Buffer until concentration was < 0.1 mg/ml.

Proteins were dialysed overnight at 4 °C into either 1X PBS + 10% glycerol or SPR Tris Buffer for subsequent assays, using Slide-A-Lyzer™ Dialysis cassettes, 7K MWCO. Protein concentrations were measured and the purity of samples was confirmed by SDS-PAGE (section 2.2.3). Samples were frozen on dry ice and stored in aliquots at -20 °C.

2.2.5.2 HA-tagged Affimer protein production for microarrays

Affimer sequences were subcloned from the pBSTG phagemid vector into kanamycin-resistant pET-lectra vectors with C-terminal 8xHis-tag and C-terminal HA-tag sequences. The HA-tag was located between the Affimer and His-tag sequences. Affimer DNA was amplified from the pBSTG vector using the Affimer T1 and T2 pET-lectra primers (Table 2.2) in a Phusion polymerase PCR (section 2.2.2.1) and digested with *SapI*. The DNA fragment was ligated into the similarly digested pET-lectra vector (see section 2.2.2 for details).

BL21 Star™ (DE3) *E.coli* cells were transformed with plasmid DNA and 200 µl starter cultures were grown at 37 °C, 1050 rpm in a 96-well plate for 6 – 8 h in LB broth kanamycin (50 µg/ml) + 1% glucose. Cultures were used to inoculate 3 ml of LB broth kanamycin in round bottom 24-well plates and grown at 37 °C, 1050 rpm until OD_{600} reached ca. 0.8. Protein expression was induced with 0.5 mM IPTG and cultures were left overnight at 22 °C, 1050 rpm.

Affimer proteins were purified from lysate using His Mag Sepharose™ Ni beads (GE Healthcare) on a KingFisher Flex™ robotic platform. All purification steps were carried out at room temperature. Induced cells were pelleted at 4816 *xg* for 10 min and incubated for 20 min with 300 µl lysis solution [0.1 mg/ml lysozyme;

1% Triton™ X-100 (Sigma-Aldrich); 10 U/ml Benzonase® Nuclease, Purity > 99% (Novagen®, Merck Millipore); 1X Halt™ Protease Inhibitor Cocktail, EDTA-free; in Lysis Buffer]. Cell debris was pelleted at 4816 *xg* for 20 min and clarified lysate collected.

The His Mag Sepharose™ Ni beads (50 µl/well) were washed x 3 and resuspended with Lysis Buffer, before incubation with 300 µl Affimer lysate and 150 µl Lysis Buffer for 90 min. Beads were washed x 5 with 1 ml Wash Buffer for 10 min and proteins eluted by incubation with 70 µl Elution Buffer for 10 min. Protein concentrations were measured and the purity of samples was confirmed by SDS-PAGE (section 2.2.3). Samples were flash frozen in liquid nitrogen and stored in aliquots at -80 °C.

2.2.6 Phage display methods

2.2.6.1 Chemical biotinylation of SH2 targets

Purified SH2 domain proteins without a BAP tag were chemically biotinylated for phage display. A 5 mg/ml solution of EZ-Link™ NHS-SS-Biotin in dimethyl sulfoxide (DMSO) was added to the protein (volumes calculated according to the manufacturer's instructions) and incubated at room temperature for 1 h. Excess biotin was removed using Zeba™ Spin Desalting Columns, 7K MWCO, according to the manufacturer's instructions. Glycerol was added to a final concentration of (v/v) 40% and the sample stored at -20 °C. Successful biotinylation was confirmed via ELISA by binding of the biotinylated target to Nunc-Immuno™ Maxisorp™ strips overnight at 4 °C and incubation with High Sensitivity Streptavidin-HRP, 1:1000 in Blocking Buffer (section 2.1.6), for 1 h at room temperature. HRP was detected using SeramunBlau® fast TMB (Seramun Diagnostica GmbH). Absorbance at 620 nm was measured.

2.2.6.2 Anti-His tag ELISA

ELISAs to show successful immobilisation of BAP-tagged and chemically biotinylated SH2 domains to streptavidin-coated plates were performed. Streptavidin-coated strips were blocked overnight with 10X Blocking Buffer and washed x6 with PBST. Purified SH2 domains (10 µl at ≥0.5 mg/ml) were incubated in the wells for 2 h at room temperature. After 6 x PBST washes, Anti-6X His tag®-HRP antibody (Abcam), 1:5000 in Blocking Buffer, was added for 1

h at room temperature. HRP was visualised using SeramunBlau® fast TMB (Seramun Diagnostica GmbH). Absorbance at 620 nm was measured.

2.2.6.3 Phage Display

Phage display was completed over four panning rounds, using previously constructed Affimer phage libraries (see Tiede et al., 2014 for details). Streptavidin-coated wells were pre-blocked overnight at 4 °C with Blocking Buffer. The Affimer phage libraries were pre-panned three times at room temperature for 40 min; 5 µl of each phage library (10^{12} cfu) was added to 100 µl Blocking Buffer in the streptavidin-coated wells.

Biotinylated SH2 targets were bound to panning wells, 20 µl target in 100 µl Blocking Buffer, and incubated at room temp for 1-2 h. Wells were washed x 6 with PBST and the pre-panned phage transferred to the target-coated wells for 2 h. Panning wells were washed x 27 with PBST and phage eluted using 0.2 M Glycine (pH 2.2) for 10 min, neutralised with 1 M Tris-HCl (pH 9.1), then eluted again with 100 mM triethylamine for 6 min, and neutralised with 1 M Tris-HCl (pH 7). Eluted phage were used to infect cultures of ER2738 cells in 2TY medium + 12 µg/ml tetracycline (OD_{600} ca. 0.6) for 1 h at 37 °C, with no shaking.

Phage-infected ER2738 cells were pelleted, re-suspended in 2TY medium, plated onto LB agar carbenicillin (100 µg/ml) and grown overnight at 37 °C. Colonies were counted and cells scraped. Cells were diluted to an OD_{600} of ca. 0.2 in 2TY carbenicillin (100 µg/ml) and incubated for 1 h at 37 °C, 230 rpm. Cultures were infected with M13KO7 helper phage (ca. 1 x 10^{14}/ml) and left for 1 h at 37 °C, 90 rpm, after which kanamycin was added (50 µg/ml) and cells left to grow overnight at 25 °C, 170 rpm. Phage-infected cultures were pelleted and the phage-containing supernatant used in the subsequent panning round. The leftover phage were precipitated using 20% (w/v) polyethylene glycol 8000, 2.5 M NaCl and re-suspended in 320 µl of TE Buffer.

Streptavidin-coated wells were used for the first panning round, followed by streptavidin-coated magnetic beads (Dynabeads®; Life Technologies) and NeutrAvidin-coated wells in the final panning round. An additional fourth panning round was completed for a selection of targets on streptavidin-coated wells; an extra three pre-panning steps were utilised in this panning round. For competitive pans, an additional incubation of target-bound phage with 2.5 µg of non-biotinylated target was performed for 24 h at room temperature before elution.

2.2.6.4 Phage ELISA

ER2738 colonies from final pan plates were grown in 200 µl of 2TY carbenicillin (100 µg/ml) at 37 °C, 1050 rpm for 6 h. 25 µl aliquots were inoculated into 200 µl of 2TY carbenicillin and grown for a further 1 h at 37 °C, 1050 rpm. M13KO helper phage (titre ca. 10^{14}/ml) were diluted 1:1000 in 2TY carbenicillin and 10 µl added per well. After 30 min at room temperature, 450 rpm, kanamycin was added to 50 µg/ml. Cultures were incubated overnight at room temperature, 750 rpm. Cells were then pelleted and the phage-containing supernatant used for the ELISA. The remaining 175 µl of the original cultures were stored at -80 °C in 40% (v/v) glycerol, to be used for DNA minipreps.

Wells of Nunc-Immuno™ Maxisorp™ F96 plates were incubated with 50 µl of 5 µg/ml streptavidin (Molecular Probes® Life Technologies) in PBS at 4 °C overnight. Plates were blocked with Blocking Buffer overnight at 37 °C, washed with PBST, and 50 µl of biotinylated targets (1:1000 in 2X Blocking Buffer) were added to wells for 1 h at room temperature. Negative control wells contained Blocking Buffer only. After washing with PBST, 10 µl of 10X Blocking Buffer and 40 µl of phage-containing supernatant were added to wells. Plates were incubated for 1 h at room temperature, washed x 1 with PBST, and phage detected with Anti-Fd-Bacteriophage-HRP antibody (Seramun Diagnostica GmbH, 1:1000 in Blocking Buffer), 50 µl per well. After a further h at room temperature, plates were washed x 10 with PBST and HRP-conjugated antibody detected using SeramunBlau® fast TMB (Seramun Diagnostica GmbH). Absorbance at 620 nm was read after 3 min and 10 min.

Plasmid DNA of selected Affimer clones was purified for DNA sequencing; phage-infected ER2738 cultures were grown from the glycerol stocks and mini-prepped (see section 2.2.2.7). DNA was sequenced by Genewiz using the sequencing primer detailed in Table 2.10 (section 2.2.2.9).

2.2.7 SH2 specificity phage ELISAs

ELISAs to check specificity of Grb2 SH2 binders for their intended target were conducted as phage ELISAs (see above section), using a 1:20 dilution of purified BAP-tagged SH2 domains for immobilisation (section 2.2.4, automated purification method). Each Affimer clone was tested against all 43 SH2 domains.

2.2.8 Surface Plasmon Resonance

Full-length Grb2 protein was produced from the pET28a vector using the same method as SH2 domain production (section 2.2.4). The protein also contained an N-terminal His-tag and no BAP tag. Grb2 protein samples were further purified and dialysed into SPR Tris Buffer using SEC, which also functioned as a method to separate the Grb2 monomer from the dimer (section 2.2.4.3). Only monomeric fractions were used in surface plasmon resonance (SPR). Experiments were conducted using a BIAcore® 2000 instrument (GE Healthcare) and monitored using BIAcore Control Software (GE Healthcare).

The running buffer used in these experiments was SPR Tris Buffer (section 2.1.6) + 0.01% Tween-20. Amine-coupling chips (sensor chip CM5, GE Healthcare) were used for Grb2 immobilisation; the chip surface consisted of carboxymethylated dextran covalently coupled to a gold surface, which binds molecules covalently via their amine groups. Each chip contained four flow cells, one of which was left un-coupled to Grb2 as a background control (referred to as blank). Binding of protein to an immobilised ligand on these chips is recorded via a change in the refractive index at the surface, and reported in terms of resonance units (RU). For most proteins, 1000 RU = 1 ng of protein bound/mm^2 of flow cell surface.

For immobilisation, flow cells in a CM5 sensor chip were primed with 0.1 M sodium acetate (pH 5.6) and the dextran matrix activated using 0.2 M *N*-(3-dimethylaminopropyl)-*N′*-ethylcarbodiimide hydrochloride (EDC; Sigma-Aldrich), mixed with 0.05 M *N*-Hydroxysuccinimide (NHS); 35 µl at a flow rate of 5 µl/min. Grb2 protein was diluted to 5 µg/ml in 0.1 M sodium acetate (pH 5.5) and immobilised onto flow cells (ca. 600 RU), at a flow rate of 5 µl/min. Excess Grb2 was removed using a high salt wash (1M NaCl) and un-reacted sites on the surface were capped using 1M ethanolamine-HCl, pH 8.5 (Sigma-Aldrich); 35 µl at a flow rate of 5 µl/min. For the blank control, only EDC/NHS activation and ethanolamine-HCl capping was peformed, with no exposure of the surface to Grb2 protein.

To measure binding, Affimer concentrations of 6.25, 12.5, 25, 50, 100, 200 and 400 nM in 0.1 M sodium acetate (pH 5.6) were flowed over the immobilised Grb2 and the blank chip surface, at a flow rate of 80 µl/min for 1 – 3 min. A 1M NaCl wash was used for chip regeneration between measurements. The sensogram

generated by each single run was corrected by subtracting the blank chip response. Binding curves were fitted and the association and dissociation rate constants (k_a and k_d) were calculated using BIAevaluation 3.2 software (GE Healthcare), allowing the determination of the equilibrium dissociation constant (K_D), using the equation $K_D = k_d / k_a$.

2.2.9 Fluorescence polarisation assay

Fluorescence polarisation assays were performed on Grb2-SH2 Affimer clones, to test their competitive binding of the Grb2 SH2 in competition with a fluorescein isothiocyanate-labelled phosphopeptide (FYp); FITC-GABA-S-pY-V-N-V-Q, which was kindly provided by Dr Michael Webb, and synthesised by Dr Katherine Horner (see McAllister et al., 2014 for details on peptide synthesis). All Affimer and Grb2 SH2 samples were dialysed into SPR Tris Buffer prior to use. Assays were set up in 96 well plates and analysed using a Tecan Spark™ 10M microplate reader. Affimer solutions (20 μM) were set up in triplicate and sequentially diluted by a factor of two in SPR Tris Buffer across 12 wells. A fluorescein isothiocyanate-labelled phosphopeptide (FYp) was added to these wells to a final concentration of 20 nM. Grb2 SH2 protein was added to wells to a final concentration of 0.25 μM, the samples were mixed and the fluorescence polarisation measured in each well.

Polarisation values for each Affimer concentration were plotted using a logarithmic scale ($\log_{10}$) for the concentration values, and the resultant sigmoidal curve fitted using the logistic function on Origin 9.1 software. From this fit, half maximal inhibitory values (IC_{50}) values were calculated automatically by Origin.

2.2.10 Immunoprecipitation of Grb2 from U-2 OS cell lysate

U-2 OS cells were washed with ice-cold PBS and lysed in Mammalian Lysis Buffer (50 mM Tris; 150 mM NaCl; 1% (v/v) Nonidet P-40 (Sigma); pH 7.4), for 30 min on ice. Cell debris was pelleted at 13,000 rpm for 10 min and the lysate collected. A bicinchoninic acid (BCA) assay was performed to determine total lysate protein concentration.

In the manual method, 10 μl Amintra Ni-NTA resin (Expedon) was incubated with 250 μg of purified His-tagged Affimer protein in 1X PBS + 10% glycerol for 90 min at 4 °C. Excess Affimer was washed off the resin and 100 μl U-2 OS lysate was incubated with the Affimer-loaded resin overnight at 4 °C. Resin samples

were washed x 3 with Mammalian Lysis Buffer and bound proteins eluted by addition of SDS-PAGE sample buffer (20 µl) and heating to 95 °C for 10 min.

In the automated method, pull-downs were performed on a KingFisher Flex™ robotic platform. His-tagged Affimer proteins were produced in 50 ml BL21 Star™ (DE3) cultures and clarified lysate was obtained after cell lysis and centrifugation to remove cell debris (section 2.2.5.1). Cell lysate (80 µl) was incubated for 10 min with; 25 µl Dynabeads™ His-Tag Isolation & Pulldown; 1X Casein Blocking Buffer (Sigma-Aldrich); in PD Wash Buffer (total volume of 200 µl). Beads were then collected, washed with 1 ml PD Wash Buffer, and incubated for 90 min with U-2 OS lysate (ca. 500 µg – 1 mg) in PD Binding Buffer. The beads were washed a further three times before incubation for 10 min in 50 µl PD His Elution Buffer to elute bound proteins.

Samples were analysed using SDS-PAGE and western blotting, to detect presence of His-tagged Affimer proteins and Grb2. For specific antibody dilutions, see Table 2.3 (section 2.1.5).

2.2.11 Protein microarrays

Protein microarrays were conducted using HA-tagged Affimer reagents (section 2.2.5.2) and BAP-tagged SH2 domain proteins (section 2.2.4.2).

SH2 domain protein samples were diluted to the appropriate concentration in 1X PBS + 20% glycerol and 10 µl samples added to wells in a 384-well microarray plate (Genetix). Samples were added to microplates in a set layout so that identification of each protein in the array was possible after printing. Proteins were spotted onto the surface of streptavidin-coated 3D-functionalized glass slides (PolyAn), using an ArrayJet Marathon™ non-contact printer. The system buffer contained 47% glycerol; 0.06% Triton™ X-100 (Sigma-Aldrich); 0.04% ProClin™ 200 (Sigma-Aldrich); in ddH_2O. Each protein spot consisted of 100 ρl solution, with a typical spot size of 200 µm. Proteins were left to dry onto the surface overnight, in a controlled environment of 18 – 19 °C and 50 – 55% humidity (using the ArrayJet JetMosphere™ system). Buffer-only spots (1X PBS + 20% glycerol) were also printed as negative controls.

After drying, slides were scanned at 532 nm using a GenePix® 4300A scanner (Molecular Devices) to visualise and analyse the printed protein spots for any drying artefacts. Slides were then secured in microarray cassettes which enclosed the arrays in separate wells, allowing an individual Affimer to be

incubated with each array. Slides were blocked with Blocking Buffer 1 (0.1 M Tris-HCl; 50 mM ethanolamine; 0.05% Tween-20; pH 9.0) for 15 min at room temperature, 140 µl/well. Wells were washed x3 with PBST and blocked additionally with Blocking Buffer 2 (2X Casein Blocking Buffer (Sigma-Aldrich); 0.1 M Tris-HCl, pH 8.5) for 30 min at room temperature, 140 µl/well.

After blocking, dilutions of Affimer in Blocking Buffer 2 (70 µl/well) were incubated with the miniarrays for 1 h at room temperature, followed by 3x PBST washes. Bound Affimer was detected using an AlexaFluor™ 647 conjugated HA-tag antibody (see Table 2.3) diluted in Blocking Buffer 2 (70 µl/well), for 1 h at room temperature in the dark. Negative control miniarrays were included on each slide; these controls were incubated with Blocking Buffer 2 and HA-tag antibody only.

Slides were washed x3 with PBST, x1 with 1X PBS and x1 with ddH_2O before centrifugation at 200 *xg* for 5 min to dry. Slides were scanned at 635 nm using a GenePix® 4300A scanner to detect bound HA-tag antibody. Images were analysed using image analysis software GenePix® Pro 7, which automatically detected spots and identified proteins according to the print layout. The local background signal surrounding each spot was also read to enable background correction for each spot. Each miniarray was analysed separately, with the mean fluorescence at 635 nm after subtraction of background fluorescence (F635 – B635) calculated for each SH2 target from the five replicate spots.

For optimisation of the assay, the array design consisted of 14 mini-arrays per slide, with 10 replicates of each SH2 target arranged in columns. The concentrations of SH2 domain targets tested ranged between 10 – 80 µM and the concentrations of Affimer tested ranged between 0.2 – 5 µg/ml. The concentrations of HA-tag antibody tested ranged from 0.1 – 2 µg/ml (1:500 – 1:10,000 dilution in Blocking Buffer 2).

In the final array design, 14 mini-arrays were printed per slide, with five replicates of 41 SH2 targets arranged in columns. The size of each miniarray was 6x6 mm, with a 3 mm gap between each miniarray. The horizontal pitch between spots was 0.254 mm and the vertical pitch 0.254 mm. The final concentrations of proteins used were 70 µM SH2 domain; 5 µg/ml Affimer; and 1 µg/ml HA-tag antibody (1:1000).

For analysis of Affimer binding specificities, the F365 – B635 calculated for each SH2 protein spot against that Affimer clone was averaged over three

experimental repeats. The Affimer was considered to be a positive hit if the signal for the intended target was ≥50x that of the signal for the buffer-only control spot. Cross-reactions to other targets were deemed significant if the signal totalled ≥10% of the intended target signal.

2.2.12 Purified protein ELISA

ELISAs to test binding of HA-tagged Affimer proteins to their BAP-tagged SH2 target were performed. Wells of Nunc-Immuno™ Maxisorp™ F96 plates were incubated with 50 µl of 5 µg/ml streptavidin (Molecular Probes® Life Technologies) in PBS at 4 °C overnight. Plates were blocked with Blocking Buffer overnight at 37 °C, washed with PBST, and 50 µl of 10 µg/ml SH2 protein in Blocking Buffer added per well. For streptavidin only controls, 50 µl of Blocking Buffer only was added.

SH2s were incubated in the wells for 2 h at room temperature, followed by 1 x wash with PBST and incubation with 50 µl of 10 µg/ml Affimer protein in Blocking Buffer, for 1 h at room temperature. Each Affimer was tested against both SH2-containing and streptavidin-only wells. Wells were washed with PBST and incubated with 50 µl HA-tag antibody (Abcam, see Table 2.3), 1:20,000 in Blocking Buffer, for 1 h at room temperature. After 1 x wash with PBST, wells were incubated with 50 µl anti-mouse-HRP antibody (see Table 2.3), 1:10,000 in Blocking Buffer for 1 h at room temperature.

Plates were washed x 6 with PBST and HRP was detected using SeramunBlau® fast TMB (Seramun Diagnostica GmbH). Absorbance at 620 nm was read after 3 min and 10 min, before the reaction was stopped with 1 M H_2SO_4 and the absorbance read again at 450 nm.

2.2.13 Mammalian cell culture

Cell lines used in this study were stored in cryovials in liquid nitrogen, in complete medium and 10% dimethyl sulfoxide (DMSO; Sigma-Aldrich). Cell culture was conducted under sterile conditions in a laminar flow hood to prevent bacterial contamination.

HEK293, Phoenix-AMPHO and U-2 OS cells were cultured in DMEM (high glucose, see section 2.1.8) supplemented with 10% (v/v) foetal bovine serum (FBS; Gibco™) and 1% (v/v) penicillin-streptomycin. MCF-7 cells were cultured in RPMI-1640 medium (see section 2.1.8) supplemented with 10% FBS and 1%

penicillin-streptomycin. Once transduced with Affimer DNA, cells were cultured in growth medium + 10% FBS; with the addition of 1 µg/ml puromycin for stably transfected cell lines. Antibiotic-free growth medium was used in all assays. Cultures were maintained in angle neck 75 cm^2 flasks with vented caps, at 37 °C with 5% CO_2.

2.2.13.1 Thawing cell lines

Cells were taken from liquid nitrogen stores and thawed at 37°C in a water bath. Once the contents of the cryovial had thawed (2 – 3 min), this was added to a 25 cm^2 flask containing 5 ml pre-warmed growth medium. Cells were incubated at 37 °C for 1 – 2 days to allow attachment to the flask and passaged once ca. 70% confluent.

2.2.13.2 Passaging cells

Cells were passaged once 70 – 80% confluent. Growth medium and 0.05% trypsin-EDTA were pre-warmed at 37 °C. Cells were washed x2 with DPBS and incubated with 2 ml trypsin-EDTA at 37 °C for 5 min to detach cells. Trypsin was neutralised by addition of 10 ml growth medium, and cells pelleted by centrifugation at 1500 rpm for 5 min. Pelleted cells were re-suspended in growth medium and cell solution was distributed to new flasks, or used to seed 6-well or 24-well plates, and incubated once more at 37 °C, 5% CO_2.

For counting cells, a 10 µl sample of cell solution was added to 10 µl Trypan Blue (Corning) and the sample applied to a Countess™ Cell Counting Chamber Slide and counted using a Countess™ II Automated Cell Counter.

2.2.14 Production of cell lines transiently expressing His-tagged Affimer proteins

Affimer DNA was amplified from the pBSTG phagemid vector using Affimer pcDNA primers (Table 2.2) in a Phusion polymerase PCR; with the modification of a 60 °C annealing temperature (section 2.2.2.1), and digested with *BamHI* and *NotI*. The DNA fragment was ligated into the similarly digested pcDNA5 vector (Thermo Fisher Scientific catalog no. V601020). Plasmid DNA was purified and sent for DNA sequencing to confirm successful insertion of Affimer DNA.

HEK293 cells were seeded in 6-well plates at 1 x 10^5 cells/ml in DMEM + 10% FBS and incubated overnight (to be ca. 60% confluent at time of transfection).

Purified Affimer-pcDNA5 plasmid DNA (2.4 µg) was mixed with 5 µl Lipofectamine® 2000 transfection reagent in a total volume of 140 µl Opti-MEM™ for 20 min at room temperature. Growth medium on the plated HEK293 cells was replaced with Opti-MEM™ and the DNA transfection mixture added to wells. Cells were incubated with DNA and transfection reagent for 18 h overnight before medium was replaced with DMEM + 10% FBS. After 48 h, the relevant assay was performed on transfected cells. Successful expression of Affimer proteins were confirmed by SDS-PAGE and western blot analysis of cell lysates to detect the His-tag. For antibody dilutions, see Table 2.3.

2.2.15 Production of cell lines stably expressing DD-tagged Affimer proteins

Affimer DNA was amplified from the pBSTG phagemid vector using Affimer pRetroX primers (Table 2.2) in a KOD polymerase PCR (section 2.2.2.1) and digested with *BglII* and *NcoI*. The DNA fragment was ligated into the similarly digested puromycin-resistant retroviral vector pRetroX-PTuner (ClonTech, Takara). Plasmid DNA was purified and sent for DNA sequencing to confirm successful subcloning of Affimer DNA.

For the addition of a helical linker between the Affimer and destabilisation domain (DD) sequences, a QuikChange-style linear amplification reaction (section 2.2.2.2) was performed, using the Affimer-pRetroX-PTuner plasmid DNA as the template and the following primers:

Forward primer sequence (5' – 3')	GGAAGCTGCCGCCAAGGAGGCCGCTGCTAAGGCCGCTG CCCCGCGGCCGCAGATCTCTG
Reverse primer sequence (5' – 3')	CCTCCTTGGCGGCAGCTTCCTTGGCAGCGGCCTCGGCCA GTTCCGGTTTTAGAAGCTCCAC

Plasmid DNA was purified after the amplification reaction and successful insertion of the helical linker sequence confirmed by DNA sequencing.

Phoenix-AMPHO cells in 25 cm^2 flasks (ca. 70% confluent) were transduced with 2 µg of purified Affimer-pRetroX plasmid DNA, using 8 µl TransIT®-293 Transfection Reagent (Mirus) in 4 ml serum-free DMEM. After 72 h, virus-containing supernatant was collected, filtered through a 0.45 µm membrane and used to transduce viral DNA into U-2 OS cells (ca. 50% confluent). Viral

supernatant supplemented with 8µg/ml Polybrene (Sigma-Aldrich) was incubated with U-2 OS cells for 6 h. Supernatant was replaced with serum-free DMEM and after 48 h, cells were selected for successful transduction using DMEM + 10% FBS supplemented with 2 µg/ml puromycin.

After selection, successful stabilisation of Affimer proteins conjugated to the DD was tested by addition of Shield1™ ligand (Takara) to the growth medium. Cells were seeded 1.25 x 10^5 in 6-well plates in DMEM + 10% FBS and left to grow for 36 h. Shield1™ concentrations of 50 nM – 1 µM were added to wells for 4 h. Cells were washed with ice-cold 1X PBS and lysed with 100 µl Mammalian Lysis Buffer. Lysates were analysed using SDS-PAGE and western blotting to confirm expression of DD-tagged Affimer proteins. For antibody dilutions, see Table 2.3.

2.2.16 Production of cell lines stably expressing His-tagged Affimer proteins

Affimer DNA was amplified from the pET11a vector using the Affimer pBABE primers (Table 2.2) in a KOD polymerase PCR; with the modification of a 68 °C annealing temperature (section 2.2.2.1), and digested with *BamHI* and *SalI*. The DNA fragment was ligated into the similarly digested puromycin-resistant retroviral vector pBABE-puro (Addgene catalog no. 1764). Plasmid DNA was purified and sent for DNA sequencing to confirm successful insertion of Affimer DNA.

Phoenix-AMPHO cells in 25 cm^2 flasks (ca. 70% confluent) were transduced with 2 µg of purified Affimer-pBABE plasmid DNA, using 8 µl TransIT®-293 Transfection Reagent (Mirus) in serum-free DMEM. After 72 h, virus-containing supernatant was collected, filtered through a 0.45 µm membrane and used to transduce viral DNA into U-2 OS or MCF-7 cells (ca. 50% confluent). Viral supernatant supplemented with 8µg/ml Polybrene (Sigma-Aldrich) was incubated with cells for 6 h. Supernatant was replaced with serum-free medium and after 48 h, cells were selected for successful transduction using medium + 10% FBS supplemented with 2 µg/ml puromycin.

After selection, cells seeded in 75 cm^2 flasks were washed with ice-cold 1X PBS and lysed with 1 ml Mammalian Lysis Buffer. Lysates were analysed using SDS-PAGE and western blotting to confirm expression of His-tagged Affimer proteins. For antibody dilutions, see Table 2.3.

2.2.17 SiRNA knockdown in mammalian cell lines

Short interfering (si) RNA pools were purchased from Dharmacon (GE Healthcare) for gene silencing of both GRB2 (encoding Grb2 protein) and PLCG1 (encoding PLCγ1 protein). RNA sequences in each pool are detailed below in Table 2.11. As controls, siGENOME Non-Targeting siRNA Control Pools #1 and #2 (Dharmacon, referred to as NT1 and NT2) were used. In addition, knockdown of Polo-like Kinase 1 (PLK1) was performed in every experiment using siGENOME SMARTpool Human PLK1 (Dharmacon), to confirm successful siRNA transfection by induction of apoptosis.

SiRNA stock solutions (2 µM in 1X siRNA Buffer, see section 2.1.6) were added to duplicate wells in 6-well plates (50 µl/well). Lipofectamine^{TM} RNAiMAX transfection reagent (2.5 µl/well) was mixed with Opti-MEM^{TM} (350 µl/well) and incubated for 5 min at room temperature. This mix was then added to all siRNA-containing wells in the 6-well plates (350 µl/well), and in addition a negative control well not containing siRNA. Transfection reagent was incubated with siRNA for 20 min at room temperature, with mixing.

Table 2.11. SiRNA sequences used for knock down of specific genes encoding proteins of interest.

Target	siRNA pool	Target sequences
Human GRB2	siGENOME SMARTpool Human GRB2 (2885) siRNA, 5 nmol	**1:** UGAAUGAGCUGGUGGAUUA **2:** CGCCAAAUAUGACUUCAAA **3:** GAACGAAGAAUGUGAUCAG **4:** GUACAAGGCAGAGCUUAAU
Human PLCG1	siGENOME SMARTpool Human PLCG1 (5335) siRNA5, nmol	**1:** CCAACCAGCUUAAGAGGAA **2:** GAAGUGAACAUGUGGAUCA **3:** GAGCAGUGCCUUUGAAGAA **4:** CCAAGAAGGACUCGGGUCA

Cells to be transfected were trypsinised, counted, and diluted in antibiotic-free growth medium to 5 x 10^4 cells/ml. This cell solution was added to each well on the 6-well plates, 1.6 ml/well. Plates were left at room temperature for 1 h before being placed back at 37 °C, 5% CO_2 for 72 h. In each experiment, non-targeting and PLK1 siRNA control wells were also used.

2.2.18 Erk phosphorylation assays

Once cell lines transiently or stably expressing Affimer proteins were established, cells were subjected to assays measuring Erk phosphorylation after EGF stimulation. Erk phosphorylation assays were conducted in each cell line as below.

2.2.18.1 Erk phosphorylation assay on transiently transfected HEK293 cells

HEK293 cells transiently expressing His-tagged Affimer proteins from the pcDNA vector were plated at 1 x 10^5/ml in 6-well plates during transfection (section 2.2.14). Cells incubated with transfection reagents, but no Affimer DNA, were used as controls. Forty-eight h post-transfection, medium in wells was replaced with serum-free medium for 90 min, before addition of human EGF (25 ng/ml). Plates were incubated at 37 °C for 10 min.

Medium was removed and cells washed with ice-cold DPBS, before scraping into 50 µl Mammalian Lysis Buffer and incubating on ice for 10 min. Lysate samples were centrifuged at 13,000 rpm for 10 min to pellet cell debris, before total protein concentrations for each sample were determined. Samples were analysed by SDS-PAGE and western blot to quantitate total Erk, phospho-Erk, Affimer protein, and Grb2 (section 2.2.3), with an equal quantity of total protein loaded per well (for antibody dilutions, see Table 2.3, section 2.1.5).

2.2.18.2 Erk phosphorylation assay on stably transduced U-2 OS cells expressing DD-tagged Affimer proteins

For U-2 OS cells stably expressing DD-tagged Affimer proteins from the pRetroX-PTuner vector, cells were plated in 6-well plates at 7.5 x 10^4 cells/ml in DMEM + 10% FBS containing Shield1™ concentrations of 0, 50, 100, 200 and 500 nM to induce protein stabilisation. As Shield1™ is supplied in 100% ethanol, ethanol was added to the medium so that the total volume was the same for all concentrations.

Cells were incubated at 37 °C, 5% CO_2 overnight (16 h) after plating. Medium in wells was then replaced with serum-free medium supplemented with Shield1™ concentrations as before. After 90 min, human EGF was added to wells to a final concentration of 25 ng/ml and plates were incubated at 37 °C for 5 min. Cells were harvested, lysed and samples subject to SDS-PAGE and western blot

analysis as above for the transiently transfected HEK293 cells; except that the DD-tag rather than the His-tag was used for detection of Affimer proteins (see Table 2.3, section 2.1.5).

2.2.18.3 Erk phosphorylation assay on stably transduced cells expressing His-tagged Affimer proteins

U-2 OS cells stably expressing His-tagged Affimer proteins from the pBABE vector were plated in 6-well plates at 5 x 10^4 cells/ml, in DMEM + 10% FBS. MCF-7 cells stably expressing His-tagged Affimer proteins were plated at 2 x 10^5 cells/ml in RPMI-1640 medium. For these cell lines, wild-type cells not transduced with Affimer DNA were used as controls.

All cells were incubated at 37 °C, 5% CO_2 for 36 h after plating. Medium in wells was then replaced with serum-free medium for 90 min before addition of human EGF; 25 ng/ml for U-2 OS and 100 ng/ml for MCF-7s. As multiple timepoints of EGF stimulation were being tested (0, 5 and 30 min), EGF was added to wells at different times so that all wells on a plate could be harvested at the same time. Plates were incubated at 37 °C after addition of EGF. Cells were harvested, lysed and subject to SDS-PAGE and western blot analysis as above for the transiently transfected HEK293 cells.

2.2.19 Co-immunoprecipitation of co-expressed Affimer and Grb2 proteins from mammalian cell lysate

For HEK293 and U-2 OS cells expressing His-tagged Affimer proteins, co-immunoprecipitation assays were also performed to confirm the binding of Affimer reagents to Grb2. Cells were seeded in 6-well plates, EGF-stimulated and lysates were prepared as before (see section 2.2.18.1 and 2.2.18.2), with cells lysed in a volume of 100 µl Mammalian Lysis Buffer rather than 50 µl. Lysate from non-stimulated cells were also prepared for each Affimer clone, in addition to wild-type cell controls.

Co-immunoprecipitation was performed on a KingFisher Flex™ robotic platform. Mammalian cell lysate (100 µl) was incubated for 90 min with; 25 µl Dynabeads™ His-Tag Isolation & Pulldown; 0.5X Casein Blocking Buffer (Sigma-Aldrich); in PD Binding Buffer (200 µl final volume). Beads were collected and washed three times with 300 µl PD Wash Buffer. Proteins were eluted by incubation for 10 min in 30 µl PD His Elution Buffer. Samples were analysed using SDS-PAGE and

western blotting, to detect presence of His-tagged Affimer proteins and Grb2. For specific antibody dilutions, see Table 2.3 (section 2.1.5).

For U-2 OS cells stably expressing DD-tagged Affimer proteins, co-immunoprecipitation assays were also performed on lysates. The assay was conducted as above, with the modification of capturing Grb2 from the lysate instead of the Affimer proteins. Grb2 was captured using a recombinantly expressed Affimer which binds the N-terminal SH3 domain, termed N-D7. Affimer N-D7 was produced in 50 ml BL21 Star™ (DE3) cultures and clarified lysate was obtained after cell lysis and centrifugation to remove cell debris (section 2.2.5.1).

N-D7 lysate (80 µl) was incubated for 10 min with; 25 µl Dynabeads™ His-Tag Isolation & Pulldown; 1X Casein Blocking Buffer (Sigma-Aldrich); in PD Wash Buffer (total volume of 200 µl). Beads were then collected, washed with 1 ml PD Wash Buffer, and incubated for 90 min with the Affimer-expressing U-2 OS lysate (500 µl) in PD Binding Buffer. The beads were washed a further three times before incubation for 10 min in 50 µl PD His Elution Buffer to elute bound proteins. Samples were subject to SDS-PAGE and western blot analysis to determine the presence of Grb2 and the DD-tagged Affimer proteins (see Table 2.3, section 2.1.5 for antibody dilutions).

2.2.20 Immunofluorescent imaging of cell lines

Cells were plated in 24-well plates onto glass coverslips coated with 0.01% Poly-L-lysine (Sigma-Aldrich). Seeding densities for each cell line were the same as detailed in section 2.2.18, with 1 ml cell solution plated per well. U2-OS cells stably expressing His-tagged Affimer proteins were additionally stimulated with EGF (25 ng/ml) for imaging; this was conducted as in section 2.2.18.3, but with all reagent volumes halved. Cells were not lysed after EGF stimulation.

Cells were washed with DPBS for 2 min, before incubation with 4% paraformaldehyde for 15 min. After 1 x PBS wash, 0.1% Triton X-100 (Sigma-Aldrich) in 1X PBS was added for 5 min. Cells were washed with PBS again and blocked for 10 min with 1% milk (diluted in 1X PBS). After a PBS wash, primary antibody solution to detect His-tagged Affimer and Grb2 proteins (antibodies diluted in 1% milk solution, see Table 2.3 for dilutions) was incubated with cells for 1 h at room temperature. Cells were washed x 3 with PBS and incubated with fluorescently-labelled secondary antibodies (see Table 2.3) in 1% milk solution,

plus Hoechst 33342 (1:1000) to stain cell nuclei. Secondary antibodies were incubated with cells in the dark for 1 h at room temperature. Cells were washed x 3 with PBS before mounting of the stained coverslips onto glass slides using ProLong™ Diamond Antifade Mountant. Slides were left to dry at room temperature overnight in the dark, before storing at 4 °C. Immunofluorescent images were taken using a Nikon Eclipse Ts2R-FL inverted microscope and analysed using NIS-Elements software (Nikon).

Chapter 3

Characterisation of Grb2 SH2-binding Affimer reagents

Chapter 3

Characterisation of Grb2 SH2-binding Affimer reagents

3.1 Introduction

Growth factor receptor-bound protein 2 (Grb2) is an SH2-containing adaptor protein, ubiquitously expressed and critical in several signalling pathways including those that become dysregulated in disease (Morlacchi et al., 2014). The Grb2 SH2 domain is flanked by two SH3 domains and links activated membrane receptors to intracellular signalling proteins (Grebien et al., 2011). Numerous processes such as cell division, cell motility and angiogenesis depend upon Grb2 activity; this has led to the protein being studied abundantly in cancer research, and has highlighted it as a possible drug target (Morlacchi et al., 2014). The Grb2 SH2 interacts with its ligands via binding to the phosphotyrosine-containing motif pY-X-N-X; where pY is the phosphotyrosine, N is asparagine and X is any residue (Giubellino et al., 2008 , Papaioannou et al., 2016). Through this binding of its SH2 domain, Grb2 associates with pY residues on the cytoplasmic portion of activated growth factor receptors, such as EGFR (Wong et al., 1999, Sorkin et al., 2000), FGFR-3 (Kanai et al., 1997) and VEGFR-3 (Salameh et al., 2005). The Grb2 SH3 domains then recruit Son of Sevenless 1 (Sos1) to membrane-bound Ras, which activates Ras through GDP-GTP exchange. Activation of Ras initiates the mitogen-activated protein kinase (MAPK) cascade (Tari and Lopez-Berestein, 2001). The stimulated MAPKs Erk1 and 2 translocate to the nucleus and trigger gene expression through phosphorylation of transcription factors such as Myc. This in turn initiates cellular processes including proliferation, differentiation and survival; key events that are aberrant in cancer (see Figure 3.1) (Dharmawardana et al., 2006).

In parallel to the MAPK pathway Grb2 can also mediate the PI3K/Akt pathway, through binding of the C-terminal SH3 domain to proline-rich sequences within Grb2-associated binders Gab1 or Gab2 (Belov and Mohammadi, 2013). Gab1 and 2 are also adaptor proteins that bind to PI3K and initiate the PI3K/Akt signalling cascade, which regulates cell proliferation and survival (Liu et al., 2009). This pathway can also be activated directly by Ras (Ijaz et al., 2018) (see Figure 3.1).

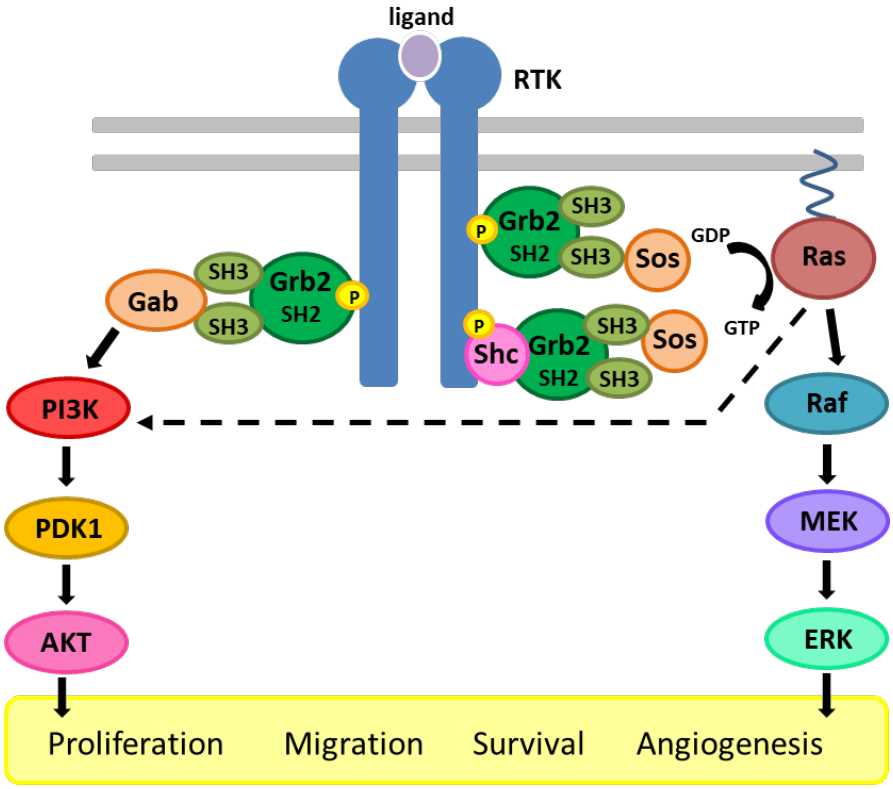

Figure 3.1. Simplified schematic of MAPK and PI3K pathway activation by Grb2. *Binding of growth factors to their respective receptors (such as EGF to the EGFR) causes autophosphorylation of tyrosine residues on the cytoplasmic tail of the receptor (depicted as a yellow circle labelled with P). This creates a docking site for the SH2 domain of Grb2, which recruits Sos1 to the membrane via its SH3 domains. Alternatively, the Grb2 SH2 binds the receptor indirectly through proteins such as Shc. Sos1 is then able to activate membrane-bound Ras, stimulating the release of GDP from Ras in exchange for GTP. The active Ras-GTP complex triggers the MAPK cascade, which leads to phosphorylation of the MAPKs Erk1/2. Additionally, receptor-bound Grb2 can associate with Gab proteins via its SH3 domains, which initiates the PI3K/Akt pathway, leading to the phosphorylation and activation of Akt. Both Erk1/2 and Akt can then initiates various cellular processes through regulation of transcription factors and gene expression.*

Additionally, Grb2 has been shown to associate indirectly with activated receptors through other proteins including Cbl, SHP-1 and Shc, as well as associating with cytoplasmic proteins such as Src and Bcr-Abl (jaz et al., 2018). Through these associations, Grb2 regulates numerous cellular pathways.

Grb2 exists in an equilibrium between the monomeric and dimeric forms, with a recent study highlighting that only the monomeric form of Grb2 is relevant to oncogenic signalling (Ahmed et al., 2015). This work demonstrated that only monomeric Grb2 is capable of binding to Sos1 and upregulating MAPK

signalling, and that the dimer is inhibitory to this process. Dimer dissociation was initiated by phosphorylation of tyrosine 160 (Y160) on Grb2, or binding of the SH2 domain to a pY-containing ligand. This self-dissociation mediated by the SH2 domain therefore acts as a switch for regulation of MAPK signalling and hence cancer progression (Ahmed et al., 2015).

Inhibitors of the Grb2 SH2 domain have shown promising results in decreasing cell motility, angiogenesis and metastasis in cellular and animal models of cancer (Soriano et al., 2004, Giubellino et al., 2007, Hsiao et al., 2013). Gay et al. (1999) used a peptidomimetic Grb2 SH2 inhibitor, CGP78850, to demonstrate that inhibition of Grb2 SH2 prevents hepatocyte growth factor (HGF)-induced cell motility in the epidermoid carcinoma cell line A-431, through the blocking of cytoskeletal rearrangements needed for this process. Two non-hydrolyzable phosphotyrosyl mimetics termed C60 and C126 were synthesised by Gao et al. (2000) as Grb2 SH2 domain inhibitors. C60 and C126 exhibited anti-angiogenic properties in *in vitro* assays (Soriano et al., 2004), and B16-F1 murine melanoma cells pre-treated with C60 also showed inhibition of cell migration and metastasis when implanted as xenografts in nude mice (Giubellino et al., 2007).

Although these reports establish the therapeutic potential of Grb2 SH2 inhibitors in cancer treatment, the compounds have not been taken into preclinical trials, with the exception of a limited study on C60 (Morlacchi et al., 2014). As metastasis in general is still poorly understood at a molecular level (Giubellino et al., 2007), studying the interactions involved in metastatic pathways, such as those regulated by the Grb2 SH2, would benefit our understanding of metastasis and aid the process of developing treatments.

Affimer reagents binding to the Grb2 SH2 domain were used in proof-of-principle studies to determine the suitability of the Affimer as a SH2 domain research reagents. The Grb2 SH2 was chosen as a target due to its extensive characterisation in contrast with many other SH2 domains (Machida and Mayer, 2005, Kraskouskaya et al., 2013). This would allow a direct comparison of Grb2 SH2 Affimer binders with previously isolated inhibitors and binding reagents. Additionally, the knowledge of Grb2 SH2-mediated pathways would allow specific endpoints to be measured in functional cell-based assays; such as phosphorylation of known downstream targets of Grb2.

3.2 Production of Grb2 SH2-binding Affimer and recombinant Grb2 proteins

3.2.1 Isolation and production of Grb2 SH2 Affimer reagents

Affimer reagents that bound the Grb2 SH2 domain had previously been isolated by the Tomlinson group via phage display screening of the Affimer Type II phage library (Tiede et al., 2014, Tiede et al., 2017; see Chapter 1, section 5.3). Forty-eight clones from the final pan had been randomly selected and tested using phage ELISA. Clones were also tested for binding to SH2 domains of other Grb family members (Figure 3.2A). All binding clones showed specificity for the Grb2 SH2 and were analysed by DNA sequencing, with 30 unique clones identified (data not shown).

Sixteen of those binders were selected to be taken forward for further characterisation in this project, based on a combination of factors: the frequency they occurred in the sequenced population, their absorbance signal in the phage ELISA, and the sequence of their variable regions (VRs) because as much variation as possible was desired in the sequence of clones. A sequence alignment of the VRs of all 16 Affimer clones can be seen in Figure 3.2B, revealing a consensus sequence of B-X-Y-X-N-Hy-X-X-P (where B is a basic residue; Hy is a hydrophobic residue; X is any amino acid, see abbreviations page for amino acid code). This consensus was present in the first VR for 13 of the 16 clones, but also found in the second VR in three clones. Residues 3 - 6 of this consensus corresponds to the native Grb2 SH2 binding motif of pY-X-N-X, (Papaioannou et al., 2016, Nioche et al., 2002). Indeed, 10 of the 16 Affimer clones contained this native sequence (with a non-phosphorylated tyrosine) in one of their variable regions. Five other binders contained the motif with an alternative aromatic residue replacing Y. Binder F5 was the only clone not to contain a similar sequence to this motif.

All Affimer-encoding sequences had previously been subcloned into the pET11a expression vector, with the exception of clones 8; 12; B5; F5; F1 and D6. These were therefore subcloned into pET11a from the pBSTG phagemid vector for production (Chapter 2, section 2.2.2.1). Affimer proteins with a C-terminal 8x histidine (His) tag were produced from the pET11a vector, in 50 ml cultures of

A

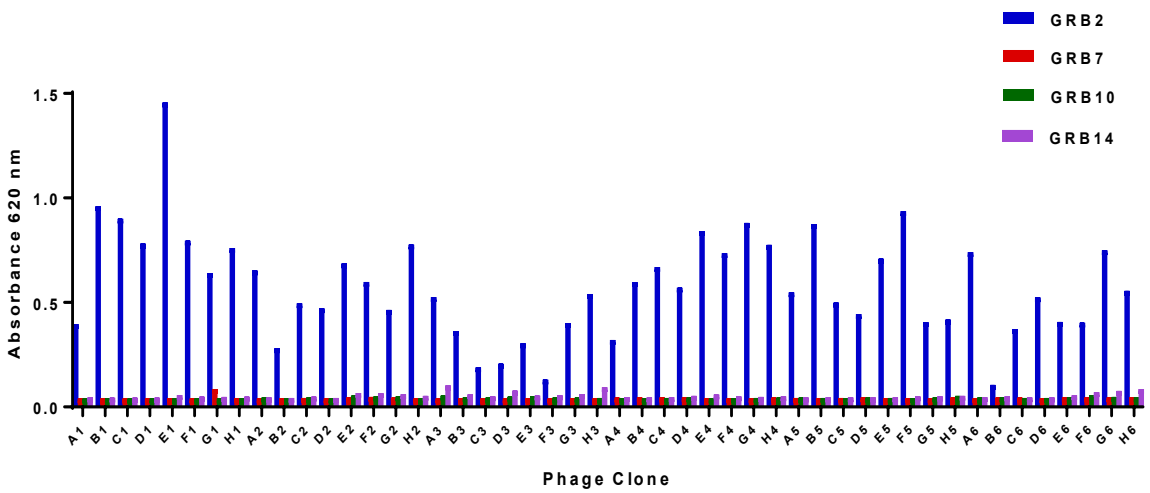

B

AFFIMER	VR 1	VR 2
D2	D-P-K-K-**Y**-V-**N**-V	N-P-V-D-K-F-D-K-I
F1	R-W-**Y**-V-**N**-V-S-L-P	D-N-M-D-N-M-N-K-I
H4	R-W-**Y**-V-**N**-I-K-F-P	N-W-T-E-F-N-S-K-T
C2	Q-W-**Y**-V-**N**-T-M-S-P	E-V-Y-H-I-K-N-K-R
12	F-Q-P-I-**Y**-I-**N**-I-V	P-D-E-P-R-Y-V-L-G
D6	P-W-**Y**-Q-**N**-V-P-Y-P	R-E-E-R-N-M-N-A-M
B4	K-W-**Y**-Q-**N**-V-M-F-P	E-S-I-D-Y-P-D-H-E
D1	K-W-**Y**-M-**N**-T-M-F-P	E-P-G-R-F-N-E-M-L
D5	F-S-H-A-**Y**-M-**N**-V-V	V-G-G-G-G-N
C1	R-H-**W**-V-**N**-V-P-F-P	G-D-G-**F**-D-**N**-A-L-H
H1	R-K-L-**W**-E-**N**-Y-K-E	A-M-R-M-Y-Y-P-E-W
A4	H-V-L-**W**-E-**N**-A-G-P	H-T-R-Y-E-Y-F-V-Y
8	Q-W-S-**W**-Q-**N**-A-V-D	V-R-P-R-G-L-F-W-D
F5	D-W-W-E-A-G-V-F-M	W-N-E-I-N-Y-M-F-D
A6	H-E-Y-P-M-H-Q-H-N	P-L-**F**-M-**N**-V-P-L-P
B5	N-K-E-Q-R-H-W-S-E	F-Q-**Y**-V-**N**-W-P-V-P
Cons.	**B**-X-**Y**-X-**N**-**Hy**-X-X-**P**	

Figure 3.2. Isolation of Grb2 SH2-binding Affimer reagents. ***(A)*** *Phage ELISA results from Grb2 SH2 Affimer library screen (Tiede et al., 2017). Phage clones were incubated in wells containing immobilised Grb2 SH2 and bound phage were detected with anti-phage-HRP antibody after washing. HRP substrate TMB was added and absorbance read at 620 nm after 3 min, for 48 clones. Binding to SH2 domains of family members Grb7, Grb10 and Grb14 was also tested.* ***(B)*** *Alignment of variable regions (VRs) of sixteen Grb2 SH2-binding Affimer clones. Alignment was performed using MacVector 13.5.2. A consensus sequence can be seen in VR1 as follows; Basic residue (B) – X – Tyrosine – X – Asparagine – Hydrophobic residue (Hy) – X – X – Proline, where X is any amino acid. Residues that resemble the native Grb2 SH2 binding motif of pY-X-N-X are in bold, including motifs where the Y residue is replaced with another aromatic residue.*

BL21 Star™ (DE3) *E. coli* cells by IPTG-induction at 30 °C overnight (Chapter 2, section 2.2.5). Three clones; A4, B5 and D5, gave lower yields than desired. For these, conditions were optimised to 400 ml cultures and a lower temperature of 20 °C overnight. It is not clear why these clones gave poorer yields, as Affimer sequences have been codon optimised for production in *E. coli* (Tiede et al., 2014). Additionally, they differed from the other Grb2 SH2 Affimer clones only in the variable regions, and even these sequences were similar to other clones. Only Affimer D5 differed significantly, containing a truncated second VR (6 amino acids) followed by a scaffold truncation of 4 amino acids, which could account for poor protein stability.

Affimer proteins were purified from lysates using nickel affinity chromatography and dialysed into appropriate buffers for future assays; either 1X PBS + 10% glycerol for pull-down assays, or SPR Tris Buffer for surface plasmon resonance and fluorescence polarisation assays. After dialysis the absorbance at 280 nm (A_{280}) of each elution was measured and protein concentrations were calculated from these values using the Beer-Lambert Law (molar extinction coefficients were determined using ExPASy ProtParam software).

Total yields for this set of Affimer reagents typically ranged between 1.5 – 10 mg per 50 ml culture, and 5 – 8 mg for the three clones produced in 400 ml cultures. SDS-PAGE analysis of dialysed proteins determined that purity of binders was sufficient for further assays (Figure 3.3A). All Affimer proteins appeared at the expected molecular weight (MW) of 12 - 13 kDa, with the exception of D5 which was seen at ca. 24 kDa (theoretical MWs calculated using ExPASy ProtParam software). This indicated possible formation of a stable dimer by this binder; which could be mediated by the previously mentioned truncated VR and scaffold region that differed from other clones.

3.2.2 Recombinant Grb2 production and purification

Both the isolated SH2 domain of Grb2 and the full-length protein were recombinantly produced and purified for use in characterisation assays *in vitro*. pET28 vectors encoding Grb2 sequences with an N-terminal 6xHis-tag were purchased from the Pawson Lab (Samuel Lunenfeld Research Institute, Canada). His-tagged Grb2 proteins were firstly produced in BL21 Star™ (DE3)

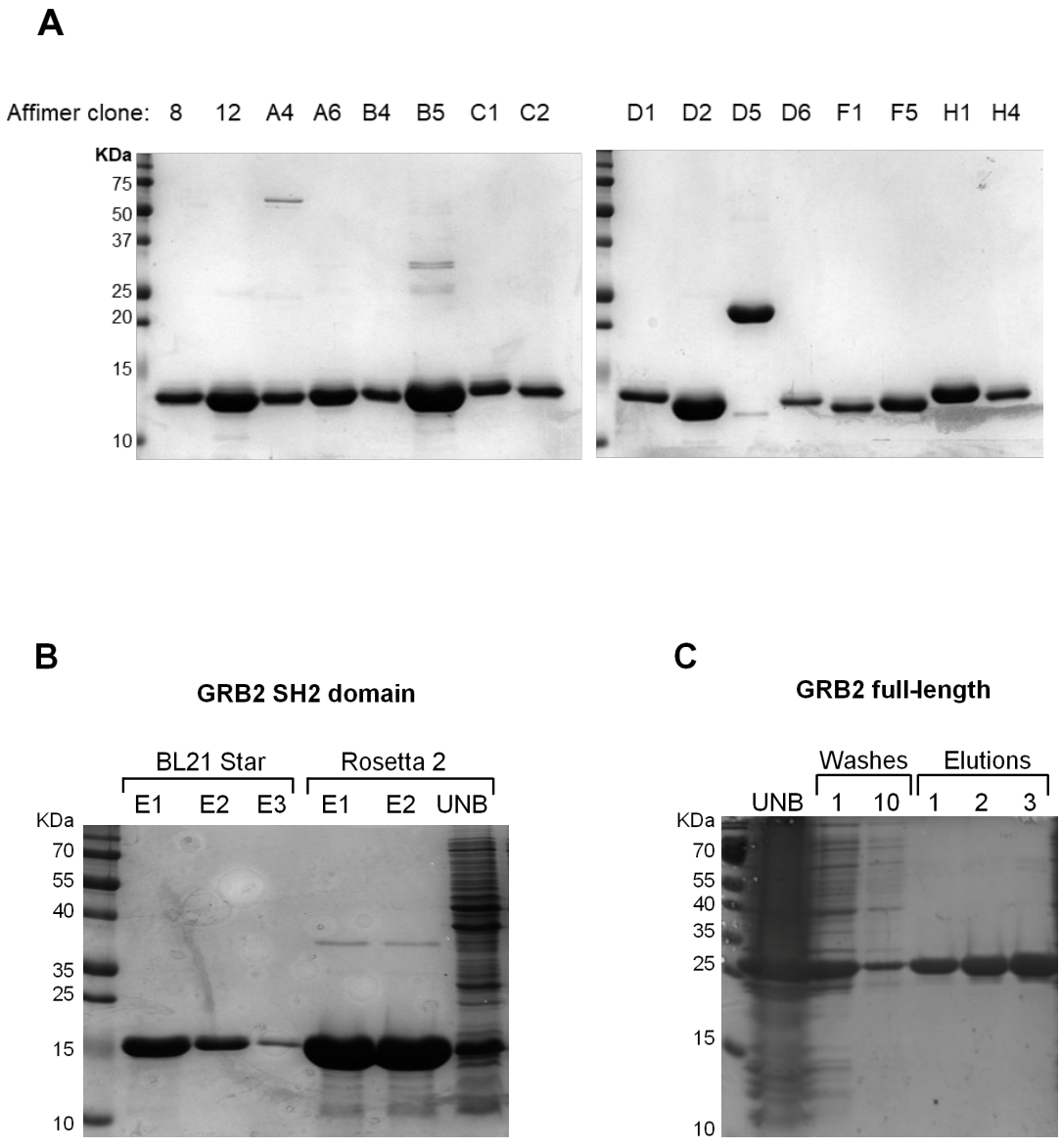

Figure 3.3. Production of Grb2 SH2-binding Affimer and Grb2 proteins. *(**A**) SDS-PAGE analysis of purified Grb2-SH2 Affimer proteins. Ni-NTA purified proteins were dialysed into PBS + 10 % glycerol prior to electrophoresis. MW of Affimer proteins ranged from ca. 12 – 13 kDa. Analysis showed possible dimerisation of binder D5 (ca. 24 kDa). **(B)** SDS-PAGE analysis of recombinantly produced Grb2 SH2 domain. Ni-NTA purified elution fractions (denoted by E) are shown both BL21 Star™ (DE3) and Rosetta™ 2 (DE3) E. coli. Unbound protein fraction (UNB) was also run for the Rosetta™ 2 (DE3) production, to observe whether a sufficient quantity of Ni-NTA resin was used. The SH2 domain can be visualised at the expected MW of ca. 16 kDa. **(C)** SDS-PAGE analysis of recombinantly produced full-length Grb2 protein from Rosetta™ 2 (DE3) E. coli. Unbound protein fraction (UNB), wash fractions and Ni-NTA purified elution fractions are shown. Grb2 can be visualised at ca. 30 kDa, as expected. All gels depicted contain 15% acrylamide.*

E. coli, but later optimised in Rosetta™ 2 (DE3) *E. coli*, as a higher yield was obtained from this strain (Chapter 2, section 2.2.4). The Rosetta™ 2 (DE3) strain is a BL21 derivative, designed to enhance the production of eukaryotic proteins that contain codons rarely used in *E. coli*. Rosetta™ cells supply tRNAs for rare codons on a chloramphenicol-resistant plasmid.

Expression was induced using IPTG in 400 ml cultures overnight at 18 °C. Proteins were purified from lysate using nickel affinity chromatography and total protein yields of 5.32 mg and 6.83 mg were achieved for the SH2 and full-length protein, respectively. Eluted fractions analysed by SDS-PAGE showed protein bands at the expected MW of ca. 16 kDa for Grb2 SH2 (Figure 3.3B) and ca. 30 kDa for Grb2 (Figure 3.3C) (based on theoretical MWs calculated using ExPASy ProtParam software). Protein concentrations were calculated using the Beer-Lambert law by measuring A_{280} of elution fractions. Molar extinction coefficients were calculated as 15470 $M^{-1}cm^{-1}$ for the SH2 domain and 39545 $M^{-1}cm^{-1}$ for the full length protein.

As Grb2 and its SH2 domain are known to form dimers in solution (McDonald et al., 2008), an attempt was made to separate the monomeric species from the dimeric by size exclusion chromatography (SEC). This separation was desired due to the indication that only the monomeric form of Grb2 is relevant to oncogenic signalling, as discussed in the introduction of this chapter (Ahmed et al., 2015). As well as separation of monomeric and dimeric species, SEC allowed buffer exchange from Elution Buffer to the SPR Tris Buffer. Issues relating to successful monomer and dimer separation of Grb2 will be detailed in the discussion of this chapter.

For the SH2 domain, two peaks were seen in the A_{280} elution trace as expected, at elution volumes of 63.5 ml and 76.4 ml (see Figure 3.4A). As SEC separates molecules on the basis of size, with larger molecules eluting quicker than smaller ones, these peaks were thought to correspond to the dimeric and monomeric species, respectively. However no molecular weight markers were run for comparison, so it was not possible to definitively conclude this. For the Grb2 full-length protein, two species were also seen as indicated by two peaks in A_{280} trace at 152 ml and 177 ml (data not shown). Full-length Grb2 fractions were then analysed by SDS-PAGE without denaturation of the sample (no heating or

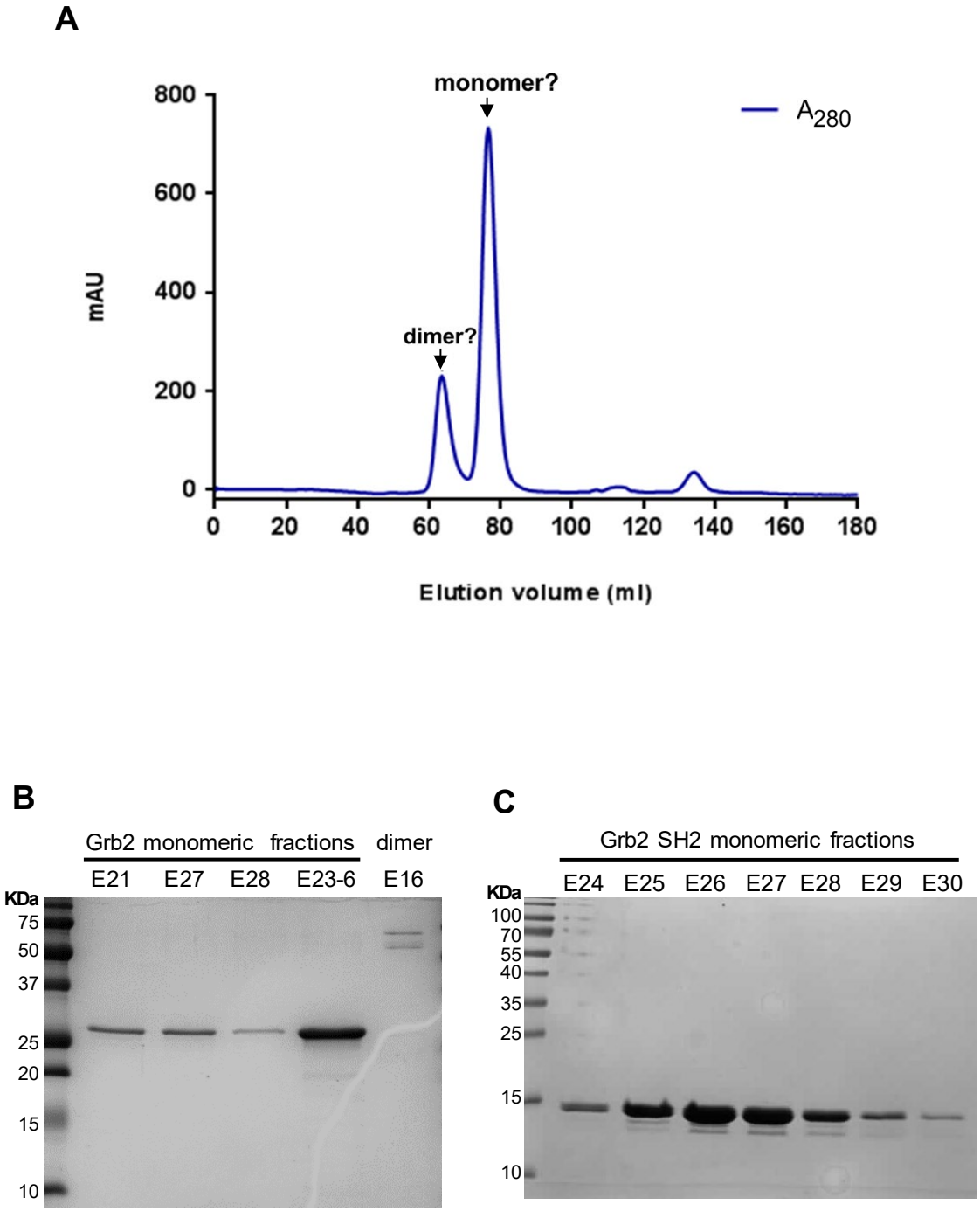

Figure 3.4. Size exclusion chromatography of purified Grb2 proteins. ***(A)*** *Chromatogram from size exclusion chromatography (SEC) for the Grb2 SH2 domain, showing absorbance at 280 nm. Ni-NTA purified elution fractions were subject to SEC to separate monomeric and dimeric species. Two peaks in A_{280} can be visualised, thought to correspond to the dimeric and monomeric proteins (labelled). Fractions were subject to SDS-PAGE without sample denaturation on 15% acrylamide gels. Monomeric fractions were visualised at the expected MW of ca. 30 kDa for the full-length Grb2* ***(B)*** *and ca. 16 kDa for the SH2 domain* ***(C)****. E23-26 for full length Grb2 = pooled and concentrated fractions 23-26. Dimer (E16) = dimeric fraction (MW ca. 60 kDa).*

addition of β-mercaptoethanol), to determine whether the MWs of the two samples corresponded to the monomeric and dimeric proteins. Four fractions appearing to be monomeric (E23 – 26), which covered an elution volume of 170.5 – 182.5 ml, were pooled and concentrated before analysis (Figure 3.4B). Un-concentrated monomeric fractions (E21, E27, E28) and a dimeric fraction from the first peak (E16; 150 - 153 ml) were analysed for comparison. The dimer was seen at the expected MW of ca. 60 kDa, with an additional protein band at a higher MW ca. 70 kDa. Monomeric fractions were sufficiently pure and bands were seen at the expected MW of ca. 30 kDa. For the SH2 domain, seven fractions appearing to be monomeric (E24 – E30) which covered an elution volume of 71.71 ml – 83.71 ml, were also analysed for purity (Figure 3.4C). These showed bands slightly lower than the expected MW for the Grb2 SH2 domain (16 kDa) at ca. 14 – 15 kDa.

3.3 Grb2 SH2 Affimer reagents bind Grb2 with nanomolar affinity

Determining the binding affinity of Affimer clones for Grb2 was important for predicting their efficacy as research reagents, in comparison with antibodies and other engineered protein scaffolds. Interactions of SH2 domains with their native ligands are generally in the low nanomolar range (Pawson and Gish, 1992); therefore if Affimer reagents were to compete with these for the Grb2 SH2 in intracellular assays, high binding affinities were needed.

Surface plasmon resonance (SPR) is a label-free detection method which is a well validated platform for measuring biomolecular interactions with high sensitivity (Nguyen et al., 2015). This method eliminates the need for molecular labels, which can cause steric hindrance or change protein structure; thus affecting the affinity of the labelled protein for its binding partner. To estimate the binding affinities of Grb2 SH2 Affimer binders for their target, six of the 16 Affimer clones were used in SPR; 8, A4, B5, F1, F5 and H1. These clones were taken forward due to their high production yields or their VR sequences. A mixture of clones were chosen that contained the Y-X-N motif in the first VR (F1), in the second VR (B5), or a W in place of the Y (8, A4, H1), or neither of these motifs (F5), to see if affinities varied dramatically between different clones. SPR was conducted using full-length His-tagged Grb2 protein. Grb2 was immobilised on

CM5 sensor chips using amine coupling and Affimer concentrations ranging between 6.25 nM - 400 nM were tested for each clone. A flow cell with an activated and capped surface, but no immobilised Grb2, was used as a control for subtracting any background binding by Affimer proteins (see Chapter 2, section 2.2.8 for more detail). All Affimer clones tested showed binding to Grb2, in accordance with phage ELISAs.

Binding curves were fitted using BiaEvaluation 3.2 software and mean K_D values calculated for each clone from the concentration range. Values ranged from 11.8 nM – 35.3 nM (see Figure 3.5), showing binders A4 and F5 to have the highest affinity for Grb2. As can be seen in Figure 3.5, the dissociation curves did not follow the 1:1 Langmuir binding model used for fitting.

Poor fitting of the dissociation phase can be caused by several factors; such as a multivalent analyte, or surface effects like mass transport and re-binding of the analyte to the surface (Edwards et al., 1995, Glaser, 1993). The effect of mass transport should have been minimal in these experiments, as a high flow rate (80 µl/min) and a low surface Grb2 density (ca. 600 RUs immobilised) were used. This could therefore be due to a multivalent analyte; the binding model used for fitting assumes a 1:1 stoichiometry, which may not be the case for this Affimer-Grb2 interaction. Additionally, if the Affimer proteins had formed dimers or multimers in solution (creating a heterogenous analyte sample) this would also have the seen effect on curve fitting. An extra SEC purification step to ensure isolation of monomeric Affimer proteins could be used in future to reduce this possibility, as was performed for the Grb2 protein samples.

Although the curve fitting was inadequate for highly accurate measurements of the K_D values, this data gave an estimated range of low nanomolar affinity for these clones. To gain more precise measurements, SPR could be repeated with SEC-purified Affimer proteins, using immobilisation of the Affimer protein on the surface and Grb2 as the analyte. Alternatively, isothermal titration calorimetry (ITC) could be implemented to determine the stoichiometry of the binding interaction if it is not a 1:1 ratio.

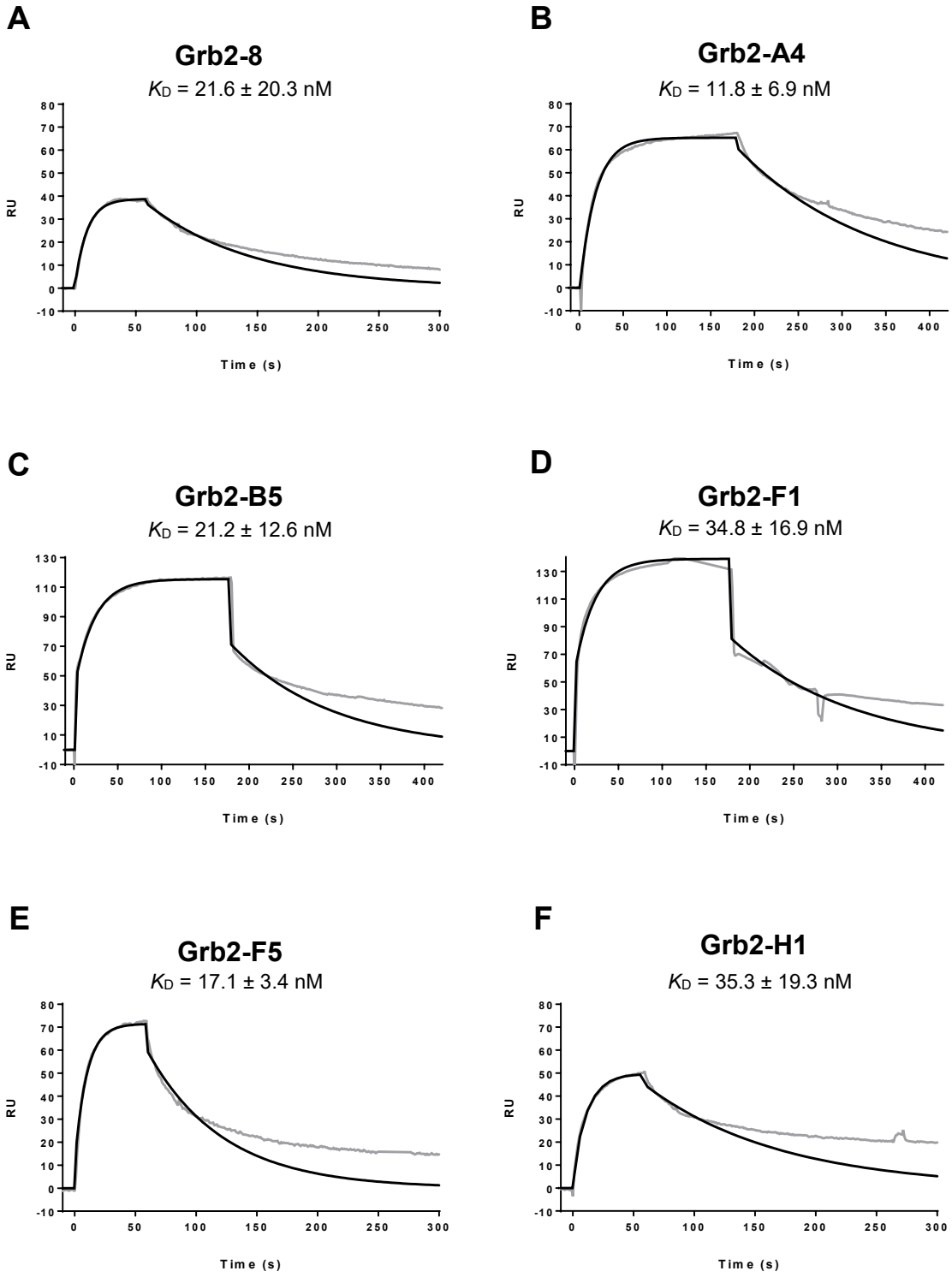

Figure 3.5. Grb2 SH2-binding Affimer reagents show high binding affinity for their target. *SPR traces for six Grb2 SH2 Affimer clones; 8* ***(A)****, A4* ***(B)****, B5* ***(C)****, F1* ***(D)****, F5* ***(E)*** *and H1* ***(F)****. Traces shown in grey for 100 nM Affimer bound to full-length immobilised Grb2 (RU = response units, subtracted from control cell curve). Binding curves were fitted using the 1:1 Langmuir binding model (shown in black). Injection time varied from 60 – 180 seconds for different Affimer clones. All graphs show 240 seconds dissociation phase.* K_D *values were calculated using a concentration range of 6.25 – 400 nM Affimer and show mean ± SD.*

3.4 Grb2 SH2 Affimer reagents capture endogenous Grb2 from U2-OS cell lysate

Next, an immunoprecipitation assay was performed to test the ability of all 16 Affimer clones to capture endogenous target protein from cell lysate (Chapter 2, section 2.2.10). Endogenous protein was chosen over precipitation of recombinant target, as this would accurately test a potential application of these Affimers as co-immunoprecipitation reagents. Endogenous protein is also present at lower concentrations than recombinantly expressed target and would therefore be a more stringent test of the binding capabilities of the reagents. Additionally this assay would confirm binding of all Affimer reagents to the Grb2 SH2 domain in its native conformation, within the full-length protein. Lysate containing endogenous levels of Grb2 was prepared from U2-OS (human osteosarcoma) cells. The first attempted method of pull-down utilised Amintra Ni-NTA resin, loaded with Affimer and incubated with cell lysate overnight at 4 °C. A yeast-SUMO binding Affimer (YS-10) (Tiede et al., 2014) was used as a negative control, as well as Ni-NTA resin only. After washing, resin-bound protein samples were analysed by western blot to verify pull-down of endogenous Grb2 from the lysate by Affimer binders. Although no band for Grb2 was seen in the YS-10 Affimer control, a faint band for Grb2 (at the expected MW of ca. 25 kDa) could be seen in the resin-only negative control (Figure 3.6A). This indicated non-specific binding of Grb2 to the Ni-NTA resin.

To resolve this issue, the assay was repeated using magnetic His-tag isolation and pull-down Dynabeads™ on a KingFisher Flex robotic platform (Tiede et al. 2017). Western blot analysis of this method showed that all but two Grb2 SH2 Affimer samples contained detectable levels of Grb2 (ca. 25 kDa), whereas the YS-10 and resin-only controls did not (Figure 3.6B). Detection of His-tagged proteins showed sufficient loading of the beads with Affimer (band at ca. 12 kDa). This signified the successful binding and pull-down of endogenous Grb2 from cell lysate by Grb2 SH2 Affimer binders.

Binders that consistently recovered a greater quantity of Grb2 over all experimental repeats included clones 8, A4, D5 and H4. Interestingly, although binder F5 pulled down the highest levels of Grb2 when using Ni-NTA resin for capture, it was inconsistent at pulling out any detectable Grb2 when using the His-Tag Dynabeads™ on the KingFisher Flex robotic platform. Affimer clones A6

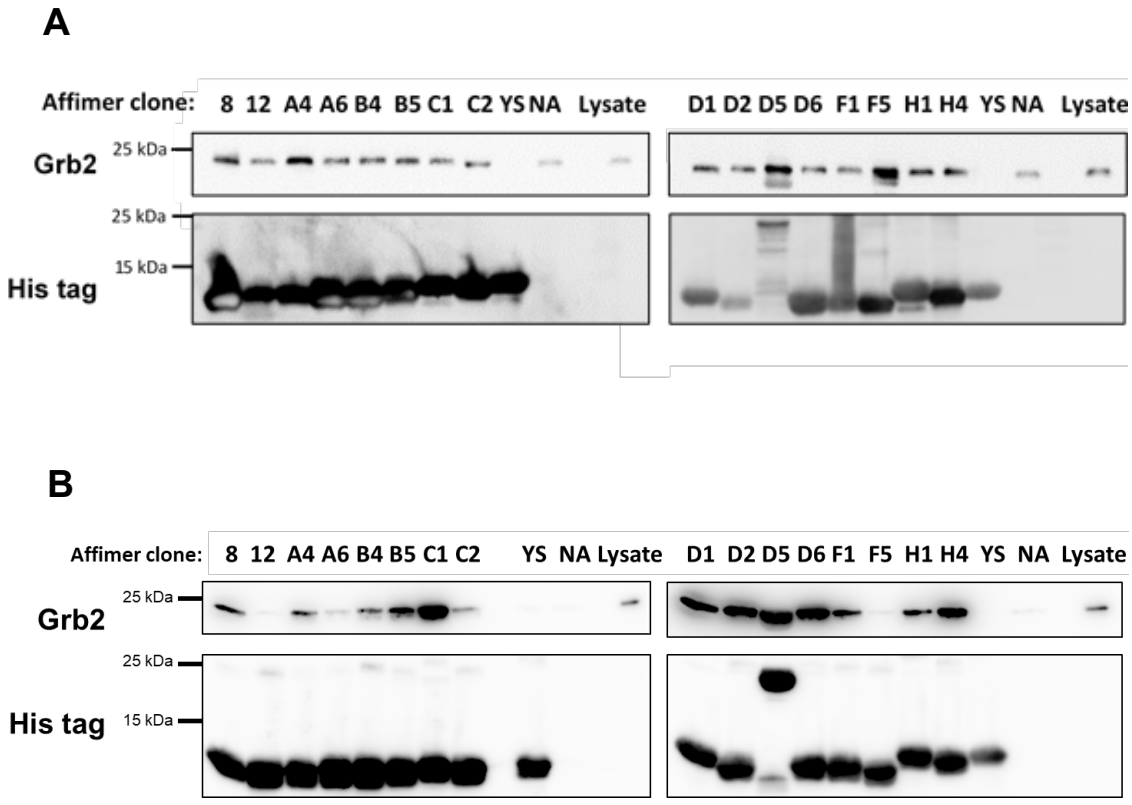

Figure 3.6. Western blots showing pull-down of endogenous Grb2 from cell lysate by Grb2 SH2 Affimer reagents. *Immunoprecipitation of endogenous Grb2 from U2-OS cell lysate, by Grb2 SH2 Affimer proteins bound to* ***(A)*** *Ni-NTA resin or* ***(B)*** *His-Tag Dynabeads™. After washing, proteins were eluted from beads and subject to western blotting to detect Grb2 (ca. 25 kDa) and His-tagged Affimer binders (ca. 12 kDa). HRP-conjugated antibodies detected using Luminata™ Forte chemiluminescent HRP substrate. Lysate = lysate not incubated with beads as a positive control for Grb2 (20 µg total protein). YS = ySUMO-binding Affimer, used as a negative control. NA = beads incubated with lysate but no Affimer. Western blots are representative of 5 experimental repeats.*

and C2 also captured much lower amounts than previously seen with the Ni-NTA resin repeats, and Affimer 12 failed to pull out Grb2 in this method. This could be due to the more stringent washing steps in the automated method. The level of Grb2 captured from lysate did not appear to correlate with Affimer expression levels or their capture on the beads, as can be seen from the His-tag western blots.

These results did not correlate completely with binding affinity data from SPR; in particular the inconsistent results seen with F5 in this assay, which had demonstrated reproducible binding to Grb2 in SPR experiments. Binder A4 showed robust pull-down of Grb2, which was consistent with this clone having one of the highest binding affinities. Other clones tested in SPR (8, B5, F1 and H1) also showed reliable capture of Grb2.

3.5 Grb2 SH2 Affimer reagents competitively bind the SH2 domain

To determine whether the Grb2 SH2 Affimer binders could compete for the pY binding site of the Grb2 SH2 domain, a fluorescence polarisation assay was performed (McAllister et al., 2014). This assay measured the displacement of a fluorescein (FITC)-conjugated Grb2 SH2-binding phosphopeptide, FITC-GABA-S-pY-V-N-V-Q (referred to as FYp; Figure 3.7A), from the binding site by the Affimer proteins (Chapter 2, section 2.2.9).

Fluorescence polarisation was calculated automatically on a Tecan Spark^{TM} 10M microplate reader, using the ratio of parallel and perpendicular polarised light emitted by the FYp (see Figure 3.7B). A Grb2 SH2 binding curve with the FYp was plotted to confirm binding of the SH2 domain to the peptide (Figure 3.8A). A binding curve was also plotted for the full-length Grb2 protein as a comparison. EC_{50} values of 206 ± 18 nM and 239 ± 13 nM were calculated from these curves for the SH2 domain and full protein, respectively.

Using the binding curves shown in Figure 3.8A, estimated K_D values of 155 ± 6 nM and and 118 ± 12 nM were calculated for the FYp with Grb2 and Grb2 SH2, respectively. These values were similar to those reported by McAllister et al. (2014) for the monomeric full-length Grb2 and Grb2 SH2 species, but much lower than the K_D value they recorded for the SH2 dimer of 4.8 ± 1.2 μM. This indicated

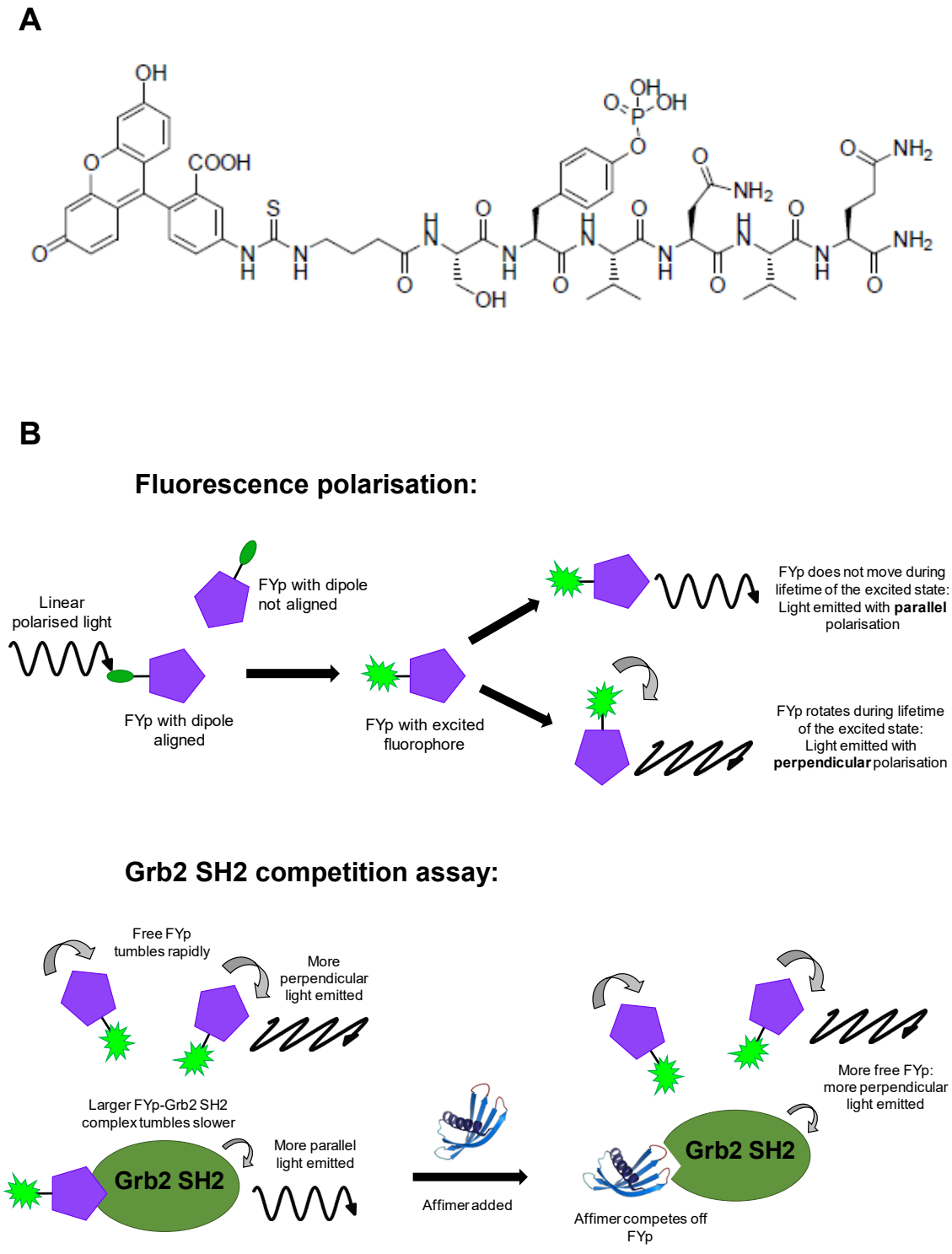

Figure 3.7. Fluorescence polarisation assay to measure competitive inhibition of the Grb2 SH2 domain by Affimer reagents. ***(A)*** *FITC-labelled Grb2 SH2 phosphopeptide ligand (FYp) used in the fluorescence polarisation competition assay. Chemical formula =* $C_{56}H_{68}N_{11}O_{19}PS$*, MW = 1262.25 Da. (McAllister et al., 2014)* ***(B)*** *Schematic of fluorescence polarisation and the assay designed to test the ability of Affimer binders to compete for the phosphopeptide-binding pocket of the Grb2 SH2 domain. FYp = peptide depicted in* ***(A)****.*

A

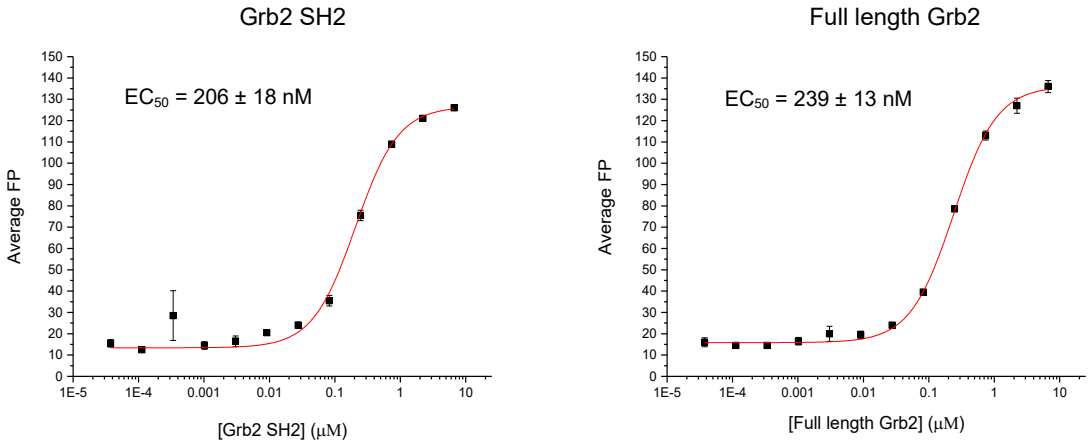

B

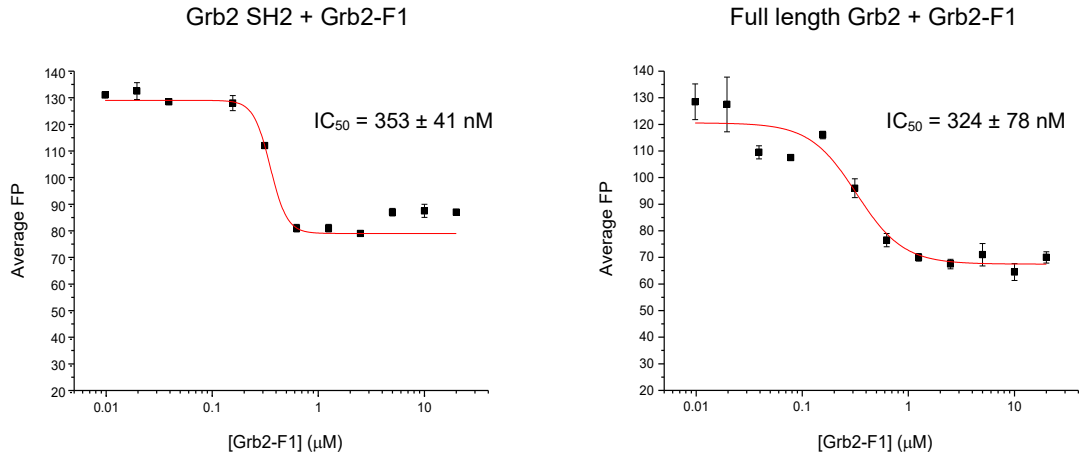

Figure 3.8. Optimisation of a fluorescence polarisation competition assay for the Grb2 SH2 domain. ***(A)*** *Fluorescence polarisation (FP) was used as a measure of binding between the FYp and Grb2 SH2, as well as full-length Grb2. Fluorescent polarisation was plotted for Grb2 protein concentrations of 37.6 pM - 6.66μM ([FYp] = 20nM) and* EC_{50} *values calculated. Data shown as mean ± SEM of replicates from two experimental repeats.* ***(B)*** *Competitive inhibition of the Grb2 SH2 and full-length Grb2 protein by Grb2 SH2 Affimer F1. Serial dilutions of Affimer ranging from 0.01 μM – 20 μM were set up in triplicate and the fluorescent polarisation measured in each well ([FYp] = 20nM; [Grb2 SH2] = 0.25μM). Data shown as mean ± SEM of replicates from one experimental repeat.*

that the protein samples contained mostly the monomeric species, and any dimerisation that had occurred after SEC had not had a significant effect on the affinity of Grb2 for its substrates; and thus on the results of these experiments.

Optimisation of competitive inhibition by Affimer proteins was then carried out using binders F1 and H1, to determine the optimal concentration range of Affimer for calculating the half maximal inhibitory concentration (IC_{50}). These two clones were selected because they had been confirmed to bind Grb2 via both SPR and pull-down, and had high production yields. Interestingly, Affimer F1 never showed full inhibition of FYp binding by the Grb2 SH2. This binder was also tested for competing for the full-length protein to compare any differences in IC50s (Figure 3.8B), showing IC_{50} values of 353 ± 41 nM and 324 ± 78 nM for F1 with the SH2 domain and full-length protein, respectively. This showed the ability of the Affimer to compete with the FYp for the full length Grb2 with similar potency as the isolated SH2 domain.

In further assays testing all 16 Affimer clones, the isolated Grb2 SH2 domain protein was used, at 0.25 μM final concentration. This concentration had shown ~ 80% of the maximum change in polarisation of FYp (Arkin et al., 2004). A final Affimer concentration range of 0.01 μM – 20 μM was used.

A dose-dependent decrease in fluorescence polarisation was seen for all Affimer binders, indicating displacement of the FYp from the Grb2 SH2 domain. Binding curves were plotted using these data (Figure 3.9, n = 3) and IC_{50} values calculated for each binder. IC_{50}s ranged from 270.9 nM – 2.32 mM, with the majority between 1 – 2 μM and suggested that F1, A4 and D5 were the most potent inhibitors (Table 3.1).

Table 3.1. IC_{50} values of Grb2 SH2 Affimer binders. *Binders ranked from best competitive inhibitor to worst. IC_{50} values were calculated from Affimer titration curves using a Logistic fit on OriginPro 9.1.*

Affimer	IC_{50} (μM)
F1	**0.27** ± 0.02
A4	**0.77** ± 0.06
D5	**0.80** ± 0.08
F5	**1.16** ± 0.15
D6	**1.22** ± 0.07
8	**1.42** ± 0.05
B5	**1.43** ± 0.04
B4	**1.49** ± 0.25
D1	**1.93** ± 0.09
H1	**1.98** ± 0.14
D2	**2.04** ± 0.13
C1	**2.34** ± 0.11
H4	**2.63** ± 0.09
12	**2.67** ± 0.61
C2	**4.49** ± 0.78
A6	**2317.67** ± 24607.08

GRB2-8
IC_{50} = 1.42 μM
± 0.05

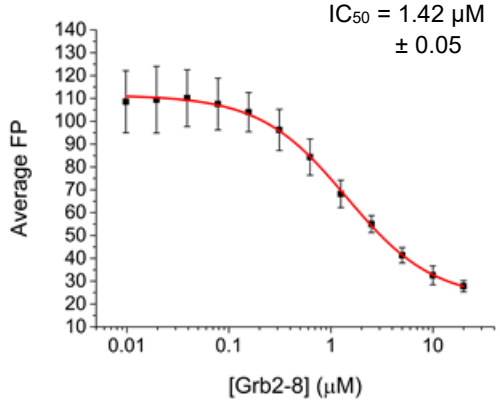

GRB2-12
IC_{50} = 2.67 μM
± 0.61

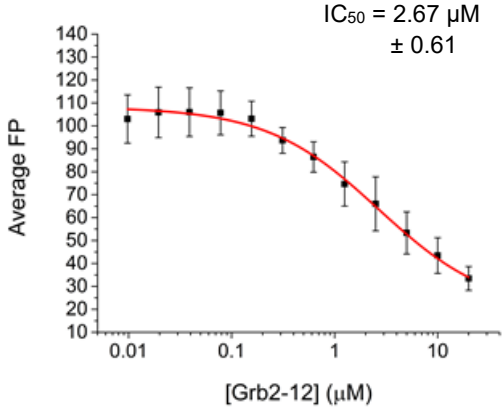

GRB2-A4
IC_{50} = 0.77 μM
± 0.06

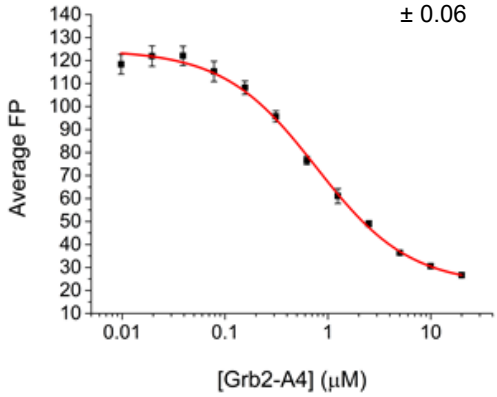

GRB2-A6
IC_{50} = 2.32 mM
± 24.61

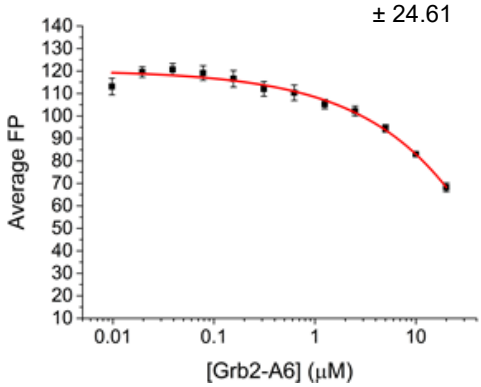

GRB2-B4
IC_{50} = 1.49 μM
± 0.25

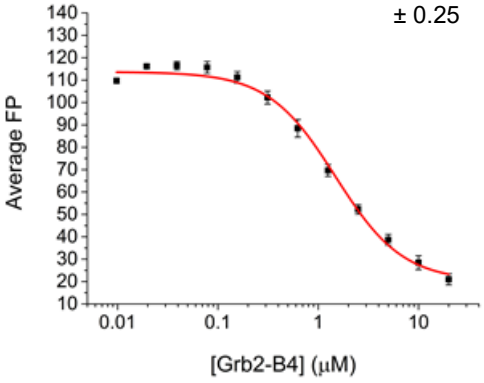

GRB2-B5
IC_{50} = 1.43 μM
± 0.04

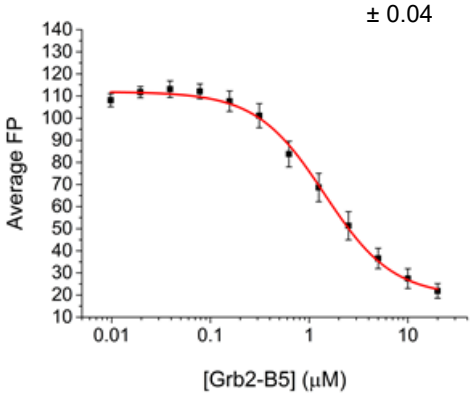

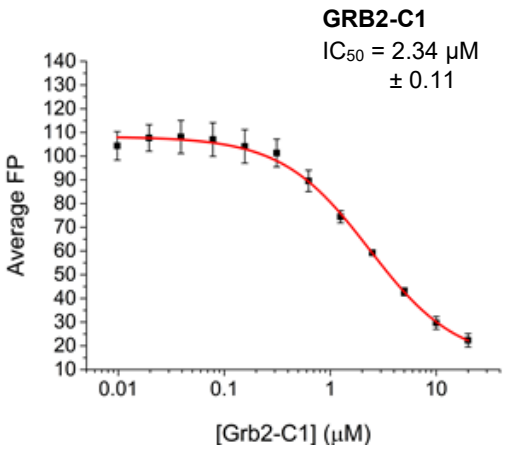
GRB2-C1
IC50 = 2.34 µM
± 0.11
Average FP
[Grb2-C1] (µM)

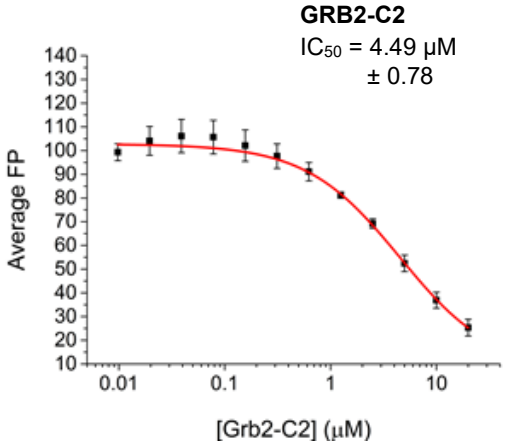
GRB2-C2
IC50 = 4.49 µM
± 0.78
Average FP
[Grb2-C2] (µM)

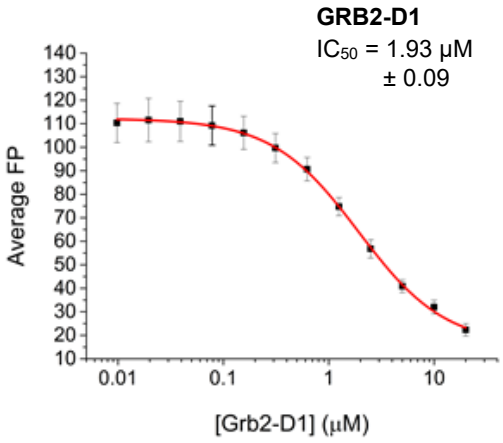
GRB2-D1
IC50 = 1.93 µM
± 0.09
Average FP
[Grb2-D1] (µM)

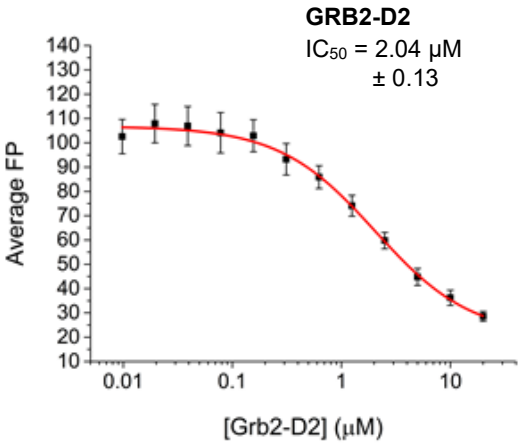
GRB2-D2
IC50 = 2.04 µM
± 0.13
Average FP
[Grb2-D2] (µM)

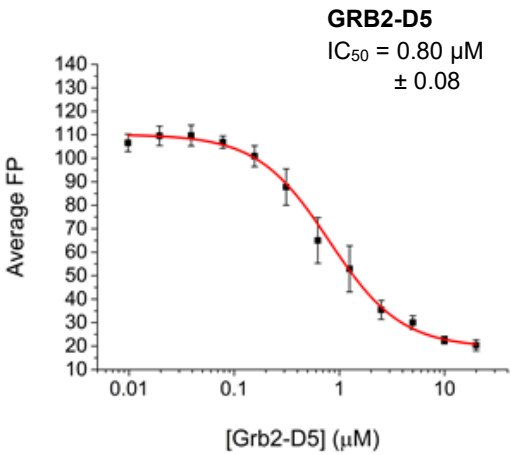
GRB2-D5
IC50 = 0.80 µM
± 0.08
Average FP
[Grb2-D5] (µM)

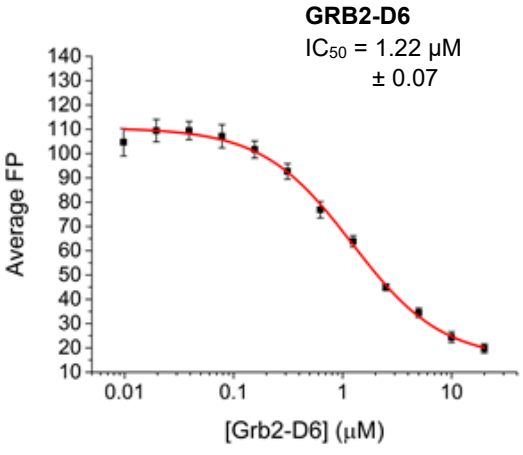
GRB2-D6
IC50 = 1.22 µM
± 0.07
Average FP
[Grb2-D6] (µM)

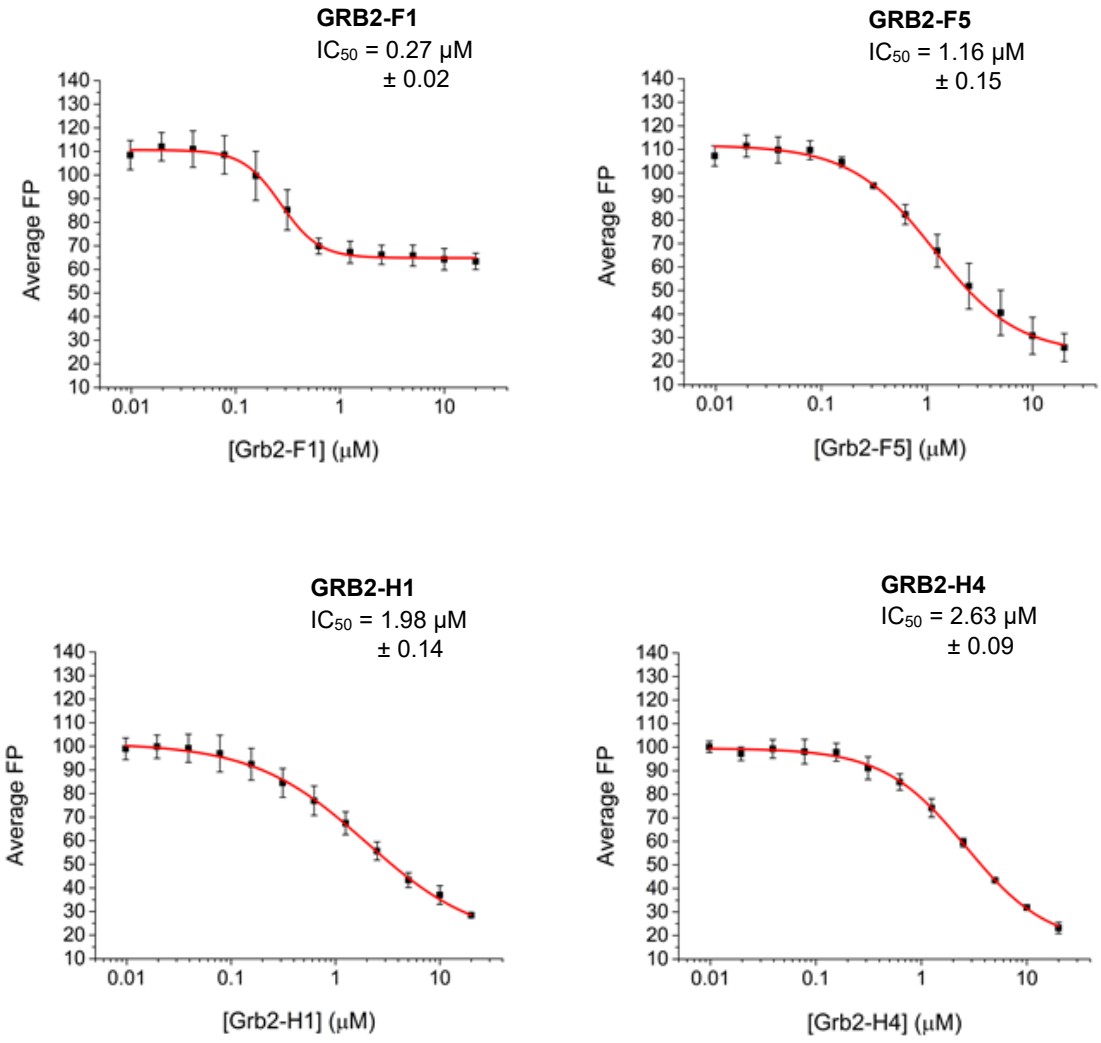

Figure 3.9. Grb2 SH2 Affimer reagents compete with a Grb2 SH2-binding phosphopeptide for the binding site of the SH2 domain. *Competitive inhibition of the Grb2 SH2 protein by 16 Grb2 SH2-binding Affimer proteins. Fluorescence polarisation (FP) was used as a measure of binding between the Grb2 SH2 and a FITC-labelled phosphopeptide ligand (FYp). Disruption of this interaction by Affime proteinrs was measured as a decrease in fluorescence polarisation. Serial dilutions of Affimer were incubated with Grb2 SH2 and FYp; concentrations were set up in triplicate and ranged from 0.01 µM – 20 µM. [FYp] = 20nM; [Grb2 SH2] = 0.25µM. Binding curves were then plotted to calculate IC_{50} of each Affimer. All IC_{50}s were calculated using OriginPro 9.1, using a logistic fit of sigmoidal curves. Data shown as mean ± SEM of three independent experiments.*

For the majority of clones, the binding curve did not plateau at the highest Affimer concentration tested. This will have affected accurate measurement of IC_{50} values; however, the main purpose of this assay was to rank the Affimer clones in their ability to inhibit the SH2 domain binding site, for selection of clones to take forward in cell-based inhibition assays. The data were therefore deemed sufficient for this purpose, as it was still possible to visualise the most potent inhibitors with this concentration range.

3.6 Specificity of Grb2 SH2 Affimer reagents for their target

To further test the specificity of the Grb2 SH2 Affimer clones, a phage ELISA was performed to check the binding of each Affimer to 43 different SH2 domains (see Appendix B). The SH2 domains were recombinantly produced with N-terminal 6x His-tag and biotin acceptor peptide (BAP) sequences; the latter is biotinylated *in vivo*, removing the need for chemical biotinylation (Beckett et al., 1999). This BAP sequence (G-L-N-D-I-F-E-A-Q-K-I-E-W-H-E) was cloned on to the N-terminus of the SH2 sequences encoded in pET28 vectors, before the His-tag sequence, using a QuikChange-style reaction (see Chapter 2, section 2.2.2.2).

Purified SH2 proteins were subjected to western blot analysis to confirm biotinylation (Figure 3.10). Biotinylated proteins were observed at the expected MWs for all SH2 domains. For the majority, this was ca. 17 – 20 kDa (theoretical MWs ranged from 17.3 – 21.1 kDa as calculated by ExPASy ProtParam). The PLCγ1 and 2 tandem SH2s (labelled PLCG1T and PLCG2T) have MWs of ca. 33 kDa, and the Stat family SH2 constructs are much larger at ca. 63 – 70 kDa. These Stat constructs also include the coiled coil and DNA-binding domains of the proteins, which are N-terminal to the SH2 domain. This is because the isolated recombinant SH2s are unstable, and require the presence of the other domains for stability. A band can also be seen for the Stat SH2s at ca. 16 kDa, signifying potential cleavage of the proteins. Additionally, an extra band at ca. 25 – 30 kDa can be seen for Abl2; this was likely the dimeric form of the domain, as this and other recombinant SH2 proteins have been previously shown to form dimers when expressed from the same constructs (Mersmann et al., 2010). Although some SH2 domains show almost undetectable signals in Figure 3.10, bands were revealed when the membrane was overexposed.

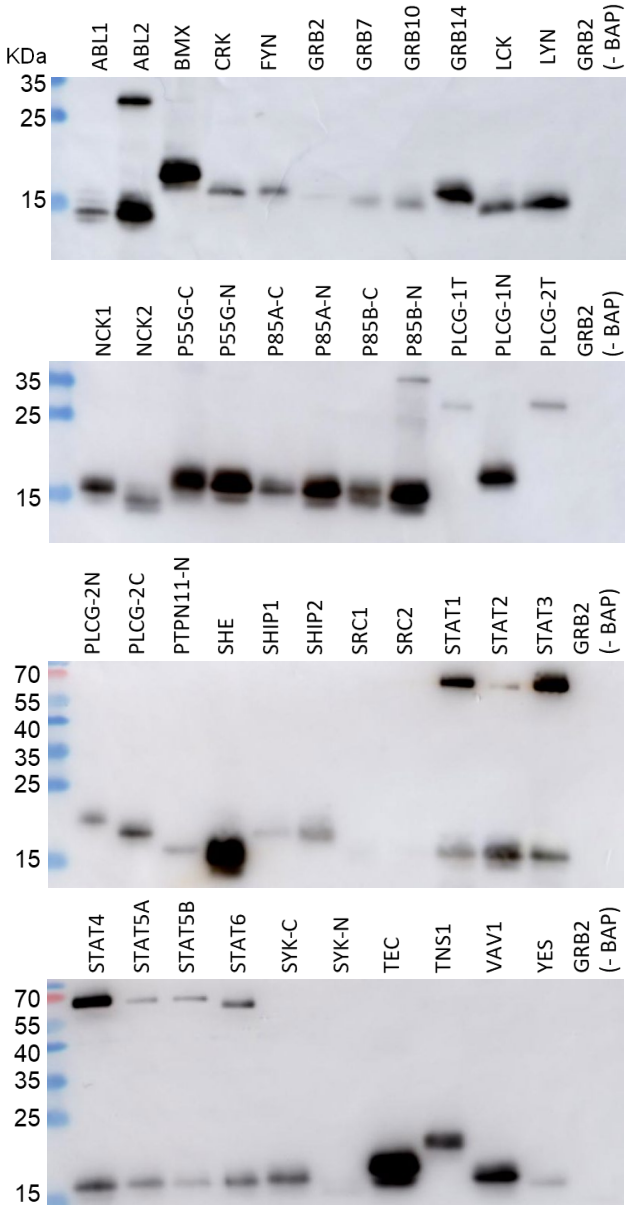

Figure 3.10. Production of biotinylated BAP-tagged SH2 domains. *Purified SH2 domain protein samples were probed for biotinylated proteins via western blot; 5 µl samples were diluted 1:5 in Elution Buffer were subject to SDS-PAGE on 15% acrylamide gels and transferred to nitrocellulose membranes. Biotin was detected with High Sensitivity Streptavidin-HRP, 1:5000. HRP visualised with Luminata™ Forte chemiluminescent substrate. Purified non-biotinylated Grb2 SH2 protein was loaded as a negative control. MW marker = PageRuler Prestained.*

Following isolation of the recombinant biotinylated SH2 domains these were immobilised onto streptavidin coated wells for the phage ELISA experiments. All Affimer binders showed binding to the Grb2 SH2 domain in the phage ELISAs as can be seen in Figure 3.11. Binding to Grb2 SH2 is labelled in green, and substantial off-target binding is labelled in red. Binders 8, 12, A4, A6, B5, H1 and H4 appeared to be the most specific, with little or no binding to other SH2s compared with the negative control. However, cross-reactivity was seen with other clones. Affimer reagents frequently showed cross-binding to the Abl2 and Crk SH2s; binding to Abl2 was seen with five clones and Crk with four. Clones D1 and D6 were the most cross-reactive, displaying considerable binding to three other SH2 domains (including Abl2 and Crk). F1 and C1 each bound two other SH2s (Abl2 and Vav1) and the remaining clones bound only one other SH2 domain. This assay was performed only once, due to a less labour-intensive method for testing specificity of Affimer reagents being established (Chapter 5).

3.7 Discussion

Affimer reagents binding to the Grb2 SH2 domain were previously isolated via phage display, with a hit rate of 92% seen in phage ELISA (absorbance signal ≥ 5x that of the streptavidin-only control) and 30 unique clones identified from DNA sequencing of 48 randomly selected clones (Tiede et al., 2014). This was a high success rate in comparison to other Grb2 SH2 screens using ScFv and Fab libraries, which had hit rates of 4 – 33% and 2 – 6 unique clones identified (Colwill et al., 2011).

Binding to the SH2 domains of other Grb family members (Grb7, Grb10 and Grb14) was also tested in the phage ELISA Tiede et al., 2017). All clones showed very low or no cross reactivity to other Grb SH2s (Figure 3.2A). In a similar specificity test on Grb2 SH2-binding ScFvs (Pershad et al., 2010), only four of 48 clones were specific for Grb2, yielding two unique sequences, Applying the same criteria for specific binding to our ELISA (a Grb2 signal of ≥10x the signal of control SH2s), 26 of 48 clones were specific for Grb2; that is 54% of clones tested, compared with 8% of the ScFvs. This result demonstrated the potential for Affimer proteins to differentiate between the structurally similar SH2 domain proteins with high specificity for their intended target. However, although pairwise

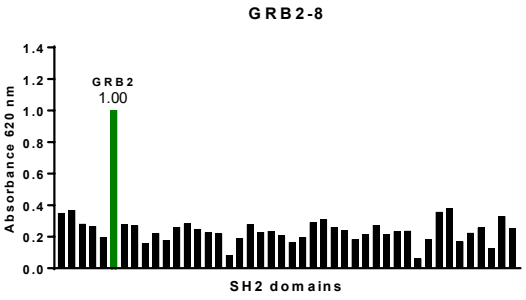
GRB2-8
GRB2
1.00
Absorbance 620 nm
SH2 domains

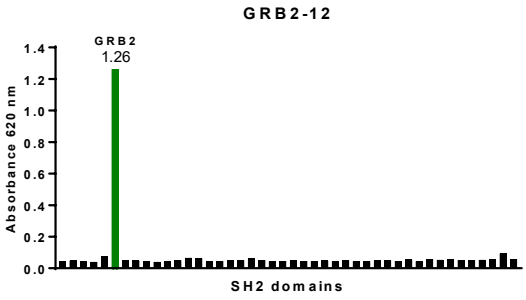
GRB2-12
GRB2
1.26
Absorbance 620 nm
SH2 domains

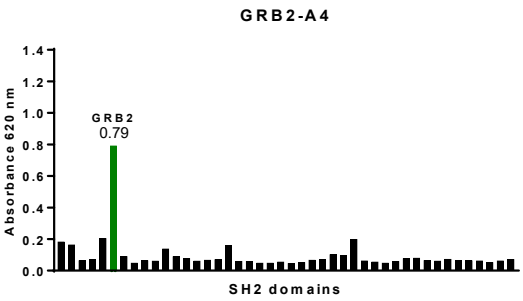
GRB2-A4
GRB2
0.79
Absorbance 620 nm
SH2 domains

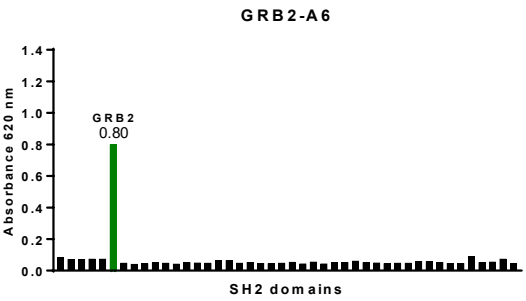
GRB2-A6
GRB2
0.80
Absorbance 620 nm
SH2 domains

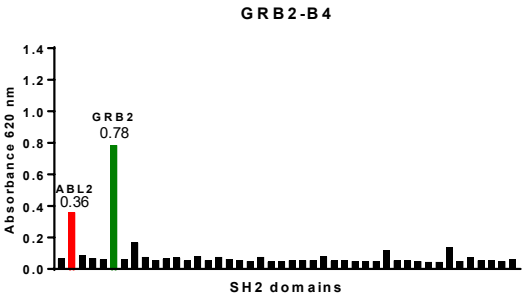
GRB2-B4
ABL2
0.36
GRB2
0.78
Absorbance 620 nm
SH2 domains

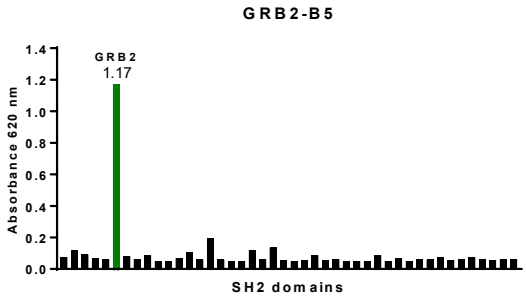
GRB2-B5
GRB2
1.17
Absorbance 620 nm
SH2 domains

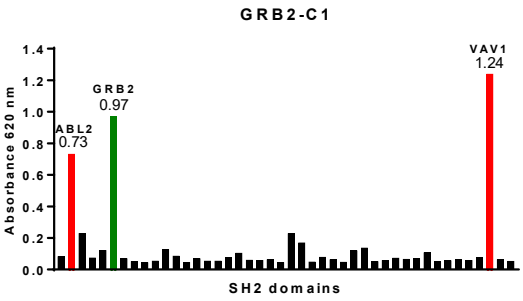
GRB2-C1
ABL2
0.73
GRB2
0.97
VAV1
1.24
Absorbance 620 nm
SH2 domains

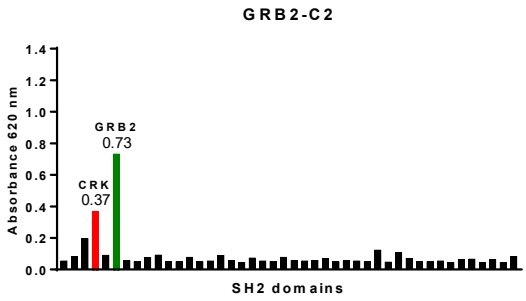
GRB2-C2
CRK
0.37
GRB2
0.73
Absorbance 620 nm
SH2 domains

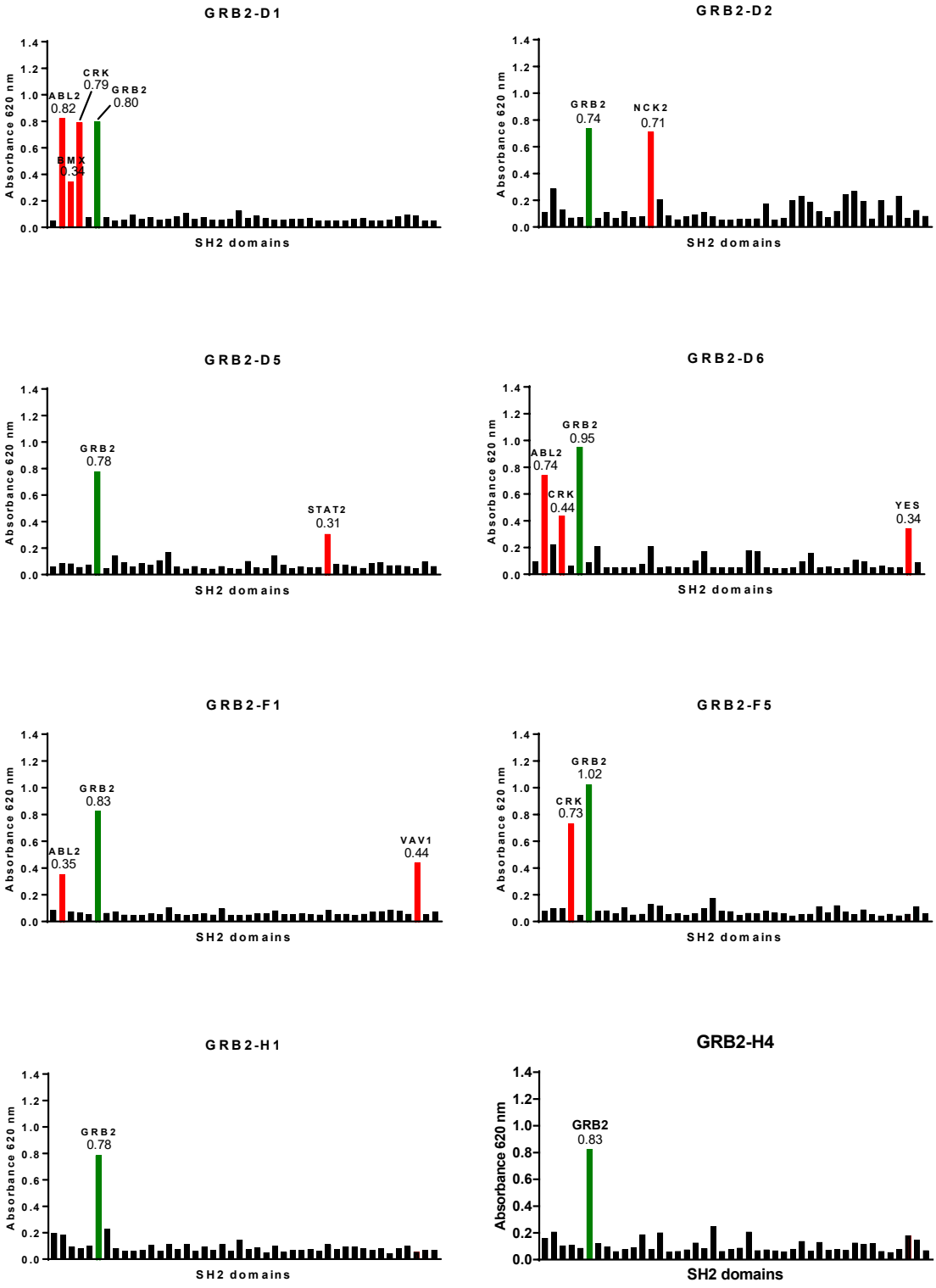

Figure 3.11. Testing specificity of Grb2 SH2 Affimer clones by phage ELISA. *Phage ELISA graphs for 16 Grb2 SH2 Affimer binders. Phage for each clone were incubated individually with 43 biotinylated SH2 domains immobilised in streptavidin-coated wells. Bound phage detected using Anti-fd bacteriophage-HRP, 1:1000. After 10x TBST washes, TMB was added and absorbance was read at 620 nm after 10 min incubation. Each clone was also tested against a streptavidin only well as a negative control. Green bars indicate binding to the intended target, red bars indicate substantial off-target binding.*

sequence homology between the Grb SH2s ranges from 30% – 70%, the identity between Grb2 and other family members remains the lowest at 30 – 32%.

The Grb2 SH2 domain binds its natural substrates via selective recognition of the binding motif pY-X-N-X (Giubellino et al., 2008). Following the sequencing and alignment of Grb2 SH2 Affimer clones (Figure 3.2B), a consensus sequence of B-X-Y-X-N-Hy-X-X-P was found predominantly in the first VR (where B is a basic residue; Hy is a hydrophobic residue; X is any amino acid). This shares similarities with the native binding sequence; in fact, 10 of the 16Affimer clones contained the native Grb2 SH2 binding sequence (with a non-phosphorylated tyrosine) in one of their variable regions. Five other clones contained the motif with an alternative aromatic residue replacing Y. This indicated that these binders could likely interact with the phosphotyrosine binding site in the Grb2 SH2 via this peptide sequence.

Production and purification of Affimer proteins showed that metal affinity chromatography gave sufficient levels of purity for use in further assays. An interesting result was the apparent molecular weight of binder D5, which was seen at ca. 24 kDa in SDS-PAGE, even after sample denaturation (Figure 3.3A). This could be explained by the formation of a stable dimer by the Affimer; this topic will be discussed in greater detail in Chapter 5.

Grb2 and its isolated SH2 domain are known to form a domain-swapped dimer in solution (McDonald et al., 2008), which has a reduced binding affinity for ligands compared with the monomeric form (Benfield et al., 2007). Thus dimer formation could have interfered with the measurement of binding affinities and IC_{50} values of Affimer binders for the Grb2 SH2. In addition, monomeric Grb2 was the physiologically relevant species for this work, as demonstrated by Ahmed et al. (2015). In that study it was shown that although Grb2 exists in a monomer-dimer equilibrium, only the monomeric form binds to Sos1 and upregulates MAPK signalling; the dimer is inhibitory to this process.

The monomeric species was therefore isolated for both the full-length Grb2 and SH2 domain proteins via SEC (Figure 3.4). However, this step may have been ineffective, as previous studies (McDonald et al., 2008) have found that even after separation of monomeric and dimeric forms of Grb2 SH2, samples re-equilibrated to yield a mixture of both species. Despite this, the EC_{50} and K_D values calculated from Grb2 control binding curves in the fluorescence

polarisation assay indicated successful isolation of the monomer for both full length Grb2 and the SH2 domain, because they corresponded to previously reported EC_{50} and K_D values for the monomeric protein species (McAllister et al. 2014).

Generally, substitution of the phosphate group in SH2 ligands results in a dramatic decrease in affinity for the target SH2 domain (Machida and Mayer, 2005) and therefore phosphopeptides are expected to be more potent SH2 binders than non-phosphorylated peptides. However, the Grb2 SH2 Affimer proteins still demonstrated binding affinities estimated in the low nanomolar range, as measured by SPR (Figure 3.5). This range is similar to that reported for SHP2 SH2 domain-binding monobodies (Wojcik et al., 2010); it is also comparable to the K_Ds reported for Grb2 SH2-binding fragments, which ranged from 0.49 nM – 0.30 µM (Colwill et al., 2011), as well as phosphopeptide binders that displayed K_D values of 100 nM and 37 nM (Gram et al., 1997). Higher affinities have been achieved with other Grb2 SH2 inhibitors however, with some compounds displaying low-picomolar K_Ds for the domain (Shi et al., 2003).

Grb2 SH2 Affimer reagents have shown the ability to capture endogenous Grb2 from U2-OS cell lysate, with binders 8, A4, D5 and H4 consistently pulling out the highest levels of Grb2. Although antibody fragments have been isolated with low nanomolar binding affinities for the Grb2 (Colwill et al., 2011), these fragments lacked the ability to immunoprecipitate either overexpressed or endogenous Grb2 from clarified lysate, with the exception of one Fab antibody. Both the ScFv and monoclonal antibodies that showed nanomolar K_Ds in SPR failed to bind Grb2 in immunoprecipitation assays. Conversely, 14 of the 16 Grb2-SH2 Affimer clones tested in the present work were able to consistently pull out endogenous Grb2 from cell lysate (Figure 3.6). These results demonstrate the ability of the Affimer reagents to bind low levels of endogenous target, in the context of the whole protein rather than just the isolated SH2 domain. As well as identifying a potential application for these Affimer binders as research reagents, this also has positive implications for their use in functional cell-based assays.

The fluorescence polarisation competition assay displayed competitive binding of Grb2 SH2 by all Affimer clones tested, with IC_{50} values ranging from 270.9 nM – 2.32 mM (Figure 3.9). Excluding the worst two binders with IC_{50}s of 4.49 µM

and 2.32 mM, this range is reduced to 0.27 ± 0.02 – 2.67 ± 0.61 μM, which is comparable with the IC_{50} values for some Grb2 SH2-binding phosphopeptides (Gram et al., 1997). These phosphopeptides were found to have IC_{50}s ranging from 0.2 ± 0.02 – 1.9 ± 0.6 μM, and contained a consensus sequence of pY-M/E-N-W. The lowest IC_{50} of 270.9 nM for binder F1 is also comparable to that of a bicyclic peptide inhibitor of the Grb2 SH2 (Quartararo et al., 2012) which had an IC_{50} of 350 ± 60 nM. This demonstrates that the inhibitory ability of the Grb2 SH2 Affimer binders is equal to previously developed Grb2 SH2 inhibitors.

The majority of Grb2-SH2 Affimer reagents that had consistently captured Grb2 in pull-down assays also showed lower IC_{50} values, with the exception of H4 which displayed a higher IC_{50} of 2.63 ± 0.09 μM. Results for clones A4 and D5 were again promising, showing two of the three lowest IC_{50} values. Affimer A6 had by far the highest IC_{50} of 2.32 ± 24.6 mM, and was arguably not effective at competing off the peptide at all. This clone had shown mixed results in pull-down of Grb2. Any discrepancies between the performance of individual Affimer clones in the pull-down and fluorescence polarisation assays could be explained by the location of their binding to Grb2 SH2, or their affinity.

For example, an Affimer that performed well at capturing Grb2 from lysate might be unable to successfully compete for the SH2 in the fluorescence polarisation assay if it bound the SH2 outside the phosphopeptide binding site, or had a lower affinity for the domain than the FYp. However, the native substrate motif Y-X-N-X (Figure 3.2B), which was expected to bind Grb2 in the phosphopeptide binding pocket, did not seem to correlate with the relative ability of Affimer proteins to displace FYp. Of the top four competitors, binders F1 and D5 contain this sequence; A4 has another aromatic residue (W) in place of Y; and F5 does not contain any version of this sequence. Conversely, of the worst four competitors three contained the motif; H4, 12 and C2. The worst inhibitor, A6, contained the sequence with an F residue in place of Y. This may imply that other residues within the variable regions are likely to be important for Affimer binding to the Grb2 SH2. Such residues could be identified by alanine scanning mutagenesis, ideally coupled with X-ray crystallography of an Affimer-SH2 domain complex.

The specificity of isolated binders was then further tested via phage ELISA against 43 recombinantly produced SH2 domains. This showed high levels of specificity of Affimer reagents for their intended target, with seven out of 16 Grb2

SH2 Affimer clones showing little or no cross-binding to other SH2s (ca. 44% of characterised binders) and the remaining clones only showing significant off-target binding to three SH2 domains at most (Figure 3.11). An Abl SH2-binding monobody isolated by Wojcik et al. (2010) showed cross-reactivity to three other SH2s in a protein microarray, indicating that the specificity of most SH2-binding Affimer proteins (all except D1 and D6) is favourable when compared with similar non-antibody reagents raised against SH2s.

As mentioned, the domains that Affimer reagents most frequently showed cross-binding to were the Abl2 and Crk SH2s. The reason for this is not particularly clear, as the Abl2 and Crk SH2 domains share only 36% and 41% sequence identity with the Grb2 SH2, respectively (alignments performed using NCBI protein BLAST tool); not a particularly high homology for SH2 domains. Additionally, the reported binding motif for the Crk SH2 is pY-X-X-P, which was not present in any of the clones (Songyang et al., 1993, Tinti et al., 2013). However, the reported motif for the Abl2 SH2 is pY-E-N-P; although this motif was also not present in the clones, the preference for an N residue at pY + 2 is the same binding preference as the Grb2 SH2 (Tinti et al., 2013, Liu et al., 2012). This residue could have therefore conferred the cross-reactivity of the Affimer reagents for the Alb2 domain, as many contained a Y-X-N motif in their VRs.

The results of these initial assays assisted in selection of clones to take forward for mammalian cell-based assays (detailed in Chapter 6). Affimer clones 8, A4, D5, F1 and H1 were chosen based on their specificity for Grb2; their ability to capture endogenous Grb2 from lysate; their capacity to competitively inhibit the SH2; or a combination of all qualities. In conclusion, Grb2 SH2 Affimer reagents had shown good potential in proof-of-principle studies for the Affimer as a SH2 domain reagent. Preliminary characterisation data indicated good specificity for their target SH2 domain over family member SH2s; further investigation of specificity showed the isolation of seven highly specific clones when tested against a panel of 43 SH2 domains. They had also demonstrated low nanomolar binding affinities, the ability to bind endogenous full-length protein in mammalian cell lysate, and the capability to compete for the SH2 binding site with a phosphorylated ligand.

Chapter 4

Isolation of Affimer binders against a subset of SH2 domains

Chapter 4

Isolation of Affimer binders against a subset of SH2 domains

4.1 Introduction

Phage display is a well-established technique that allows the selection of binding molecules to a wide range of targets. This technique has been utilised for the isolation of Affimer reagents since the creation of the Affimer Type II phage library, and has resulted in the successful screening of over 350 targets (Tiede et al., 2017). As phage display screening had been efficient in isolating specific Affimer reagents for the Grb2 SH2 domain (Chapter 3; Tiede et al., 2014), it was decided to use this method for screening of further SH2 domains. The aim of this work was to isolate binders against a large subset of the SH2 domain family, to work towards the goal of raising specific binding reagents against all SH2 domains.

During phage display negative selection against closely-related targets can be incorporated to favour selection for a specific member of a homologous protein family (Mersmann et al., 2010, Moghaddam et al., 2003, Tang et al., 2017). Additionally, it is a high-throughput approach that makes no pre-conceptions about the binding site(s) on the target and enables the isolation of reagents to multiple target proteins in a rapid time-frame. Of all the molecular display techniques, it has proven the most popular approach (Wu et al., 2016).

In phage display, a binding peptide or protein is displayed on the surface of the bacteriophage the by the bacteriophage, with the DNA encoding the peptide or protein encapsulated inside. This method was first described by G. Smith in 1985 and has since become one of the most effective ways of isolating large numbers of peptide and protein binders, as well as antibodies (Smith, 1985). *E. coli* filamentous bacteriophage (f1, fd, M13) are commonly used for phage display. The binding reagent is encoded as a fusion protein, mostly with coat proteins pIII or pVIII. The minor coat protein pIII is displayed at one end of the phage as five copies (Bazan et al., 2012) and is commonly used for fusion with proteins. By contrast there are some 2,700 copies of the small major coat protein pVIII that is most commonly fused with peptides for peptide display selection. In filamentous phage systems the foreign DNA is inserted either into the phage

genome, which encodes all proteins needed for replication and assembly of phage or, more commonly, into a phagemid vector. Phagemid vectors are plasmids that only carry an antibiotic resistance marker, a phage packaging signal and in addition to the bacterial origin of replication they also carry a phage origin of replication; allowing the production of single stranded copies of phagemid DNA within the *E. coli* cells (Kehoe and Kay, 2005). Use of these phagemids therefore require the addition of helper phage to provide the proteins needed for phagemid replication, including wild-type pIII and other structural proteins forming the phage coat. Addition of helper phage allows the assembly of phage particles with the displayed foreign peptides (Paschke, 2006; Li and Caberoy, 2010).

Phage-display of protein/peptide libraries ensures a physical link between phenotype (the displayed protein/peptide) and genotype (the encoding DNA). A schematic of the phage display process used with Affimer proteins can be seen in Figure 4.1. The libraries can be used in a screening process against a desired target, where binding clones are separated from non-specific clones by rounds of affinity selection, also known as biopanning (Wu et al., 2016).

During biopanning, a phage display library is incubated with the target that has been immobilised onto a solid surface such as microtitre plate wells or magnetic beads. This incubation is followed by extensive washing to remove non-binding phage. Binding phage are then eluted, usually using extremes of pH or by high salt, and are amplified in *E. coli* host cells. Three to five rounds of biopanning are usually used to obtain an enriched phage pool of high affinity binders (Wu et al., 2016). After biopanning, phage-infected host cells can be plated onto agar plates, allowing individual clones to be picked and tested for binding to the target antigen via ELISA or other assays (Li and Caberoy, 2010; Bazan et al., 2012).

Phage display has been previously utilised to raise binding reagents against SH2 domains, including antibody fragments and monobodies (Colwill et al., 2011; Wojcik et al., 2010; Sha et al., 2013). Phage display has been used to isolate Affimer binders against a range of targets. Proof-of-principle studies on yeast small ubiquitin-like modifier (ySUMO), fibroblast growth factor 1 (FGF1) and platelet endothelial cell adhesion molecule (CD31), showed this to be an effective method for identifying Affimer reagents that bind with high affinity to the

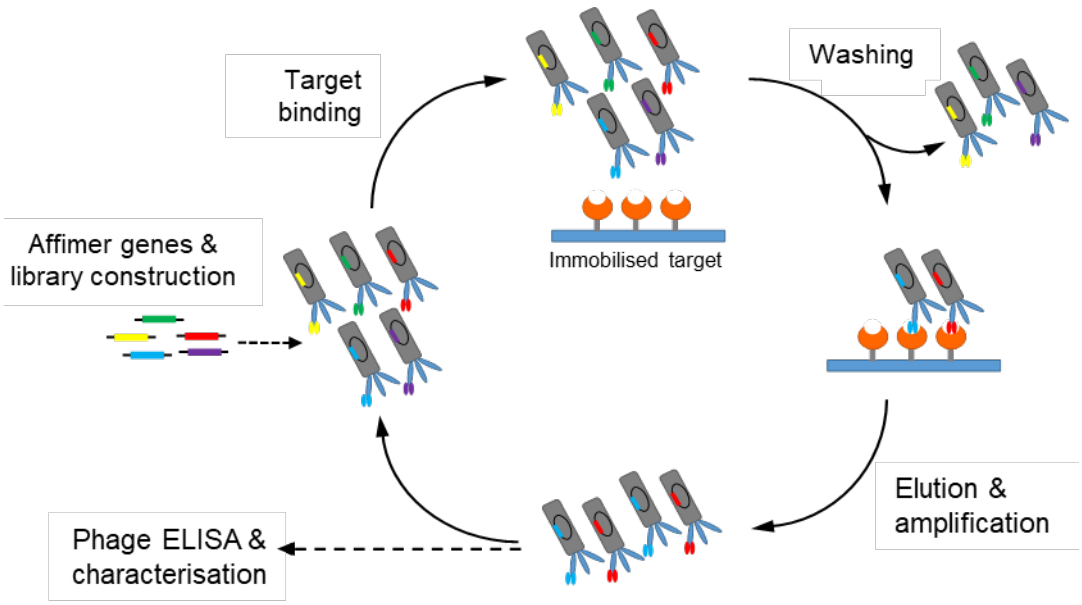

Figure 4.1. Isolation of Affimer reagents using phage display. *Schematic showing the stages in biopanning of an Affimer phage display library. Affimer clones are displayed on the surface of bacteriophage with the encoding DNA encapsulated inside. The target is immobilised through biotinylation and binding to a streptavidin-coated surface, and is then incubated with the phage library. Stringent washing steps remove any non-binding clones, and the binding clones are eluted using extremes in pH. These clones are then amplified through infection of E. coli and the process is repeated two – three more times. After biopanning is complete, individual clones are assessed for binding to the target in relation to a streptavidin-only control. Binding clones are then sent for DNA sequence analysis.*

protein of interest (Tiede et al., 2014). Affimer binders have now been successfully raised against diverse targets using this technique; including soluble proteins, small organic molecules, extracellular receptors and viral proteins (Tiede et al., 2017).

As phage display screening had successfully yielded promising Affimer binders for the Grb2 SH2 domain, the process was used in the following work to further screen a subset of 42 other SH2 domains. These SH2 domains were chosen because the constructs encoding them had been previously purchased by Avacta, and were therefore readily available to the candidate for screening. It is envisioned that all 120 SH2 domains will eventually be screened using the Affimer phage library, however this was beyond the scope of this project.

4.2 Optimisation of screening using PLCγ, Grb and Ship SH2 domains

Before a large-scale screen of multiple SH2 domains was attempted, optimisation of the phage display screening protocol was carried out using SH2 domains from PLCγ, Grb and Ship proteins. Phage display screening and phage ELISAs on PLCγ targets was conducted by master's students Eleanor Foy and Grace Reddy, using chemically biotinylated and BAP-tagged SH2 proteins, respectively. Screening and phage ELISAs on BAP-tagged Grb and Ship targets was performed by master's student Naomi Gibson. Work carried out by students is detailed in the relevant Figure legends.

This optimisation was used to maximise the success rate of the large-scale screen and ensure Affimer binders were isolated against a large number of the SH2 targets. In all SH2 screens, Affimer libraries of both scaffold Types (I and II; see Chapter 1, section 1.5.1) were screened. Two different Type I libraries were included; the Type I 9x9 library where each variable region (VR) contains nine randomised amino acids (as with the Affimer Type II library) and the Type I 6x12 library, where variable region one (VR1) contains six residues and variable region two (VR2) contains 12 residues. All libraries were mixed and screened together during phage display.

4.2.1 PLCγ SH2 domain protein production and biotinylation

SH2 domain proteins of the PLCγ isoforms one and two were initially used for optimising phage display. PLCγ proteins contain two SH2 domains each, these being positioned adjacent to each other within the protein sequence and are termed the N- and C-terminal SH2. Five different PLCγ SH2 constructs were tested; the PLCγ1 N-terminal SH2 (PLCγ1-N); the PLCγ2 N-terminal SH2 (PLCγ2-N); the PLCγ2 C-terminal (PLCγ2-C); the PLCγ1 N- and C-terminal SH2s in tandem (PLCγ1-T); and the PLCγ2 N- and C-terminal SH2s in tandem (PLCγ2-T). The isolated PLCγ1-C domain was not available to screen, as it had not been purchased by Avacta.

pET28 vectors encoding PLCγ SH2 sequences with an N-terminal 6xHis-tag were purchased from the Pawson Lab (Samuel Lunenfeld Research Institute, Canada). As with the Grb2 proteins, His-tagged PLCγ SH2 proteins were firstly produced in BL21 Star™ (DE3) *E. coli*, as this strain provided sufficient yields for

phage display screening. Expression was IPTG-induced in 400 ml cultures overnight at 18 °C. Proteins were purified from lysate using nickel affinity chromatography and eluted fractions analysed by SDS-PAGE (Figure 4.2A). This showed protein bands at a MW of ca.18 kDa for the isolated SH2 domains and ca.30 kDa for the tandem SH2s, corresponding to the theoretical MW range of 17.9 – 18.7 kDa for the single SH2 domain constructs and 30.4 – 31.3 kDa for the tandem SH2 constructs (calculated using ExPASy ProtParam software).

Protein concentrations were estimated using the Beer-Lambert law by measuring A_{280} of elution samples. These values were only estimates, because the proteins were not dialysed from the Elution Buffer and so contained a high concentration of imidazole (300 mM) which can interfere with spectrophotometry readings. Elution Buffer not containing protein was always used as a reagent blank to try to reduce this effect. Total PLCγ SH2 protein yields were estimated at ca.1.7–4.8 mg from 400 ml cultures.

For phage display screening of the Affimer library, chemical biotinylation of target proteins is performed for immobilisation onto streptavidin-coated surfaces used during panning rounds. PLCγ SH2 proteins were biotinylated immediately after purification, in elution buffer, using EZ-Link™ NHS-SS-Biotin, an amine-reactive biotinylation reagent (methods section ref). Biotinylation of the SH2 proteins was checked via western blot analysis (Figure 4.2B), where bands corresponding to the theoretical MW of the proteins could be seen. Strong biotinylation of all targets was observed, with the exception of PLCγ2-T where only weak signals in both ELISA and western blot analysis were detected. Biotinylation of this target was repeated twice but similar results were seen. No other instances of biotinylation of this construct were found in the literature for comparison. This protein was still used for phage display screening with the other SH2 domain proteins.

4.2.2 Phage display screening of five chemically biotinylated PLCγ SH2 domains failed for four targets

At first, the same phage display protocol used for screening of the Grb2 SH2 domain was utilised, as this showed great success and isolated over 30 unique binders (Tiede et al., 2014). In this protocol, three panning rounds were

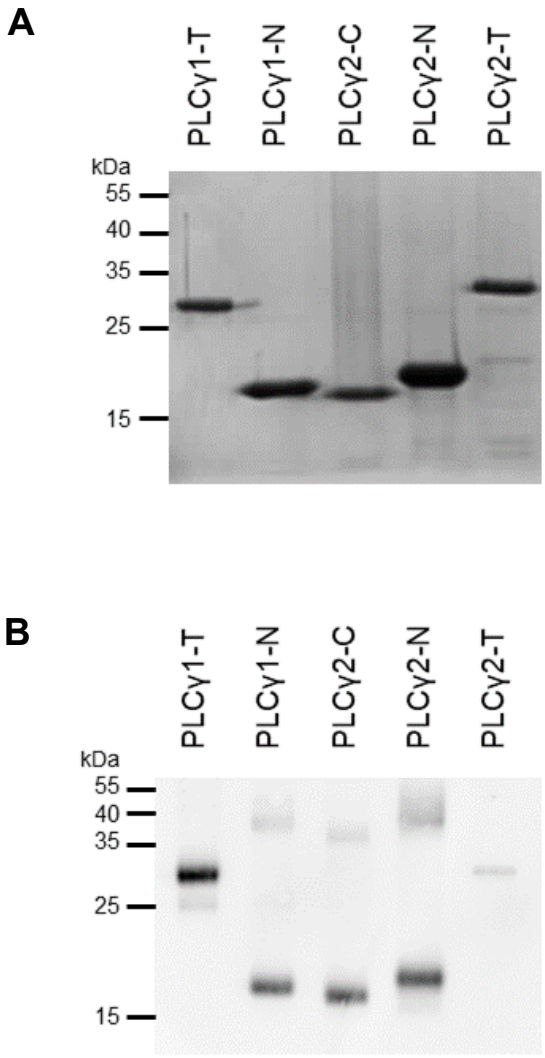

Figure 4.2. Production and biotinylation of His-tagged PLCγ SH2 domain proteins. ***(A)*** *SDS-PAGE analysis of recombinantly produced PLCγ SH2 domains (-N, -C and -T denote the N-terminal or C-terminal SH2, or both in tandem). Ni-NTA purified elution samples used in phage display screening were electrophoresed on 15% acrylamide gel and proteins detected with Coomassie Blue. SH2 Domains can be visualised at ca. 18 kDa for the single SH2 domains and ca. 30 kDa for the tandem SH2s.* ***(B)*** *Western blot detection of biotinylated PLCγ SH2 domains. After chemical biotinylation using NHS-SS-biotin, 5 µl SH2 protein samples were electrophoresed and transferred to nitrocellulose membranes. Membranes were incubated with High Sensitivity Streptavidin-HRP, 1:5000 to detect biotin. HRP was detected with Luminata Forte. MW marker = PageRuler Prestained.*

conducted using the chemically biotinylated SH2 proteins (Chapter 2, section 2.2.6). The first pan utilised streptavidin-coated wells as the binding surface, the second used streptavidin-coated beads, and the third used neutravidin-coated wells. Altering the binding surface between pans reduces background such that non-specific Affimer clones that bind to the streptavidin-coated surface rather than the immobilised target can be eliminated. Phage display was performed on all targets, using a standard first pan and competitive second and third pans. For competitive pans, an additional incubation of target-bound phage with 2.5 µg of non-biotinylated target protein was performed for 24 h at room temp before elution.

The expected amplification in colony numbers of 10-fold or more (Frei and Lai, 2016) was not observed in pan three when compared with negative control plates (see Table 4.1A). An additional fourth panning round was therefore completed in which streptavidin-coated wells were used, as in pan one. After this fourth pan, there was still no amplification in colony numbers seen for PLCγ1-T, PLCγ1-N, PLCγ2-T and PLCγ2-C (see Table 4.1B). PLCγ2-N plates showed a ca. 21-fold amplification compared to the negative control, indicating successful isolation of PLCγ2-N SH2-binding Affimer clones.

PLCγ2-N phage were therefore taken forward to confirm specific target binding via phage ELISA. Sixty-four clones were randomly selected and each tested

Table 4.1. Colony numbers from phage display screening of PLCγ SH2 domains. *Colony numbers on 10µl target (positive) plates and negative control plates were counted and total colony numbers for 8 ml cultures estimated for each PLCγ target, after three **(A)** and four **(B)** panning rounds. Successful amplification of positive clones seen for PLCγ2-N is highlighted in green. Panning was performed by student Eleanor Foy.*

A Pan 3

Target	Positive	Negative
PLCγ1-T	2.24×10^4	2.18×10^4
PLCγ1-N	1.81×10^4	1.18×10^4
PLCγ2-T	1.19×10^4	1.10×10^4
PLCγ2-N	4.69×10^4	2.23×10^4
PLCγ2-C	2.08×10^4	1.28×10^4

B Pan 4

Target	Positive	Negative
PLCγ1-T	6.16×10^3	6.32×10^3
PLCγ1-N	4.03×10^4	4.29×10^4
PLCγ2-T	1.55×10^4	1.59×10^4
PLCγ2-N	5.41×10^4	2.56×10^3
PLCγ2-C	5.57×10^4	4.93×10^4

against wells containing immobilised biotinylated PLCγ2-N, or streptavidin only wells. Clones were additionally tested against other PLCγ SH2 targets to check for cross-binding. Absorbance readings from all plates were plotted for each clone to visualise specificity of phage for PLCγ2-N (Figure 4.3A). Of the 64 tested, 23 clones showed as positive hits in the ELISA (determined as having a signal for the intended target ≥ 5x higher than the streptavidin-only control) corresponding to a 36% hit rate. Most binding clones displayed specific binding to PLCγ2-N, despite the PLCγ2-T construct also containing the PLCγ2-N SH2. This lack of binding to the tandem SH2 protein could be because the epitope recognised by binders in the PLCγ2-N is not accessible in the presence of the PLCγ2-C domain. Some binding to PLCγ1-N was also seen for seven clones. The 23 binding clones were analysed by DNA sequencing, identifying four unique binders, all of which were Affimer Type II. An amino acid alignment of the VRs in these clones was performed using MacVector 13.5.2 (Figure 4.3B) and revealed a consensus sequence of Y-X-Ar-Hy-X-X-Hy in VR2 (refer to abbreviations section for amino acid abbreviations). Clone PLCγ2N-B8 occurred most frequently in the sequenced population, constituting 11 of the 23 sequenced clones. This clone showed specificity for PLCγ2-N in the phage ELISA as did clones PLCγ2N-B3 and PLCγ2N-E2. Clone PLCγ2N-C2 occurred eight times in the sequenced binders and displayed some cross-binding to PLCγ1-N in the ELISA, as well as to PLCγ1-T to a lesser extent.

4.2.3 Addition of an N-terminal biotin acceptor peptide to SH2 domain constructs and optimisation of protein production

As the screen had been unsuccessful for all but PLCγ2-N, the sequences of the PLCγ SH2 domains were analysed to determine whether biotin could be binding to free lysine residues near the phosphotyrosine-binding sites. As lysine contains a primary amine in the side chain, amine-reactive biotinylation reagents can label these residues instead of the N-terminus of a protein. If the SH2 domains were labelled with a biotin near the phosphotyrosine-binding site, this could orientate the SH2 targets so that their binding surface is not accessible to the phage, or block interactions with the Affimer-displaying phage. Protein sequences were aligned using PyMOL v1.7.4. A lysine residue can be seen at position 52 of

A

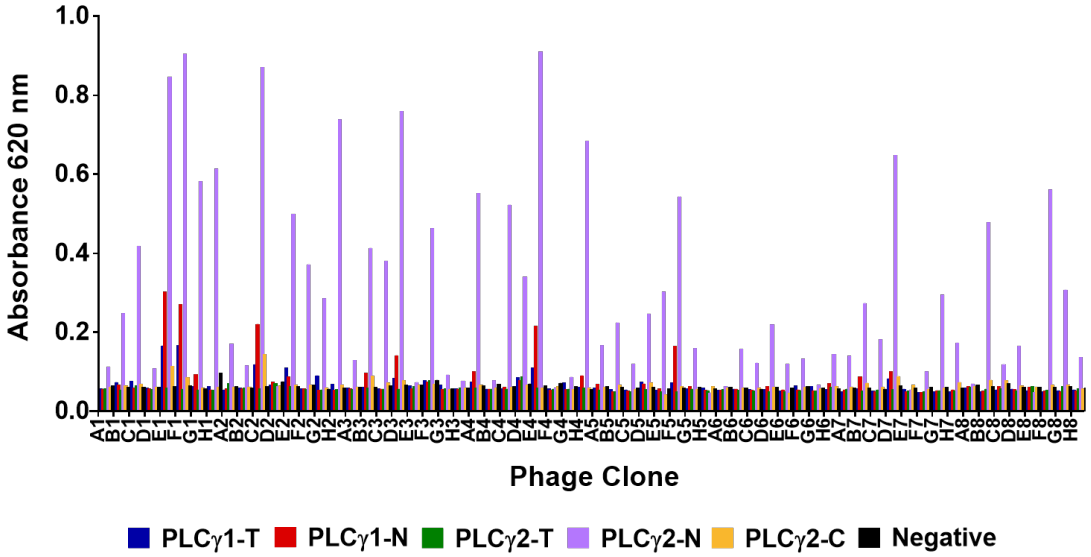

B

Clone	Type	VR 1	VR 2	Frequency
PLCγ2N-B3	II	KQTVVEPTQ	SYWFLPMKQ	1
PLCγ2N-B8	II	AQYMPHWR	YNWLDEGYS	11
PLCγ2N-C2	II	MSKHEISEV	RYYAWAGWA	8
PLCγ2N-E2	II	WAGNFVMYQ	GLWDAGIHL	2
	consensus:		YXAHXXH ry y	

Figure 4.3. Isolation of PLCγ2-N SH2-binding Affimer clones. ***(A)*** *Phage ELISA results from the PLCγ2-N SH2 Affimer library screen. Phage clones were incubated in wells containing immobilised PLCγ2-N SH2 and bound phage were detected with anti-phage-HRP antibody after washing. HRP substrate TMB was added and absorbance read at 620 nm after 3 min, for 48 clones. Cross-binding to SH2 domains of PLCγ1-N, PLCγ1-T, PLCγ2-C and PLCγ2-T were also tested.* ***(B)*** *Alignment of variable regions (VRs) of the 4 unique PLCγ2-N SH2-binding Affimer clones. Alignment was performed using MacVector 13.5.2. A consensus sequence can be seen in VR2 as follows; Y – X – Ar (aromatic side chain) – Hy (Hydrophobic residue) – X – X – Hy, where X is any amino acid. Residues that conform to the consensus are in red. Frequency = number of times the clone occurred in the sequenced population. Phage ELISA and sequence analysis was performed by student Eleanor Foy.*

PLCγ1-C and PLCγ2-C that is not present in PLCγ1-N and PLCγ2-N sequences (Figure 4.4A). This lysine is within the phosphotyrosine-binding region (F-L-I/V-R-**K**/E-R sequence), corresponding to the highly conserved phosphotyrosine-binding F-L-V-R-E-S sequence in Src (Russell et al., 1992; Campbell and Jackson, 2003). Another lysine residue is present at position 69 in all targets except for PLCγ2-N; this residue is present on the binding 'face' of the domains, on the βD strand of the central β sheet (Campbell and Jackson, 2003). Biotinylation of the proteins at this position could result in blocking of the phosphotyrosine-binding site or unfavourable orientation of the SH2 domains, and may explain why only the screen for PLCγ2-N was successful.

To overcome this problem, a biotin acceptor peptide (BAP) sequence was inserted at the N-terminus of the SH2 sequences, before the 6xHis-tag (as mentioned in Chapter 3, section 3.6). Incorporation of a BAP sequence on the terminus of a protein is a method for ensuring site-directed biotinylation, away from the binding site. This peptide mimics the biotin acceptor function of the biotin carboxyl carrier protein (BCCP) sub-unit of acetyl CoA carboxylase, binding endogenous biotin within *E. coli* cells when recombinantly expressed (Beckett et al., 1999). This removes the need to chemically biotinylate a target for phage display. Insertion of the BAP sequence into the SH2-encoding pET28 vectors was achieved using a QuikChange-style reaction (Chapter 2, section 2.2.4) and was also performed for plasmids encoding SH2 domains of the Grb family (Grb7, Grb10, Grb14), and Ship1 and Ship2 proteins. Translation of the DNA sequencing results showed correct incorporation of the BAP sequence (G-L-N-D-I-F-E-A-Q-K-I-E-W-H-E) for all SH2 constructs (Figure 4.4B).

For SH2 domains containing the BAP tag, protein production was carried out as before in BL21 Star™ (DE3) *E. coli* cells. However, total protein yields for PLCγ SH2s were estimated at ca. 0.87 – 0.29 mg per 400 ml culture, which was significantly lower than previous production yields. Culture samples revealed this was due to low production levels, as shown by SDS-PAGE (data not shown). SH2 proteins were therefore produced in Rosetta™ 2 (DE3) *E. coli* (see Chapter 3, section 3.2.2) and cultures were induced at a lower temperature of 18 °C, in accordance with previous studies detailing SH2 domain production (Pershad et al., 2010; Mersmann et al., 2010). A higher yield was obtained from this strain

A

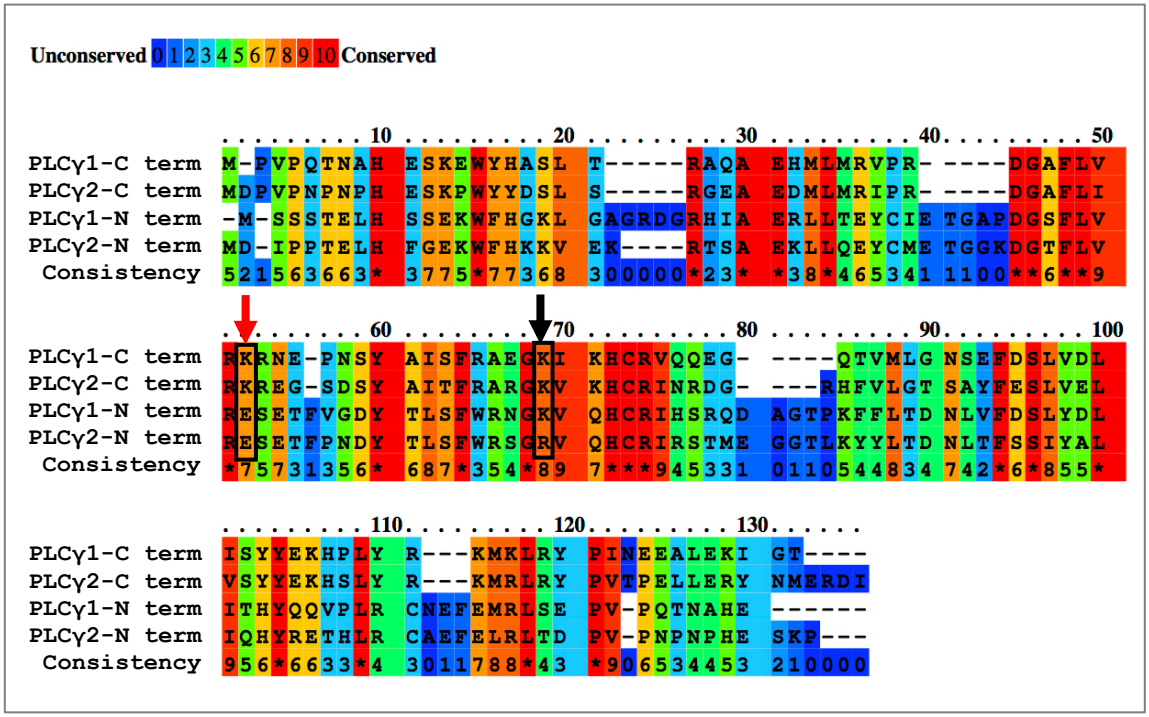

B

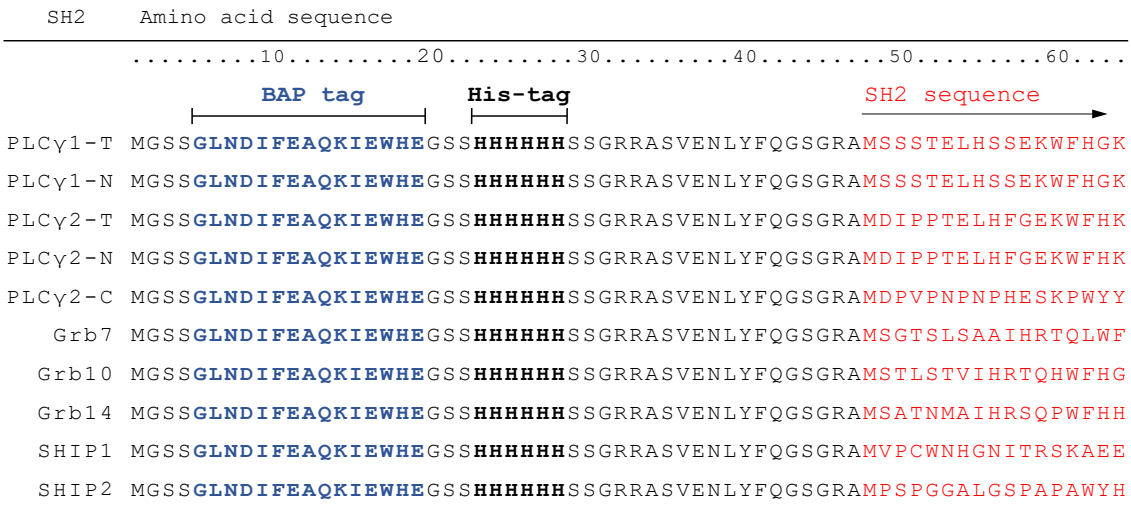

Figure 4.4. Insertion of BAP tag into SH2 domain sequences. (A) *Alignment of PLCγ SH2 domain sequences using PyMOL v1.7.4 revealed a lysine in the phosphotyrosine-binding region of C-terminal PLCγ SH2 domains, but not N-terminal PLCγ SH2s at position 52 (red arrow). Addtionally a lysine was present in all SH2 domains except for the N-terminal PLCγ2 domain at position 69, on the binding face of the proteins (black arrow). These two positions are indicated with arrows and outlined in boxes.* ***(B)*** *Alignment of PLCγ, Grb and Ship family SH2 domain amino acid sequences using MacVector 13.5.2 showed successful insertion of an N-terminal BAP sequence (blue), before the His-tag (bold) and SH2 domain sequences (red).*

using this method (typically ca. 2 – 7 mg per 400 ml for PLCγ SH2s). Proteins were purified from lysate using nickel affinity chromatography and elution fractions analysed by SDS-PAGE (Figure 4.5A) and western blot (Figure 4.5B) analysis, to check purity and successful *in vivo* biotinylation.

As seen in Figure 4.5A, protein bands were visualised slightly lower than the expected MWs of the PLCγ proteins with the BAP tag; the theoretical MWs had been calculated as 19.9 – 20.8 kDa for the single domains and 33.4 – 33.5 kDa for the tandem domains. However, the successful addition of the BAP tag on the proteins was suggested by the increase in MW of the BAP-containing PLCγ2-N sample compared with the non-tagged PLCγ2-N control. Proteins did not appear as pure as previous PLCγ samples with an extra band observed at ca. 25 kDa for all PLCγ proteins samples, signifying a contaminant in the samples (indicated by black arrows). However, a Rosetta^{TM} 2 lysate control was not run on these gels, and therefore this theory could not be confirmed. Additionally, several faint bands at ca. 15 kDa and below can be seen for some of the samples, indicating potential degradation of proteins.

For the Grb and Ship proteins, similar results to the PLCγ samples were seen in the SDS-PAGE analysis. Two elution fractions were analysed for each of these targets. The BAP-tagged Grb family samples showed protein bands at ca. 16 kDa which was slightly lower than the calculated MWs (18.5 – 18.7 kDa). Ship proteins showed bands at a higher MW, ca. 17 - 18 kDa, which was closer to their calculated MWs of 18.6 and 18.8 kDa. Like the PLCγ samples, a common band was visualised at ca. 25 kDa, as well as other bands particularly in Grb10 and Grb14 samples. The presence of this band in all SH2 samples suggested this was perhaps an endogenous protein containing a histidine-rich region, which enabled it to bind the Ni-NTA resin used in purification.

A western blot was then performed on samples to detect biotinylated proteins, to determine successful biotinylation of BAP-tagged SH2 proteins *in vivo* (Figure 4.5B). Elution one was used for the Grb and Ship SH2s. Bands corresponding to the SDS-PAGE gels and the calculated MWs of the BAP-tagged SH2 proteins were observed for all targets in the western blots, and no band was seen in the negative controls, indicating successful biotinylation of these SH2 domains.

Extra bands were also seen in PLCγ2, Grb and Ship samples, which correlated with the MW of the SH2 dimers. By error, samples had not been reduced before

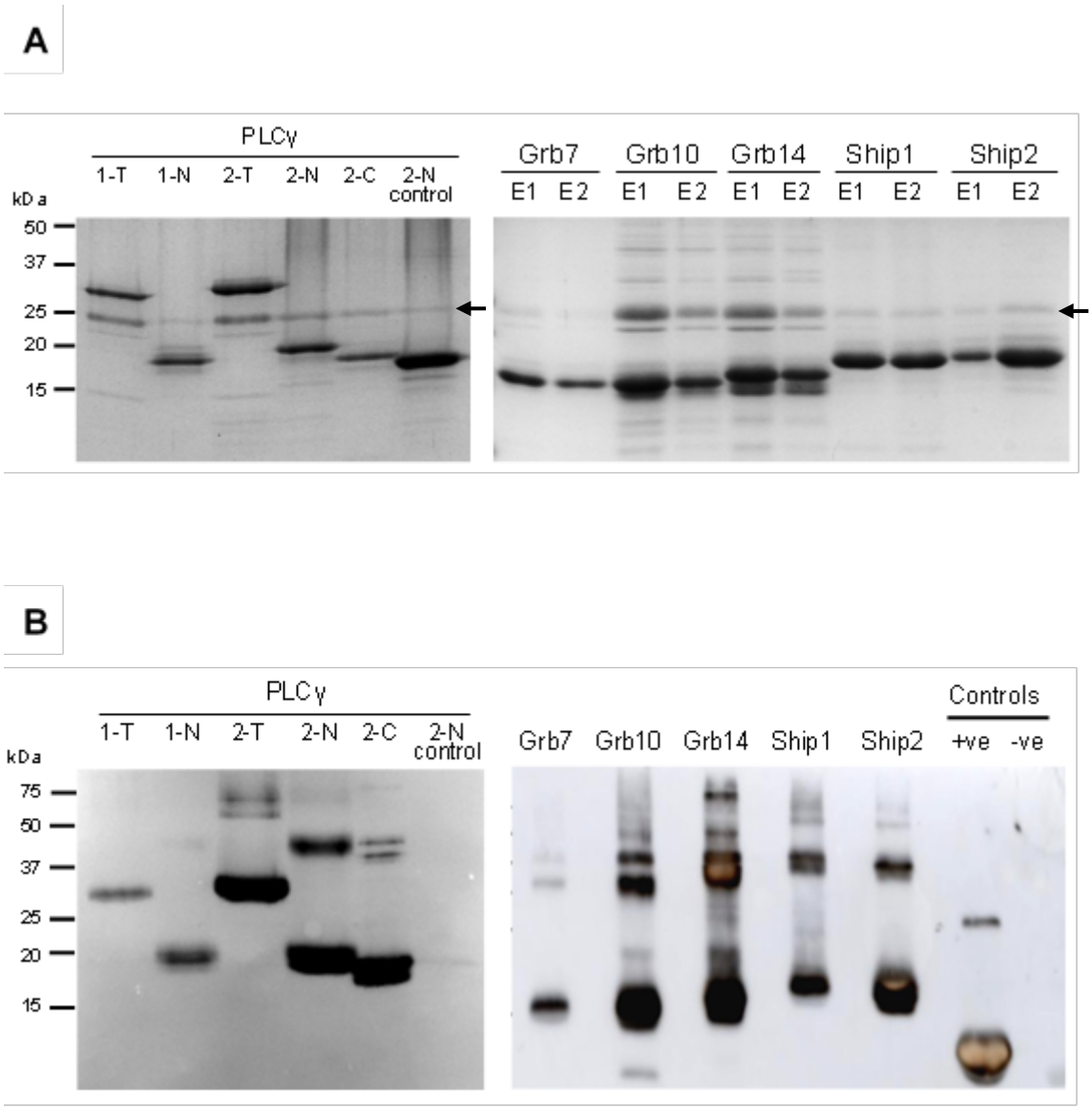

Figure 4.5. Production and biotinylation of BAP-tagged SH2 domain proteins. ***(A)*** *SDS-PAGE analysis of Ni-NTA purified elution fractions of recombinantly produced BAP-tagged PLCγ, Grb and Ship SH2 domains. For Grb and Ship proteins, two elution fractions (denoted E1 and E2) were analysed. PLCγ2-N control = non-BAP-tagged PLCγ2-N protein. Domains can be visualised at ca. 18 kDa for isolated PLCγ SH2 domains and ca. 30 kDa for the tandem PLCγ SH2s. Grb family SH2s were seen at ca. 16 kDa and Ship SH2s at ca. 17 -18 kDa. Black arrows indicate a non-specific band seen at ca. 25 kDa in most samples* ***(B)*** *Western blots detecting biotinylated proteins in elution fractions shown in (A); for Grb and Ship E1 samples were used. Controls on Grb/Ship blot = chemically biotinylated Grb2 SH2 (+ve) and non-biotinylated Grb2 SH2 (-ve). Samples were electrophoresed and transferred to nitrocellulose membranes. Membranes were incubated with High Sensitivity Streptavidin-HRP, 1:5000 to detect biotin and HRP detected with Luminata Forte. MW marker = Precision Plus Protein™, gels contained 15% acrylamide. Protein production was performed by students Grace Reddy and Naomi Gibson.*

electrophoresis, as this was the method that had previously been used for chemically biotinylated SH2 proteins to avoid de-coupling of the biotin molecule from the proteins. Therefore, it is likely that these bands are indeed the biotinylated dimers of the SH2 proteins. A strong dimer band was seen in the PLCγ2-N western blot that was not present at all in SDS-PAGE; indicating that dimerisation had occurred rapidly, in the time between the two analyses being conducted.

The common band seen at ca. 25 kDa in the SDS-PAGE analysis was not present in either western blot. This showed that the contaminant protein was not biotinylated and therefore should not be immobilised on the streptavidin-coated surface with the SH2 domain. However, because the protein samples were quite impure compared to previous batches of SH2s, pre-panning against lysate from Rosetta™ 2 (DE3) cells not expressing any SH2 domains was included in all further screens (detailed in the following section).

In addition to western blot analysis, an ELISA was conducted on the BAP-tagged PLCγ SH2 domains to check that the proteins could be efficiently captured on streptavidin-coated wells used in phage display. Proteins were incubated in wells for 2 h, before six TBST washes and detection of the His-tag with an anti-His HRP-conjugated antibody. As seen in Figure 4.6, all constructs except PLCγ1-T showed signals above that of the streptavidin-only control. This did reflect the biotin western blot, which had shown a weaker signal for PLCγ1-T. However the western blot had shown the presence of biotinylated PLCγ1-T in the sample, so it decided to take PLCγ1-T forward with the other samples without optimisation of immobilisation for this protein . This assay demonstrated successful capture of four out of the five biotinylated His-tagged SH2 proteins on the surface.

4.2.4 Phage display screening of BAP-tagged SH2 domains successfully isolated SH2-binding Affimer clones

The phage display screens were conducted as previously for PLCγ SH2s, with the addition of Rosetta™ 2 (DE3) lysate in the pre-panning steps for all panning rounds. This was used to reduce the isolation of non-specific Affimer clones which bound any impurities in the SH2 samples. By adding the lysate to a streptavidin-coated pre-pan well, any endogenous biotinylated proteins in the

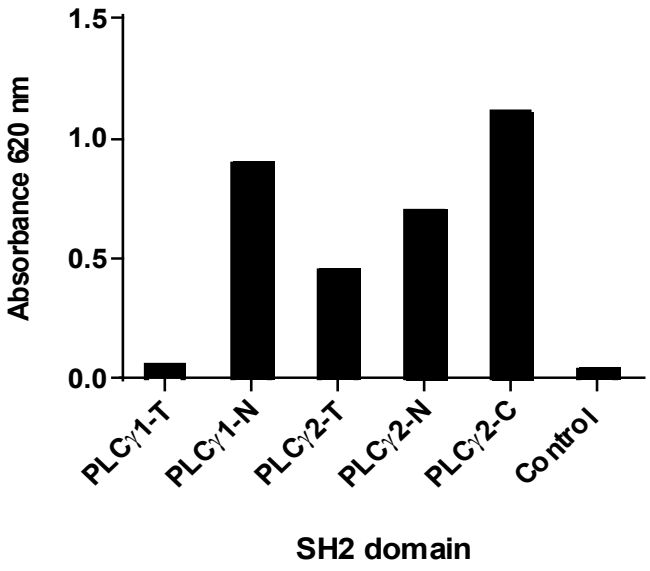

Figure 4.6. Immobilisation of BAP-tagged SH2 domain proteins on streptavidin-coated plates. *ELISA using PLCγ SH2 domains to check successful capture of biotinylated BAP-tagged SH2 proteins on the streptavidin-coated wells used in phage display. 10 µl SH2 protein elutions were incubated in streptavidin-coated wells for 1 h at room temperature. After 6x washes, captured SH2 domains were detected via the His-tag with 1:1000 Anti-His-HRP. HRP was detected using TMB substrate and absorbance measured at 620 nm. Streptavidin-only well was used as the negative control. Data shown for one experimental repeat. ELISA was performed by student Grace Reddy.*

lysate would be immobilised on the well. Exposing the Affimer phage library to these proteins would capture and remove any non-specific binders from the library, before it was panned against the SH2 domain samples.

4.2.4.1 PLCγ SH2 domain screens

PLCγ pan three plates showed substantial amplification in colony numbers (≥10x negative plates) for all targets except PLCγ2-C, which contained ca. three-fold less colonies than the negative control (Table 4.2A). PLCγ1-T plates showed the largest amplification of ca. 137-fold. Phage ELISAs were performed on 48 clones for each target, testing clones against all PLCγ SH2 domains to check for cross-binding. Only PLCγ1-T phage showed any binding to immobilised targets; all other plates showed no binding of phage to the intended target or cross-binding to other targets (data not shown).

Table 4.2. Colony numbers from phage display screening of BAP-tagged PLCγ SH2 domains. *Colony numbers on 10µl target (positive) plates and negative control plates were counted and total colony numbers for 8 ml cultures estimated for each PLCγ target, after three* ***(A)*** *and four* ***(B)*** *panning rounds. Successful amplifications of positive clones are highlighted in green. Panning was performed by student Grace Reddy.*

A Pan 3

Target	Positive	Negative
PLCγ1-T	6.59×10^6	4.80×10^4
PLCγ1-N	2.82×10^6	9.60×10^4
PLCγ2-T	1.02×10^7	2.64×10^5
PLCγ2-N	8.21×10^6	8.80×10^4
PLCγ2-C	2.40×10^4	7.20×10^4

B Pan 4

Target	Positive	Negative
PLCγ1-T	1.05×10^7	2.16×10^5
PLCγ1-N	2.94×10^6	$6.40\ 10^4$
PLCγ2-T	4.14×10^6	4.0×10^4
PLCγ2-N	1.44×10^7	$1.2\ 10^5$

A hit rate of 27% was seen in the PLCγ1-T ELISA (inclusion criteria being an absorbance value for the target ≥ 5x the value for the negative control, see Figure 4. 7). Most PLCγ1-T binding phage showed specificity for PLCγ1-T, with cross-binding to PLCγ1-N evident for some clones. However, cross-reactivity was expected as the tandem constructs contain both the -N and -C domains. As the PLCγ1-C SH2 was not available to test in this work, the apparent specificity of some clones for PLCγ1-T in the ELISA would suggest that these Affimer clones bind to the C-terminal SH2 domain of PLCγ1. A fourth panning round was then conducted on all PLCγ targets, excluding PLCγ2-C which had shown no amplification in colony numbers by pan three. Again, amplification was seen for all targets compared with the negative control plates, ranging from ca. 49 – 120-fold (Table 4.2B). Phage ELISAs were conducted on 48 clones for each SH2 and showed successful isolation of clones to all targets, however, with varying hit rates (Figure 4.8). Hit rates ranged from 4 – 88%, with both PLCγ1-T and PLCγ2-N showing lower hit rates than in their previous screens.

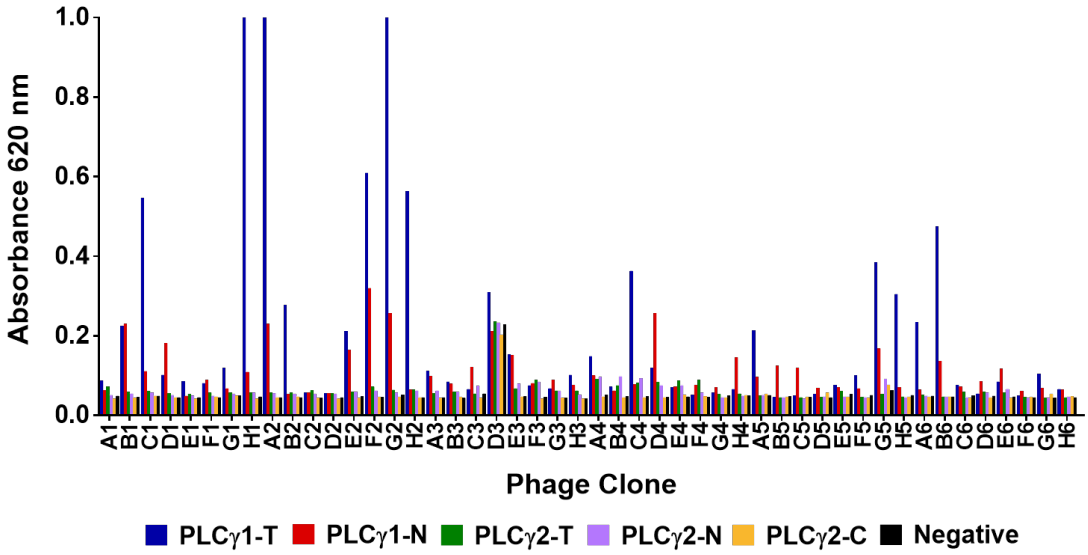

Figure 4.7. Phage ELISA testing binding of PLCγ1-T pan 3 phage clones to their target and cross-binding to other PLCγ SH2s. *Phage ELISA results from the pan 3 pool of the BAP-tagged PLCγ1-T SH2 screen. Phage clones were incubated in wells containing immobilised PLCγ1-T SH2 protein and bound phage were detected with anti-phage-HRP antibody after washing. HRP substrate TMB was added and absorbance read at 620 nm after 10 min, for 48 clones. Cross-binding to SH2 domains of PLCγ1-N, PLCγ2-T, PLCγ2-C and PLCγ2-N was also tested. Phage ELISA was performed by student Grace Reddy.*

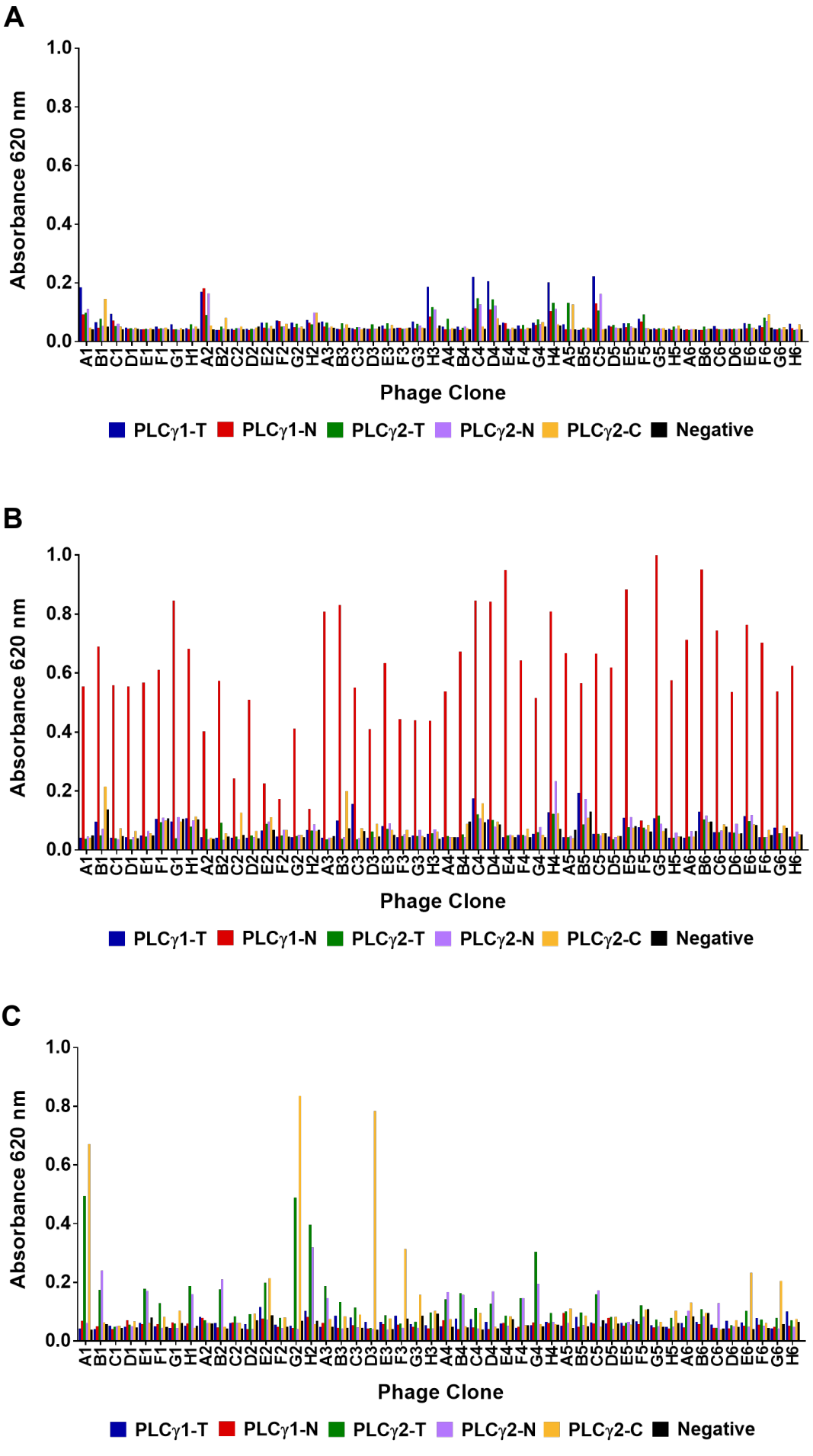
A
B
C
Absorbance 620 nm
1.0
0.8
0.6
0.4
0.2
0.0
A1 B1 C1 D1 E1 F1 G1 H1 A2 B2 C2 D2 E2 F2 G2 H2 A3 B3 C3 D3 E3 F3 G3 H3 A4 B4 C4 D4 E4 F4 G4 H4 A5 B5 C5 D5 E5 F5 G5 H5 A6 B6 C6 D6 E6 F6 G6 H6
Phage Clone
PLCγ1-T
PLCγ1-N
PLCγ2-T
PLCγ2-N
PLCγ2-C
Negative

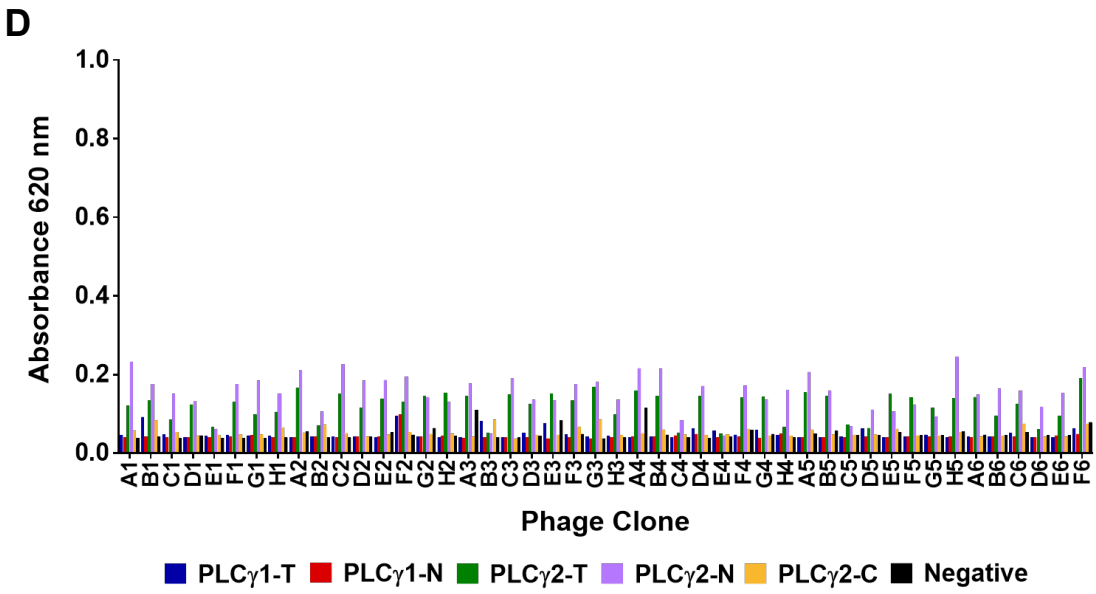

Figure 4.8. Phage ELISAs testing binding of PLCγ SH2 Affimer clones to their target and cross-binding to other PLCγ SH2s. *Phage ELISA results from the pan 4 pools of the BAP-tagged PLCγ SH2 screens;* ***(A)*** *PLCγ1-T,* ***(B)*** *PLCγ1-N,* ***(C)*** *PLCγ2-T, and* ***(D)*** *PLCγ2-N. Phage clones were incubated in wells containing immobilised PLCγ SH2 proteins and bound phage were detected with anti-phage-HRP antibody after washing. HRP substrate TMB was added and absorbance read at 620 nm after 10 min, for 48 clones per target. Cross-binding to SH2 domains of other PLCγ SH2s was also tested. Phage ELISAs were performed by student Grace Reddy.*

Specificity of clones also varied between targets, with all PLCγ1-T and PLCγ2-T clones showing cross-reactivity with other and PLCγ constructs, whilst PLCγ1-N phage showed high levels of specificity. PLCγ1T-A5 showed only binding to PLCγ2-T and PLCγ2-C, indicating this could be a PLCγ2 C-terminal binder. Additionally, clones PLCγ2T-A1 and PLCγ2T-G2 showed cross-binding to PLCγ2-C and another two clones, PLCγ2T-D3 and PLCγ2T-F3, showed specific binding to PLCγ2-C with no cross-binding to other SH2 domains. This indicated the isolation of PLCγ2-C binding clones despite the failure of the phage display screen for this target.

4.2.4.2 Grb and Ship SH2 domain screens

The Grb and Ship SH2 domains were also screened using the same protocol for three panning rounds. In parallel, a screen was performed on these targets that utilised standard pans throughout, instead of competitive panning for the second

and third pans. This was due to the relatively low colony numbers seen on positive plates during the PLCγ screens (compared with previous Affimer screens, data not published); it was thought that competitive panning could be too stringent for SH2 targets and could result in a loss of isolated clones.

This comparison of the two panning methods was used to determine which would isolate the greatest number of unique binders for SH2 domains. However, by pan three in the standard panning screens a substantial amplification in colony numbers (≥ 10x) was seen only for targets Grb7 and Ship1 when compared with negative plates (Table 4.3A). Amplification was much higher for competitive panning (ca. 176 – 676x), with all targets showing sufficient amplification (Table 4.3B). Clones from both screens for all targets were used for ELISAs, to further compare standard and competitive panning.

For each target, 48 clones were tested against all Grb family SH2s (including Grb2) and Ship SH2s. For Grb7 and Grb10, clones showed mostly specific binding with little or no cross-reactivity (Figure 4.9 and 4.10). Clone Grb10-G8 from standard panning appeared to bind Ship2 preferentially to Grb10, and one competitive clone (Grb10-E7) bound Grb7. Grb14 clones conversely showed

Table 4.3. Colony numbers from phage display screening of BAP-tagged Grb and Ship SH2 domains. *Estimated colony numbers for standard* ***(A)*** *and competitive panning* ***(B)*** *screens for Grb and Ship family SH2s after 3 panning rounds. Colonies counted on 10µl target (positive) plates and negative control plates, and total numbers for 8 ml cultures estimated for each target. Successful amplifications of positive clones are highlighted in green. * denotes too many colonies to count. Panning was performed by student Naomi Gibson.*

A

Pan 3 standard

Target	Positive	Negative
Grb7	7.32×10^6	2.80×10^5
Grb10	4.64×10^5	9.60×10^4
Grb14	1.96×10^6	2.32×10^5
Ship1	2.95×10^6	1.44×10^5
Ship2	3.52×10^5	2.08×10^5

B

Pan 3 comp

Target	Positive	Negative
Grb7	*	8.0×10^3
Grb10	3.29×10^6	$<8.0 \times 10^3$
Grb14	1.75×10^7	3.20×10^4
Ship1	5.41×10^6	8.0×10^3
Ship2	2.83×10^6	1.6×10^4

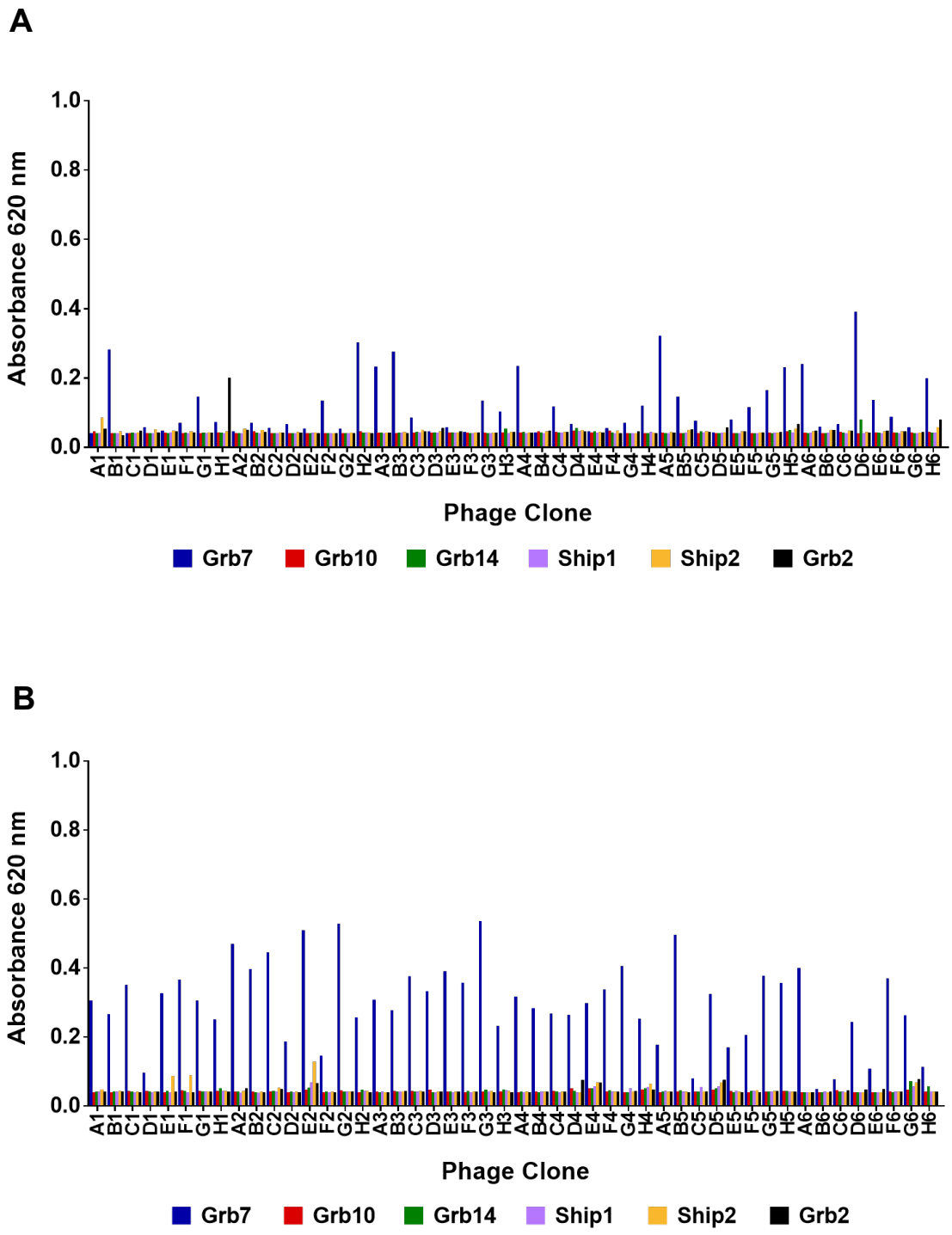

Figure 4.9. Phage ELISA testing binding of Grb7 Affimer clones to their target and family member SH2s. *Phage ELISA results testing the pan three pools from the BAP-tagged Grb7 SH2 standard panning screen* ***(A)*** *and competitive panning screen* ***(B)****. Phage clones were incubated in wells containing immobilised Grb7 SH2 protein and bound phage were detected with anti-phage-HRP antibody after washing. HRP substrate TMB was added and absorbance read at 620 nm after 10 min, for 48 clones. Cross-binding to SH2 domains of Grb10, Grb14, Grb2, Ship1 and Ship2 was also tested. ELISAs were performed by student Naomi Gibson.*

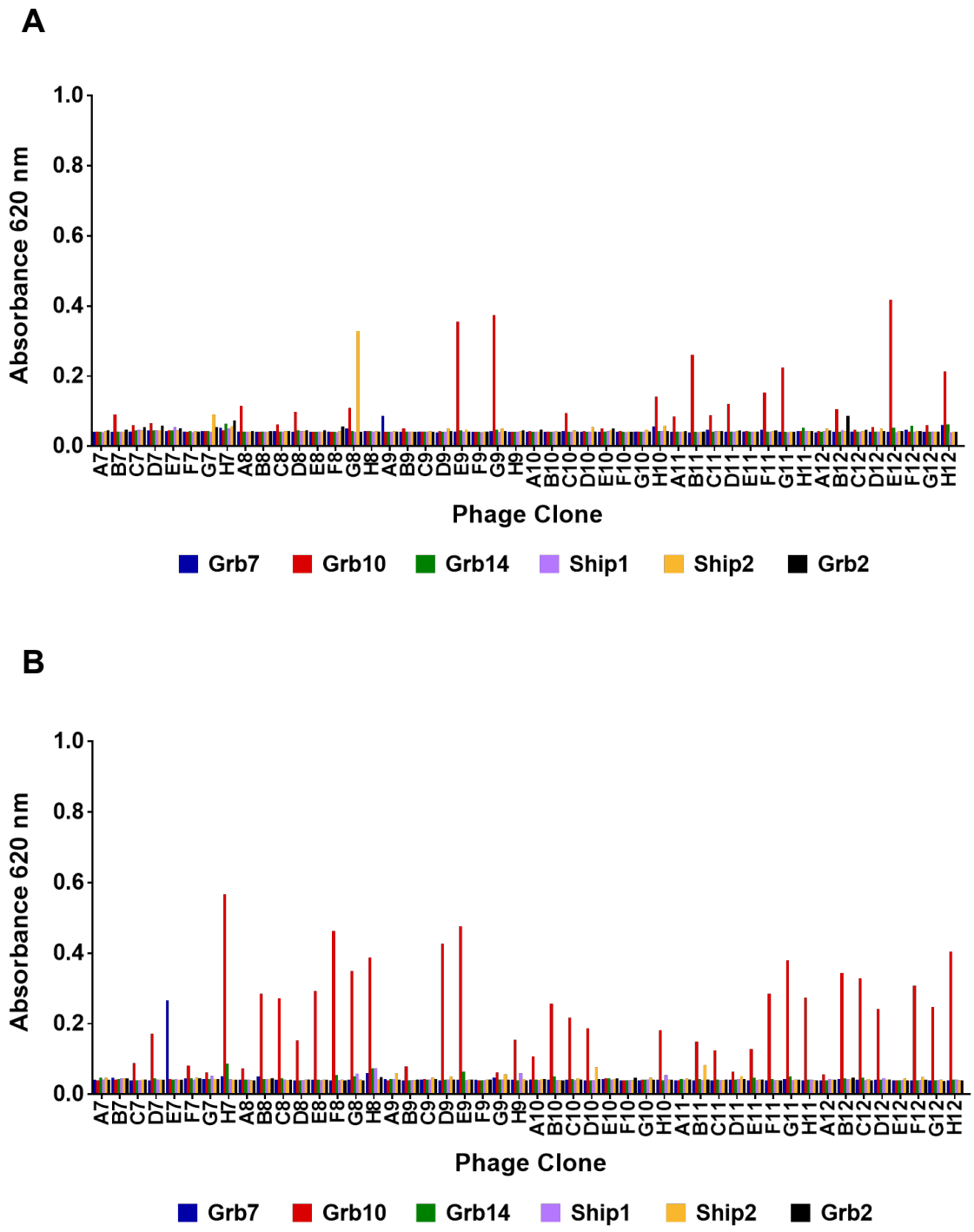

Figure 4.10. Phage ELISA testing binding of Grb10 Affimer clones to their target and family member SH2s. *Phage ELISA results testing the pan three pools from the BAP-tagged Gr10 SH2 standard panning screen* ***(A)*** *and competitive panning screen* ***(B)****. Phage clones were incubated in wells containing immobilised Grb10 SH2 protein and bound phage were detected with anti-phage-HRP antibody after washing. HRP substrate TMB was added and absorbance read at 620 nm after 10 min, for 48 clones. Cross-binding to SH2 domains of Grb7, Grb14, Grb2, Ship1 and Ship2 was also tested. ELISAs were performed by student Naomi Gibson.*

substantial cross-reactivity, particularly with Grb7 and Grb10 (Figure 4.11). The only clones that showed substantial absorbance values and bound specifically to Grb14 were standard panning clones Grb14-B3, Grb14-C3, Grb14-H5 and competitive panning clone Grb14-F3. ELISA hit rates for all Grb targets were much higher for clones from competitive panning (42 – 92%) compared with clones from standard panning (10 – 13%).

Ship1 phage from both screens showed high specificity for the Ship1 SH2 (Figure 4.12), with no cross-binding seen for any competitive phage clones. Similarly, Ship2 competitive panning phage displayed a high level of specificity with no cross-reactivity seen for any clones (Figure 4.13B). In contrast, Ship2 clones from standard panning showed much cross-reactivity, predominantly with Grb2 (Figure 4.13A). For both targets, hit rates were comparable between the two panning methods, with rates of 50 – 52% for Ship1 and 25% for both Ship2 screens.

Addition of the BAP tag for SH2 domain immobilisation had resulted in the successful screening of nine out of 10 targets; including those for which screening had previously failed. For most of these targets, competitive panning had shown superior results to standard panning in terms of colony amplification and number of hits in phage ELISAs. However, DNA sequencing to quantify the numbers of isolated clones was needed to complete the comparison of the two screening methods. Phage clones that were positive hits in the ELISAs were sent for DNA sequence analysis for all targets; for PLCγ SH2s this was 47 in total, up to 10 clones per target. For Grb and Ship families, a total of 237 clones were analysed, ranging from 34 to 61 clones per target. For targets PLCγ1-T, PLCγ2-T and PLCγ2-N, the criteria for sending a clone for analysis was lowered to include some showing a signal only ≥ 3x higher than background in the ELISA.

4.2.5 Alignments of the variable regions in PLCγ SH2-binding Affimer clones

DNA sequences of clones were translated to proteins and amino acid alignments of the VRs were performed using MacVector 13.5.2. For PLCγ1-T, a total of 13 unique sequences were identified; 10 from the pan three pool and three from the pan four pool. PLCγ1T-A5, the binder that had shown specificity for PLCγ2-T and

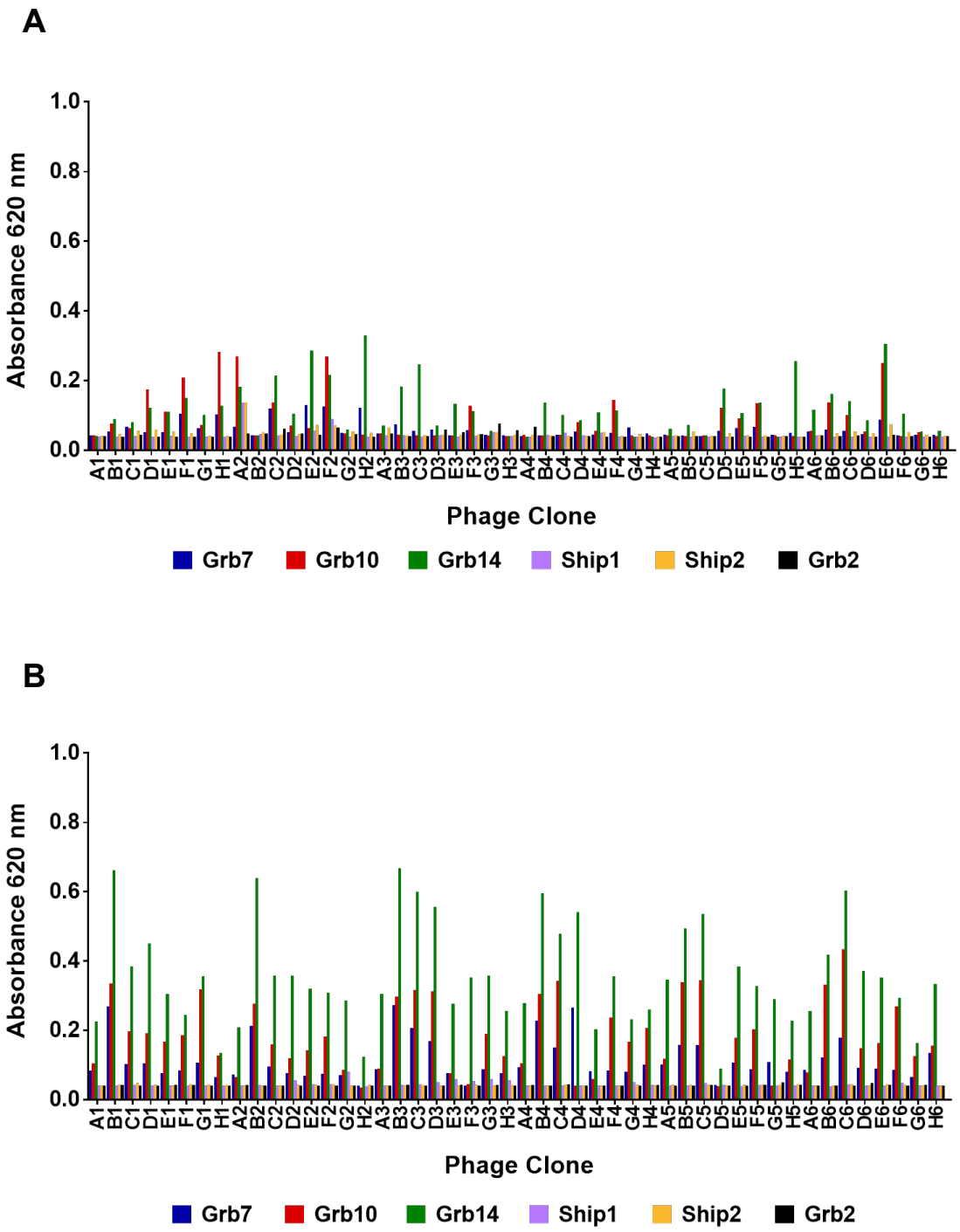

Figure 4.11. Phage ELISA testing binding of Grb14 Affimer clones to their target and family member SH2s. *Phage ELISA results testing the pan three pools from the BAP-tagged Gr14 SH2 standard panning screen* ***(A)*** *and competitive panning screen* ***(B)****. Phage clones were incubated in wells containing immobilised Grb14 SH2 protein and bound phage were detected with anti-phage-HRP antibody after washing. HRP substrate TMB was added and absorbance read at 620 nm after 10 min, for 48 clones. Cross-binding to SH2 domains of Grb7, Grb10, Grb2, Ship1 and Ship2 was also tested. ELISAs were performed by student Naomi Gibson.*

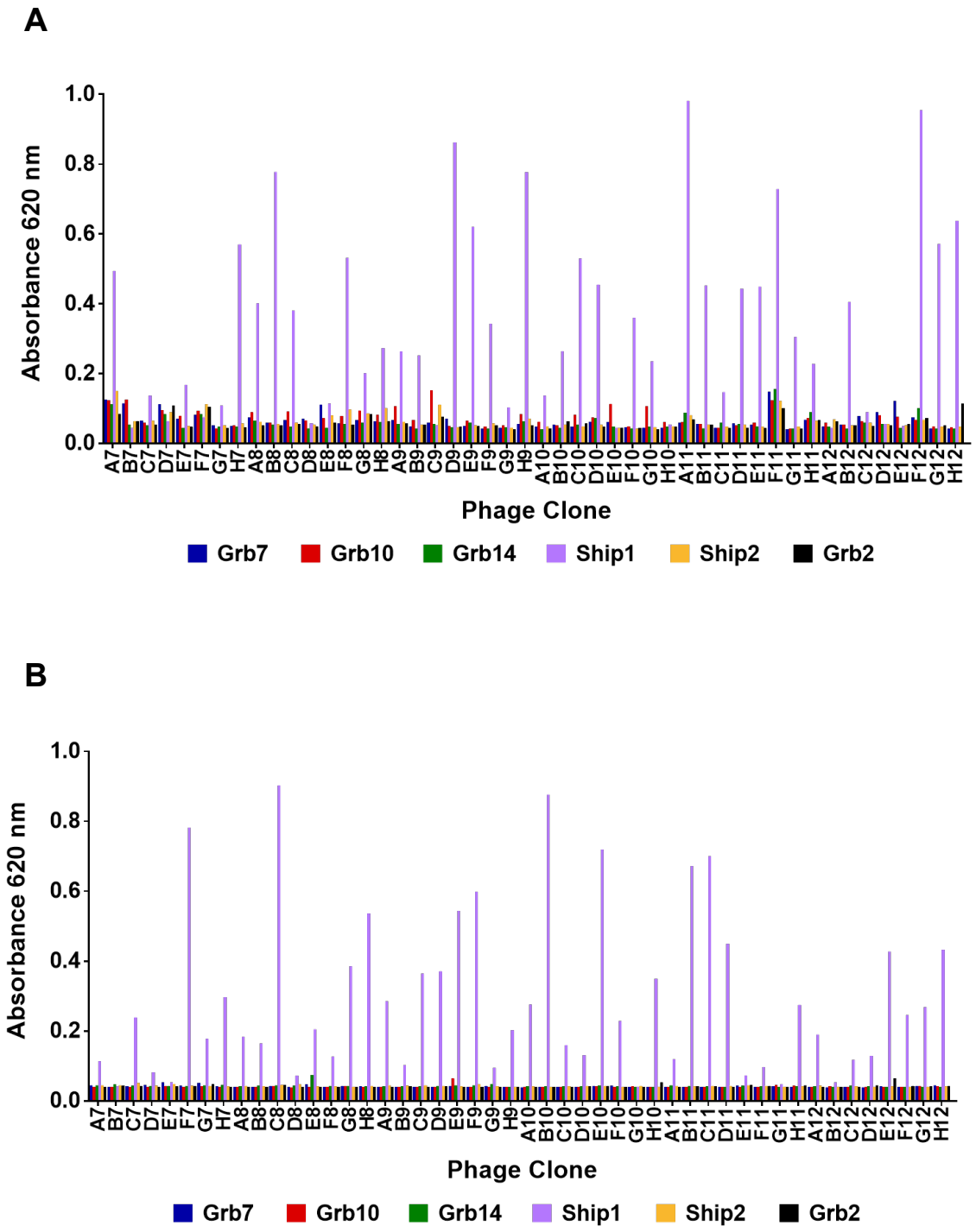

Figure 4.12. Phage ELISA testing binding of Ship1 Affimer clones to their target and cross-binding to other SH2s. *Phage ELISA results testing the pan three pools from the BAP-tagged Ship1 SH2 standard panning screen* ***(A)*** *and competitive panning screen* ***(B)****. Phage clones were incubated in wells containing immobilised Ship1 SH2 protein and bound phage were detected with anti-phage-HRP antibody after washing. HRP substrate TMB was added and absorbance read at 620 nm after 10 min, for 48 clones. Cross-binding to SH2 domains of Grb7, Grb14, Grb10, Grb2 and Ship2 was also tested. ELISAs were performed by student Naomi Gibson.*

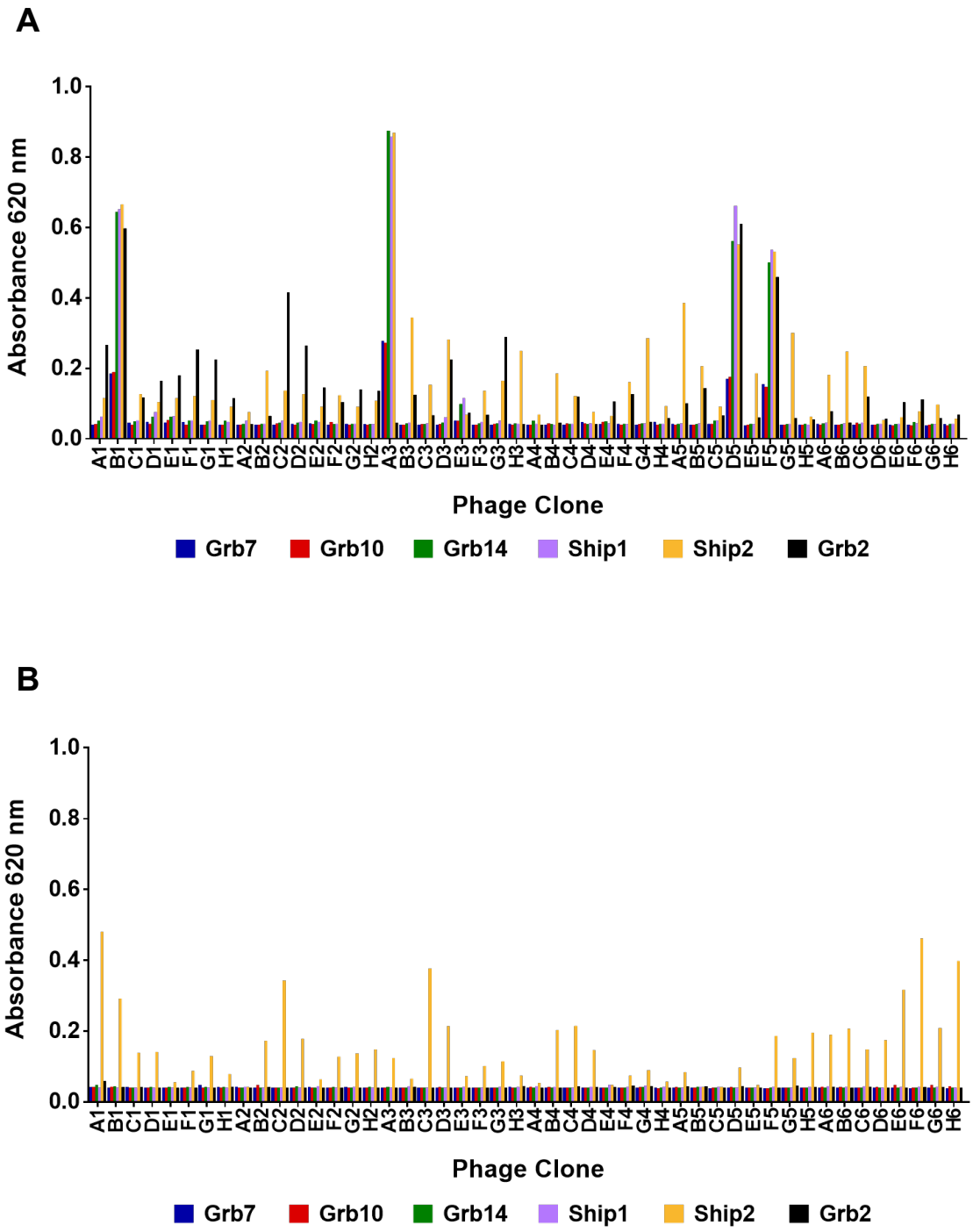

Figure 4.13. Phage ELISA testing binding of Ship2 phage clones to their target and family member SH2s. *Phage ELISA results testing the pan three pools from the BAP-tagged Ship2 SH2 standard panning screen* ***(A)*** *and competitive panning screen* ***(B)****. Phage clones were incubated in wells containing immobilised Ship2 SH2 protein and bound phage were detected with anti-phage-HRP antibody after washing. HRP substrate TMB was added and absorbance read at 620 nm after 10 min, for 48 clones. Cross-binding to SH2 domains of Grb7, Grb14, Grb10, Grb2 and Ship1 was also tested. ELISAs were performed by student Naomi Gibson.*

PLCγ2-C in the ELISA, was the only Type I scaffold. Interestingly, no binders from the pan three pool were the same as in the pan four pool. When clones from both pans were aligned, a consensus sequence of B-Ar-Hy-X-X-F-P (see abbreviations page) was revealed in the VR1 (Figure 4.14A). The pan four Type II clones, which both bound non-specifically to all PLCγ constructs in the phage ELISA (except PLCγ2-C) only contained the first part of the consensus sequence, and not the F-P residues. The specificities of PLCγ1-T clones determined in phage ELISA did not appear to correlate with any VR sequences, with both cross-reactive and specific clones sharing the consensus sequence in VR1. The PLCγ2-binding clone PLCγ1T-A5 only contained three amino acids corresponding to the consensus sequence.

Two unique clones, both from the Type II library, were found for PLCγ1-N; PLCγ1N-B7 which appeared nine times and PLCγ1N-E10 which appeared once (Figure 4.14B). Neither had been isolated in the PLCγ1-T screen. Although similarities were seen in VR1, no consensus was revealed upon alignment. Neither clones contained the B-Ar-Hy-X-X-F-P consensus seen in the PLCγ1-T clones, in either region. This was not surprising, as these clones had shown specificity for PLCγ1-N in the ELISA and did not bind to PLCγ1-T.

Three unique clones were identified from analysis of PLCγ2-T binders (Figure 4.15A). Clone PLCγ2T-D3, which was previously mentioned as binding specifically to PLCγ2-C in the ELISA, was the same as clone PLCγ2T-A1. PLCγ2T-A1 had shown binding to both PLCγ2-T and PLCγ2-C in the ELISA. The other 2 unique clones, which had shown binding to PLCγ2-N rather than PLCγ2-C, both contained the sequence Hx-X-Hx-X-Ac in their VR1.

Analysis of PLCγ2-N binders revealed eight unique clones. Binder PLCγ2N-C8 was identified as clone PLCγ2T-B1. A consensus of Ar-X-X-Ac was revealed in VR1 (Figure 4.15B), with five of the clones containing this sequence. Clone PLCγ2N-F8, which had additionally bound PLCγ1-T and PLCγ1-N in the ELISA, did not contain the consensus. In VR2, a motif of F/Y-Q/N was seen for the first two amino acids. No clones that had been identified in the non-BAP-tagged target screen were isolated in this screen. Only clone PLCγ2N-E3 from the non-BAP screen contained the Ar-X-X-Ac motif in VR1 and clone PLCγ2N-B8 was

A

	Clone	Type	VR 1	VR 2	Frequency
Pan 3:	PLCγ1T-A8	II	LKFLITNFP	KFPFNTDPI	1
	PLCγ1T-B8	II	YKLLMPAFP	NFDRHAIGR	2
	PLCγ1T-B10	II	YRFMITAMP	NGHKPIV	1
	PLCγ1T-C7	II	MRFVITNFP	YKNDKISDM	2
	PLCγ1T-C8	II	FMVTDFPQW	NGTRQMWVA	2
	PLCγ1T-C10	II	IGILMMQFP	KDINYKIIT	1
	PLCγ1T-E9	II	FRILMSGFP	QGPNAYEKF	1
	PLCγ1T-E10	II	VRFLFKTIP	HAPNHQGIT	1
	PLCγ1T-G9	II	TSEWIQSDL	KEYMANQIK	1
	PLCγ1T-G10	II	IKFVEFPQW	QKAHKAVMM	1
Pan 4:	PLCγ1T-A2	II	MKYISHEWTD	LMFNRDPPR	2
	PLCγ1T-C4	II	LHFSMDGGY	AMNWALREF	5
	PLCγ1T-A5	I	TKSGPFTFH	REIGKSRDV	1
		consensus:	BAHXXXFP ry		

B

Clone	Type	VR 1	VR 2	Frequency
PLCγ1N-B7	II	WMDNFWRRM	QVHGNPWMD	9
PLCγ1N-E10	II	HENTTFYSN	KYPHTWNIS	1

Figure 4.14. Isolation of PLCγ1 SH2-binding Affimer clones. ***(A)*** *Alignment of the variable regions (VRs) of the 13 unique PLCγ1-T Affimer clones, isolated from both pan 3 and pan 4 phage pools in the screen against the BAP-tagged SH2 domain. A consensus sequence can be seen in VR1 as follows; B – Ar – Hy – X – X – X – F – P, (Ar = aromatic residue, Hy = hydrophobic residue, X is any amino acid).* ***(B)*** *Alignment of VRs of the two unique PLCγ1-N SH2-binding Affimer clones isolated against the BAP-tagged SH2 domain. Alignments were performed using MacVector 13.5.2. Residues that conform to a consensus are in red.*

A

Clone	Type	VR 1	VR 2	Frequency
PLCγ2T-A1	II	HRWWYDNFV	LAGHYAPSV	3
PLCγ2T-B1	II	VIMLTWSPE	DQHMYEGWD	1
PLCγ2T-G4	II	QYMSITADD	YNYSRKRHN	1

B

Clone	Type	VR 1	VR 2	Frequency
PLCγ2N-A7	II	PWERIDISD	YQYYNNLKM	3
PLCγ2N-A8	II	HTFTWKWWY	NEDIESYEL	1
PLCγ2N-B7	II	VHWFRYDME	FQKRHYGIP	1
PLCγ2N-B11	II	RFVPEGLAE	YQDMFWGYN	1
PLCγ2N-B12	II	EGNFYWPDE	YQGWFQSWP	1
PLCγ2N-C8	II	VIMLTWSPE	DQHMYEGWD	1
PLCγ2N-F8	II	MEERISVDD	FNLIKWRRY	1
PLCγ2N-H8	II	QPHPRYDDD	FNYSQHWND	1
	consensus:	AXXA r c	AA rm	

Figure 4.15. Isolation of PLCγ2 SH2-binding Affimer clones. ***(A)*** *Alignment of the variable regions (VRs) of the three unique PLCγ2-T SH2-binding Affimer clones, isolated against the BAP-tagged SH2.* ***(B)*** *Alignment of the VRs of unique PLCγ2-N SH2-binding Affimer clones, isolated in the BAP-tagged SH2 screen. A consensus sequence can be seen in VR1 as follows; Ar – X – X – Ac (Ar = aromatic residue, Ac = acidic residue, X = any amino acid). Two conserved residues (Ar – Am) can also be seen in VR2 (where Am = Amide residue). Alignments were performed using MacVector 13.5.2. Residues that conform to a consensus are in red.*

the only clone to contain the F/Y-N/Q motif in VR2. Conversely, no clones isolated against the BAP-tagged PLCγ2-N contained the Y-X-W-Hy-X-X-Hy consensus seen in VR2 of the clones from the non-BAP-tagged screen. In total, 49 unique Affimer clones had been isolated against the PLCγ SH2s.

4.2.6 Alignments of the variable regions in Grb family SH2-binding Affimer clones

Forty-eight unique clones were identified by DNA analysis for the Grb7 SH2; 30 from competitive panning (Figure 4.16A) and 20 from standard panning (Figure 4.16B), with two clones appearing in both screens. All but one clone were the Type II scaffold. A conserved motif of Y-X-N was seen in VR2 of clones from both screens, with competitive clones containing this motif as part of a larger consensus sequence (I/L-Y-G-X-X-Y-X-N). For two standard panning clones Grb7-H1 and Grb7-A3, as well as competitive clone Grb7-D4, the Y-X-N motif was found in VR1 rather than VR2. Interestingly, clone Grb7-H1 had shown preferential binding to Grb2 in the phage ELISA. As the Affimer binders previously isolated against Grb2 (Chapter 3) also contained a conserved Y-X-N motif in VR1, this is not surprising.

A total of 12 unique Affimer clones were isolated against the Grb10 SH2; five from standard panning (Figure 4.17A) and nine from competitive panning (Figure 4.17B), with two clones appearing in both pools. Sequencing revealed that standard panning clone Grb10-G8, which had appeared to cross-bind to Ship2 in the ELISA, was the same as Grb10-H12, which was specific for Grb10. This indicates a possible contamination in well G8 and this was in fact a specific Grb10 binder. Additionally, competitive pan clone Grb10-E7, which had shown binding to Grb7 and not Grb10 in the phage ELISA, was identified as clone Grb7-H6 from the Grb7 standard panning. This Affimer was therefore excluded from future Grb10 binder analysis.

Another interesting result was standard pan clone Grb10-E9, which contained an extra five amino acids in VR1 (14 in total). Consensus sequences of Ar-X-X-X-X-X-Hy in VR1 of standard pan clones (Figure 4.17A) and W-X-F-P-X-A-Hy-M in VR1 of competitive pan clones (Figure 4.17B) were revealed. When final unique clones from both screens were aligned together, the consensus in VR2 was

A

Clone	Type	VR 1	VR 2	Frequency
Grb7-A1	II	PKYQRIDQP	WIYIGYDN	1
Grb7-B1	II	VSPFPMQQP	FIHGYAYAN	1
Grb7-C1	II	QASDRYWHS	DSEYANPIY	5
Grb7-E1	II	ADVSEWWRD	RLRMHGYDN	1
Grb7-F1	II	HNMMEPNE	FIYGHGYDN	1
Grb7-G1	II	RETVTWMPT	SIYGDDYDN	1
Grb7-H1	II	IIENGGWTL	NLFQRGYAN	1
Grb7-A2	II	PYGQSVTPG	FYFTNWYAN	1
Grb7-B2	II	HAVNGKWMA	KIYGPFYAN	1
Grb7-C2	II	EPKMSYAYY	RIYGKHYHN	1
Grb7-D2	II	QDAHMMLHT	FPYGYIYAN	1
Grb7-E2	II	PDAHLHESV	FPYGRYYSN	1
Grb7-G2	II	WQENNFGMQ	SGWYSNPQF	4
Grb7-A3	II	TVYPEHPWD	MPWMPYYQN	2
Grb7-B3	II	VHPYLHPYA	YLYGRDYEN	1
Grb7-C3	II	HIDADSKTS	RPYGFFYDN	1
Grb7-D3	II	GWKVGWGFE	YPYGEFYNN	1
Grb7-E3	II	ATFPHEYPV	NDCGAHYHN	2
Grb7-G3	II	QLSWGYPAT	YIYGPEYSN	1
Grb7-A4	II	VFHDTEDVI	SGWYANPQF	1
Grb7-C4	II	MTNQTHHWE	LIYGPYYNN	3
Grb7-D4	II	RWYENRFYP	GEERHAYLT	1
Grb7-E4	II	TNTNQHAPR	YLYGVTYDN	1
Grb7-H4	II	NNDGPNVYS	YPHGRWYAN	1
Grb7-A5	II	QQHWSKQHE	FHYYNYLSM	1
Grb7-C5	II	IMPQDTTIT	LIYAPWYHN	1
Grb7-D5	II	RQPYNQLHQ	FTYENYMEW	1
Grb7-G5	II	AVKVDVNSP	LLFGPMYNN	1
Grb7-H5	II	MWYEAKYDH	YPFGYYYNN	1
Grb7-G6	II	MKLMEPKEW	FLYGPYYNN	1
	consensus:		IYGXXYXN /L	

B

Clone	Type	VR 1	VR 2	Frequency
Grb7-F2	II	YLRDRHWAH	KIADINYAN	1
Grb7-H2	II	GMYPPEMWT	YLYGKKYAN	1
Grb7-E6	II	YYQQQSPGY	YPYGLFYAN	1
Grb7-C4	II	DAPNLPVAQ	NFYHQMYDN	1
Grb7-A4	II	HITQSKDLH	FLYGTMYQN	1
Grb7-F5	II	TVYPEHPWD	MPWMPYYQN	1
Grb7-D6	II	MWYEAKYDH	YPFGYYYNN	1
Grb7-H4	II	TKEKSIPQK	KFHHIYANG	1
Grb7-G3	II	WVEVWYGTH	EYSRAYSNP	1
Grb7-G1	II	WTWAGGYST	ASIYANPHL	1
Grb7-A5	II	ELMAMLRSE	NSLYANPIY	1
Grb7-B1	II	LEWDPQFST	DSYYDNPMY	1
Grb7-A6	II	FHYAMSEN	LSLYDNYPI	1
Grb7-H5	II	ADKSTRRRA	ASEYNNPIY	1
Grb7-H6	II	PPDHADRMD	NHYYSNPQY	1
Grb7-G5	II	EGMGDVRPE	NWYENYPEY	1
Grb7-H1	II	KYYQNMMLP	GFLMGMGHS	1
Grb7-B3	II	MHPAQPNVQ	NKMMHKYYE	1
Grb7-B5	II	TLSHVIKHP	DKKLNMYYE	1
Grb7-A3	I	PQPYANFIA	RSMFAPAEA	1
	consensus:		YXN	

Figure 4.16. Isolation of Grb7 SH2-binding Affimer clones. *Alignment of the variable regions (VRs) of unique Grb7 SH2-binding Affimer clones isolated using* ***(A)*** *competitive panning and* ***(B)*** *standard panning. A consensus sequence can be seen in VR2 of competitive clones as follows; I/L-Y-G-X-X-Y-X-N (X = any amino acid). A consensus of Y-X-N was also seen in VR2 of standard clones. Alignments were performed using MacVector 13.5.2. Residues that conform to a consensus are in red.*

A

Clone	Type	VR 1	VR 2	Frequency
Grb10-E9	II	MMWTEWEPELYVFG	KWPPMSQLM	3
Grb10-H10	II	TQQISYQRS	QWEWTMAVM	2
Grb10-A8	II	ASEGSQNWQ	SWMFPQALL	4
Grb10-G8	II	SSHFGESTI	DEFANTPWL	2
Grb10-F11	II	MEVFEWWKS	NVFGKAHFT	1
	consensus:		AXXXXXH r y	

B

Clone	Type	VR 1	VR 2	Frequency
Grb10-H7	II	MMWTEWEPELYVFG	KWPPMSQLM	8
Grb10-B8	II	SNGMAMAPH	KWYFPNAVM	4
Grb10-D7	II	RQESPMIRD	WWYFPSAIM	1
Grb10-H8	II	AQESMSDKT	VWYFTAAHM	1
Grb10-D9	II	SVTQPTRLQ	QWYFPMATM	2
Grb10-H10	II	KQGNSAKQT	DWSFQMAHM	1
Grb10-F12	II	HGHGGIQVE	EWSFKMAQL	1
Grb10-D12	II	GEQLKYQMS	DWMFPRAIL	1
Grb10-C10	II	ASEGSQNWQ	SWMFPQALL	3
	consensus:		WXFPXAHM y	

Figure 4.17. Isolation of Grb10 SH2-binding Affimer clones. *Alignment of the variable regions (VRs) of unique Grb10 SH2-binding Affimer clones isolated using* ***(A)*** *standard panning and* ***(B)*** *competitive panning. A consensus sequence can be seen in VR2 of standard clones as follows; Ar-X-X-X-X-X-Hy (Ar = aromatic residue, Hy = hydrophobic, X = any amino acid). In VR2 of competitive clones, the consensus was W-X-F-P-A-Hy-M. Alignments were performed using MacVector 13.5.2. Residues that conform to a consensus are in red.*

W-X-F-X-X-A-Hy-M. No Grb10 binders contained the Grb7 Y-X-N motif, which was expected as no cross-binding to Grb7 was seen with these clones in the phage ELISAs.

For the Grb14 SH2, seven unique clones were isolated. Standard panning yielded six clones (Figure 4.18A) and competitive panning three (Figure 4.18B). Alignment of the VRs revealed no consensus sequence in either region. However, three clones that showed specific binding to Grb14 in phage ELISA did share a conserved motif of Ar-Hy-X-B in VR2 (shown in red, Figure 4.18A). One clone (standard pan clone Grb14-H1/competitive pan clone Grb14-C3) appeared 39 times out of the 50 clones sequenced. This high occurrence suggests it is a potent binder, however it also showed cross-binding to Grb7 and Grb10 in the ELISAs. Standard pan clones Grb14-E2, Grb14-E3 and Grb14-H5 contained the Grb7-binding motif Y-X-N in one of their VRs, although Grb14-E3 and Grb14-H5 did not show any binding to Grb7 in the phage ELISA. In total, 67 unique clones were isolated against the Grb family SH2 domains (Grb7, 10 and 14), with the majority of those (48) raised against Grb7.

4.2.7 Alignments of the variable regions in Ship SH2-binding Affimer clones

Analysis of Ship1 SH2 pools revealed 16 unique clones isolated from standard panning (Figure 4.19A) and 13 from competitive (Figure 4.19B), with three repeated sequences; a total of 26 unique Affimer clones. Like the PLCγ and Grb family binders, these were mostly Type II scaffolds with the exception of five clones. Upon alignment, no consensus sequence was displayed in either VR.

A total of 27 unique clones were isolated against the Ship2 SH2; as with Ship1, 16 from standard panning (Figure 4.20A) and 13 from competitive (Figure 4.20B), with two sequences appearing in both pools. Unlike other targets, the majority of these Ship2 binders were from the Type I scaffold library.

Indeed, competitive panning exclusively isolated Type I Affimer reagents. Clones that had shown specific binding to Ship2 in the ELISA (Ship2-B2, -B4, -E5, -G4, -G5 and -H3) were all Type I, with the exception of Ship2-G5. A conserved feature of Ar-Hy was revealed in VR1 at amino acid positions four and five. No consensus was seen when split into cross-reactive and specific clones. In total,

A

Clone	Type	VR 1	VR 2	Frequency
Grb14-H1	II	EPKLYENQQ	PMVIPARWT	2
Grb14-B4	I	DPYSQE	QQRYIQHEWVWV	1
Grb14-H2	II	WEDWGW	ILNQKNRLK	2
Grb14-E2	II	PHPYISRE	FFYENNNTH	2
Grb14-E3	II	SDYHYGQPV	TYRPNYANR	2
Grb14-H5	II	TTMYSNGPY	TWLLHSEAR	1

B

Clone	Type	VR 1	VR 2	Frequency
Grb14-C3	II	EPKLYENQQ	PMVIPARWT	37
Grb14-F3	II	ARPEEPHWW	YKDNVYYFL	1
Grb14-D4	II	PHPYISRE	FFYENNNTH	2

Figure 4.18. Isolation of Grb14 SH2-binding Affimer clones. *Alignment of the variable regions (VRs) of unique Grb14 SH2-binding Affimer clones isolated using* ***(A)*** *standard panning and* ***(B)*** *competitive panning. Similar motifs in VR2 of three Grb14-specific binding clones are highlighted in red. Alignments were performed using MacVector 13.5.2.*

A

Clone	Type	VR 1	VR 2	Frequency
Ship1-H9	II	HELLTFLKY	SHRIINNLG	2
Ship1-C8	II	AHGPPDYHM	SIYFPMNYW	3
Ship1-F9	II	TLPYSLPGN	TQINFTMYI	4
Ship1-F11	II	FSFHSWSFQ	WQKYPFMLN	1
Ship1-F12	II	TWARYVWPQ	FNPWLHTNK	2
Ship1-D11	II	MYIGENLHW	WFFLLLGDL	1
Ship1-D9	II	VEYYDMTEL	WENRNFKSA	1
Ship1-A11	II	KEEWYPYQK	YLKAAFIEF	1
Ship1-D10	II	NADDRIEGE	FLKMLFGFM	1
Ship1-A8	II	VVEVKLLYD	RIRLRWTEH	3
Ship1-H11	II	SNAFTFTSQ	KIRAFWWPD	1
Ship1-G10	I	EAGNWN	KAWSSFPHLWEY	1
Ship1-F10	II	LTWESNLPY	VTWLYRGHSL	1
Ship1-H7	II	LSADTVYHS	EMMIWFINF	3
Ship1-E11	II	QAHVNISHS	EFRLMWPLL	1
Ship1-A7	II	YRRLLFFHH	APGNIIMIE	1

B

Clone	Type	VR 1	VR 2	Frequency
Ship1-H7	I	KHVFKIYTY	QAMEQYLHL	4
Ship1-A9	II	ADFHHNEWL	VPVKFYYVT	1
Ship1-G8	I	KYMQVRKFE	TEAQLFGVE	4
Ship1-B10	II	VEYYDMTEL	WENRNFKSA	4
Ship1-C7	I	QTGRMVPHE	LHFTGFWHG	1
Ship1-H8	II	HMLRTQQKY	PLFGLFFHI	1
Ship1-F7	I	RVGVWE	MHYIQVVNPFE	2
Ship1-B11	II	AMMPNLEDI	KEFFAVEWSR	1
Ship1-H9	II	IRPPPKPDY	TFTWFVQGK	1
Ship1-D9	II	QVMPDEPHG	EWMLHRHYL	1
Ship1-C8	II	HELLTFLKY	SHRIINNLG	1
Ship1-F10	I	ELMFHY	RHLPMAQGMSYT	1
Ship1-H11	II	YRRLLFFHH	APGNIIMIE	1

Figure 4.19. Isolation of Ship1 SH2-binding Affimer clones. *Alignment of the variable regions (VRs) of unique Ship1 SH2-binding Affimer clones isolated using* ***(A)*** *standard panning and* ***(B)*** *competitive panning. Alignments were performed using MacVector 13.5.2.*

A

Clone	Type	VR 1	VR 2	Frequency
Ship2-D2	I	GSSSFP	RWYYQGTMLWVT	1
Ship2-D3	I	SALYGE	WFTFINKSINYG	1
Ship2-B4	I	STYFGE	SMRITVNGWDTW	1
Ship2-C1	I	QFWDRY	RMEYSMKGVIMA	1
Ship2-B2	I	MGWQLN	HYKFHGSLVTVH	1
Ship2-A5	I	PTQPIM	LWEFTPNSTIVH	1
Ship2-C2	I	YSKYGD	NVMIVNARFHVK	1
Ship2-G4	I	RMFYGT	MMTWQDQVFDVT	1
Ship2-E5	I	KAYYGE	SVQVSQHMINVG	1
Ship2-G5	II	KYHDGYGPEPE	GLWWTPAHF	2
Ship2-B1	II	KAMMFSYYP	KYIRRFRTY	1
Ship2-F5	II	GWFFMGKRW	KPMILGIFR	1
Ship2-D5	II	VKHVWFRHR	SKGHILRHH	1
Ship2-B3	II	APHERRHHE	NRYLKIRIG	1
Ship2-A3	II	PPRQTLRRVK	SRRLMPQKW	1
Ship2-H3	I	QPLMFAGPT	MYVNTVYVG	1
	consensus:	AH ry		

B

Clone	Type	VR 1	VR 2	Frequency
Ship2-B2	I	VNDFIN	KFIYVNNRLNYS	1
Ship2-D6	I	DSQPVQ	TYRYFQEYVSIV	1
Ship2-G6	I	YTSPVA	HRWDRWQYHVV	1
Ship2-B6	I	RTPSGY	TVAWLNHQWHVG	1
Ship2-F5	I	ESFSIK	KIQWTQFGYQEQ	1
Ship2-C2	I	QGVYVD	NYMFTAAGWQHT	1
Ship2-H5	I	AGMYMD	QYKITTEGVKWD	2
Ship2-A6	I	IGHFND	WIRLQDRKYFHG	1
Ship2-E6	I	KGVFMH	SYQISQGHVAVF	1
Ship2-D2	I	MGWFGP	KAIVTPDYHASW	1
Ship2-C4	I	KAYYGE	SVQVSQHMINVG	1
Ship2-B1	I	RMFYGT	MMTWQDQVFDVT	2
Ship2-A1	I	NTHWDHQNY	IYKNWKLIG	4
	consensus:	AH ry		

Figure 4.20. Isolation of Ship2 SH2-binding Affimer clones. *Alignment of the variable regions (VRs) of unique Ship2 SH2-binding Affimer clones from standard panning* ***(A)*** *and competitive panning* ***(B)*** *screens. A conserved feature of Ar-Hy can be seen in VR1 of clones from both screens. Alignments were performed using MacVector 13.5.2. Residues conforming to the conserved residues are in red.*

53 unique clones were raised against the Ship SH2 domains.

Addition of the BAP tag for SH2 domain immobilisation had resulted in the successful screening for nine out of 10 SH2 targets. Although screening had failed for the isolated PLCγ2-C domain, two unique PLCγ2-C binding clones had been identified from both the PLCγ2-T (PLCγ2T-A1) and PLCγ1-T (PLCγ1T-A5) screens.

This strategy had therefore isolated reagents to all 10 SH2 domains tested in this work. For targets Grb7 and Grb10, more unique clones had been isolated in competitive panning than standard panning. The opposite was true for the other three targets Grb14, Ship1 and Ship2. However, overall the number of isolated clones remained similar between the two methods for each target, differing by a maximum of ten clones (Grb7 screen). Therefore, it was decided to continue using competitive panning for future SH2 domain screens. This was because the binders isolated by competitive panning had shown higher signals in phage ELISAs, which has previously correlated with a higher affinity binders. .

4.3 Phage display screening of 32 BAP-tagged SH2 domains

4.3.1 Production of BAP-tagged SH2 domains for screening

Addition of the BAP tag for immobilisation during phage display was performed as previously described (Chapter 2, section 2.2.4; see section 4.2.3) for 32 more SH2 domains (see Appendix B for all targets). pET28 vectors encoding these SH2 sequences with an N-terminal 6xHis-tag had been purchased from the Pawson Lab (Samuel Lunenfeld Research Institute, Canada).

For SH2s containing the BAP tag, protein production was carried out in Rosetta™ 2 (DE3) *E. coli*. A high-throughput method was utilised as only small yields of proteins were required for phage display screening. In this method, 3 ml cultures were induced with 0.5 mM IPTG overnight at 18 °C. His-tagged SH2 proteins were captured from culture lysates on a KingFisher™ Flex robotic platform using His Mag Sepharose Ni beads (GE Healthcare), washed and eluted in 130 µl Elution Buffer. The Elution Buffer also contained 1 mM TCEP HCl to reduce any disulphide bonds formed between cysteine residues in the SH2 proteins. This was because SH2 domains, which are usually found in proteins present the reducing cell cytoplasm, do not contain disulphide bonds

(with the exception of the Csk SH2 which was not present in the screened domains; Mills et al. 2007). It was desirable to keep the proteins in their natural conformation as much as possible for screening. Estimated total yields ranged from ca. 16 – 173 µg.

Elution samples were then subjected to western blot detection of biotin, to check successful *in vivo* biotinylation of proteins. These results can be seen in Chapter 3, section 3.6 (Figure 3.10); as this was the same batch of proteins that was used for specificity ELISAs on Grb2 Affimer clones. Biotinylated protein bands were observed corresponding to the theoretical MWs of all SH2 domains. For the majority, this was ca. 16 – 19 kDa; the Stat family SH2 constructs are much larger at ca. 63 – 70 kDa as explained in Chapter 3, section 3.6. Although some SH2 domains show almost undetectable signals, bands were revealed when the membrane was overexposed. In addition to western blot analysis, an ELISA was conducted on the BAP-tagged SH2 domains to check that the proteins could be efficiently captured on streptavidin-coated wells used in phage display (see section 4.2.3). Proteins were captured onto streptavidin-coated wells via the BAP tag, and detected via the His-tag with an anti-His HRP-conjugated antibody. As seen in Figure 4.21, all constructs showed signals above that of the streptavidin-

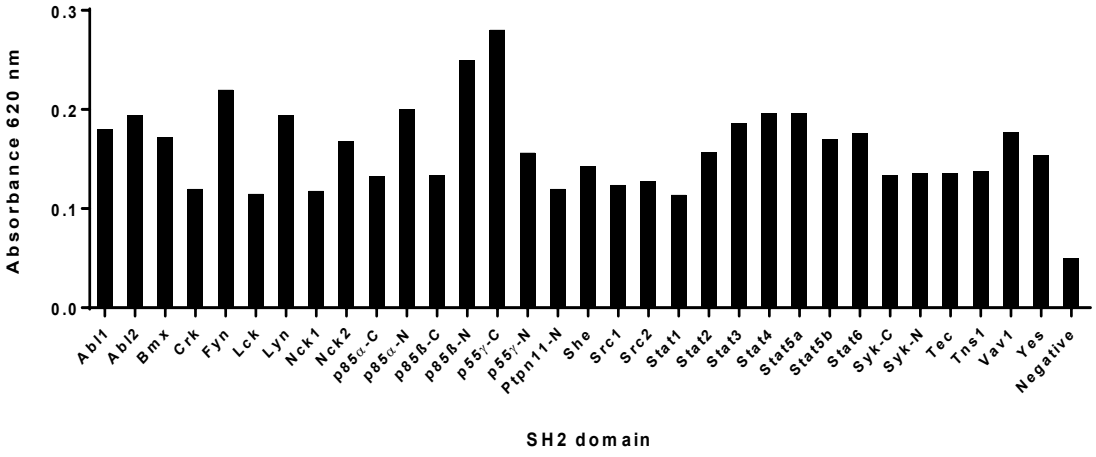

Figure 4.21. Immobilisation of BAP-tagged SH2 domain proteins on streptavidin-coated plates. *ELISA to check successful capture of biotinylated BAP-tagged SH2 proteins on the streptavidin-coated wells used in phage display. 10 µl SH2 protein elutions were incubated in streptavidin-coated wells for 1 h at room temperature. After 6x washes, captured SH2 domains were detected via the His-tag with 1:1000 Anti-His-HRP. HRP was detected using TMB substrate and absorbance measured at 620 nm. Streptavidin-only well was used as the negative control.*

only control well. This indicated successful capture of the biotinylated His-tagged SH2 proteins on the surface, though this experiment was conducted only once.

4.3.2 Phage display screening of BAP-tagged SH2s and ELISA results

In these SH2 screens, another phage library was also screened in addition to the Type I and II libraries; namely the single-VR1 Type II library. In this library, VR1 contains nine variable amino acids as with the original Type II library, but VR2 has been replaced with the three amino acids A-A-E to remove the second binding region. This library had not been created when the previous SH2 screens were performed; it was decided to include it for the large-scale screen to expand the variety of Affimer clones available. This library had also shown favourable results compared with the two-loop Type II library for some targets in initial screens (data not published).

The screens were conducted as previously described for BAP-tagged PLCγ, Grb and Ship SH2s, including the addition of Rosetta™ 2 (DE3) lysate in the pre-panning steps for all panning rounds (see section 4.2.4). Competitive pans were conducted in second and third panning rounds. This work was carried out by the candidate and Dr Christian Tiede of the Tomlinson group. Target protein production, confirmation of botinylation and testing immobilisation to streptavidin-coated wells was carried out by the candidate. Phage display screening and phage ELISAs were conducted by the candidate and Dr Tiede concurrently, on an equal number of targets.

Pan three plates showed a substantial amplification in colony numbers (≥ 10x negative plate) for 18 of the targets (Table 4.4A). Colony numbers were low for some targets, but amplification compared with negative plates was still notable. For the 14 targets in which sufficient amplification in colony numbers had not been achieved, a fourth panning round was conducted as for the PLCγ proteins. After this, colony amplification was seen for only six of these targets, with eight failing (Lck, Ptpn11-N, Src1, Src2, Syk-C, Syk-N, Stat2 and Yes; Table 4.4B). For most, failure of the screen correlated with low protein concentration, the exceptions being Lck and Syk-C.

Table 4.4. Colony numbers from phage display screening of BAP-tagged SH2 domains. *Colony numbers on 10µl target (positive) plates and negative control plates were counted and total colony numbers for 8 ml cultures estimated for each SH2 target, after three **(A)** and four **(B)** panning rounds. Successful amplifications of positive clones are highlighted in green. Panning was performed by the candidate in conjunction with Dr Christian Tiede.*

A

SH2 target	Positive	Negative
Abl1	1.19×10^7	4.16×10^4
Abl2	5.89×10^7	4.99×10^5
Bmx	2.38×10^7	9.12×10^4
Crk	5.47×10^7	9.44×10^4
Fyn	8.32×10^6	3.62×10^5
Lck	2.56×10^5	1.78×10^5
Lyn	1.28×10^5	7.28×10^4
Nck1	2.32×10^5	4.64×10^4
Nck2	1.20×10^5	6.40×10^4
p85α-C	2.24×10^5	4.56×10^4
p85α-N	1.54×10^7	1.79×10^5
p85β-C	1.12×10^5	2.26×10^5
p85β-N	1.92×10^7	2.24×10^5
p55γ-C	3.52×10^5	2.03×10^5
p55γ-N	9.50×10^7	1.09×10^5
Ptpn11-N	3.20×10^4	3.20×10^4
She	1.79×10^5	2.40×10^3
Src1	8.00×10^2	1.60×10^3
Src2	8.00×10^2	1.60×10^3
Stat1	2.56×10^5	3.20×10^3
Stat2	9.60×10^3	3.20×10^3
Stat3	$>8.00 \times 10^6$	8.00×10^2
Stat4	$>8.00 \times 10^6$	8.00×10^2
Stat5a	2.72×10^5	1.60×10^3
Stat5b	4.48×10^5	3.20×10^3
Stat6	2.56×10^4	2.40×10^3
Syk-C	4.80×10^3	8.00×10^2
Syk-N	1.60×10^3	4.00×10^3
Tec	3.76×10^4	1.60×10^3
Tns-1	4.48×10^5	4.00×10^3
Vav1	8.00×10^6	3.20×10^3
Yes	9.60×10^3	2.40×10^3

B

SH2 target	Positive	Negative
Lck	2.48×10^6	4.70×10^5
Lyn	8.00×10^6	1.47×10^5
Nck1	1.05×10^7	7.20×10^4
Nck2	4.96×10^6	2.27×10^5
p85α-C	6.24×10^6	2.88×10^5
p85β-C	1.54×10^7	1.76×10^5
p55γ-C	3.04×10^6	3.84×10^4
Src1	3.12×10^4	4.00×10^4
Ptpn11-N	6.56×10^5	2.82×10^5
Src2	6.72×10^6	7.36×10^5
Syk-C	9.68×10^4	2.16×10^4
Syk-N	1.36×10^6	4.32×10^5
Stat2	3.76×10^4	3.44×10^4
Yes	2.72×10^5	1.12×10^5

Phage ELISAs were conducted on 48 clones per target for the other 24 SH2 domains that had been successfully screened; the exception being Stat6 for which only 24 clones were available on the positive plate. Owing to the large number of ELISAs conducted, specificity of clones was not tested at this stage, rather each clone was tested against a target-coated well and a streptavidin-only well as a control.

Hit rates in ELISAs varied from 0 – 100%, with the target Nck2 showing no positive hits. Targets Stat1, Stat5a, Stat6 and Tns1 also showed no positive hits when following the criteria of signal ≥ 5x that of the negative control well. However, when the threshold was lowered to ≥ 3x that of the negative control, hit rates for these targets were raised to 2% for Stat1 (one hit), 29% for Stat5a, 4% for Stat6 (one hit) and 38% for Tns1.

ELISA signals for most of these targets were low across all phage clones tested, suggesting possible degradation or poor immobilisation of the target in these cases. For some, poor ELISA results did correlate with low protein concentration. Targets with the highest hit rates included Abl2 (100%), p55γ-N (100%), Bmx (98%) and p85β-N (98%). For over half of the targets the hit rates were ≥ 50%. Results from each target ELISA can be seen in Figure 4.22.

Four targets for which either the screen or phage ELISA had failed were successfully re-screened after production of new batches of protein; Lck, Nck2, Src1 and Syk-N. Four pans were conducted on all targets, showing colony amplification for all cases. For Lck, the number of colonies on the positive plate was very high, so 96 clones were tested in the ELISA. For the other targets, 48 clones were tested as standard. ELISA hit rates varied from 15% (Nck2) to 91% (Lck) (Figure 4.23).

In total, phage display screening was successful for 27 out of the 32 SH2 domains. For most of these targets, stab plate cultures containing all 48 clones were sent for DNA sequence analysis . For targets that had shown considerably lower hit rates, such as Lyn, Nck2, Src1, Stats 5a - 6 and Tec, fewer clones were analysed.

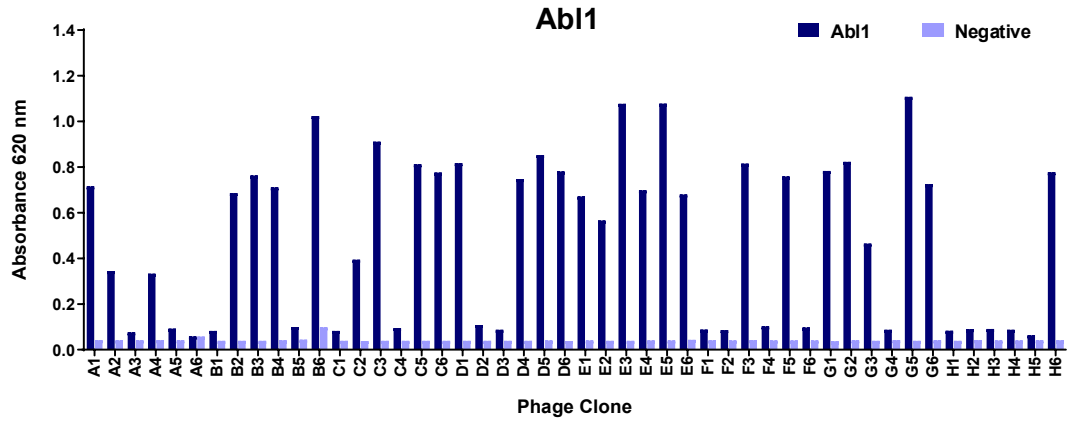
Abl1
Abl1
Negative
Absorbance 620 nm
Phage Clone

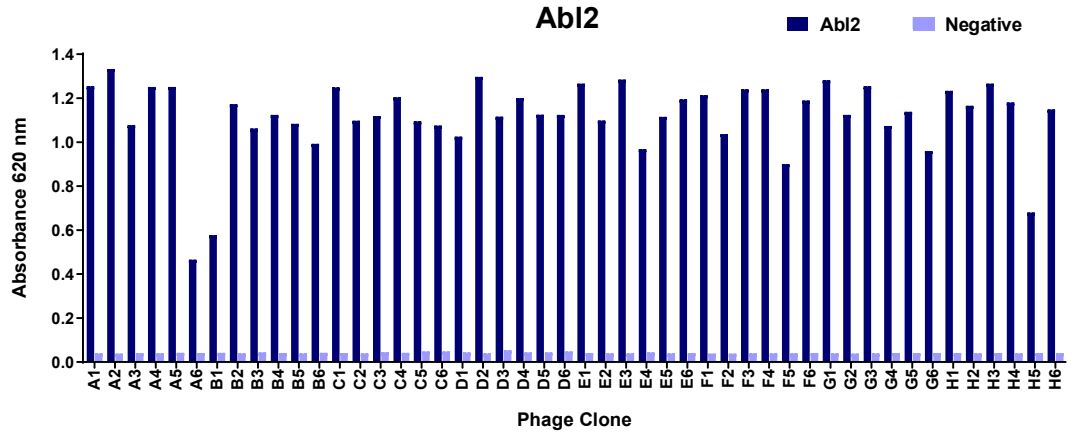
Abl2
Abl2
Negative
Absorbance 620 nm
Phage Clone

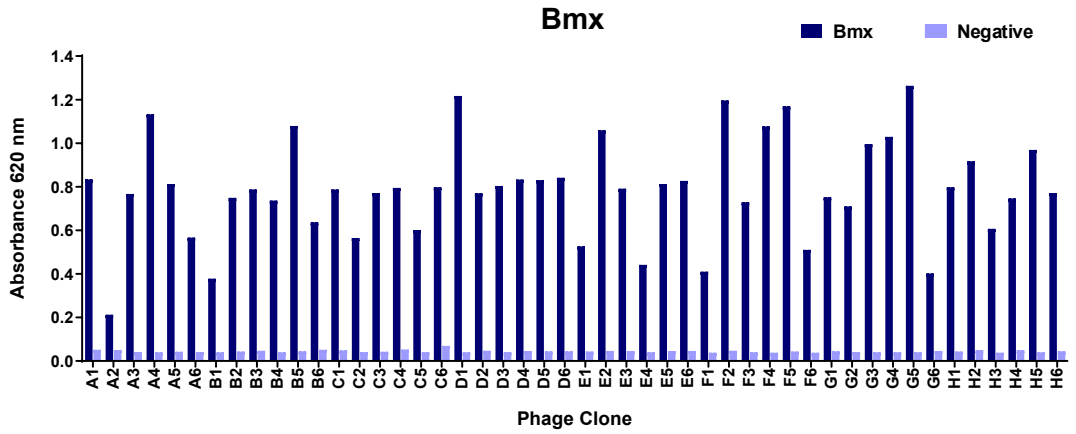
Bmx
Bmx
Negative
Absorbance 620 nm
Phage Clone

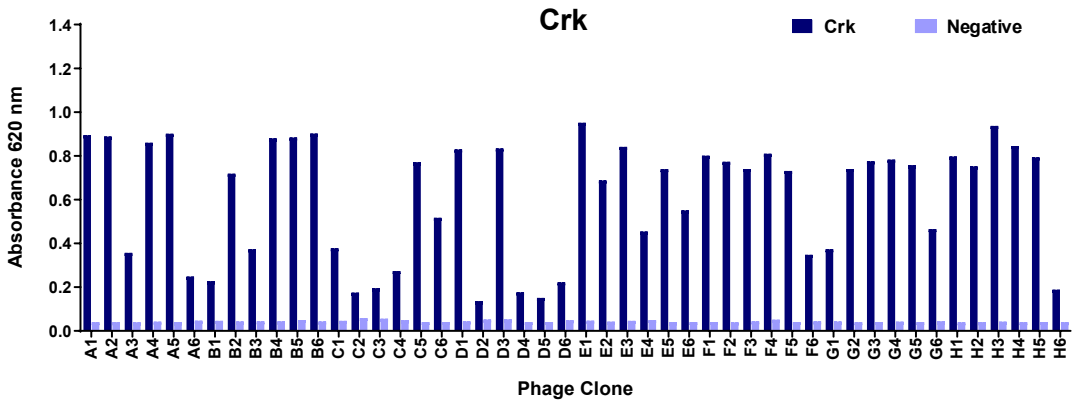
Crk
Crk
Negative
Absorbance 620 nm
Phage Clone

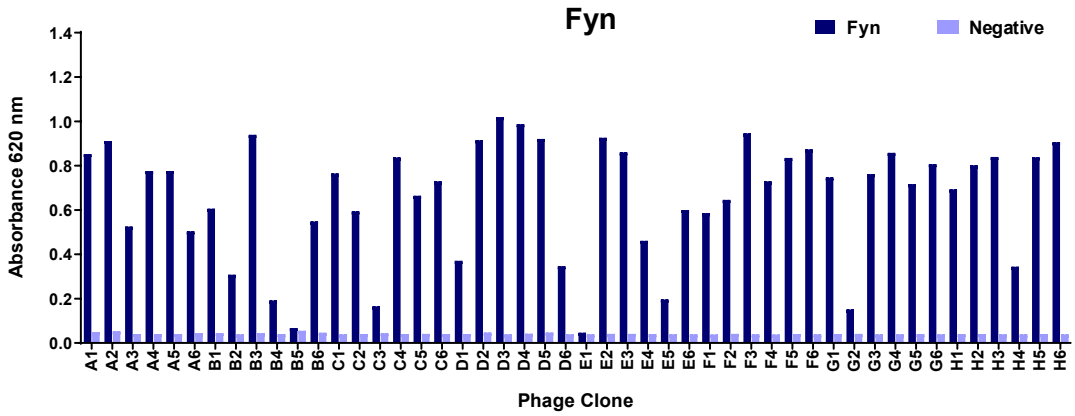
Fyn
Fyn
Negative
Absorbance 620 nm
1.4
1.2
1.0
0.8
0.6
0.4
0.2
0.0
A1 A2 A3 A4 A5 A6 B1 B2 B3 B4 B5 B6 C1 C2 C3 C4 C5 C6 D1 D2 D3 D4 D5 D6 E1 E2 E3 E4 E5 E6 F1 F2 F3 F4 F5 F6 G1 G2 G3 G4 G5 G6 H1 H2 H3 H4 H5 H6
Phage Clone

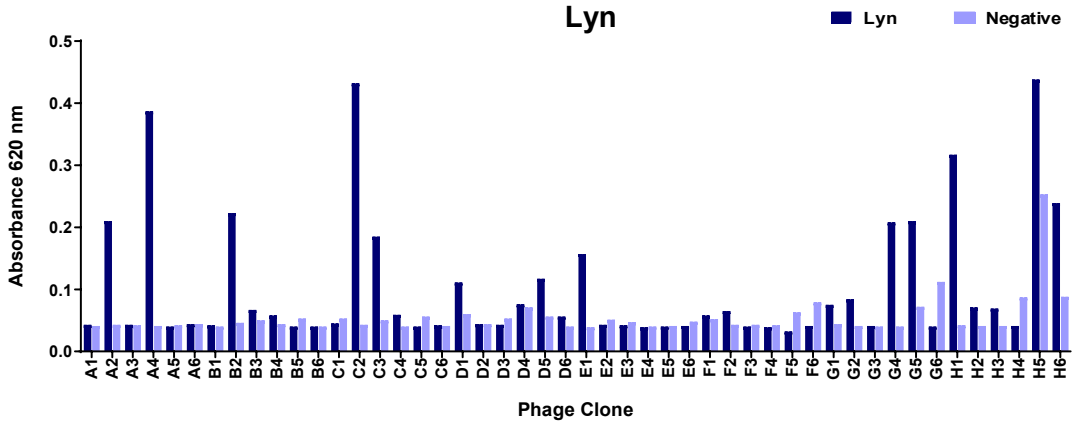
Lyn
Lyn
Negative
Absorbance 620 nm
0.5
0.4
0.3
0.2
0.1
0.0
A1 A2 A3 A4 A5 A6 B1 B2 B3 B4 B5 B6 C1 C2 C3 C4 C5 C6 D1 D2 D3 D4 D5 D6 E1 E2 E3 E4 E5 E6 F1 F2 F3 F4 F5 F6 G1 G2 G3 G4 G5 G6 H1 H2 H3 H4 H5 H6
Phage Clone

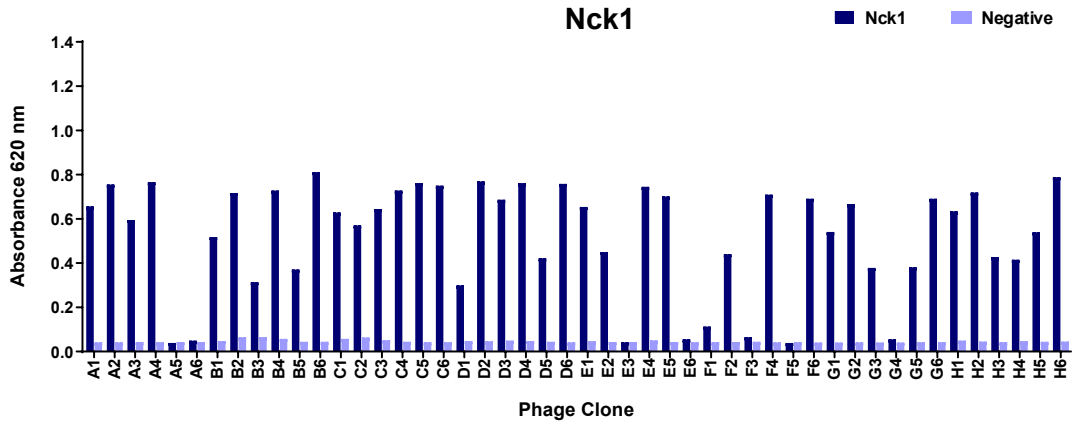
Nck1
Nck1
Negative
Absorbance 620 nm
1.4
1.2
1.0
0.8
0.6
0.4
0.2
0.0
A1 A2 A3 A4 A5 A6 B1 B2 B3 B4 B5 B6 C1 C2 C3 C4 C5 C6 D1 D2 D3 D4 D5 D6 E1 E2 E3 E4 E5 E6 F1 F2 F3 F4 F5 F6 G1 G2 G3 G4 G5 G6 H1 H2 H3 H4 H5 H6
Phage Clone

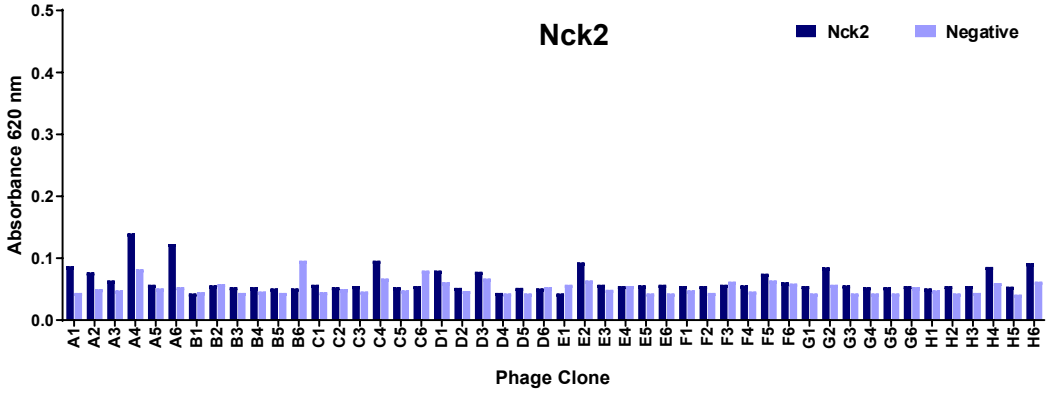
Nck2
Nck2
Negative
Absorbance 620 nm
0.5
0.4
0.3
0.2
0.1
0.0
A1 A2 A3 A4 A5 A6 B1 B2 B3 B4 B5 B6 C1 C2 C3 C4 C5 C6 D1 D2 D3 D4 D5 D6 E1 E2 E3 E4 E5 E6 F1 F2 F3 F4 F5 F6 G1 G2 G3 G4 G5 G6 H1 H2 H3 H4 H5 H6
Phage Clone

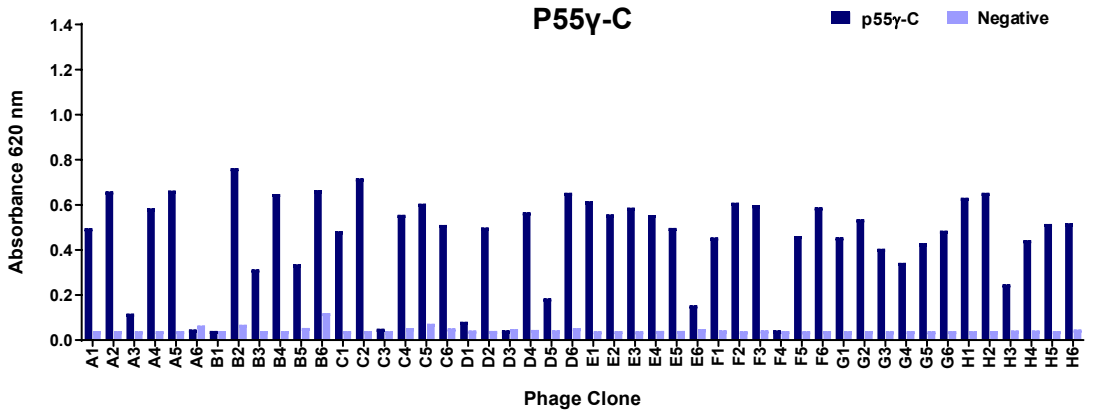
P55γ-C
p55γ-C
Negative
Absorbance 620 nm
Phage Clone

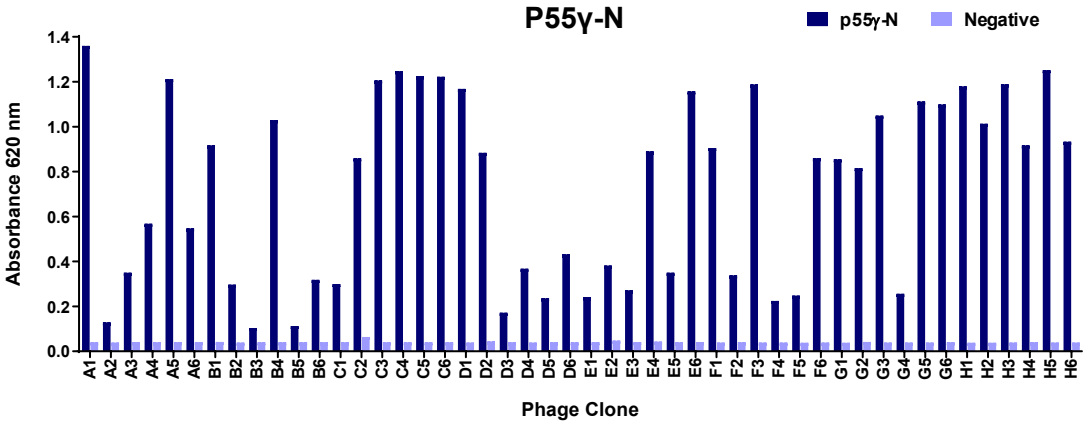
P55γ-N
p55γ-N
Negative
Absorbance 620 nm
Phage Clone

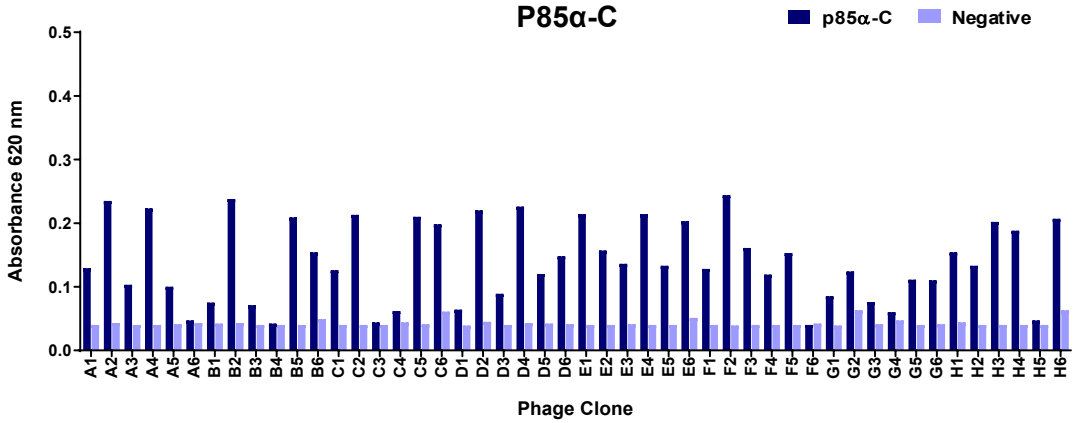
P85α-C
p85α-C
Negative
Absorbance 620 nm
Phage Clone

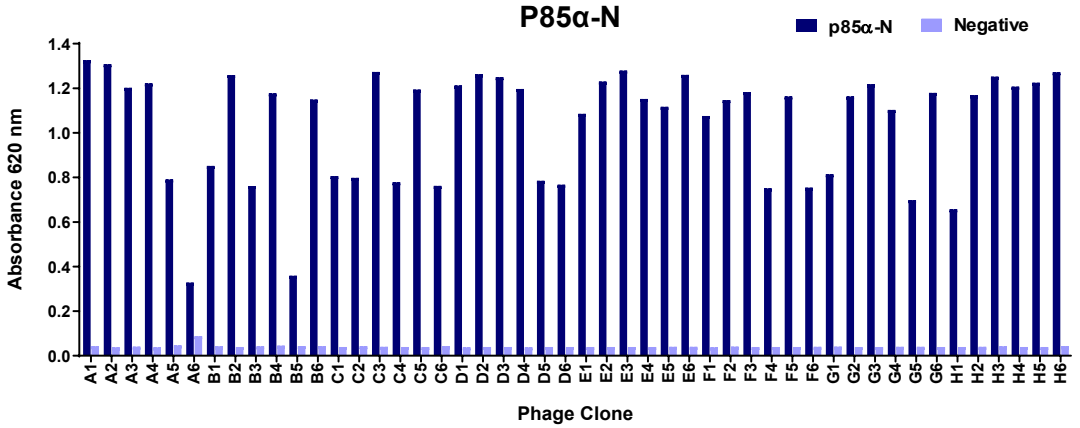
P85α-N
p85α-N
Negative
Absorbance 620 nm
Phage Clone

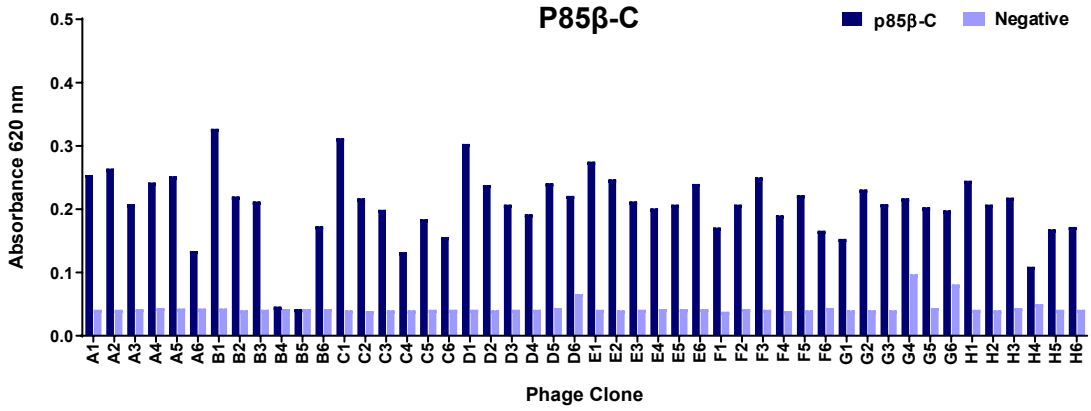
P85β-C
p85β-C
Negative
Absorbance 620 nm
0.0
0.1
0.2
0.3
0.4
0.5
A1 A2 A3 A4 A5 A6 B1 B2 B3 B4 B5 B6 C1 C2 C3 C4 C5 C6 D1 D2 D3 D4 D5 D6 E1 E2 E3 E4 E5 E6 F1 F2 F3 F4 F5 F6 G1 G2 G3 G4 G5 G6 H1 H2 H3 H4 H5 H6
Phage Clone

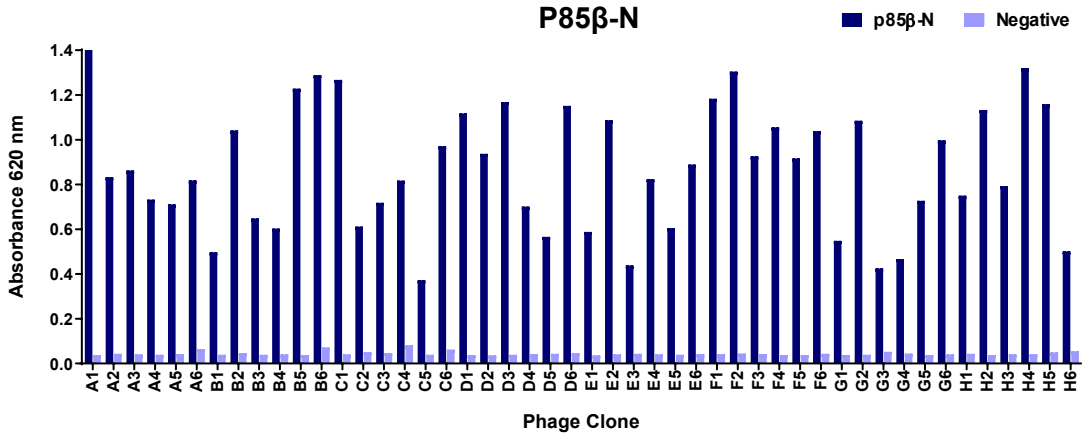
P85β-N
p85β-N
Negative
Absorbance 620 nm
0.0
0.2
0.4
0.6
0.8
1.0
1.2
1.4
A1 A2 A3 A4 A5 A6 B1 B2 B3 B4 B5 B6 C1 C2 C3 C4 C5 C6 D1 D2 D3 D4 D5 D6 E1 E2 E3 E4 E5 E6 F1 F2 F3 F4 F5 F6 G1 G2 G3 G4 G5 G6 H1 H2 H3 H4 H5 H6
Phage Clone

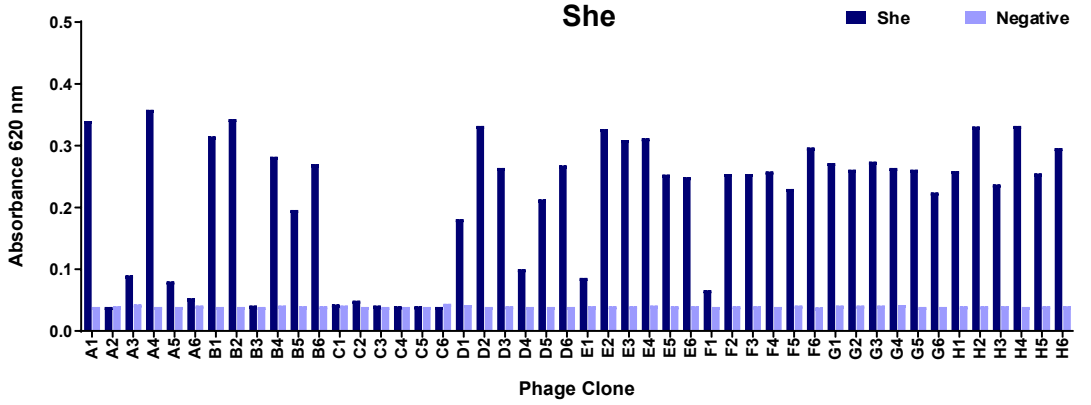
She
She
Negative
Absorbance 620 nm
0.0
0.1
0.2
0.3
0.4
0.5
A1 A2 A3 A4 A5 A6 B1 B2 B3 B4 B5 B6 C1 C2 C3 C4 C5 C6 D1 D2 D3 D4 D5 D6 E1 E2 E3 E4 E5 E6 F1 F2 F3 F4 F5 F6 G1 G2 G3 G4 G5 G6 H1 H2 H3 H4 H5 H6
Phage Clone

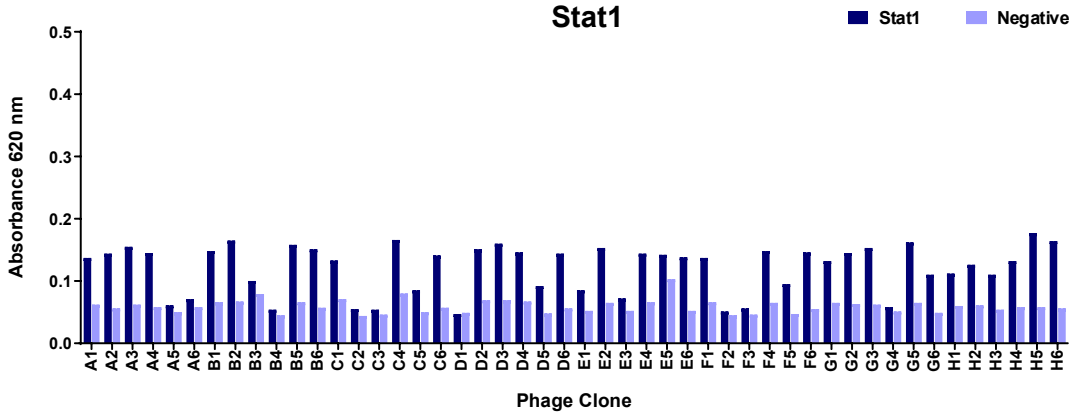
Stat1
Stat1
Negative
Absorbance 620 nm
0.0
0.1
0.2
0.3
0.4
0.5
A1 A2 A3 A4 A5 A6 B1 B2 B3 B4 B5 B6 C1 C2 C3 C4 C5 C6 D1 D2 D3 D4 D5 D6 E1 E2 E3 E4 E5 E6 F1 F2 F3 F4 F5 F6 G1 G2 G3 G4 G5 G6 H1 H2 H3 H4 H5 H6
Phage Clone

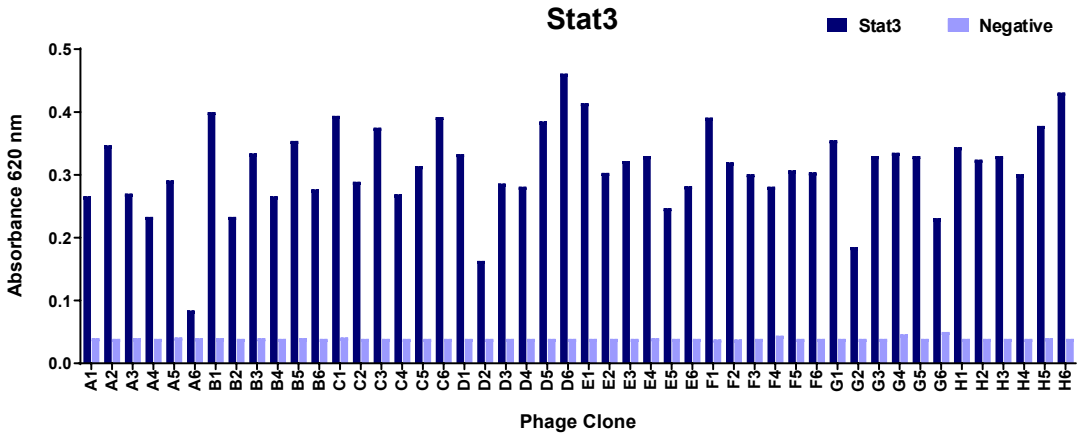
Stat3
Stat3
Negative
Absorbance 620 nm
0.5
0.4
0.3
0.2
0.1
0.0
A1 A2 A3 A4 A5 A6 B1 B2 B3 B4 B5 B6 C1 C2 C3 C4 C5 C6 D1 D2 D3 D4 D5 D6 E1 E2 E3 E4 E5 E6 F1 F2 F3 F4 F5 F6 G1 G2 G3 G4 G5 G6 H1 H2 H3 H4 H5 H6
Phage Clone

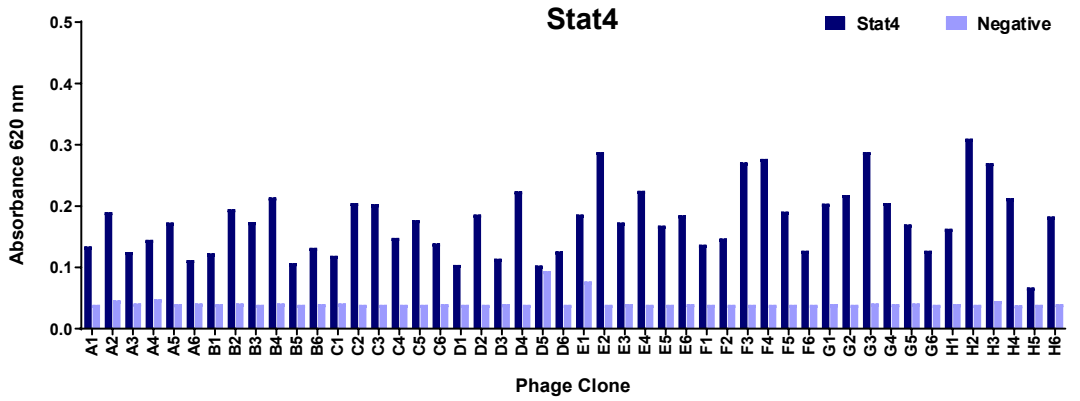
Stat4
Stat4
Negative
Absorbance 620 nm
0.5
0.4
0.3
0.2
0.1
0.0
A1 A2 A3 A4 A5 A6 B1 B2 B3 B4 B5 B6 C1 C2 C3 C4 C5 C6 D1 D2 D3 D4 D5 D6 E1 E2 E3 E4 E5 E6 F1 F2 F3 F4 F5 F6 G1 G2 G3 G4 G5 G6 H1 H2 H3 H4 H5 H6
Phage Clone

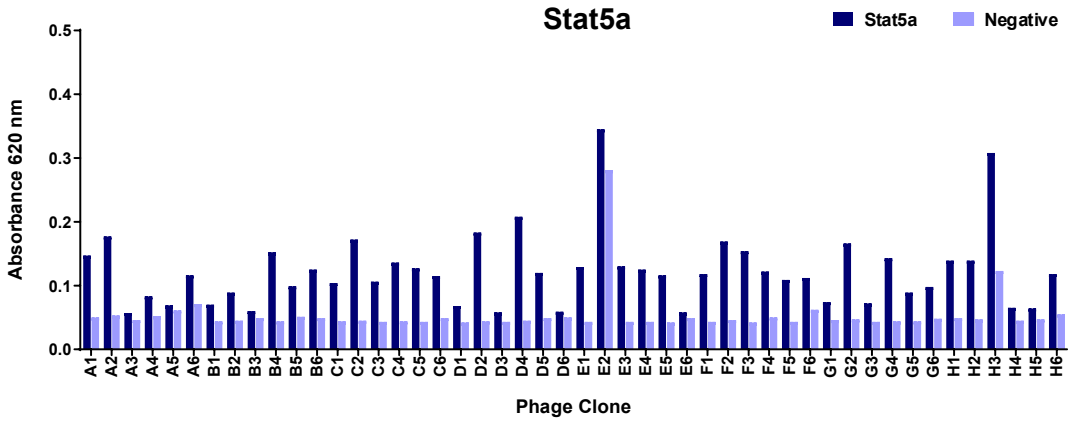
Stat5a
Stat5a
Negative
Absorbance 620 nm
0.5
0.4
0.3
0.2
0.1
0.0
A1 A2 A3 A4 A5 A6 B1 B2 B3 B4 B5 B6 C1 C2 C3 C4 C5 C6 D1 D2 D3 D4 D5 D6 E1 E2 E3 E4 E5 E6 F1 F2 F3 F4 F5 F6 G1 G2 G3 G4 G5 G6 H1 H2 H3 H4 H5 H6
Phage Clone

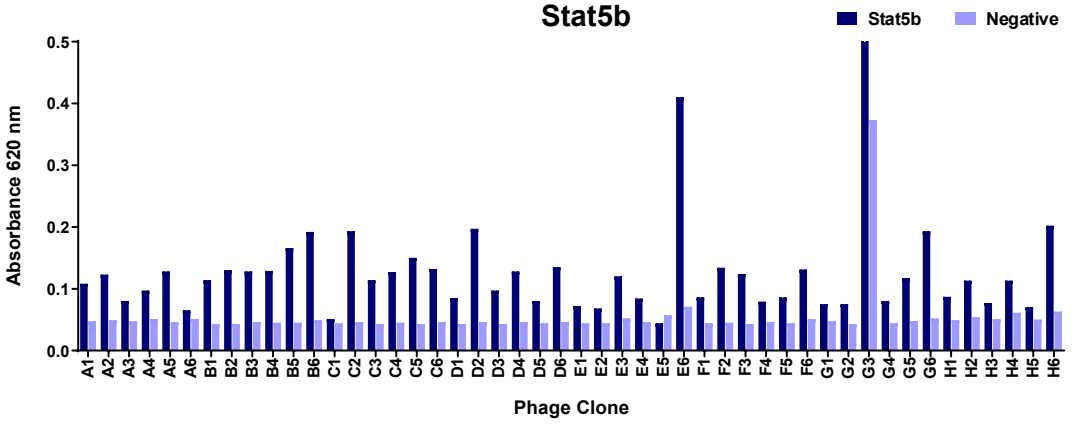
Stat5b
Stat5b
Negative
Absorbance 620 nm
0.5
0.4
0.3
0.2
0.1
0.0
A1 A2 A3 A4 A5 A6 B1 B2 B3 B4 B5 B6 C1 C2 C3 C4 C5 C6 D1 D2 D3 D4 D5 D6 E1 E2 E3 E4 E5 E6 F1 F2 F3 F4 F5 F6 G1 G2 G3 G4 G5 G6 H1 H2 H3 H4 H5 H6
Phage Clone

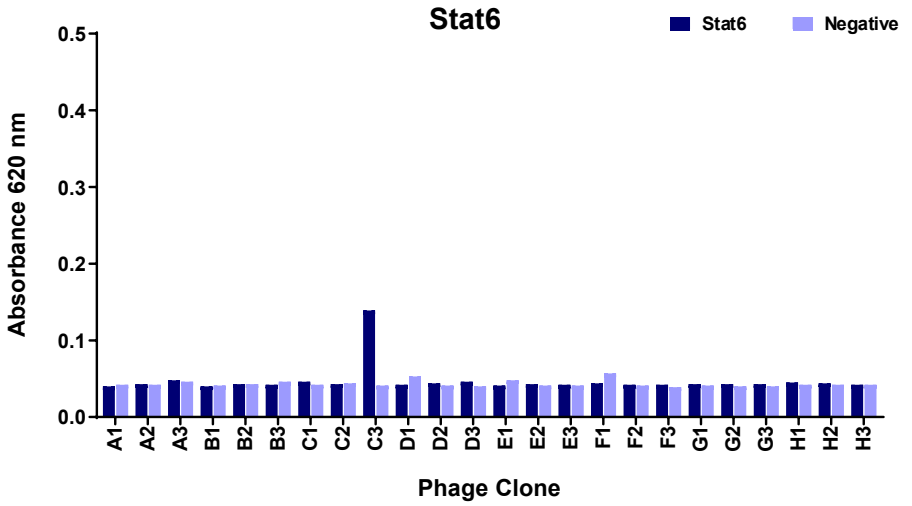
Stat6
Stat6
Negative
Absorbance 620 nm
0.5
0.4
0.3
0.2
0.1
0.0
A1 A2 A3 B1 B2 B3 C1 C2 C3 D1 D2 D3 E1 E2 E3 F1 F2 F3 G1 G2 G3 H1 H2 H3
Phage Clone

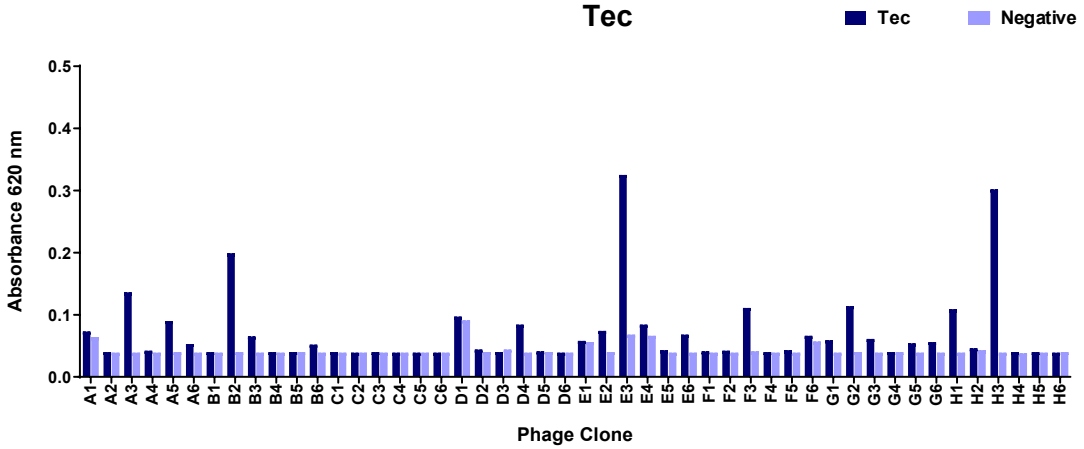
Tec
Tec
Negative
Absorbance 620 nm
0.5
0.4
0.3
0.2
0.1
0.0
A1 A2 A3 A4 A5 A6 B1 B2 B3 B4 B5 B6 C1 C2 C3 C4 C5 C6 D1 D2 D3 D4 D5 D6 E1 E2 E3 E4 E5 E6 F1 F2 F3 F4 F5 F6 G1 G2 G3 G4 G5 G6 H1 H2 H3 H4 H5 H6
Phage Clone

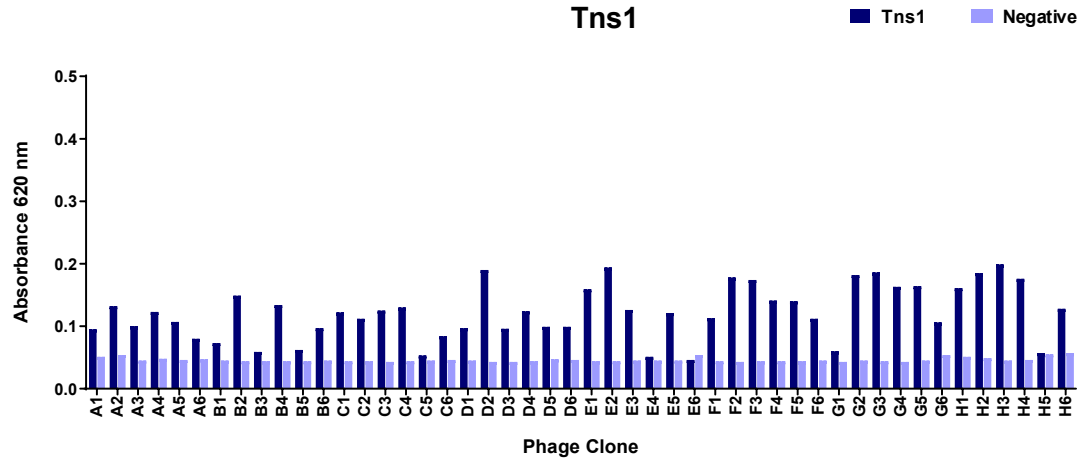
Tns1
Tns1
Negative
Absorbance 620 nm
0.5
0.4
0.3
0.2
0.1
0.0
A1 A2 A3 A4 A5 A6 B1 B2 B3 B4 B5 B6 C1 C2 C3 C4 C5 C6 D1 D2 D3 D4 D5 D6 E1 E2 E3 E4 E5 E6 F1 F2 F3 F4 F5 F6 G1 G2 G3 G4 G5 G6 H1 H2 H3 H4 H5 H6
Phage Clone

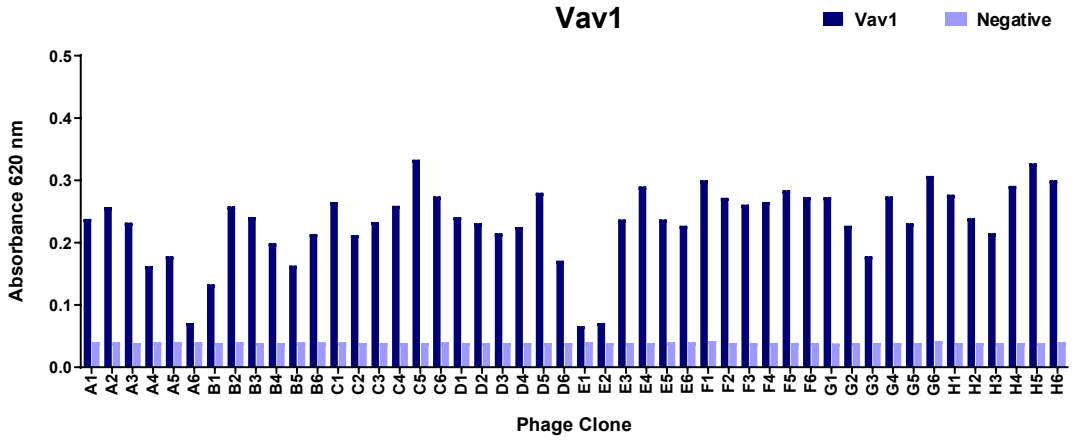

Figure 4.22. Phage ELISAs testing binding of Affimer clones to multiple SH2 targets. *Phage ELISA results for successfully screened BAP-tagged SH2 domains. Phage clones were incubated in wells containing immobilised SH2 protein and bound phage were detected with anti-phage-HRP antibody after washing. HRP substrate TMB was added and absorbance read at 620 nm after 10 min, for 48 clones (Stat6 = 24 clones). Binding to streptavidin-only wells (negative) was also tested. Phage ELISAs were performed by the candidate (14 targets) and Dr Christian Tiede (10 targets).*

A

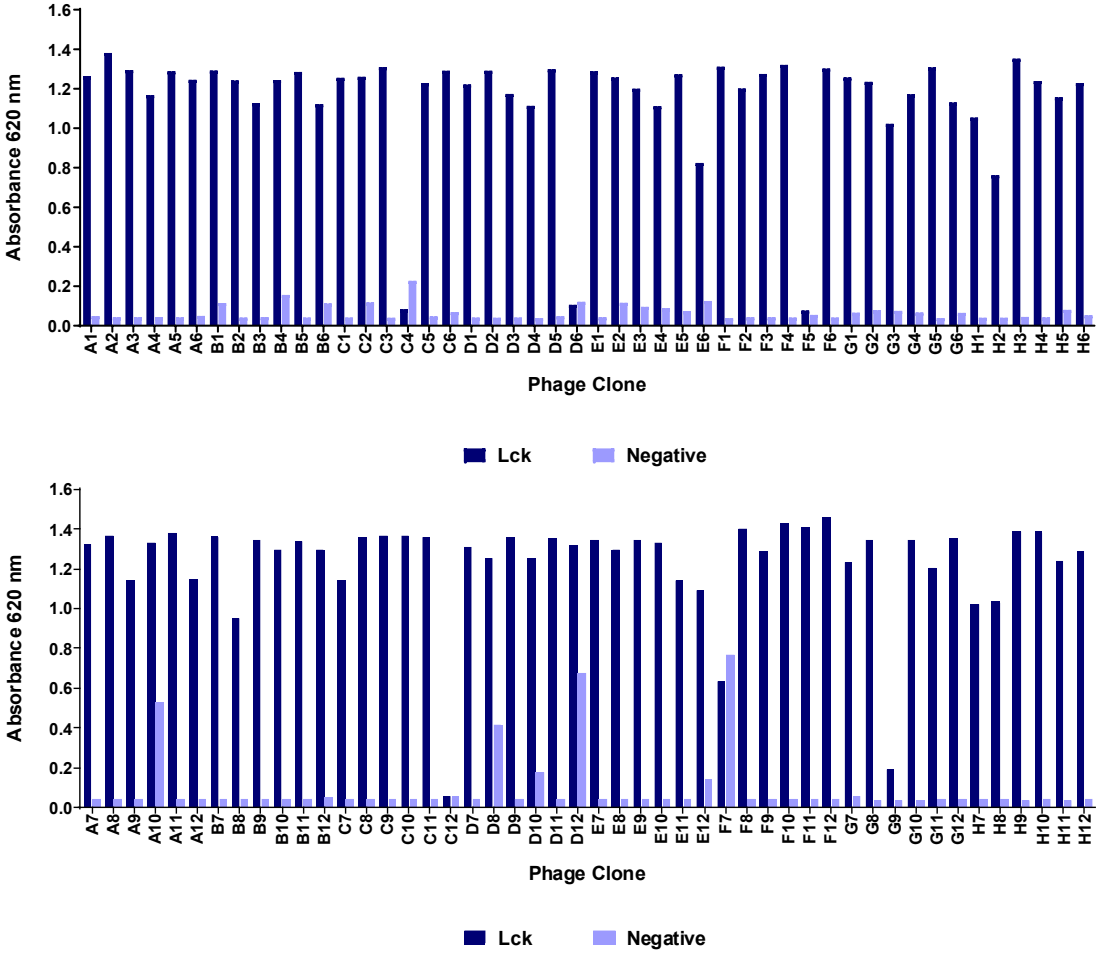
Absorbance 620 nm
1.6
1.4
1.2
1.0
0.8
0.6
0.4
0.2
0.0
A1 A2 A3 A4 A5 A6 B1 B2 B3 B4 B5 B6 C1 C2 C3 C4 C5 C6 D1 D2 D3 D4 D5 D6 E1 E2 E3 E4 E5 E6 F1 F2 F3 F4 F5 F6 G1 G2 G3 G4 G5 G6 H1 H2 H3 H4 H5 H6
Phage Clone
Lck
Negative
Absorbance 620 nm
1.6
1.4
1.2
1.0
0.8
0.6
0.4
0.2
0.0
A7 A8 A9 A10 A11 A12 B7 B8 B9 B10 B11 B12 C7 C8 C9 C10 C11 C12 D7 D8 D9 D10 D11 D12 E7 E8 E9 E10 E11 E12 F7 F8 F9 F10 F11 F12 G7 G8 G9 G10 G11 G12 H7 H8 H9 H10 H11 H12
Phage Clone
Lck
Negative

B

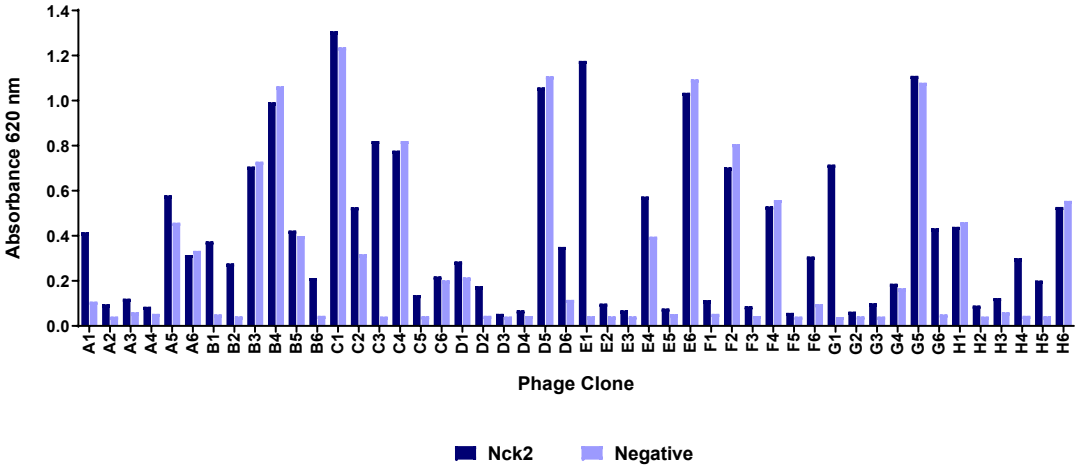
Absorbance 620 nm
1.4
1.2
1.0
0.8
0.6
0.4
0.2
0.0
A1 A2 A3 A4 A5 A6 B1 B2 B3 B4 B5 B6 C1 C2 C3 C4 C5 C6 D1 D2 D3 D4 D5 D6 E1 E2 E3 E4 E5 E6 F1 F2 F3 F4 F5 F6 G1 G2 G3 G4 G5 G6 H1 H2 H3 H4 H5 H6
Phage Clone
Nck2
Negative

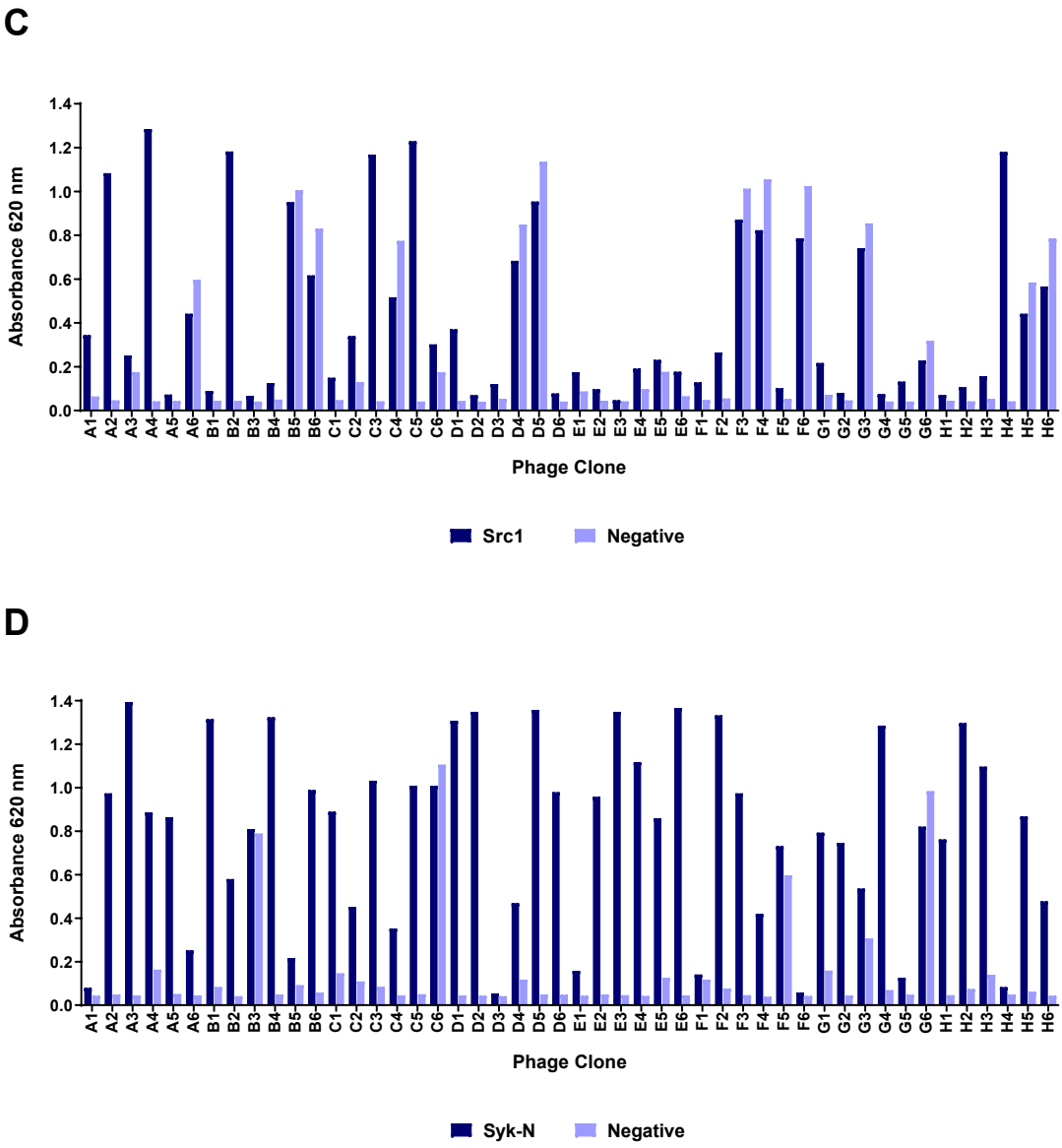

Figure 4.23. Phage ELISAs testing binding of Affimer clones from repeated SH2 screens. *Phage ELISA results for successfully re-screened BAP-tagged SH2 domains; Lck* ***(A)****, Nck2* ***(B)****, Src1* ***(C)*** *and Syk-N* ***(D)****. Phage clones were incubated in wells containing immobilised SH2 protein and bound phage were detected with anti-phage-HRP antibody after washing. HRP substrate TMB was added and absorbance read at 620 nm after 10 min, for 48 clones (Stat6 = 24 clones). Binding to streptavidin-only wells (negative) was also tested.*

4.3.3 DNA sequences and consensus alignments of the variable regions in SH2-binding Affimer clones

DNA sequencing results for Abl1-binding clones yielded six unique binders (Figure 4.24A), most of which were Type II scaffolds. Binder Abl1-A1 occurred most frequently at 17 times. Alignment of the VRs revealed a consensus of Hy-Ar-X-Ac-Y in VR1 and E-Ac-Ac-B-Ar in the VR2.

The results for Abl2 binders showed 42 unique sequences, including 29 single-loop binders. A strong consensus of P-L-X-W-L-X-L-P was revealed in VR1 (Figure 4.24B). The Abl1 and Abl2 populations did not share any of the same clones, despite the target protein sequences being ca. 89% homologous. However, Abl1-B3 had a similar VR1 to the Abl2 binders and in particular clones Abl2-A2 and Abl2-G2. This suggests that these binders may cross-reactive with both isoforms.

Twenty-two unique sequences were isolated for Bmx SH2-binding clones. In VR1 a consensus of Y-X-N/S can be seen (Figure 4.24C). No consensus was found in VR2, although the two most frequently occurring clones both contained an I-B-L-B motif.

As Bmx is a member of the Tec non-receptor tyrosine kinase family, binders isolated against the Tec SH2 domain were compared to the Bmx binders. Six unique Tec-binding clones were identified (Figure 4.24D). A consensus sequence of Hy-Ar-X-X-X-Ar-Hx-L was shown in VR2. No clones contained the Y-X-N/S motif seen in the Bmx binders, and conversely no Bmx clones contained the consensus found in the Tec binders.

For Crk, 21 unique clones were isolated from the sequenced population (Figure 4.25A). In an alignment of the Type I binders, a consensus sequence of H-D-Y-Y-Ar-Hx was revealed. When aligned with the Type II clones, this is reduced to D-Ar-Ar-Ar.

Clones had been isolated to Src family members Fyn, Lck, Lyn and Src1. As these targets are very similar in their sequences, the clones raised against these binders were compared for any homologous binding motifs. Sequence analysis for Fyn-binding clones showed 20 unique binders, however, two of these (Fyn-B5 and Fyn-E1) had shown no binding in the ELISA. After alignment, a consensus sequence of P-Ar-X-Hy was revealed in VR2 while the non-binding clones Fyn-B5 and Fyn-E1 did not contain this sequence (Figure 4.25B).

A

Clone	Type	VR 1	VR 2	Frequency
Abl1-A1	II	LINWGEYMD	EEDHYTQMH	17
Abl1-C1	I	VHRYWPVWV	FPLDPQTNL	16
Abl1-C2	II	NVVYVDAGF	EDEHIAIWF	2
Abl1-G2	II	EHLMDEYSD	EEYSYQKHS	2
Abl1-B3	II	GMLYYWPPD	AAE	2
Abl1-B6	II	YFQIEGYPQ	YYYRFIHMD	2

B

Clone	Type	VR 1	VR 2	Frequency
Abl2-E1	II	QPLEWLELP	AAE	2
Abl2-B3	II	MPLDWLPMP	AAE	2
Abl2-D4	II	PPLPWLKVP	AAE	2
Abl2-F6	II	APLDWLYLP	AAE	1
Abl2-D3	II	APLMWLDMP	AAE	1
Abl2-F5	II	APLPWLIFP	AAE	1
Abl2-E2	II	APLPWLSYP	AAE	1
Abl2-F2	II	APLQWLDFP	AAE	1
Abl2-H6	II	HALTWLSLP	AAE	1
Abl2-E3	II	HPLEWLDLP	AAE	1
Abl2-D2	II	HPLPWLKLP	AAE	1
Abl2-D6	II	IALEWLNLP	AAE	1
Abl2-C4	II	KALVWLDLP	AAE	1
Abl2-F3	II	KPLPHLMLP	AAE	1
Abl2-G3	II	KPLTWLDLP	AAE	1
Abl2-G2	II	KPLYYHPPD	AAE	1
Abl2-A5	II	KPVPWLDLP	AAE	1
Abl2-B5	II	MPLDWLPIP	AAE	1
Abl2-C5	II	MPLTWLDIP	AAE	1
Abl2-E5	II	NPLKWLDLP	AAE	1
Abl2-B4	II	PPLPWFHTP	AAE	1
Abl2-E6	II	PPLSWIDLP	AAE	1
Abl2-H5	II	PWGYIPYRS	AAE	1
Abl2-D5	II	QALEHLNLP	AAE	1
Abl2-B1	II	RRWAFSSIE	AAE	1
Abl2-H4	II	TPVPWLILP	AAE	1
Abl2-C1	II	VPLDWLDLP	AAE	1
Abl2-A6	II	VPLPWLKIP	AAE	1
Abl2-C6	II	PFPLYYGHI	AAE	1
Abl2-D1	II	HPVSWLNLP	AKHHMPNVT	1
Abl2-A1	II	APLDWLDLP	EDHNAGNFS	1
Abl2-H3	II	KPLPWLKMP	ESKNQIPMG	1
Abl2-B6	II	FPVYYWPPD	FDQAMRMLG	1
Abl2-F1	II	SPLPWLDLK	FSDAGNIGF	1
Abl2-E4	II	PGVAWLPLP	HNRLAYQAD	1
Abl2-H1	II	PPLDWLDLD	KRPFNFAKF	1
Abl2-G6	II	MPLYWLELP	LEDAHPYMI	1
Abl2-A2	II	KALYYWPPD	NMGPDPMHH	1
Abl2-G5	II	PPVHWLHLP	RNANSNKAI	1
Abl2-H2	II	RPLPWLDLA	SDYPRASAV	1
Abl2-G4	II	KALHWLHLP	VTMAPEMSP	1
Abl2-A3	II	APPYYWPPD	YPYTIMHLQ	1
	consensus:	PLXWLXLP		

C

Clone	Type	VR 1	VR 2	Frequency
Bmx-G1	II	IRYSSFATQ	RSMPMIKLH	9
Bmx-A1	II	FKYFSSHKI	RYQSIIHLK	5
Bmx-H4	II	FKYFSSHKI	RYHSIIHLK	2
Bmx-D1	II	GNIVQQWYH	DTPGMWHWN	2
Bmx-A5	II	PRWLSHEIR	QIVPRVQLM	2
Bmx-A3	I	MPAYFEKWY	FSDEEFNPW	2
Bmx-F3	II	EQAWGPILN	EMYEVRYYH	2
Bmx-A4	II	YHEYQNGAF	WYPYNLWLK	2
Bmx-E4	I	HYMNWDRLW	TYLKMDTSM	1
Bmx-G3	II	RWYVNAIDP	AAE	1
Bmx-H3	II	LWYWNADDP	AAE	1
Bmx-C2	II	QWYVNVQGI	AAE	1
Bmx-A2	II	LMFQSFIRK	RKIPLVQLT	1
Bmx-G2	II	MWYANSPHY	RQDQQHTVP	1
Bmx-F6	II	GTNYENAMF	VGIKMMPEY	1
Bmx-H2	II	WAHYYYRSF	WQGRTIRLL	1
Bmx-E2	II	WAQYDNGSF	WQGRTRRLL	1
Bmx-F1	II	VKWTSYHIQ	KYININIL	1
Bmx-C5	II	QWFYSRVIE	RPMPLIMLN	1
Bmx-F5	II	SDQMYGMAR	WFHKPTFHT	1
Bmx-H5	II	QWYENWPEV	FAESYPQVM	1
Bmx-G6	II	SRYVSYGVT	RIHPRIKLL	1
	consensus:	YXN S		

D

Clone	Type	VR 1	VR 2	Frequency
Tec-E3	II	FPDNMVWRQ	IFLPIFTLL	2
Tec-F3	II	DVSLIADET	EIFRAVWNL	1
Tec-G2	II	VFSIKHTQK	ELYKYTYSL	1
Tec-B2	II	HEASKYEW	EPHMLYIMW	1
Tec-A3	II	VELEHNPDS	TYYTYILTA	1
Tec-H1	II	HRRVHPLDA	VLLGWRLVE	1
	consensus:		HAXXXAXL yr r	

Figure 4.24. Unique Affimer clones raised against Abl SH2s and Tec family SH2s. ***(A)*** *Alignment of the variable regions (VRs) of Abl1 SH2 Affimer clones.* ***(B)*** *Alignment of the VRs of Abl2 SH2 Affimer clones. A consensus sequence can be seen in VR1 as follows; P-L-X- W-L-X-L-P.* ***(C)*** *Alignment of VRs of the unique Bmx SH2-binding Affimer clones. . A consensus sequence of Y-X-N/S was revealed in VR1.* ***(D)*** *Alignment of Tec SH2-binding Affimer VRs. A consensus of Hy-Ar-X-X-X-Ar-X-L is shown in VR2. Alignments were performed using MacVector 13.5.2. Residues that conform to a consensus are in red.*

A

Clone	Type	VR 1	VR 2	Frequency
Crk-A3	I	YHDYYATHE	DRDWQTRVL	2
Crk-B3	I	QHDYYWDAT	KAHDLKAIM	2
Crk-D2	I	IHDYYFQNS	SKDMTFVNV	2
Crk-E6	I	YHDYYYAAE	GSARYTPST	1
Crk-E4	I	EHDWYFSTK	NQRPTSQAF	1
Crk-C4	I	YHDYAFSTT	PGDLDWKDS	1
Crk-D5	I	VHDYYMTDF	RGNINLIAD	1
Crk-C2	I	MHDYFFSMD	MQEKNPMPP	1
	consensus :	HDYYAH rx		

Clone	Type	VR 1	VR 2	Frequency
Crk-A2	II	TVDYTNQQH	KDRLTWGFW	8
Crk-A1	II	FYDWPGNEYQSI	VAWMKNNVN	5
Crk-D1	II	QSAWTGEQH	EVHYPFSFS	3
Crk-F3	II	YDMPYPTVG	LWLKQYKGM	3
Crk-E5	II	IYDWPGGGLL	AAE	2
Crk-H3	II	DWWNFPVFN	AAE	2
Crk-H4	II	QSDDHWTWT	GSWPMSIHH	2
Crk-B2	II	WARTDIEFG	GLMTEGMWG	1
Crk-A4	II	FTAYNNGIH	LLFWRGYKD	1
Crk-C3	II	YQKEFWDDP	RARRIHFDW	1
Crk-B1	II	QYGSGDLFL	SKNIMLELM	1
Crk-E2	II	ETHYKNAVL	FFKLHDYEH	1
Crk-E3	II	TVDYSNQQY	KDNLPGGSW	1

B

Clone	Type	VR 1	VR 2	Frequency
Fyn-D2	II	QYLNSYWHG	KIMIEEDVY	3
Fyn-A2	II	DQKMDEYQD	YIFFDPWWV	3
Fyn-D3	II	YRNQSGDQD	YIYFSPWWV	2
Fyn-A4	II	IGEFAQKWA	EVWMDPWKV	2
Fyn-D1	II	ENSHMRAEE	SWYAVPWWI	2
Fyn-G2	II	HFPMWMEYQ	AAE	1
Fyn-B4	II	VFDEWWWQA	AAE	1
Fyn-D6	II	QWIGFFEG	ARSPAMITG	1
Fyn-C6	II	VFSPDVFAD	FFNFPPYWG	1
Fyn-C2	II	IANYSEFGL	GIYMYPYMV	1
Fyn-E4	II	DHHEIWRTR	GVLINYQPY	1
Fyn-E2	II	EMVWMWQLG	HIKHTDYDF	1
Fyn-A3	II	EGNIDTPYV	SWMVEPWII	1
Fyn-E6	II	PIEEPTHWA	TFFLSPWFT	1
Fyn-B5	II	GYQFEKVHM	TWWDAVYDY	1
Fyn-H4	II	QEEDMVGHH	VFPWSAAQM	1
Fyn-B2	II	QEQNLDGHH	VFPWSADVM	1
Fyn-C3	II	LPSTTMPHH	VWWAYPYMI	1
Fyn-E5	II	INLEHNYHT	YNSVLLDLF	1
Fyn-E1	I	DEWHSMMTW	FTIYVKSHI	1
	consensus :		PAXH r y	

C

Clone	Type	VR 1	VR 2	Frequency
Lck-A1	II	ITHELFMD	QKAYILRYG	29
Lck-B9	II	QWNDRTPIA	RWIGPTFIM	9
Lck-A7	II	VWHVRDPRS	QWIFNHADL	7
Lck-A9	II	QHTSPSEQW	KLFEKIITL	2
Lck-B2	II	VVGRDWQVA	KLVMPSFNY	2
Lck-C1	II	MRIQPLPY	WSFNVIELM	2
Lck-C7	II	VEWWMTPMK	AAE	1
Lck-E6	II	SVRDTVNYS	DFGIFWHMG	1
Lck-E4	II	VEHTHYHTQ	DLIIAAFEW	1
Lck-B6	II	PEHQWRVTV	DMIIPNGHR	1
Lck-A12	II	QVGGPDERF	DVGMWFRIG	1
Lck-H4	II	RMYVMNWED	ERAVHLTIG	1
Lck-A4	II	PFWIYNVTG	IFMAPHRKM	1
Lck-F9	II	VPSEFFPFW	KFLTPAQAQ	1
Lck-B10	II	MSGMGLMAA	KMLTVNTFF	1
Lck-H12	II	FKSQAMVFS	KPGTWPPWH	1
Lck-B12	II	VLSHYHVSY	NYPQFIIIQ	1
Lck-B3	II	HSDNHIITY	PFIMPRHKM	1
Lck-H6	II	PYRQFKMMF	PMLLPHNII	1
Lck-B8	II	NLYQQAVHS	PRKIYMFQL	1
Lck-G3	II	IRQHPSMHQ	PRKLTWLLP	1
Lck-G7	II	YMNGGYFPY	PWIRPHRIL	1
Lck-D10	II	NAEMGFMSR	PWITPHMRL	1
Lck-C5	II	ERPEYQAPN	QFHNHWFFF	1
Lck-A2	II	TGPHWPIAD	QKYALLRYG	1
Lck-H2	II	DAQSNWEPE	QLIIMTINW	1
Lck-G4	II	YGQTWAAS	QLITPARRY	1
Lck-E11	II	QNVQEYDTD	QYFLIRLMK	1
Lck-D3	II	PARLHGITV	RLMIPTNNV	1
Lck-H5	II	MQPKNWLSG	RWLMPNARR	1
Lck-E12	II	EQLEWEMFE	RWLWTPMQI	1
Lck-B11	II	VEGYRQPHP	SWEKAPFRF	1
Lck-A6	II	WFGGHDKSN	TYWQRIYTL	1
Lck-H7	II	PDIWHNIGV	VLIMPSFRI	1
Lck-A3	II	KRQVFASTI	YASAAIRYN	1

D

Clone	Type	VR 1	VR 2	Frequency
Lyn-A4	II	EWQKKGYVS	ERSVKWVLP	4
Lyn-A2	II	AEEFMTFMG	QFLMPRMNL	2
Lyn-C2	II	PEGSGITVA	RWNMPKRFV	1
Lyn-B2	II	PEMMNVFWV	TYIMPPGRI	1
consensus:			AHMPXXXH ry y	

E

Clone	Type	VR 1	VR 2	Frequency
Src1-A4	II	IRFLFFWVG	AAE	4
Src1-D1	II	SSWFFTRNE	DMMLGSGNY	1
Src1-A1	II	IEKRAVISS	RERRLHLTP	1
Src1-A2	II	QMFGQSPSY	RKYWLG	1

Figure 4.25. Unique Affimer clones raised against the Crk SH2 and Src family SH2s. *Alignment of the variable regions (VRs) of Crk SH2 Affimer clones* ***(A)*** *shows a consensus in VR1 of Type I binders of H-D-Y-Y-Ar-Hx (Ar = Aromatic residue, Hx = hydroxyl residue). Alignment of the VRs of Affimer clones against Src family SH2s; Fyn* ***(B)****, Lck* ***(C)****, Lyn* ***(D)*** *and Src1* ***(E)****. A consensus of P-Ar-X-Hy (Hy = hydrophobic residue) in VR2 of Fyn-binding clones, and Ar-Hy-M-P-X-X-X-Hy in VR2 of Lyn-binding clones is shown. Alignments were performed using MacVector 13.5.2. Residues that conform to a consensus are in red.*

For the Lck SH2 35 unique clones were isolated, all from the Type II libraries (Figure 4.25C). Lck-A1 occurred 29 times, indicating this could either bea potent binder and was able to successfully compete off other clones during biopanning, or it had a growth advantage (Hoen et al., 2012). No consensus was revealed for either VR when the sequences were aligned, and the only clone containing the P-Ar-X-Hy consensus seen in the Fyn binders was Lck-A4 (P-F-W-I).

Four unique clones were isolated for the Lyn SH2. Clone Lyn-A4 appeared four times in the eight sequenced clones. Alignment of the VRs showed a consensus in VR2 of Ar-Hy-M-P-X-X-X-Hy (Figure 4.25D). Comparing this Lyn-binding motif to the Lck and Fyn binders, some did show a similar sequence in their VR2, notably for clones Lck-B9, Lck-B3, Lck-G7, Lck-D10 and Lck-H7.

Of the eight sequenced Src1 SH2-binding clones, four unique binders were revealed (Figure 4.25E). Clone Src1-A4 occurred four times and was a single-loop binder. Interestingly, Src1-A2 was missing four residues of the scaffold sequence after VR2. No consensus motifs could be seen in either VR and; when compared with Affimer clones isolated against other Src family SH2s, no similar motifs were apparent.

Sequence analysis of Nck-binding clones revealed four unique binders for Nck1 and seven for Nck2 (Figure 4.26). Nck1-A1 appeared 36 times out of 48,

A

Clone	Type	VR 1	VR 2	Frequency
Nck1-A1	II	KFVYDPVAH	TNIYNRYSF	36
Nck1-F1	II	PQEHGWWHH	FPAPAYPEI	4
Nck1-F2	II	QVNVDPIVL	QNYYNQHMF	4
Nck1-G4	I	GPSDPA	KRMWQWSWKNSP	1
	consensus:	DPH y	AAXXXA rm r	

B

Clone	Type	VR 1	VR 2	Frequency
Nck2-H4	II	ASKRFKMYM	AAE	1
Nck2-G6	II	KRKKLRIRN	AAE	1
Nck2-B1	II	RKKKIRLVR	AAE	1
Nck2-A1	II	MHRSLHIRK	LNKLSIPKG	1
Nck2-E1	II	YESVSSDES	NFHMIFTHW	1
Nck2-G1	II	NKAYADSP	NVFEFKISH	1
Nck2-C3	II	YIYAPGWGL	WYFQERNVF	1
	consensus:	BBHBH y y		

Figure 4.26. Unique Affimer clones raised against Nck SH2 domains. *Alignment of the variable regions (VRs) of Nck1* ***(A)*** *and Nck2* ***(B)*** *SH2 Affimer clones. For Nck1 clones a consensus motif of D-P-Hy can be seen in VR1, and of Ar-Am-X-X-X-Ar in VR2 (where Hy = hydrophobic residue, Ar = Aromatic residue, Am = Amide residue). For Nck2 clones, a consensus of B-B-Hy-B-Hy was revealed in VR1 (B = basic residue). Alignments were performed using MacVector 13.5.2. Residues that conform to a consensus are in red.*

indicating this was a potent binder. Upon alignment of Nck1 clones, a motif of D-P-Hy was revealed in VR1 and a consensus of Ar-Am-X-X-X-Ar in VR2 (Figure 4.26A). A consensus of B-B-Hy-B-Hy was revealed in VR1 of Nck2 binders (Figure 4.26B). Clones Nck2-C3 and Nck1-A1 shared similar sequences VR1, suggesting these binders could be cross-reactive to both isoforms.

The number of unique clones isolated against the SH2 domains of PI3K ranged from 8 – 35 for each target. For the P85α-C SH2, nine unique clones were isolated, with P85αC-C1 occurring 20 times out of 48 sequences. A consensus sequence of W-X-Ar-X-X-X-X-E-Hy was revealed in VR1, which be seen in Figure 4.27A.

Sequencing of P85α-N clones showed 24 unique binders (Figure 4.27B), with a consensus sequence of W-E-E-Y-H-E revealed in VR1 of the Type I binders. The Type II binders did not share the same sequence in their VRs, however a consensus of W-M-X-P-X-X-X-Hy was seen in VR2. Interestingly, the clone that occurred most frequently, P85αN-D1, did not contain this sequence.

Eight unique clones were isolated against the P85β-C SH2; five of which were single-loop binders. The two 2-loop binders, P85βC-B4 and P85βC-B5, had shown no binding in the ELISA. A consensus sequence in VR1 of H-A-F-Ac-D-X-X-Q-D was revealed after alignment of binding clones (Figure 4.27C). This sequence was not found in non-binding clones P85βC-B4 and P85βC-B5, or in the Type I binder P85βC-H4.

P85β-N clones also yielded eight unique binders (Figure 4.27D). No consensus was revealed in either of the VRs, although four clones contained the sequence Ar-X-X-Hy in VR1 and four binders contained the sequence Am-X-X-Ar in VR2.

Thirteen unique binders were identified for P55γ-C. In the Type II binders a consensus of P-H-X-L-X-X-I-W was revealed in VR2 (Figure 4.27E).

For the P55γ-N SH2, 35 unique clones were isolated, with the majority from the Type I 6x12 library. The same consensus sequence found in the P85α-N binders of W-E-E-Y-H-E was revealed in VR1 (Figure 4.27F). None of the P55γ-N and P85α-N clones were the same, however.

The two Type II binders raised against P55γ-N also shared similar VR2s to the Type II P85α-N clones, which is highlighted in Figure 4.28. These results indicated that the isolated P55γ-N and P85α-N clones may be cross-reactive between the two SH2 domains.

A

Clone	Type	VR 1	VR 2	Frequency
p85αC-C1	II	DIWAIQHVI	DDLNFNMRD	20
p85αC-A1	II	WMWGFMDEE	IVWSTPAEE	12
p85αC-C4	II	FEFWAQYES	DPWEGMHVE	3
p85αC-D1	II	WYFQQHFEV	SPWANFSIK	3
p85αC-C3	II	WDSSVIPEY	LVILFIPQQ	2
p85αC-F4	II	WFFEQAYEV	VSWDFSPVF	2
p85αC-F6	II	GEDFMFYQL	KEPHRSMQL	1
p85αC-H5	II	WVFNTEHEV	YPWTGKGVH	1
p85αC-B4	I	KFKQRQ	MTPTFWETEYFD	1
	consensus:	WXAXXXXEH r y		

B

Clone	Type	VR 1	VR 2	Frequency
p85αN-E3	I	WEEYHE	DALVGHDKRGNA	3
p85αN-C1	I	WEEYHE	EENMRSDHLEEV	2
p85αN-E5	I	WEEYHE	DTTDPNMYHDN	1
p85αN-E2	I	HYEYHE	EGVPPRIDQDED	1
p85αN-B6	I	WEEYHE	FAQEADQEQHTM	1
p85αN-A3	I	WEEYHE	IMEDQIALEEKD	1
p85αN-F4	I	WETYHE	KEVSVGQHVVTE	1
p85αN-D6	I	MWSYEE	LDQPSIQTYDPK	1
p85αN-A4	I	WEEYHE	LDQQYKLAKQDI	1
p85αN-D3	I	HWEYHE	PMITRDIQHYED	1
p85αN-F2	I	WEEYHE	SGEDFISAIRHP	1
p85αN-D4	I	WEEYHE	VEGMSYTPWMSF	1
p85αN-B5	I	HEEYHE	VPDHVDHYSASV	1
p85αN-B3	I	HWEYHE	WQRWTDRQEYIE	1
p85αN-A2	I	IWSYDE	VDEDHHGTQIRP	1
	consensus:	WEEYHE		

Clone	Type	VR 1	VR 2	Frequency
p85αN-D1	II	YYWSHFQQS	TDINDPYER	11
p85αN-B1	II	ISMARFDGT	KYIQVELDG	6
p85αN-E4	II	YGSWSAHKM	PWMNPHFLI	2
p85αN-H2	II	FEFNYNGQF	WIMLFDDGD	2
p85αN-C6	II	WDPEYQFIG	HWMRPEKLI	1
p85αN-B2	II	SYFIAMYEY	NENYFMPLV	1
p85αN-A1	II	IMEEDYYWL	PWMMPILLI	1
p85αN-C4	II	WWLEHPASF	PWMQPITMT	1
p85αN-G3	II	LGAQDLFDY	IWMMPMKLI	1
	consensus:		WMXPXXXH y	

C

Clone	Type	VR 1	VR 2	Frequency
p85βC-C1	II	HAFDDPDQD	AAE	22
p85βC-C2	II	HAFDDHSQD	AAE	13
p85βC-D1	II	HAFEQYDID	AAE	6
p85βC-F1	II	HAFEDWQQD	AAE	2
p85βC-A3	II	YAFDDPSQD	AAE	1
p85βC-B4	II	YVAGHIHNH	WAWIRPNQD	1
p85βC-B5	II	IMFTEQYEL	WPWAANNKV	1
p85βC-H4	I	AVFPAE	AAQATRLLADLE	1
	consensus:	HAFADXXAD c m		

D

Clone	Type	VR 1	VR 2	Frequency
p85βN-A1	II	PQSDHMNAE	YGTNWLADL	13
p85βN-H2	II	DWQALPIDQ	ENNAWARIT	9
p85βN-C1	II	SYFIAMYEY	NENYFMPLV	8
p85βN-A3	I	LTKHYY	YHIKHLLIAPSL	3
p85βN-G1	I	EYDSHELYT	ELVSAPWED	1
p85βN-E3	II	HWVNAGWLE	HQNMIGNFF	1
p85βN-F1	II	HWDEHINTA	NSVYWESVA	1
p85βN-E6	II	AAVVAYITS	QEHWQHYMI	1

E

Clone	Type	VR 1	VR 2	Frequency
p55γC-C1	II	LESQETVEF	LPQRLMTIW	12
p55γC-B5	II	PPGRAGIEW	LPHYLLTIW	11
p55γC-G1	II	PKYGEVSPH	IPHLILRIW	4
p55γC-E5	II	NMMHARRQW	EPHRLFVVW	4
p55γC-E3	II	YNSVDPHYD	MPHRLLTIW	2
p55γC-C3	II	LDHDSVYEE	WLPDIKHIH	2
p55γC-E6	II	QDIATYKMW	EPQLIAAIW	1
p55γC-D5	II	TMPNKVDYH	LPHILFTLW	1
p55γC-B2	II	RVVAFNGKA	TMYNFNHFW	1
	consensus:		PHXLXXIW	

Clone	Type	VR 1	VR 2	Frequency
p55γC-F4	I	DWISTL	AGLMFATWSHFD	1
p55γC-D1	I	GRKMQM	GKWWPAWQYAYT	1
p55γC-A3	I	LHWTTHQEF	FKVYDEHMYR	1
p55γC-D3	I	NVPARKKKI	GSKWDRGAW	1

F

Clone	Type	VR 1	VR 2	Frequency
p55γN-G2	I	WEEYHE	MSRTEYRDMSDR	2
p55γN-F1	I	WEEYHE	SGQHMEPSWPII	2
p55γN-D1	I	WEEYHE	YAVIYNPAASMS	2
p55γN-D5	I	HWEYVE	AAKHQEYEDKMD	1
p55γN-G4	I	MWQFEE	ADFQPSPNDRMH	1
p55γN-E5	I	WQEYHE	ADSQPEMMFHVD	1
p55γN-G1	I	HEVVIE	AEYEHEGYEEEH	1
p55γN-C5	I	VETYEE	AHETIEPHEYPV	1
p55γN-F3	I	HWEYHE	ANEHTGDVATEA	1
p55γN-E6	I	HYEYHE	ARDTPPVQMQME	1
p55γN-B5	I	WEEYHE	DAEGEVKGSMGD	1
p55γN-B1	I	MYEYTE	DTADVPVANDHK	1
p55γN-F6	I	WETYHE	DVENNLEAHNIM	1
p55γN-C6	I	HWEFHE	EHVEETPFDPYM	1
p55γN-C3	I	WQEDHE	ESRTLMHDKIDF	1
p55γN-B2	I	WEEYHE	FSSAAFPYDHAM	1
p55γN-C2	I	WEEHHE	HDEIFQVVTPNI	1
p55γN-F4	I	WEEYHE	HSKNNIIYEMPF	1
p55γN-A3	I	HWEYHE	KADMTYDVNQPD	1
p55γN-H6	I	HWEYEE	LDQVHHRQEEFS	1
p55γN-B4	I	MWEYHE	MMTTPVPEKTD	1
p55γN-E3	I	WEEAHE	NADAILFHHNSN	1
p55γN-D2	I	HWSYDE	NPHEDDNQANMG	1
p55γN-G5	I	HWEFHE	RDTVYQAVQEHE	1
p55γN-A5	I	WEEHHE	RERKEENLILSV	1
p55γN-H2	I	WEEYHE	RQEFPMGHTDIA	1
p55γN-H5	I	WEEYHE	RVSEIPAHYSSP	1
p55γN-D4	I	WEEYWE	SKLQASRVSDDP	1
p55γN-H1	I	YEEVIE	TFVVPQEMTPHN	1
p55γN-D3	I	WEEYHE	VADYQRHDGDGA	1
p55γN-A6	I	YYTYEE	WYELPDDYMEHQ	1
p55γN-C1	I	WEEYHE	YEQQENERYKYT	1
p55γN-B3	I	HYEFHE	PNPTDKIFQWTY	1
p55γN-B6	II	EDPDLTQRIDT	AWMMPIKLE	1
p55γN-F2	II	WTDRGPYDH	PFMNPLNLL	2
	consensus:	WEEYHE		

Figure 4.27. Unique Affimer clones raised against PI3K SH2 domains. *Alignment of the variable regions (VRs) of Affimer binders raised against p85α-C* ***(A),*** *p85α-N* ***(B)****, p85β-C* ***(C)****, p85β-N* ***(D)****, p55γ-C* ***(E)*** *and p55γ-N* ***(F)*** *SH2s. Consensus sequences were revealed of W-X-Ar-X-X-X-X-E-Hy in VR1 of p85α-C clones, W-E-E-Y-H-E in VR1 of p85α-N and p55γ-N Type I clones and W-M-X-P-X-X-X-Hy in VR2 of p85α-N Type IIs. A consensus of H-A-F-Ac-D-X-X-Q-D in VR1 of p85β-C clones and, P-H-X-L-X-X-I-W in VR2 of p55γ-C clones was also seen. Alignments were performed using MacVector 13.5.2. Residues that conform to a consensus are in red.*

Clone	Type	VR 1	VR 2
p85αN-A1	II	IMEEDYYWL	PWMMPILLI
p85αN-G3	II	LGAQDLFDY	IWMMPMKLI
P85αN-E4	II	YGSWSAHKM	PWMNPHFLI
p55γN-B6	II	EDPDLTQRIDT	AWMMPIKLE
P55γN-F2	II	WTDRGPYDH	PFMNPLNLL
	consensus:		PWMMPHXLI y

Figure 4.28. Alignment of similar Affimer clones raised against PI3K p85α-N and p55γ-N SH2 domains. *Alignment of the variable regions (VRs) of Affimer binders raised against the p85α-N and p55γ-N SH2s showed similar sequences in VR2. Conserved sequences are in red. Alignments were performed using MacVector 13.5.2.*

Analysis of She SH2 domain binders revealed eight unique clones, with clone She-G1 occurring 15 times and clone She-B1 12 times (Figure 4.29). A consensus of Ar-X-Hy-X-Y was revealed in VR1, with three binders containing the motif Y-A-N-Y. In VR2 a consensus of Ar-X-X-Hy was also seen.

Binders isolated for the six Stat family members were next compared. For Stat1, 14 unique clones were found with Stat1-A1, a 2-loop Type II Affimer, appearing 31 times in the 48 sequenced clones. This clone accounted for all wells that showed the highest signals in the ELISA. Other binders that had shown signals above the background were clones Stat1-D5, Stat1-G6, Stat1-E1 and Stat1-C5.

Clone	Type	VR 1	VR 2	Frequency
She-G1	II	MYANYTDWA	RSRPKWKEI	15
She-B1	II	EQYDLQFT	TWAPEEGLE	12
She-C1	II	YYANYDVTA	YFRLGQTR	9
She-E1	I	FQGDMY	SLDPHHKVADWL	6
She-E4	II	AWSWYNMDE	TFVQVFPRF	2
She-A6	II	YYANYNMNY	RYRNAKGTS	1
She-B4	II	MHLIMYERP	TFDNIWIPD	1
She-A2	I	QSYSIS	YIVTPHSSEFWW	1
	consensus:	AXHXY r y	AXXH r y	

Figure 4.29. Unique Affimer clones raised against the She SH2 domain. *Alignment of the variable regions (VRs) of Affimer binders raised against the She SH2 domain revealed a consensus of Ar-X-Hy-X-Y in VR1 and Ar-X-X-Hy in VR2. Alignments were performed using MacVector 13.5.2. Residues that conform to a consensus are in red.*

Stat1-A1 and Stat1-D5 shared the sequence P-Ac-X-X-X-X-R-F in VR1 (Figure 4.30A).

Forty-seven unique clones were isolated against Stat3. Although groups of these binders showed similar sequences and motifs, overall no consensus was revealed for either VR (Figure 4.30B).

Sequencing of Stat4 binders revealed that all 48 clones were unique. A consensus of Hy-X-Ar-X-X-Ar can be seen in VR1, with 16 clones containing the sequence I-X-F-X-X-F (Figure 4.30C). The sequence Hy-X-Ar-X-X-Ar was also seen in Stat1-E3, Stat3-A6 and Stat3-D6 (Figure 4.30D) but was not observed in any Stat5 or Stat6 clones.

Of the seven sequenced Stat5a binders, two unique clones were identified with clone Stat5a-A2 appearing six times. Both binders contained the motif Q-X-X-P-Q in VR1, and N-Ar-N-I in VR2 (Figure 4.30E).

For Stat5b, four unique binders were isolated. A consensus of Ar-X-X-N was revealed in VR2 (Figure 4.30F); a motif also seen in binders Stat5a-D4, Stat1-A5 and Stat4-E2 (Figure 4.30G).

The one positive binder hit in the Stat6 phage ELISA, Stat6-C3, is shown in Figure 4.30H. This Affimer was a 2-loop Type II scaffold, and did not contain the consensus sequences found in the Stat5 binders. Most Stat targets pulled out primarily Type II scaffold binders.

It is important to note that as the Stat constructs encode more than just the isolated SH2 domain, the Stat binders raised in these screens may bind elsewhere in the proteins; and therefore may not be SH2-binding reagents. This may account for the lack of a consensus sequence in the binders for some Stat targets.

Eighteen unique clones were isolated against the Syk-N SH2 domain (Figure 4.31A), with clone C5 occurring the most frequently at nine times. No overall consensus was found for either VR, although groups of binders showed very similar sequences.

Analysis of Tns1-binding clones identified four unique clones. Clone Tns1-A1 constituted 43 out of 48 sequences, suggesting this was a high affinity binder. Two of the clones, Tns1-E4 and Tns1-H5, had shown no binding in the ELISA. When aligned, the two binding clones (Tns1-A1 and Tns1-C2) shared a motif of Ar-Hy-Ar in VR2, which was not seen in the non-binding clones (Figure 4.31B).

A

Clone	Type	VR 1	VR 2	Frequency
Stat1-A1	II	PDYIYQRF	WAFGMMMGP	31
Stat1-D5	II	LPEQWAKRFRIIM	AAE	2
Stat1-G6	I	PVYHKKVFF	YRVEAEGMW	1
Stat1-E1	I	NNYRKLRVT	HVFNMSSLQ	1
Stat1-C5	I	VKRVLV	LSRVHPEGDKRQ	1
Stat1-C3	I	NRKAVHPTI	AYHNGFHPR	1
Stat1-C2	I	FDSSNE	DHFYYWYLGWND	1
Stat1-G4	I	IRRLHT	FSVLYEPPYFRP	1
Stat1-A5	I	DSSKMKIWF	GHMAWYSYN	1
Stat1-B4	I	LHKTHRKTF	GKLYDLEIT	1
Stat1-E5	I	TYRFTVPRK	KYLSRHYSR	1
Stat1-E3	I	DKKIKS	PAGRGSWYKWSW	1
Stat1-F3	I	KPASKAAMY	WTDFWVFLR	1
Stat1-B3	II	KMMRHLFLH	GFQNIYQIF	1

B

Clone	Type	VR 1	VR 2	Frequency
Stat3-H2	II	HGPVRVPWQ	DYGANLPLL	2
Stat3-D4	II	WFTVWQDKM	AAE	1
Stat3-B5	II	IPEAVIPWL	AIKIHGMPY	1
Stat3-D2	II	QFEYMKPWD	AVSAWGLIH	1
Stat3-A5	II	QAQPQMGIE	DFLPFPLTI	1
Stat3-E3	II	VLGAHQSQF	DQNGIIFLW	1
Stat3-H5	II	RWQGNVPSE	EIRFYGSWD	1
Stat3-C1	II	SKVEMFRSH	ELKWNKEGI	1
Stat3-E1	II	EWDPGHPWR	ELLINMHYE	1
Stat3-G3	II	IPNASAPWF	EWMYYGDQW	1
Stat3-A3	II	TSEYLFTKQ	FLETTNRRA	1
Stat3-F2	II	QMENQFGWE	FLLIGQAPI	1
Stat3-A4	II	SEEEIFVRE	GINLTHHNI	1
Stat3-G5	II	LHKDLWRRQ	GINTSLGDV	1
Stat3-A2	II	EQQANFSKI	HFEILEMNA	1
Stat3-E5	II	SAHRQFTQE	HLMVNAGAF	1
Stat3-B2	II	WFIDGFVEQ	KLMVTKKFI	1
Stat3-C4	II	QRHVKWKEE	KMKLVETAI	1
Stat3-H1	II	PYYEGARDF	KSGDMLFLW	1
Stat3-B4	II	EQDEQFGHS	LLYWNNDDI	1
Stat3-F5	II	WVRIYSDYL	NAGADTLRE	1
Stat3-G1	II	SEKLNSQTM	NDKNIWFLW	1
Stat3-E4	II	YVPSSFSHV	NLKINNDVW	1
Stat3-D1	II	YFAPDEPQS	NNNWWWFLF	1
Stat3-C3	II	EFQYAGPWQ	PFAILGAWD	1
Stat3-F6	II	EYVWLVTMP	QIIVTGSRY	1
Stat3-A6	II	VVFNEFSKH	QLTRIYEHL	1
Stat3-H3	II	YFEPQFKQH	QNPPIAFVW	1
Stat3-D3	II	VVDWEELPQ	RFIFPDITF	1
Stat3-B1	II	EHDPTNPWT	RIQFHQQWH	1
Stat3-C6	II	TEEHLWNVV	RLVLHDGDL	1
Stat3-B3	II	HQGSGYTHN	RLYIRPTTV	1
Stat3-H6	II	SPEEETPWA	SFQVNLQWI	1
Stat3-F1	II	QSAEMWWEE	SILVTGGQV	1
Stat3-B6	II	AVKWEFASE	SLLISPDPL	1
Stat3-G2	II	TYVVDWHFG	TFINVSEKD	1
Stat3-F3	II	HETEKGPWT	TFMWHKRQE	1
Stat3-E6	II	SGTVKWMRE	TIESESHPM	1
Stat3-D5	II	YEEETFFDT	TLRINKEFI	1
Stat3-F4	II	YNRGQSPWN	TMVYWGKEF	1
Stat3-D6	II	FQYMDMWIE	VFQSSTHPF	1
Stat3-G6	II	ESHDRFRRV	VLWGSFGAI	1
Stat3-C5	II	YTVNKWATD	VMVINVNSI	1
Stat3-G4	II	TLVWQPQEP	WIRLRMHWM	1
Stat3-A1	II	IMPSPLGHS	GLKINQEWL	1
Stat3-C2	II	HEYHWSSE	LIIVNDHTI	1
Stat3-E2	II	VMTELRFFP	QYKWYDEYA	1

C

Clone	Type	VR 1	VR 2	Frequency
Stat4-G6	I	KRDGIMWEY	NLVPIGSYT	1
Stat4-C4	II	WLTVQMVKH	AAE	1
Stat4-A5	II	SITFTLFLS	AHHHEFPAE	1
Stat4-E6	II	KISFRKFNS	ASLDGNNPR	1
Stat4-C6	II	TIPLKYFTH	DVYAKYGNQ	1
Stat4-H5	II	RIIFHQFIH	DYIAPVAER	1
Stat4-C3	II	TIPFTKFEH	EMLQGLSNN	1
Stat4-A6	II	EISFRMFIS	ESTMMNMNA	1
Stat4-H3	II	TIHFRTFNS	EYIGNVFPM	1
Stat4-D3	II	AQIRWWGTK	GDELLMMGL	1
Stat4-C5	II	QTPQDWVVE	GMHWNYGVL	1
Stat4-A4	II	FIEFHKFSH	GSKMPWKMK	1
Stat4-C2	II	EGQGSVWPH	HFQLAERWG	1
Stat4-G1	II	TIVFTSFKH	HYYSNKRRG	1
Stat4-D5	II	VVWRQRMQW	IVRHWMGDF	1
Stat4-H1	II	FIHWPHMVS	KMNMKNPKQ	1
Stat4-D2	II	HQFKKYYWA	KMQYSDDQR	1
Stat4-E3	II	WIRWQWMHS	KNLVELHSM	1
Stat4-B3	II	TIPFKLFVH	KNQSDKNML	1
Stat4-E1	II	VMWPWWGVQ	NDHILHKNL	1
Stat4-D1	II	GISWSFMHS	NMIAPTNQE	1
Stat4-H6	II	HHFLSQEWA	NMIRMSNRT	1
Stat4-F2	II	HNWHYPYIY	PQVNASRFF	1
Stat4-H2	II	HTFDYPAIH	PRIGKPKPK	1
Stat4-B4	II	VDRTKQYIV	QDLMLNKGL	1
Stat4-G2	II	YVERWYAWI	QDLMLSQDV	1
Stat4-F3	II	FQNMWHSHS	QDLMLYQAP	1
Stat4-G4	II	SIPFTLFQS	QLRGQQRPE	1
Stat4-C1	II	FIPFHVFHH	QMHSLWEDHK	1
Stat4-D6	II	VLTFISFSH	QPYDTIIYK	1
Stat4-F4	II	YRYEYPLIH	QQMHHKGSN	1
Stat4-F5	II	GIAFTMFES	RKLGLSIHD	1
Stat4-A3	II	NLWKYPVMQ	RLEANLMQR	1
Stat4-E2	II	YQWNYPKIE	RVRAPTSDA	1
Stat4-B1	II	SITFKFFLS	RYHHLQLIQ	1
Stat4-B6	II	MSRNAWMDH	SDKFLFPHP	1
Stat4-F1	II	FIPFNYFNS	SSKPNYASN	1
Stat4-E5	II	SIEFKQFQS	TFTAIQSLK	1
Stat4-B5	II	SISWSWMRS	TLMNANIEG	1
Stat4-A2	II	NSQRSMVSE	TSIWSYGRL	1
Stat4-A1	II	RQWHFPEVY	TVFVEANHN	1
Stat4-D4	II	HQFHDKLWE	VAGPRHRIN	1
Stat4-H4	II	HITWSFMMS	VMIPANNMD	1
Stat4-F6	II	AMQFPTEQH	WPVFWNYPF	1
Stat4-E4	II	YINWEFLHS	YSWINADWT	1
Stat4-B2	II	AFPVKWDYQ	VLPFLNQKP	1
Stat4-G3	II	QHHQRFTQD	VLIGVHPMP	1
Stat4-G5	II	QIMFHMFYH	HWKNDPVIK	1
consensus :		HXAXXA y r r		

D

Clone	VR sequence
Stat1-E3	PAGRGSWYKWSW
Stat3-A6	VVFNEFSKH
Stat3-D6	VLWGSFGAI
consensus:	HXAXXA y r r

E

Clone	Type	VR 1	VR 2	Frequency
Stat5a-A2	II	KQQFPQSQQ	TNFNIKLIK	6
Stat5a-D4	II	IVQRPPQQA	NYIWNWNIS	1
consensus:		QXXPQ	NAN r I	

F

Clone	Type	VR 1	VR 2	Frequency
Stat5b-E6	II	KTVRGVFQD	AYRWEHNFG	1
Stat5b-G6	II	MTSMVDGTE	FKMWHWNVM	1
Stat5b-H6	II	EPKNKGAHE	IYIYGWNVG	1
Stat5b-B6	II	MFERPHQYH	VNIYHMSIS	1
consensus:			AXXN r	

G

Clone	VR sequence
Stat1-A5	GHMAWYSYN
Stat4-E2	YQWNYPKIE
Stat5a-D4	NYIWNWNIS
Stat5b-G6	FKMWHWNVM
Stat5b-E6	AYRWEHNFG
Stat5b-H6	IYIYGWNVG
consensus:	AXAN r r

H

Clone	Type	VR 1	VR 2	Frequency
Stat6-C3	II	VIYAWGGLM	HPLEMYEDE	1

Figure 4.30. Unique Affimer clones raised against Stat family proteins. *Alignment of the variable regions (VRs) of Affimer binders raised against the Stat SH2 domains; Stat1* ***(A)****, Stat3* ***(B)****, Stat4* ***(C)****, Stat5a* ***(E)****, Stat5b* ***(F)*** *and Stat6* ***(H)****. Alignment revealed a consensus of Hy-X-Ar-X-X-Ar in VR1 of Stat4 clones; this sequence was also found in other Stat family binders, shown in* ***(D)****. Alignment also revealed consensus sequences in Stat5a binders of Q-X-X-P-Q in VR1 and N-Ar-N-I in VR2, and Ar-X-X-N in VR2 of Stat5b binders.* ***(G)*** *shows more Stat binders containing similar VR sequences, sharing the consensus Ar-X-Ar-N in VR2. Alignments were performed using MacVector 13.5.2. Residues that conform to a consensus are in red.*

A

Clone	Type	VR 1	VR 2	Frequency
SykN-C5	II	PYVVNSGWF	GLLLKRHWA	9
SykN-F2	II	RTYPPFVFY	KNQNIFALY	4
SykN-D2	II	NWQPLLSYW	PKTGAQELY	4
SykN-C3	II	RTYFHGYPE	HFFRHMTHP	2
SykN-F4	II	VRKKVFSFR	AAE	1
SykN-G2	II	EVFRNPARV	ESYLMSPIF	1
SykN-D6	II	LLPHEYNPM	FFFKLFPHP	1
SykN-D5	II	SQQPWVMYW	FHPKRMVLN	1
SykN-E5	II	SVQNPVHVQ	HARYFRNGH	1
SykN-C2	II	QNKRRIHSA	KETIWSWAA	1
SykN-G1	II	REEWPWEQD	RMQLITNRI	1
SykN-D4	II	QPGHHRRML	SHHGTRIMW	1
SykN-C4	II	PEYPYMHWD	TMPLRTSQV	1
SykN-C1	II	ADCVHGCL	VLLLKTHWE	1
SykN-E4	II	WWPIYPQDP	WGMQAAFLM	1
SykN-D1	II	LPGNALTMR	PYFLNWQPF	1
SykN-A6	II	WFRMKYWTS	AAE	1
SykN-B2	II	YFRINWWQS	AAE	1

B

Clone	Type	VR 1	VR 2	Frequency
Tns1-A1	II	AEEDEEYTG	FWIYENMP	43
Tns1-E4	II	DMRDWEFTN	HDLPKLWEP	2
Tns1-C2	II	THHMSGYFN	PDYPFLWHS	1
Tns1-H5	II	WKHDYGMND	QYYWANQVV	1
		consensus:	AAHA rryr /P	

C

Clone	Type	VR 1	VR 2	Frequency
Vav1-F1	II	QYWVNIQDE	TLWQKEPFM	4
Vav1-D1	II	QYWVNDPTE	YMEFDEFEQ	4
Vav1-G2	II	LYWVNVMSE	KSMKDGVAE	3
Vav1-F4	II	VAFPTNLSE	PNIRLNYHL	3
Vav1-C1	II	NYWVNVDNE	VPKWWQPNM	3
Vav1-F2	II	LYWVNVQDE	YYMDPGMRA	3
Vav1-A1	II	EYWVNVSDE	KPPAAFRYW	3
Vav1-H3	I	RFSIPQWIR	YNEEAAEIN	2
Vav1-H5	II	QKIRQHDRW	GESKINFHL	2
Vav1-A2	II	PYWVNLPFP	PKIKNPKGN	2
Vav1-G1	II	VYWVNVPDE	RMDRQRMKN	2
Vav1-E4	II	QYWVNIADE	TYPKWSQKT	2
Vav1-H1	II	RYWVNVVDE	YPYMNDNSR	2
Vav1-E2	II	PYWVNLYTP	EQIVNEDHY	1
Vav1-E1	II	VMLRFYMTW	GEQKLNFHL	1
Vav1-G3	II	LMYGYQEIM	GFNYINNHL	1
Vav1-B1	II	RYWVNMPEP	NRKNDNMVP	1
Vav1-A5	II	EYWVNVADE	NSAQKNNRL	1
Vav1-C5	II	RYWINMAYP	NSEPEWHPY	1
Vav1-H6	II	NYWVNVDNE	RDLRKTQNM	1
Vav1-C2	II	IKGDMDEEP	SGQIKYWYP	1
Vav1-G5	II	PYWVNISDE	VRQIPHFPW	1
Vav1-D6	II	KYWVNRPFP	AAE	1
Vav1-B6	II	PYWVNVRDE	AAE	1
Vav1-B5	I	VNNYVQQYK	LIHQQVFLK	1
Vav1-B4	I	PGMNFHIPE	NQWLPAWYI	1
consensus:		YWVNHXXE Y		

Figure 4.31. Unique Affimer clones raised against Syk-N, Tns1 and Vav1 SH2 domains. ***(A)*** *Alignment of the variable regions (VRs) of Affimer binders raised against the N-terminal Syk SH2 domain.* ***(B)*** *Alignment of Tns1 binders revealed a consensus of Ar/P-Ar-Hy-Ar in VR2.* ***(C)*** *Alignment of Vav1 clones showed a consensus of Y-W-V-N-Hy-X-X-E in VR1. Alignments were performed using MacVector 13.5.2. Residues that conform to a consensus are in red.*

Twenty-six unique sequences were raised against the Vav1 SH2. A consensus of Y-W-V-N-Hy-X-X-E was revealed in VR1 (Figure 4.31C). Eighteen of the binders contain the motif Y-W-V-N in this region.

A summary table of ELISA hit rates and number of unique clones isolated for each SH2 target can be seen in Table 4.5. This includes the previously performed Grb2 SH2 screen and so in total 38 SH2 domains were successfully screened using the Affimer phage libraries. For targets which were screened more than once, both ELISA hit rates are reported. The number of clones sequenced and subsequent unique binders identified are the total number from both screens.

4.4 Discussion

In this work, Affimer binders were successfully isolated against 38 SH2 domains out of 42 screened (including PLCγ2-C). The number of Affimer clones raised against each target ranged from 1 – 48 (totalling 8 – 100% of the sequenced population for each target). In addition, for 10 constructs from PLCγ, Grb and Ship protein families, Affimer binders have been isolated that appear to be protein-specific when tested against closely-related family member SH2s in an ELISA. A hit rate of 50 – 100% was achieved in phage ELISAs for over half of the targets.

This success was not only due to the stringent phage display protocol used, but also the incorporation of an N-terminal BAP tag on the SH2 antigens. This allowed site-directed *in vivo* biotinylation of the target protein for phage display screening, removing the need for chemical biotinylation which was thought to result in blocking of the SH2 binding site. This method also allows the simple capture directly from cell lysate and presentation of the target protein away from the surface, making the binding site more easily accessible, an advantage when isolating Affimer binders that will function in cell-based assays. Previously failed screens for the PLCγ SH2s were repeated, and were successful for four of the five targets using this new immobilisation method (Figures 4.7 and 4.8).

Previous studies have recommended the use of competitive panning to reduce the isolation of cross-reactive binders and have reported >100x increase in the selectivity of clones when compared to standard panning (Hemminki et al., 1998; Mersmann et al., 2010).

Table 4.5. Summary of phage display screening and isolation of Affimer clones to BAP-tagged SH2 domains. *Final hit rates and unique clones isolated for each successfully screened SH2 domain. Targets for which the positive hit criteria was lowered to a signal ≥3x that of the negative control are highlighted in grey. For SH2s screened twice, both hit rates are shown separately in column 2.*

SH2 target	ELISA hit rate (%)	Number sequenced	Unique clones
Abl1	60	48	6
Abl2	100	48	42
Bmx	98	48	22
Crk	83	48	21
Fyn	90	48	20
Grb2	92	48	30
Grb7	73 / 15	61	48
Grb10	42 / 13	34	12
Grb14	92 / 10	52	8
Lck	91	87	35
Lyn	8	8	4
Nck1	81	48	4
Nck2	15	8	7
p85α-C	23	48	9
p85α-N	92	48	24
p85β-C	54	48	8
p85β-N	98	48	8
p55γ-C	81	48	13
p55γ-N	100	48	35
PLCγ1-T	27 / 4	21	13
PLCγ1-N	88	10	2
PLCγ2-T	8	6	3
PLCγ2-N	48 / 4	33	11
She	66	48	8
Ship1	52 / 50	54	26
Ship2	25 / 25	36	27
Src1	17	8	4
Stat1	2	48	14
Stat3	92	48	47
Stat4	31	48	48
Stat5a	29	7	2
Stat5b	2	6	5
Stat6	4	1	1
Syk-N	69	42	18
Tec	4	7	6
Tns1	38	48	4
Vav1	81	48	26

In the comparison of panning techniques conducted using Grb and Ship SH2s, competitive panning generally isolated more specific binders than standard panning (Figures 4.9 – 4.13) . This was particularly notable for Ship2, where competitive panning isolated multiple binders with no cross-reactivity, in contrast to standard panning (Figure 4.13). For Grb7 and Grb10 SH2s, competitive panning also identified more unique binders than non-competitive panning (Figures 4.16 and 4.17). The ELISA signals of binders isolated from competitive panning were also generally higher, suggesting these could bind more strongly to the target. This implied that competitive pans were successful in removing weaker binders through the incubation of phage with unbound target. Grb14 was the only target for which competitive panning clones did not show higher specificity in phage ELISAs; but this was due to the presence of one cross-reactive clone which occurred frequently in the population (Figure 4.11).

The results obtained from the Affimer libraries in this work are comparable to those achieved by the Renewable Protein Binder Working Group and colleagues, who have used antibody fragment libraries to screen against SH2 domains via phage display (Colwill et al., 2011; Mersmann et al., 2010; Pershad et al., 2010). In one of these screens of 20 SH2 domains using a scFv library, the positive hit rate in ELISA varied from 5 – 63% per target, with a quarter of the targets showing a hit rate of ≥ 50%. Of these, between 12 – 48 per target were then taken forward for a specificity ELISA testing cross-reactivity with two other SH2 domains (Shc1 and Lyn). Of these, between 4 – 96% of clones tested showed specificity for their target. Unique clones were then identified and this ranged from 1 – 19 clones per target (Pershad et al., 2010).

In another of these screens on the same 20 SH2s, positive ELISA hits ranged from 0 – 44%. The screens for the two failed targets, as well as four targets with low signals in ELISA, were repeated using immobilisation of targets to magnetic beads rather than microtiter plates for panning. These repeated screens yielded hit rates of 3 – 74%. The number of unique clones isolated per target ranged from 2 – 10 (Mersmann et al., 2010). From all the antibody screens combined, a total of 1,788 clones showed positive hits in ELISA out of 6,972 screened (26%). A total of 340 unique binders for the 20 SH2 domains were isolated from the screening of four libraries (an average of 17 antibody fragments per target).

In this study, the hit rate in ELISA ranged from 0 – 100%, with over half the targets showing a hit rate of ≥ 50%. In the specificity ELISAs on Grb and Ship family SH2s, between 2 – 100% of hits were specific for their target. This is raised to a rate of 33 – 100% per target, if the Grb14 competitive pan ELISA is excluded. The number of unique clones per target identified in this study was 1 – 48, with a total of 622 unique binders raised against 38 SH2 domains (an average of 16 Affimer clones per target).

After analysis of isolated clones, it was revealed that some of the Affimer VR sequences correlated to previously reported binding motifs of the SH2 targets. In prior studies these motifs have often included a phosphorylated tyrosine residue, to mimic natural SH2 substrates. However, as seen with the Grb2 SH2 binders characterised in Chapter 3, the Affimer VR sequences can imitate these binding motifs with a non-phosphorylated Y in place of the phosphotyrosine.

Previously reported binding motifs for PLCγ1 and PLCγ2 SH2s did not match any consensus seen within the PLCγ Affimer clones. However, a few clones did share similarities with previously observed phosphopeptide sequences; for example, PLCγ1T-B8 (Figure 4.14) contained the motif Y-X-X-L which reflected the reported preference for L at Y + 3 by the PLCγ1-N domain (Songyang et al., 1993; Liu et al., 2012). Binders PLCγ2N-B8 and PLCγ2N-B3 from the non-BAP-tagged screen also showed this sequence (Figure 4.3B). Another PLCγ2-N binder from the BAP-tagged screen, PLCγ2N-B7, contained the sequence Y-G-I-P (Figure 4.15B). This correlated to the previously found PLCγ2 SH2 binding preference of P at Y + 3 (Tinti et al., 2013).

The Grb7 SH2 has an established binding motif of pY-X-N in its substrates (where pY is a phosphotyrosine) (Pero et al., 2002). Of the 48 unique Grb7 binders, 46 contained the Y-X-N motif, with the majority appearing in VR2 (Figure 4.16). The more extended consensus seen upon alignment of competitive panning Affimer binders was I/L-Y-G-X-X-Y-X-N. This shows a preference for tyrosine or other aromatic residues N-terminal to the pY, as previously reported (Pero et al., 2002). Despite Grb2 and Grb7 having a similar binding motif, little cross-reactivity was seen for Grb7 binders. Comparison of Grb7 and Grb2 SH2 Affimer clones isolated in this project with therefore may be useful for conferring potential selectivity between Grb7 and Grb2 SH2s.

Competitive clones Grb10-D9 and Grb14-C3 also contained the previously reported substrate motifs of Y-X-X-M and Y-E-N-X, for the Grb10 and Grb14 SH2s respectively (Figures 4.17 and 4.18) (Laviola et al., 1997; Tinti et al., 2013). Findings have shown that a hydrophobic residue at the Y + 2 position is required for recruitment of the Ship1 SH2 by its ligands (Bruhns et al., 2000). This Y-X-Hy sequence was found in 11 of the 28 Affimer binders (Figure 4.19). The Ship2 SH2 was also reported to bind the same motif, but no Ship2 Affimer clones contained this sequence.

The preferred ligand binding motif of the Abl SH2 domain has been reported as pY-X-X-P by multiple studies (Colicelli, 2010; Y.J.Wang, 2010; Tinti et al., 2013). This motif can be seen in binder Abl1-B3 in VR1, but in no other isolated clones (Figure 4.24A). The Y-M-D motif seen in the first region of Abl1-A1 also forms part of an Abl1 SH2 binding motif of pY-M-D-L previously reported (Songyang et al., 1993). The Y-X-X-P motif was also seen in Abl2 clones Abl2-A2, Abl2-A3 and Abl2-G2 (Figure 4.24B). The strong consensus in Abl2 binders of P-L-X-W-L-X-L-P did not correlate to known Abl2 binding peptides; however, L has been shown to be a preferred residue at pY + 3 for the Abl2 SH2. Many of the Affimer clones contained the motif W-X-X-L as part of the consensus sequence, with W replacing Y as the aromatic residue in this sequence (Tinti et al., 2013).

It has been shown that the Bmx SH2 preferentially binds peptides containing an N at pY + 2 (Tinti et al., 2013). Nine of the Bmx clones contained this Y-X-N motif, with Bmx-H5 and Bmx-F6 also containing an E residue at Y + 1 (Y-E-N) and C2 containing a V at pY + 3 (Y-X-N-V); all which corresponded to the binding preferences reported for Bmx (Figure 4.24C) (Tinti et al., 2013). This motif is also the same seen in the Grb7 Affimer clones, suggesting these binders could be cross-reactive.

The Crk Affimer consensus of H-D-Y-Y-Ar-Hx (Figure 4.25A) did not correlate with the known phosphopeptide binding motif of pY-X-X-P for the Crk SH2 (Feller, 2001). However, three clones (Crk-A1, Crk-F3 and Crk-E5) did contain this sequence (Y-X-X-P). Additionally, these clones contained a D residue at Y + 1, which reflects previously reported binding preferences of the Crk SH2 (Songyang et al., 1993). Binder Nck1-A1 (Figure 4.26A) contained the sequence Y-D-P-V, which also corresponded to the binding motifs reported for the Nck SH2 by Songyang et al. (1993).

For the Stat1 SH2 domain, a phosphopeptide binding motif of pY-D/E-P/R-R/P/Q has been observed (Gan and Roux, 2009). A sequence corresponding to this was found in Stat1-G4, which contained the motif Y-E-P-P (Figure 4.30A). Another Stat binder also containing a similar sequence was Stat4-F4 (Y-E-Y-P) (Figure 4.30C). In a different study, the preferred Stat SH2-binding motif was described as Y-X-X-Q (Liu et al., 2012). Two Stat Affimer clones, Stat3-G3 and Stat4-C6, contained this sequence (Figure 4.30B, C). An additional nine Stat3 and Stat4 binders contained this sequence with a different aromatic residue in place of the Y. This suggested that these Affimer clones could bind in the pTyr-binding pocket of the Stat SH2s. Most of the Stat binders did not contain these known Stat SH2 domain binding motifs, and therefore could be binding outside the SH2 domain itself, as previously mentioned.

SykN-B2 contained a reported Syk-N SH2 binding motif of Y-X-X-I/L (Figure 4.31A) (Liu et al., 2012; Tinti et al., 2013). The Tns1 SH2 binding motif of Y-E-N-X was also found in a Tns1 Affimer; Tns1-A1, which had occurred 43 times in the 48 sequenced clones (Figure 4.31B) (Liu et al., 2012). Additionally, a preference for an L residue at Y + 3 was observed for the Tns1 SH2 by Tinti et al. (2013). This Y-X-X-L motif was seen in binder Tns1-C2. In a previous study (Chen et al., 2011), it was shown that the Vav SH2 domain binds a peptide with the motif Y-X-X-X-Y; this sequence is found in Vav1-B5, but in no other Vav1 clones (Figure 4.31C).

Although many similarities were seen with previously reported SH2-binding motifs, most Affimer clones did not reflect known SH2 phosphopeptides. A well-documented peptide binding motif for the Src family SH2s is the Y-E-E-I motif, which none of the Src family Affimer clones contained (Figure 4.25B - E) (Liu et al., 2012). Equally, the W-E-E-Y-H-E consensus seen in both p85α-N and p55γ-N binders (Figure 4.27B, F) did not correlate with preferred PI3K SH2 binding motifs; or even any known PI3K interacting partners in a BLAST search of the motif. For Affimer clones showing no known binding motif, this suggests that they could be binding areas outside the pY-binding pocket. Once specificities for all Affimer clones have been explored, the sequences of the VRs will be a useful tool for probing which motifs confer binding specificity for individual SH2s.

The rapid process of screening the Affimer library combined with the ease of screening multiple targets at once, results in a cost-effective method of

generating research tools to large protein families such as SH2 domains. Different research groups are attempting to screen the entire human proteome using binding reagents such as antibodies and their fragments (Colwill et al., 2011; Pershad et al., 2010; Mersmann et al., 2010). Using the Affimer library to help achieve this goal could provide a less laborious and costly option, with comparable results achieved.

Chapter 5

Testing the specificity of SH2-binding Affimer reagents

Chapter 5
Testing the specificity of SH2-binding Affimer reagents

5.1 Introduction

Testing the specificity of binding reagents is a rate-limiting step. High specificity is especially important for use of reagents in functional cell-based assays, as high concentrations of numerous other proteins within the cell presents a challenging environment for specific recognition of a protein of interest (Sha et al., 2017). Although SH2 domains have been targeted using phosphopeptides, peptidomimetics and small molecules, these have often not been able to discriminate between closely related SH2 domains, such as the Grb family SH2s or Src family kinase SH2s (Kraskouskaya et al., 2013, Quartararo et al., 2012, Kukenshoner et al., 2017). Inhibitors that were originally developed for selective inhibition are now even used as 'pan' SH2 domain probes, demonstrating the lack of truly specific binders (Kukenshoner et al., 2017). Additionally, many inhibitors claiming to be selective show a lack of data against a sufficient proportion of the SH2 domain family (Furet et al., 1998, Kraskouskaya et al., 2013).

Specificity of four SHP2 SH2-binding monobodies was tested using intracellular expression of the epitope-tagged monobodies, followed by affinity capture from lysate and mass spectroscopy to identify binding partners (Sha et al., 2013). This revealed no reproducible capture of other SH2-containing proteins, showing that non-antibody scaffolds could be effective at conferring specificity for one SH2 domain only. This could be due to the larger binding interface available in protein binders compared with small molecules and phosphopeptide mimetics. The crystal structure of an Abl SH2-binding monobody in complex with the SH2 domain revealed that one third of the binding interface lay outside the highly-conserved phosphotyrosine-binding pocket usually targeted by small inhibitors (Wojcik et al., 2010). This extra portion of the domain bound by the monobody is theorised by the researchers to be the reason for its specificity for Abl SH2s over Src family SH2 domains.

Affimer reagents have shown high specificity for previous targets, demonstrating the ability to discriminate between homologous protein isoforms (Tiede et al.,

2017, Tiede et al., 2014, Hughes et al., 2017, Tang et al., 2017). They are therefore promising tools for specific targeting of SH2 domains. In this work, the SH2-binding Affimer reagents isolated in Chapter 4 were tested for their specificity against the set of 43 SH2 domains that had been screened using phage display. A protein microarray assay was used to accomplish this.

Protein microarrays provide a versatile platform with which to characterise thousands of proteins in a high-throughput manner (Sutandy et al., 2013). The concept of microarray technology was first developed by Roger Elkins in 1989 and was evolved into the DNA microarray, which has been successfully used to determine the mRNA expression levels of thousands of genes in numerous biological samples (Trevino et al., 2007). The protein microarray was later developed and is now used for protein function analyses, study of protein-protein interactions and for determining substrate specificity (Angenendt, 2005). Indeed, microarrays have been used in numerous studies to determine specificities of monoclonal antibodies (Jeong et al., 2012, Hu et al., 2007).

Microarray technology consists of depositing nanolitre drops of up to tens of thousands of proteins onto a small surface; usually a glass slide or other substrates such as nitrocellulose (Barbulovic-Nad et al., 2006). The proteins are arranged in specific locations on the array to enable identification upon analysis. Samples or reagents are then incubated with the arrays in solution and bound proteins are detected (Govindarajan et al., 2012). Protein microarrays have become one of the most powerful tools in proteomic studies and are an effective high-throughput method for determining specificity of reagents (Sutandy et al., 2013). If a successful microarray protocol can be developed for screening Affimer specificity, this could be a very useful tool for selecting Affimer reagents for further characterisation; reducing both workload and cost due to the volume of reagents used.

5.2 Production of SH2 and Affimer proteins for protein microarrays

5.2.1 Production and purification of BAP-tagged SH2 domains

SH2 domain proteins were recombinantly produced from pET28 vectors encoding the SH2 sequences with an N-terminal 6xHis-tag and BAP-tag, as

previously described in Chapter 4 (section 4.3.1). However, instead of using the automated purification of SH2 domains on the KingFisher™ Flex robotic platform, SH2s were produced from 50 ml cultures of Rosetta™ 2 (DE3) *E. coli* and purified manually using Amintra™ Ni-NTA resin (Expedeon) (Chapter 2, section 2.2.4.1). This scale-up was to ensure a sufficient protein yield for the microarray experiments. Estimated total yields typically ranged from ca. 3 – 400 mg, with the Stat constructs in particular showing consistently low yields. The purity of elutions and successful *in vivo* biotinylation of SH2s was confirmed by western blot analysis to detect biotin (Figure 5.1). Biotinylated proteins were observed corresponding to the theoretical MWs of all SH2 domains, as well as bands at higher MWs for some of the domains. The size of these bands corresponded to the dimeric forms of the SH2s and had been observed in previous western blots of these proteins. Although some SH2 domains (Grb7, Nck2, PLCγ2-T, Ptpn11-N, Ship2, Src2 and Syk-N) show almost undetectable signals, bands were revealed when the membrane was overexposed; these low signals in the blot corresponded to a lower estimated protein concentration.

5.2.2 Cloning and production of HA-tagged Affimer reagents

For each SH2 target successfully screened by the Affimer library (Chapter 4), 3 – 5 unique clones were chosen to take forward for microarray experiments (except for targets Stat5a, Stat6 and PLCγ1-N where only 1 – 2 clones had been isolated). These clones were chosen based on their frequency in the sequenced population, their signal in phage ELISA, or a combination of both. For some targets, the choice was limited due to the low number of unique clones isolated. The 16 Grb2 SH2 Affimer reagents were also included, to compare results to the specificity phage ELISAs conducted on these clones (Chapter 3, section 3.6). Additionally, Affimer reagents previously isolated against the SH2 domains of PI3K in an earlier screen (Tiede et al. 2017) were included, as the specificities of these had also been previously determined by phage ELISA. Chosen clones for each SH2 can be seen in Appendix C; in total, 177 Affimer clones raised against 37 SH2s.

Affimer proteins used in microarray experiments were produced from pET-lectra vectors encoding the Affimer with a C-terminal 6xHis-tag and a HA-tag (YPYDVPDYA). This HA-tag was located between the Affimer and His-tag

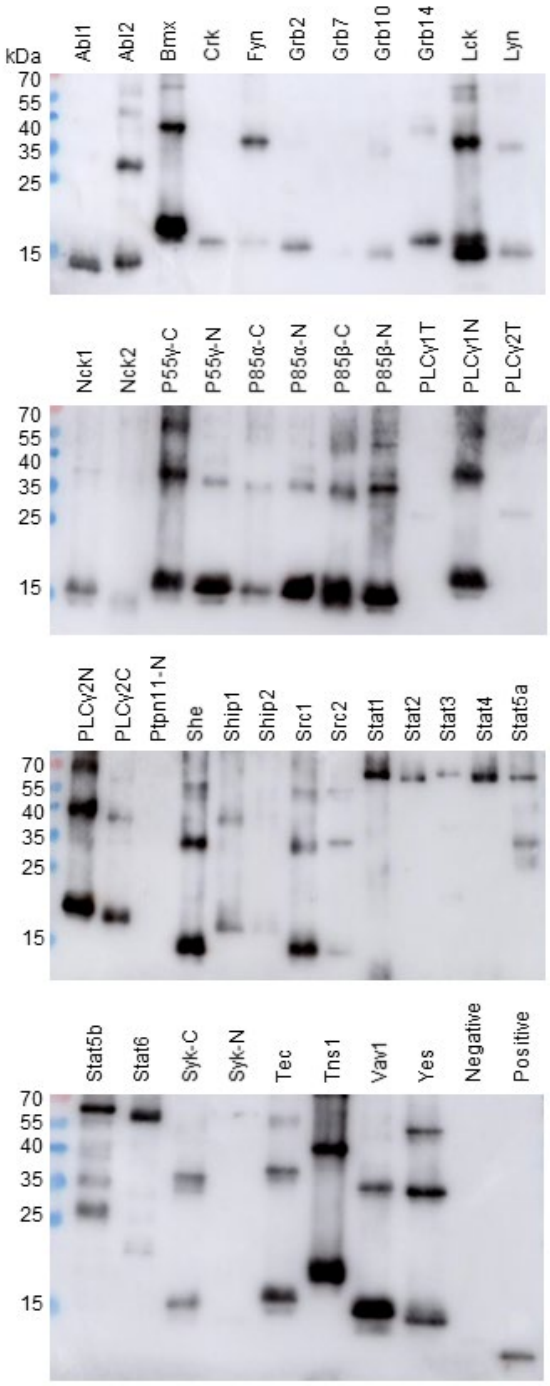

Figure 5.1. Production of biotinylated BAP-tagged SH2 domains for use in microarrays. *Western blots showing purified SH2 domain protein samples probed for biotinylated proteins. 5 µl samples diluted 1:5 in elution buffer were subject to SDS-PAGE and transferred to nitrocellulose membranes. Membranes were incubated with High Sensitivity Streptavidin-HRP, 1:5000 to detect biotin. HRP visualised with Luminata Forte. Purified non-biotinylated Grb2 SH2 and chemically biotinylated Grb2 SH2 were used as negative and positive controls, respectively. MW marker = PageRuler Prestained, gels contain 15% acrylamide.*

sequences and was included for detection of the Affimer proteins; in microarray experiments previously conducted by Avacta®, HA-tagged Affimer reagents had been successfully used and detected by an anti-HA antibody (data not published). It was therefore decided to utilise this tested strategy for the SH2 domain array (summarised in Figure 5.2). Affimer sequences (177 in total) were subcloned from the pBSTG phagemid vector into the pET-lectra expression vector and subject to DNA sequencing analysis (see Chapter 2, section 2.2.5.2). This work was carried out by the candidate and Thomas Taylor (Tomlinson group, University of Leeds). In addition to the SH2 domain Affimer reagents, the ySUMO Affimer YS-10 was also subcloned into pET-lectra, to be used as a positive control with biotinylated ySUMO in the microarray optimisation. Ligations of three clones were unsuccessful and DNA analysis showed incorrect sequences for a further six clones (shown in pink in Appendix C), leaving 168 clones to take forward. It was not attempted to repeat subcloning for the failed binders, as at least one clone per target was successful.

HA-tagged Affimer proteins were recombinantly produced from the pET-lectra vector, in cultures of BL21 Star™ (DE3) *E. coli* cells by IPTG-induction at 30 °C overnight. As previously utilised for the SH2 domains, proteins were produced from 3 ml cultures and purified using His Mag Sepharose Ni beads (GE Healthcare) on the KingFisher™ Flex robotic platform. Total yields typically ranged from ca. 15 – 130 µg and proteins showed a sufficient level of purity as

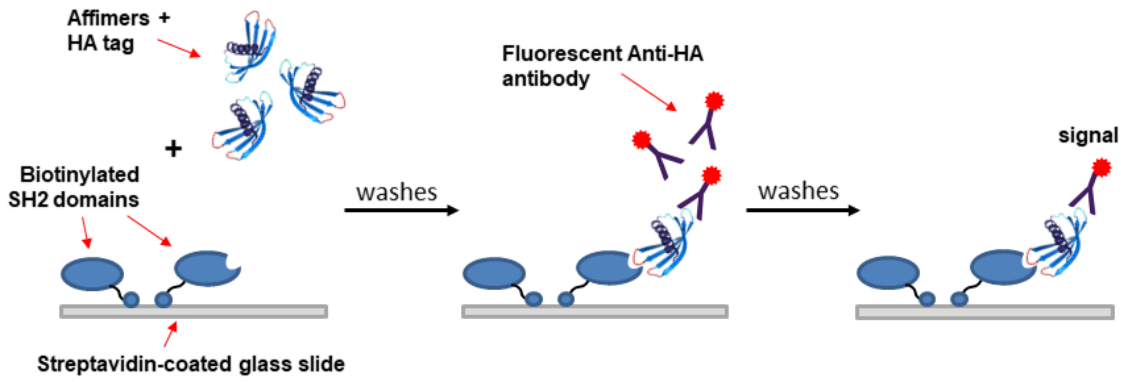

Figure 5.2. Schematic of strategy for SH2 protein microarrays using BAP-tagged SH2 domains. *Biotinylated BAP-tagged SH2 domain proteins were immobilised in an array format on streptavidin-coated glass slides and incubated with HA-tagged Affimer. Bound Affimer was then detected using a fluorescently-labelled HA-tag antibody and after washing fluorescence is read at the correct wavelength for the antibody fluorophore.*

determined by SDS-PAGE (Figure 5.3A). Clones with lower yields were re-produced in 50 ml cultures (see Figure 5.3B). These typically did not appear as pure as the KingFisher™ purified Affimer proteins, sometimes revealing an extra band at ca. 35 kDa in certain samples. Interestingly, Affimer Grb2-D5 (boxed in black, Figure 5.3A) did not appear as a stable dimer, as it did when produced from the pET11a vector (Chapter 3). This is discussed in more detail in the discussion section of this chapter.

5.3 Optimisation of microarray conditions using Grb2 SH2 Affimer reagents

Optimisation of the microarray protocol was carried out using Grb2 SH2 Affimer clones; Grb2-12, Grb2-B5, Grb2-D6 and Grb2-F5, as well as YS-10 (see Chapter 2, section 2.2.11). These clones were first tested against a sub-set of six BAP-tagged SH2 domains (including all Grb family members) and chemically biotinylated ySUMO. Three concentrations of Grb SH2s and ySUMO were tested initially; 10 and 20 µM, as well as the highest possible concentration for each protein (ranging from 50 – 80 µM). Proteins were printed in 1X PBS + 20% glycerol; addition of glycerol in printing buffer has been shown to slow spot drying and decrease variation in spot size and morphology, including the occurrence of drying artefacts (Olle et al., 2005).

Proteins were spotted onto streptavidin-coated glass slides (PolyAn) to utilise the N-terminal BAP-tag for immobilisation; enabling the same orientation of targets that was used in the phage display screens. Studies have shown that specific orientation of capture agents increases the analyte-binding capacity (up to 10-fold) of surfaces used in microarrays (Peluso et al., 2003). The strength of the streptavidin/biotin bond would also decrease the loss of immobilised SH2 during slide processing.

Slides were printed with 14 mini-arrays per slide, using buffer-only spots as a negative control. After drying overnight, slides were scanned at 532 nm to visualise the immobilised proteins (Figure 5.4). This showed no drying artefacts, although some proteins could be visualised more clearly than others. Slides were then processed, with an individual Affimer incubated with each mini-array. Slides were scanned at 635 nm to observe bound Affimer, by detection of the

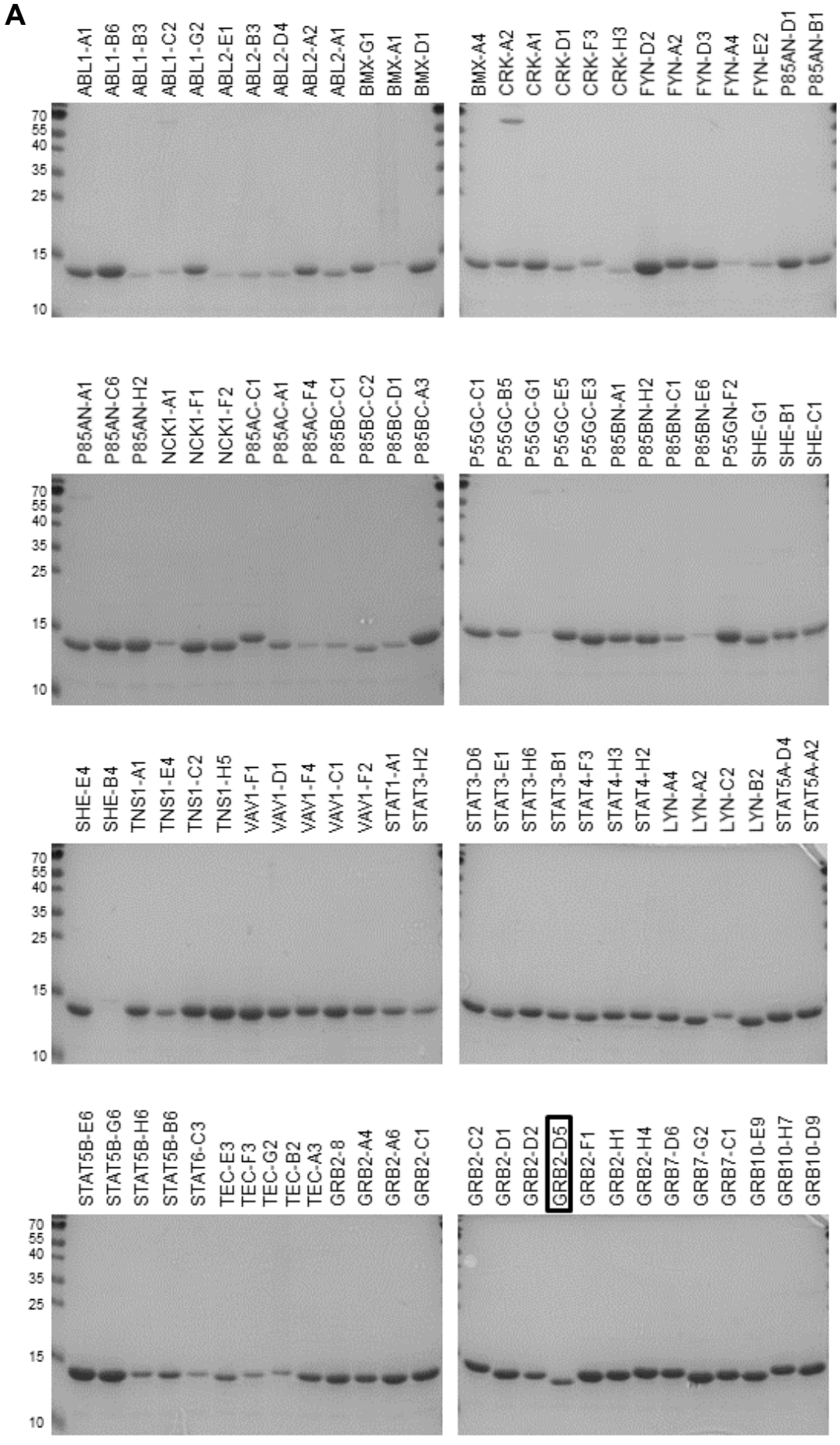
A
ABL1-A1
ABL1-B6
ABL1-B3
ABL1-C2
ABL1-G2
ABL2-E1
ABL2-B3
ABL2-D4
ABL2-A2
ABL2-A1
BMX-G1
BMX-A1
BMX-D1
BMX-A4
CRK-A2
CRK-A1
CRK-D1
CRK-F3
CRK-H3
FYN-D2
FYN-A2
FYN-D3
FYN-A4
FYN-E2
P85AN-D1
P85AN-B1
P85AN-A1
P85AN-C6
P85AN-H2
NCK1-A1
NCK1-F1
NCK1-F2
P85AC-C1
P85AC-A1
P85AC-F4
P85BC-C1
P85BC-C2
P85BC-D1
P85BC-A3
P55GC-C1
P55GC-B5
P55GC-G1
P55GC-E5
P55GC-E3
P85BN-A1
P85BN-H2
P85BN-C1
P85BN-E6
P55GN-F2
SHE-G1
SHE-B1
SHE-C1
SHE-E4
SHE-B4
TNS1-A1
TNS1-E4
TNS1-C2
TNS1-H5
VAV1-F1
VAV1-D1
VAV1-F4
VAV1-C1
VAV1-F2
STAT1-A1
STAT3-H2
STAT3-D6
STAT3-E1
STAT3-H6
STAT3-B1
STAT4-F3
STAT4-H3
STAT4-H2
LYN-A4
LYN-A2
LYN-C2
LYN-B2
STAT5A-D4
STAT5A-A2
STAT5B-E6
STAT5B-G6
STAT5B-H6
STAT5B-B6
STAT6-C3
TEC-E3
TEC-F3
TEC-G2
TEC-B2
TEC-A3
GRB2-8
GRB2-A4
GRB2-A6
GRB2-C1
GRB2-C2
GRB2-D1
GRB2-D2
GRB2-D5
GRB2-F1
GRB2-H1
GRB2-H4
GRB7-D6
GRB7-G2
GRB7-C1
GRB10-E9
GRB10-H7
GRB10-D9
70
55
40
35
25
15
10

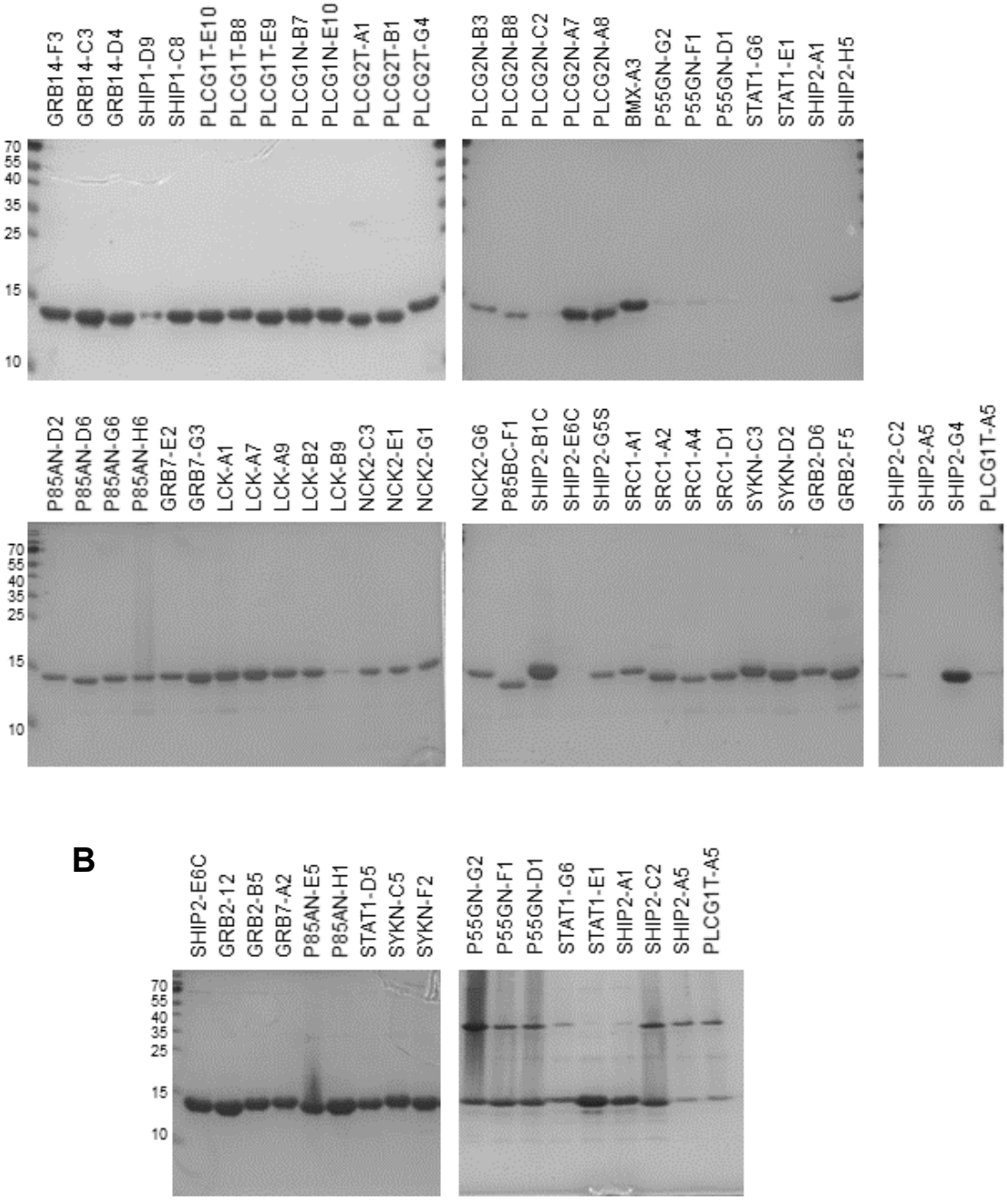

Figure 5.3. Production of HA-tagged SH2-binding Affimer proteins. ***(A)*** *SDS-PAGE analysis of purified HA- and His-tagged SH2-binding Affimer proteins. Affimer reagents purified on a KingFisher™ Flex robotic platform were electrophoresed on 15% acrylamide gels and detected with Coomassie Blue. MW of Affimer proteins ranged from ca. 13 – 14 kDa. No dimerisation of binder Grb2-D5 (black box) was seen (ca. 13 kDa). Analysis showed low yields for some clones, which were re-produced in 50 ml cultures and manually purified using Ni-NTA resin* ***(B)****. Molecular weight marker = PageRuler™ Prestained.*

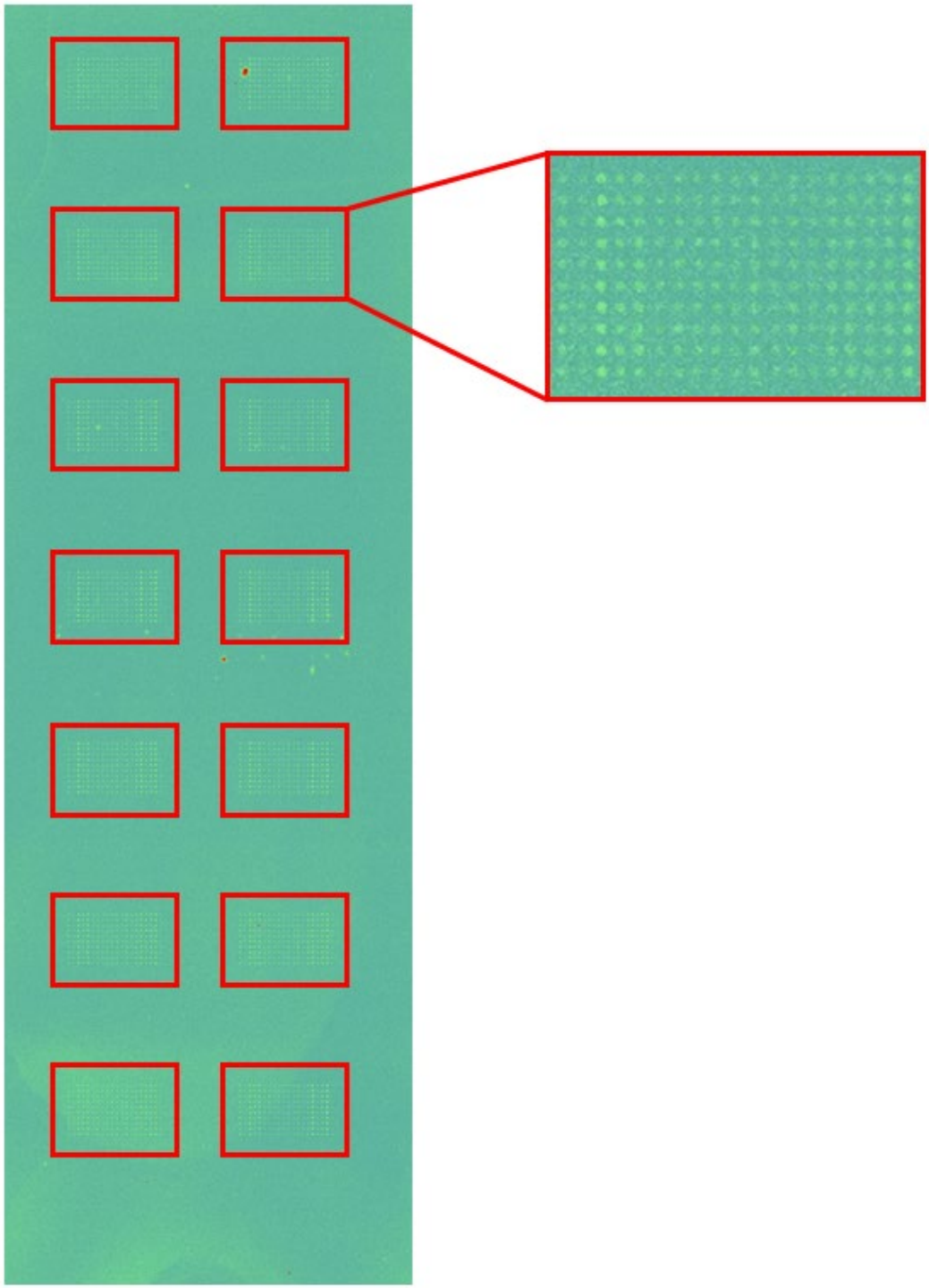

Figure 5.4. Post-print analysis of SH2 immobilisation on streptavidin-coated slides. *Streptavidin-coated slide (PolyAn) spotted with BAP-tagged SH2 domain proteins was scanned at 532 nm to visualise the immobilised proteins. SH2s were spotted in 14 identical arrays per slide, with 10 replicate spots per protein, and dried overnight in a controlled environment of 18 – 19 °C and 50 – 55% humidity. Image was captured using a GenePix 4300A scanner and analysed using GenePix® Pro 7 software; image is shown in Rainbow mode to better visualise the protein spots.*

fluorescent anti-HA-tag secondary antibody. GenePix® Pro 7 software was used to automatically detect protein spots and subtract background signal. In the initial test, dilutions of 0.5 mg/ml Affimer at 1:500 and 1:2500 were used with 1:500 and 1:2500 HA-tag antibody, respectively. Additionally, dilutions of 1:100 were tested for the YS-10 control, in case no signals at lower dilutions were seen. The 1:2500 dilutions of Affimer reagents YS-10, Grb2-12 and Grb2-B5 showed very low or no binding to the intended target, whereas Grb2-D6 and Grb2-F5 showed substantial binding to the highest Grb2 concentration of 70 μM and a lower level of binding to 10 and 20 μM Grb2 (see Figure 5.5A for examples).

When reagent dilutions of 1:500 were used, significant binding to 70 μM Grb2 was then seen for Grb2-12 and Grb2-B5. These clones also showed binding to lower Grb2 concentrations, although with a greatly decreased signal. At this dilution Grb2-D6 and Grb2-F5 showed binding to all Grb2 SH2 spots in a Grb2 concentration-dependent manner, with Grb2-D6 also showing binding to Grb7 80 μM (see Figure 5.5B for examples). For YS-10, binding to ySUMO was only visualised when using 1:100 dilutions (Figure 5.5C). The results from this test demonstrated the ability to successfully detect Affimer-SH2 interactions using this protocol, although optimisation of reagent dilutions were needed. As signals were higher and uniformity of spot morphology was maintained with 70 μM spots, this was the immobilised target concentration used in future experiments. Moreover, the streptavidin-coated slides had displayed low background signal and uniform spot morphology, indicating this surface was sufficient for the immobilisation of SH2s.

In the next set of tests, optimum Affimer and antibody dilutions were established. The same protocol was used as before, but with a larger sub-set of 20 SH2 domains tested (including two different Grb2 samples to check batch-to-batch variability of SH2s). SH2s were printed at a concentration of 70 μM and incubated with dilutions of 0.5 mg/ml Affimer at 1:100 or 1:500, followed by dilutions of HA-tag antibody ranging from 1:500 – 1:10,000. Several additional Affimer clones for different SH2 targets, including both Type II and Type I scaffolds, were tested. Some example graphs for Grb2-B5 can be seen in Figure 5.6. As expected, the signal for the intended SH2 target was consistently higher with the 1:100 Affimer dilution compared with the 1:500 dilution (examples in Figure 5.6A and B). When

A

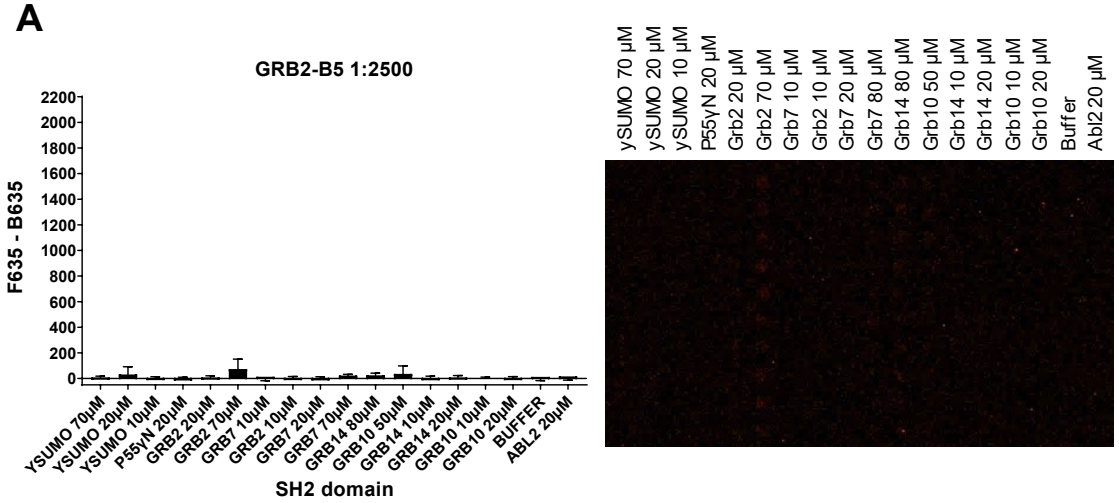
GRB2-B5 1:2500
F635 - B635
2200
2000
1800
1600
1400
1200
1000
800
600
400
200
0
YSUMO 70µM
YSUMO 20µM
YSUMO 10µM
P55γN 20µM
GRB2 20µM
GRB2 70µM
GRB7 10µM
GRB2 10µM
GRB7 20µM
GRB7 70µM
GRB14 80µM
GRB10 50µM
GRB14 10µM
GRB14 20µM
GRB10 10µM
GRB10 20µM
BUFFER
ABL2 20µM
SH2 domain
ySUMO 70 µM
ySUMO 20 µM
ySUMO 10 µM
P55γN 20 µM
Grb2 20 µM
Grb2 70 µM
Grb7 10 µM
Grb2 10 µM
Grb7 20 µM
Grb7 80 µM
Grb14 80 µM
Grb10 50 µM
Grb14 10 µM
Grb14 20 µM
Grb10 10 µM
Grb10 20 µM
Buffer
Abl2 20 µM

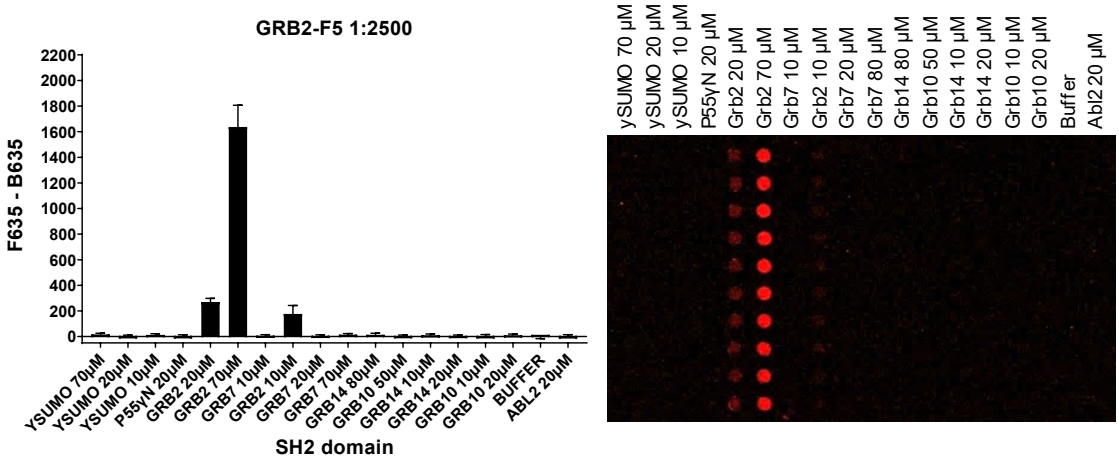
GRB2-F5 1:2500
F635 - B635
2200
2000
1800
1600
1400
1200
1000
800
600
400
200
0
YSUMO 70µM
YSUMO 20µM
YSUMO 10µM
P55γN 20µM
GRB2 20µM
GRB2 70µM
GRB7 10µM
GRB2 10µM
GRB7 20µM
GRB7 70µM
GRB14 80µM
GRB10 50µM
GRB14 10µM
GRB14 20µM
GRB10 10µM
GRB10 20µM
BUFFER
ABL2 20µM
SH2 domain
ySUMO 70 µM
ySUMO 20 µM
ySUMO 10 µM
P55γN 20 µM
Grb2 20 µM
Grb2 70 µM
Grb7 10 µM
Grb2 10 µM
Grb7 20 µM
Grb7 80 µM
Grb14 80 µM
Grb10 50 µM
Grb14 10 µM
Grb14 20 µM
Grb10 10 µM
Grb10 20 µM
Buffer
Abl2 20 µM

B

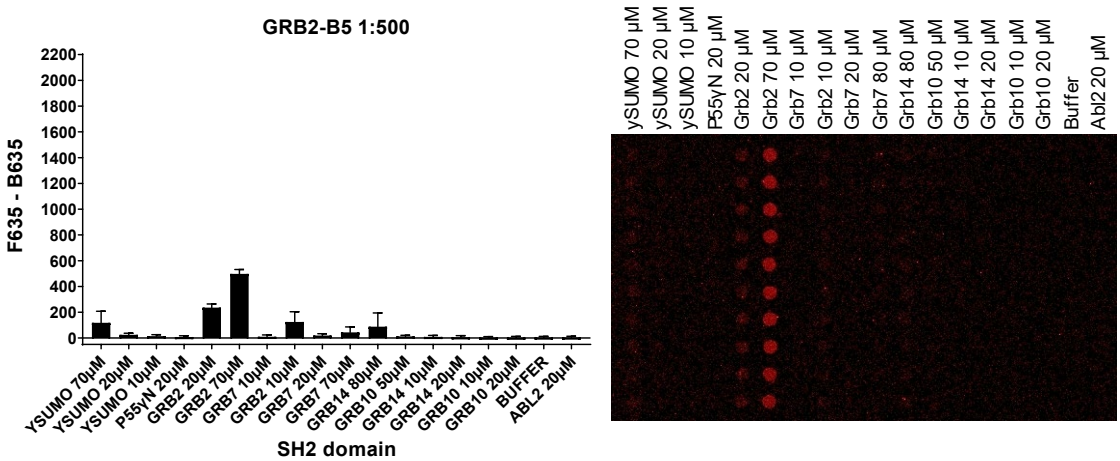
GRB2-B5 1:500
F635 - B635
2200
2000
1800
1600
1400
1200
1000
800
600
400
200
0
YSUMO 70µM
YSUMO 20µM
YSUMO 10µM
P55γN 20µM
GRB2 20µM
GRB2 70µM
GRB7 10µM
GRB2 10µM
GRB7 20µM
GRB7 70µM
GRB14 80µM
GRB10 50µM
GRB14 10µM
GRB14 20µM
GRB10 10µM
GRB10 20µM
BUFFER
ABL2 20µM
SH2 domain
ySUMO 70 µM
ySUMO 20 µM
ySUMO 10 µM
P55γN 20 µM
Grb2 20 µM
Grb2 70 µM
Grb7 10 µM
Grb2 10 µM
Grb7 20 µM
Grb7 80 µM
Grb14 80 µM
Grb10 50 µM
Grb14 10 µM
Grb14 20 µM
Grb10 10 µM
Grb10 20 µM
Buffer
Abl2 20 µM

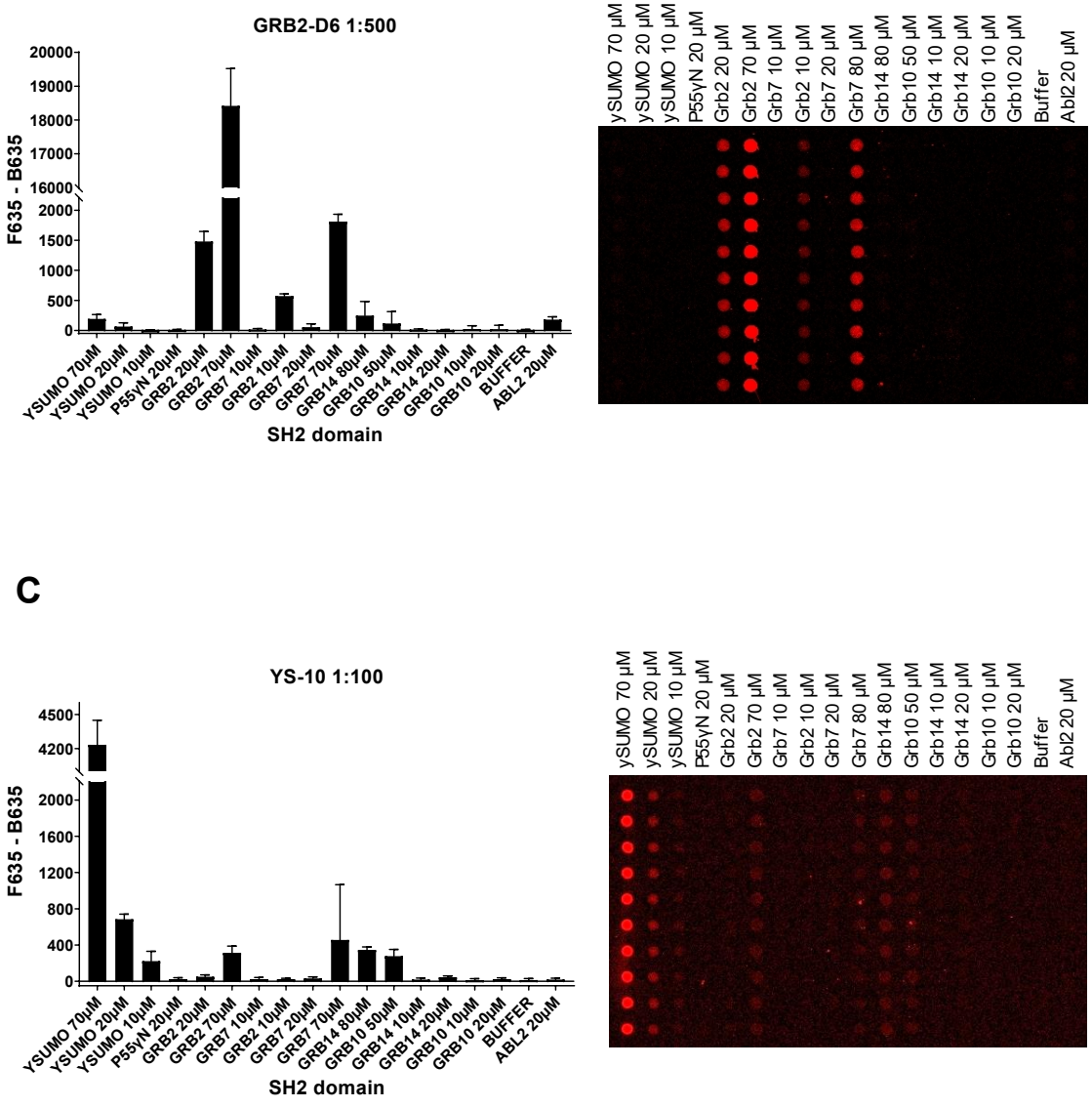

Figure 5.5. Preliminary optimisation of an SH2 protein microarray using Grb2 SH2 Affimer reagents. *Streptavidin-coated slides (PolyAn) spotted with different concentrations of BAP-tagged SH2 domain proteins were incubated with dilutions of HA-tagged Grb2 SH2 Affimer reagents (one per array). Bound Affimer was detected using an HA-tag Alexa Fluor® 647-conjugated antibody. After washing, slides were scanned at 635 nm using a GenePix 4300A scanner and analysed using GenePix® Pro 7 software.* ***(A)*** *Results for Grb2-B5 and Grb2-F5 at 1:2500 Affimer dilutions, demonstrating little to no binding of Grb2 SH2 by some reagents at this dilution.* ***(B)*** *Results for Grb2-B5 and Grb2-D6 for 1:500 dilutions, showing binding of the Grb2 SH2 by both reagents, as well as some cross-binding of Grb2-D6 to the Grb7 SH2.* ***(C)*** *The YS-10 positive control showed binding to ySUMO only at an Affimer + antibody dilution of 1:100.*

A

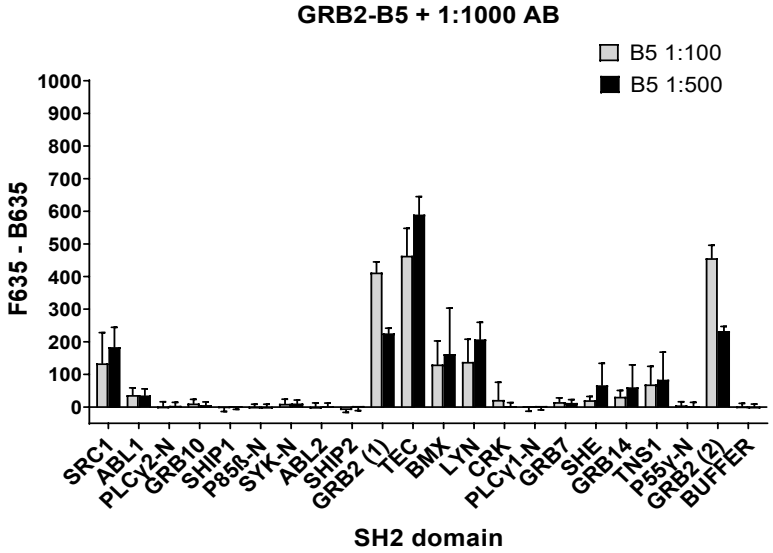

1:100 Affimer:

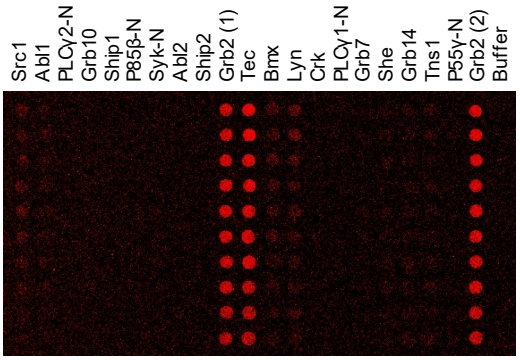

1:500 Affimer:

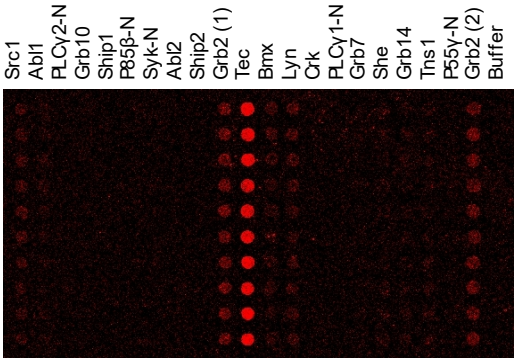

B

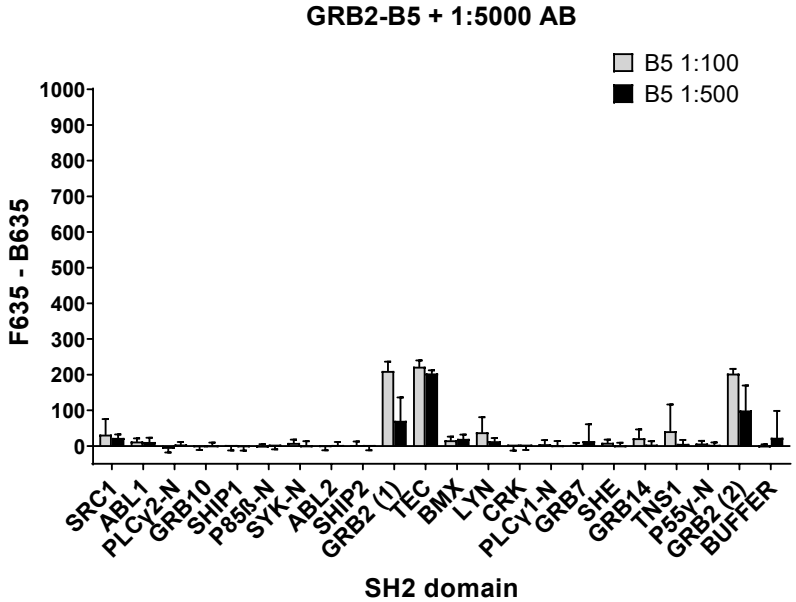

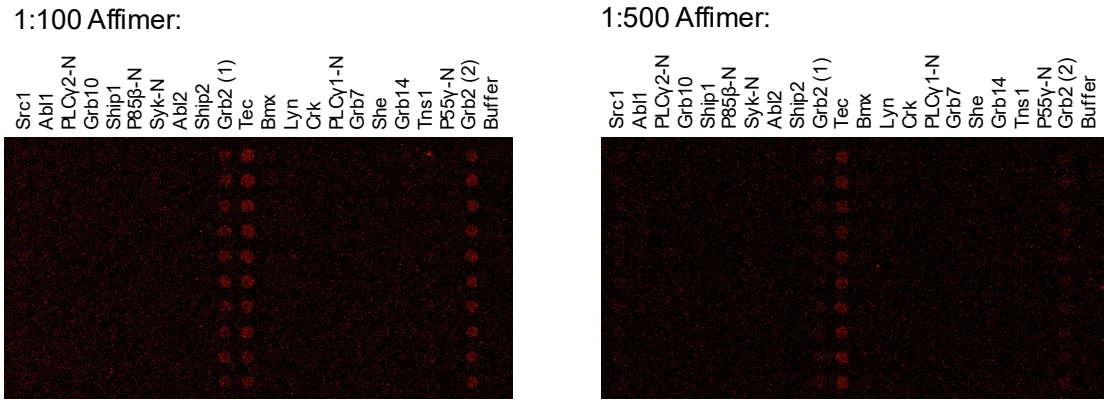

Figure 5.6. Optimisation of reagent dilutions for an SH2 protein microarray. *Streptavidin-coated slides (PolyAn) spotted with 70 µM BAP-tagged SH2 domain proteins were incubated with dilutions of HA-tagged Grb2 SH2 Affimer reagents and HA-tag Alexa Fluor® 647-conjugated antibody in blocking buffer. Slides scanned at 635 nm using a GenePix 4300A scanner and analysed using GenePix® Pro 7 software. Results for Grb2-B5 at 1:100 and 1:500 dilutions with* ***(A)*** *1:1000 antibody and* ***(B)*** *1:5000 antibody are displayed as examples, to show the increased signal seen with Affimer dilution 1:100, as well as the low signals seen with lower antibody concentrations. Graphs show mean background-corrected fluorescence for each SH2, quantified from the images to the right.*

combined with lower antibody dilutions of 1:5000 and 1:10,000, little to no signal was seen with 1:500 dilutions of some binders such as Grb2-B5 (see Figure 5.6B). Non-specific binding of the HA-tag antibody to certain SH2s was also seen in negative control wells incubated with antibody only (Figure 5.7A); antibody binding to the Tec SH2 was particularly high. The signal for this non-specific binding increased as the antibody concentration increased. This could indicate aggregation of these targets on the surface of the slide.

Based on the results of these tests, a combination of 1:100 Affimer with 1:1000 HA-tag antibody was decided upon for the final microarray experiments (final concentrations of 5 µg/ml Affimer and 1 µg/ml antibody). These dilutions showed the highest signal for specific Affimer-SH2 interactions, while showing lower signals for non-specific HA-tag antibody interactions than the 1:500 antibody dilution. Although the lower antibody concentrations of 1:5000 and 1:10,000 had shown even lower signals for these non-specific interactions, weaker Affimer

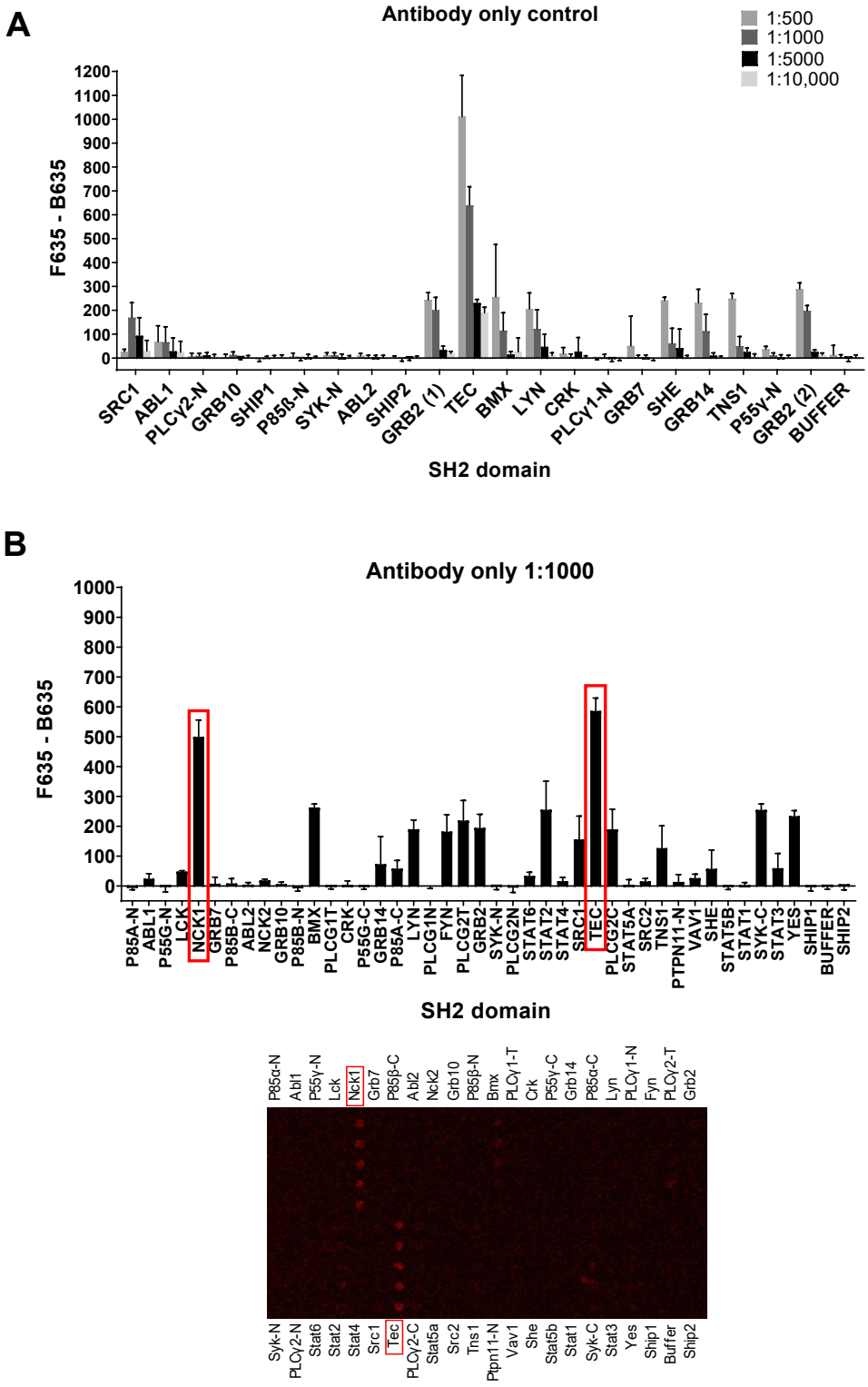

Figure 5.7. Non-specific binding of the HA-tag antibody to printed SH2 domain proteins. ***(A)*** *Antibody-only wells from optimisation shown in Figure 5.6. Streptavidin-coated slides spotted with BAP-tagged SH2 domain proteins (70 µM) were incubated with HA-tag Alexa Fluor® 647 antibody dilutions, 1:500 – 1:10,000. Slides were scanned at 635 nm using a GenePix® 4300A scanner and analysed with GenePix® Pro 7 software. Graphs show mean background-corrected fluorescence for each SH2.* ***(B)*** *The HA-tag Alexa Fluor® 647 antibody was then tested against all 43 SH2 domains at a dilution of 1:1000.*

clones such as Grb2-B5 had shown little detectable binding to their intended target for these conditions. It was a concern that lower signals in the assay would result in a loss of sensitivity and failure to detect weaker cross-reactions of Affimer reagents with other SH2s.

A final test was conducted to check non-specific binding of the HA-tag antibody to all 43 SH2 domains (listed in Appendix B). SH2s were printed onto slides at a concentration of 70 μM as before and incubated with 1:1000 antibody. Results showed high levels of antibody binding to Tec again, as well as Nck1 (boxed in red, Figure 5.7B). These two SH2 domains and their respective binders were therefore excluded from the final microarray experiments.

5.4 Protein microarrays testing specificity of SH2 Affimer reagents

The full set of the remaining 162 Affimer reagents were then tested in microarrays against the 41 SH2 domain targets (Chapter 2, section 2.2.11). Three experimental repeats were performed, using new batches of SH2 and Affimer proteins in each repeat. After the first repeat, the Stat2 SH2 was also excluded from further experiments due to high non-specific binding by the HA-tag antibody. As new batches of target proteins were produced for the final experiments, this could be the reason why this high level of antibody binding to Stat2 was not seen in the optimisation tests. The final layout of the printed arrays excluding Stat2 can be seen in Figure 5.8; containing five replicate spots for each SH2 domain, plus 10 spots for the buffer-only control.

Figure 5.9 shows results for all Affimer reagents summarised in the form of a heat map. This heat map shows the relative binding of each Affimer to each SH2 domain, by displaying the mean background-corrected signal at 635 nm averaged over the three experimental repeats. For each experimental repeat, the signal was also normalised to the buffer-only control signal. As seen in Figure 5.9, most clones showed binding with their intended target, with a few significant cross-reactions. Of the 162 Affimer reagents tested, 54 showed no binding to their intended target (exclusion criteria was a mean signal ≤ 50-fold higher than the buffer-only control). This was not in accordance with the phage ELISAs performed after screening, which had all shown binding of these clones to their

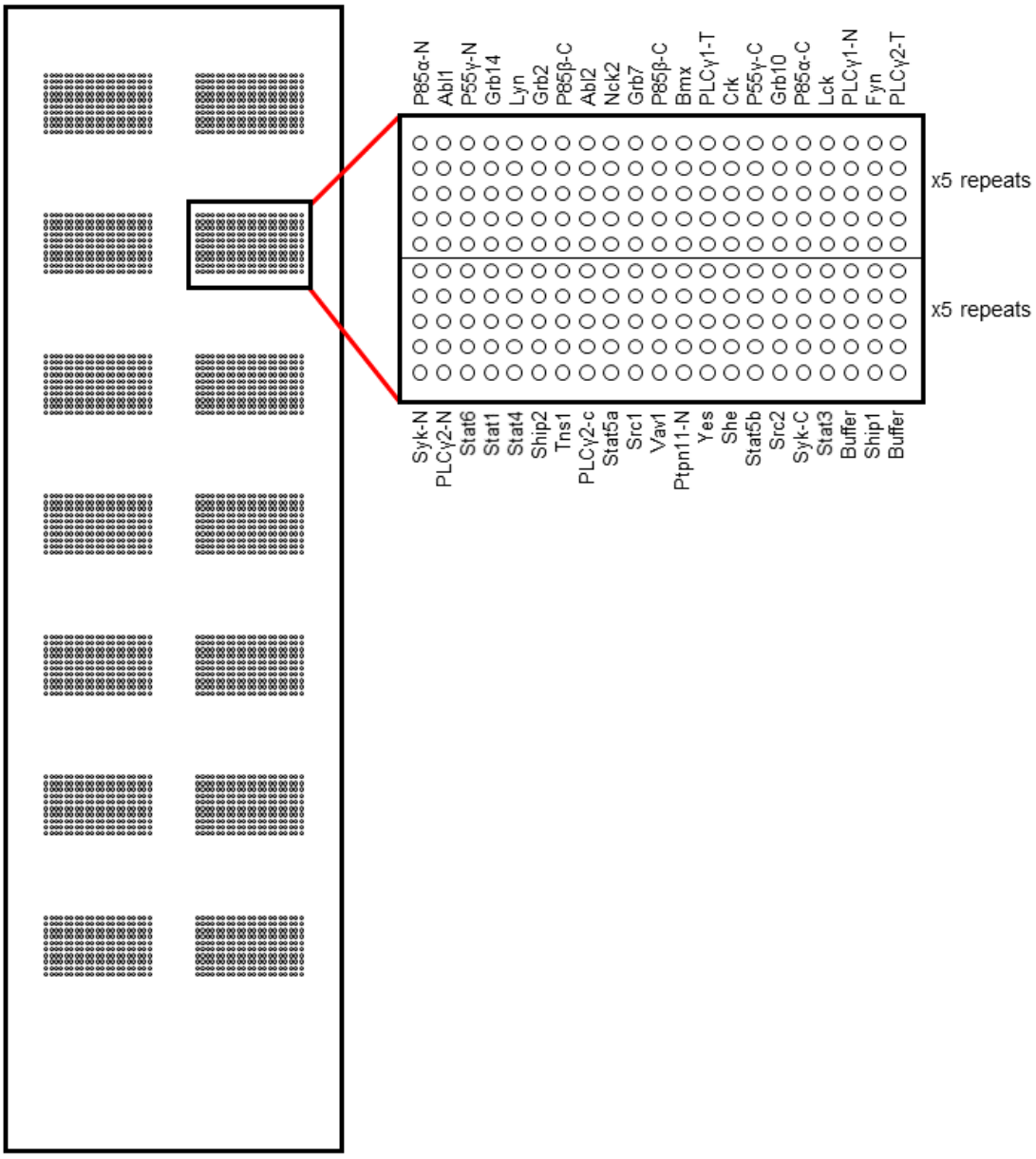

Figure 5.8. Final print layout for SH2 domain proteins in SH2 Affimer protein microarrays. *Streptavidin-coated slides (PolyAn) were spotted with 41 BAP-tagged SH2 domain proteins (70 μM) using an ArrayJet Marathon non-contact printer. Each SH2 was printed in replicates of five, with the buffer-only control printed twice to give a total of 10 buffer control spots. Fourteen identical arrays were printed per slide; use of a microarray cassette on slides allowed incubation of each array with a different Affimer reagent, totalling 13 reagents per slide plus an antibody-only control well.*

Figure 5.9. Specificities of SH2-binding Affimer reagents tested against 40 SH2 domains. *Heat map of results from SH2 protein microarrays testing specificity of SH2-binding Affimer reagents. The heat map displays the mean background-corrected fluorescent signal at 635 nm for each Affimer against each SH2 domain, averaged over three experimental repeats. In each experimental repeat, the signal was also normalised to the buffer-only control signal.*

target. Non-binding results tended to be seen for Affimer clones raised against a particular target; for example, no clones for She, Tns1, p85α-C and p85β-C showed binding to their target. Additionally, only one clone showed binding for Vav1, Stat1 and Ship2. This suggests that immobilisation and drying onto the microarray surface could have caused these targets to unfold and no longer be recognised by their Affimer reagents. Protein denaturation after microarray spotting is a well-documented problem (Ramani et al., 2012, Liotta et al., 2003, Chang Ming Li et al., 2008).

Of the 108 Affimer clones that did show binding to their target, 51 of these were specific; showing little or no cross-binding to other SH2 domains. This number included PLCγ2T-A1 which also bound the isolated PLCγ2-C, and PLCγ2N-A8 which bound the PLCγ2-T construct. Affimer reagents were deemed specific if off-target interactions were ≤ 10% of the signal shown for the intended target, in accordance with previous work on SH2 domain-binding antibody fragments (Colwill et al., 2011, Sjoberg et al., 2012). In total, positive hits were shown against 31 of the 35 SH2 domains for which binders were tested (as Tec, Nck1 and Stat2 had been excluded). Of these, specific binders were found for 22 SH2 domains.

Interesting examples of specific binders included those for targets Abl1 and Abl2 SH2s, which share 89% sequence identity. Specific Affimer clones were seen for both targets, with all Abl2 clones that were tested showing specificity (examples in Figure 5.10). Several binders raised against the SH2 domains of PI3K (p85α, p85β and p55γ subunits) also showed specificity, despite these domains sharing a pairwise sequence identity of 83 – 90%. Examples in Figure 5.11 show that specific clones were identified for p85α-N, p85β-N, p55γ-N and p55γ-C. As mentioned previously, no clones for p85α-C and p85β-C showed binding to their target. This could suggest denaturation of these targets on the microarray surface, and therefore any binders of the other PI3K SH2s that are cross-reactive with these two targets may not have been correctly identified.

Another interesting result was that seen for binder Src1-A2 (Figure 5.12). This clone showed significant binding to all SH2 domain targets, but not to the buffer-only control. This could mean that the clone is binding a sequence shared by all

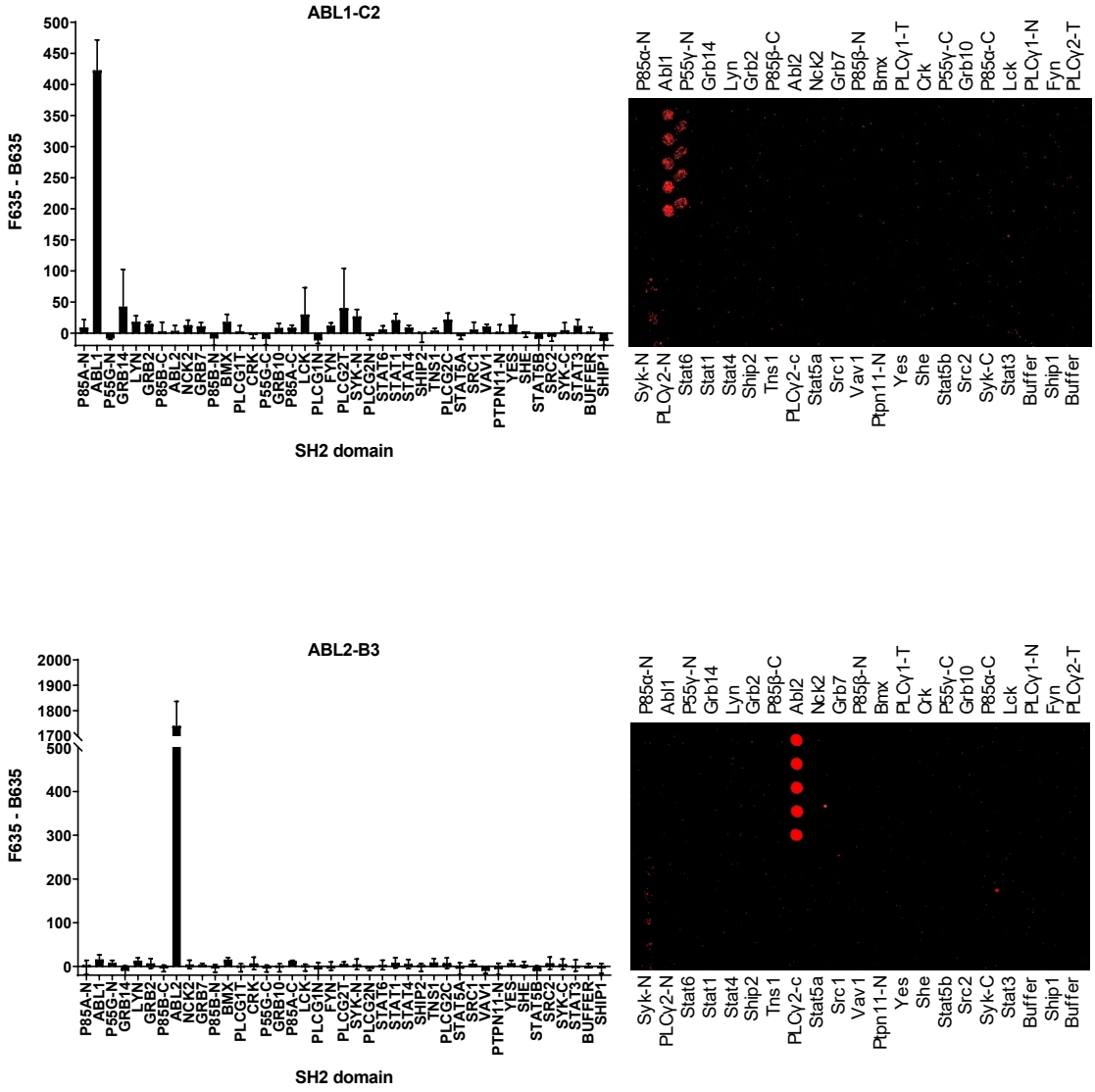

Figure 5.10. Abl SH2-binding Affimer reagents show specificity in a SH2 protein microarray. *Results from SH2 microarrays for binders Abl1-C2 and Abl2-B3 showed specific binding of these clones to one Abl isoform. Graphs show the mean background-corrected fluorescent signal at 635 nm for each SH2 domain, quantified from the images on the right using GenePix® Pro 7 software. Data is displayed as mean ± SD from one experimental repeat (five replicates per SH2).*

A

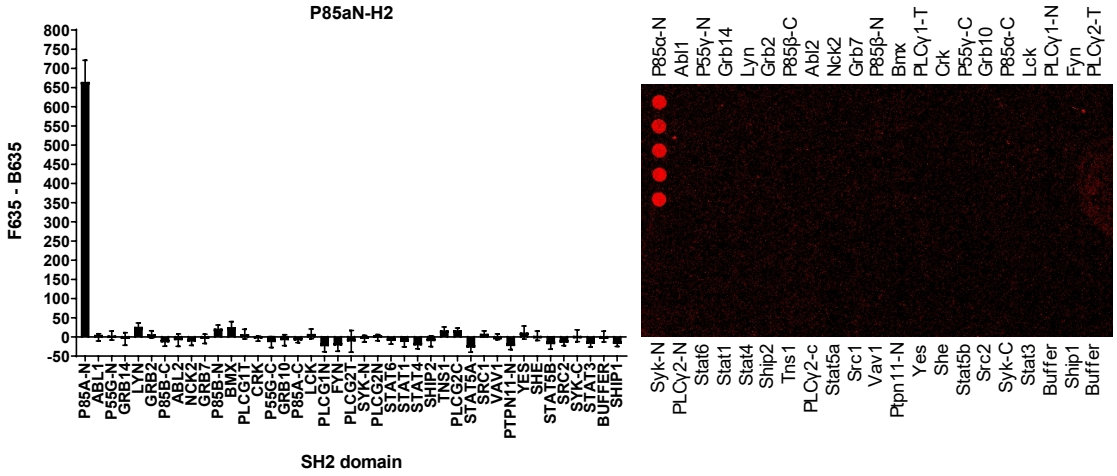
P85aN-H2
F635 - B635
SH2 domain
P85α-N
Abl1
P55γ-N
Grb14
Lyn
Grb2
P85β-C
Abl2
Nck2
Grb7
P85β-N
Bmx
PLCγ1-T
Crk
P55γ-C
Grb10
P85α-C
Lck
PLCγ1-N
Fyn
PLCγ2-T
Syk-N
PLCγ2-N
Stat6
Stat1
Stat4
Ship2
Tns1
PLCγ2-c
Stat5a
Src1
Vav1
Ptpn11-N
Yes
She
Stat5b
Src2
Syk-C
Stat3
Buffer
Ship1
Buffer

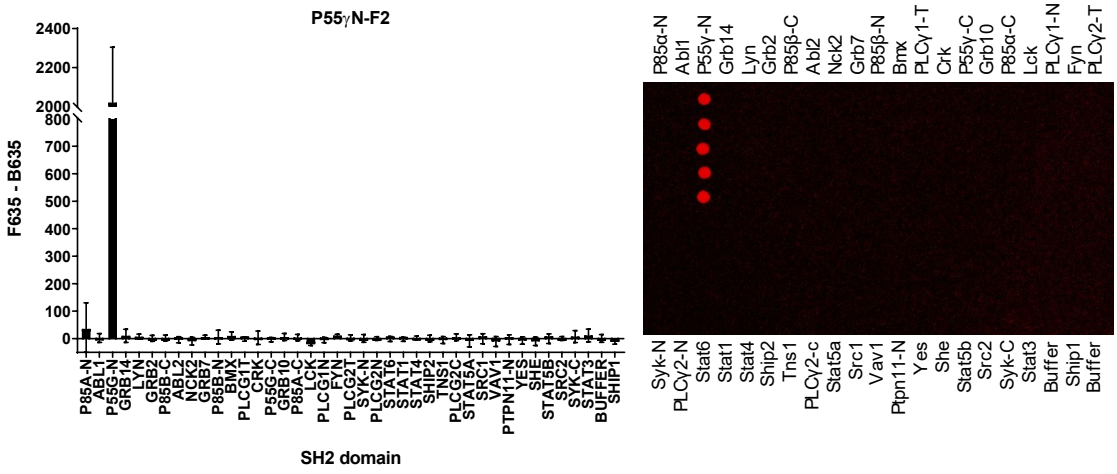
P55γN-F2
F635 - B635
SH2 domain
P85α-N
Abl1
P55γ-N
Grb14
Lyn
Grb2
P85β-C
Abl2
Nck2
Grb7
P85β-N
Bmx
PLCγ1-T
Crk
P55γ-C
Grb10
P85α-C
Lck
PLCγ1-N
Fyn
PLCγ2-T
Syk-N
PLCγ2-N
Stat6
Stat1
Stat4
Ship2
Tns1
PLCγ2-c
Stat5a
Src1
Vav1
Ptpn11-N
Yes
She
Stat5b
Src2
Syk-C
Stat3
Buffer
Ship1
Buffer

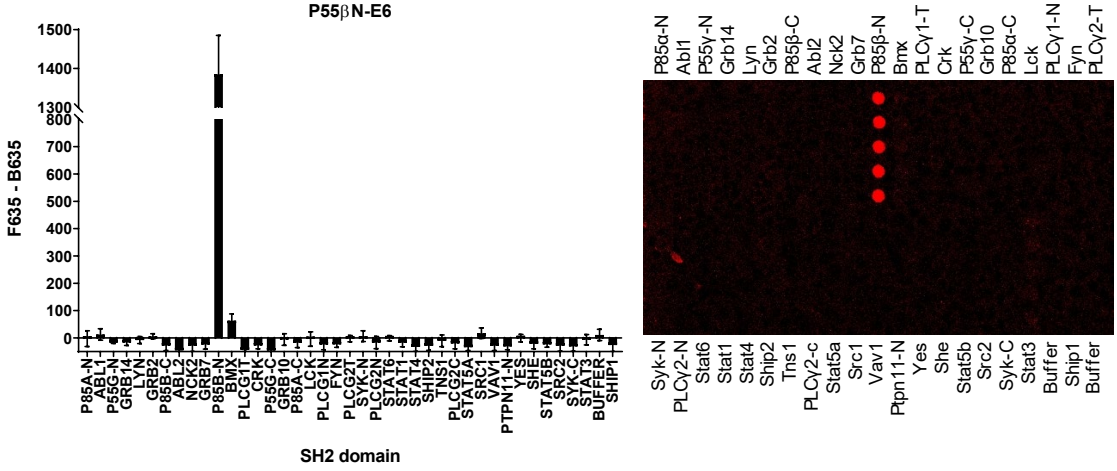
P55βN-E6
F635 - B635
SH2 domain
P85α-N
Abl1
P55γ-N
Grb14
Lyn
Grb2
P85β-C
Abl2
Nck2
Grb7
P85β-N
Bmx
PLCγ1-T
Crk
P55γ-C
Grb10
P85α-C
Lck
PLCγ1-N
Fyn
PLCγ2-T
Syk-N
PLCγ2-N
Stat6
Stat1
Stat4
Ship2
Tns1
PLCγ2-c
Stat5a
Src1
Vav1
Ptpn11-N
Yes
She
Stat5b
Src2
Syk-C
Stat3
Buffer
Ship1
Buffer

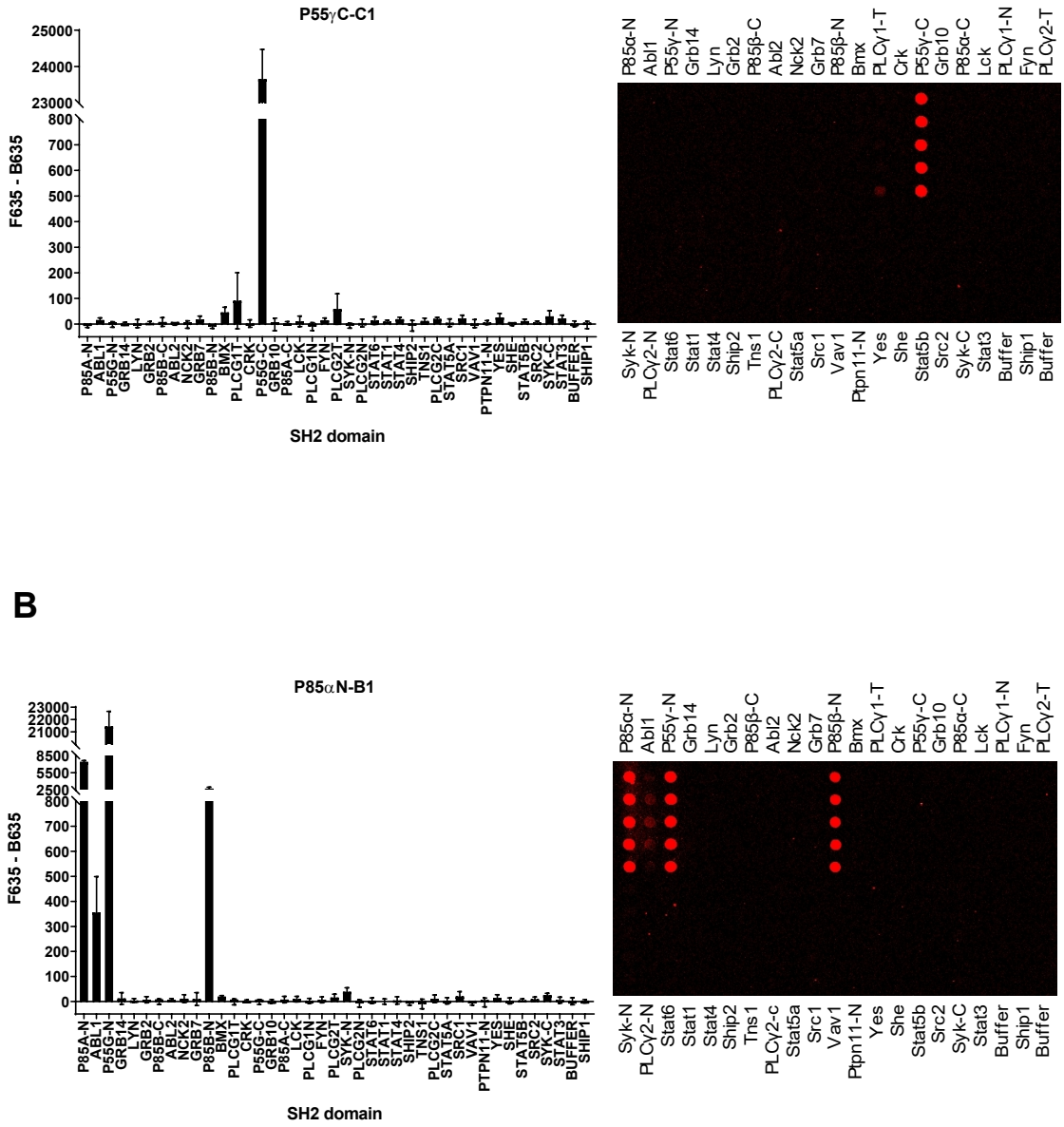

Figure 5.11. PI3K SH2-binding Affimer specificities in the SH2 protein microarray. ***(A)*** *Results from SH2 microarrays for Affimer binders against the PI3K SH2 domains revealed specific clones for p85α-N, p85β-N, p55γ-N and p55γ-C.* ***(B)*** *Cross-binding of p85α-N binder B1 to the p85β-N and p55γ-N domains. Graphs show the mean background-corrected fluorescent signal at 635 nm for each SH2 domain, quantified from the images on the right using GenePix® Pro 7 software. Data is displayed as mean ± SD from one experimental repeat (five replicates per SH2).*

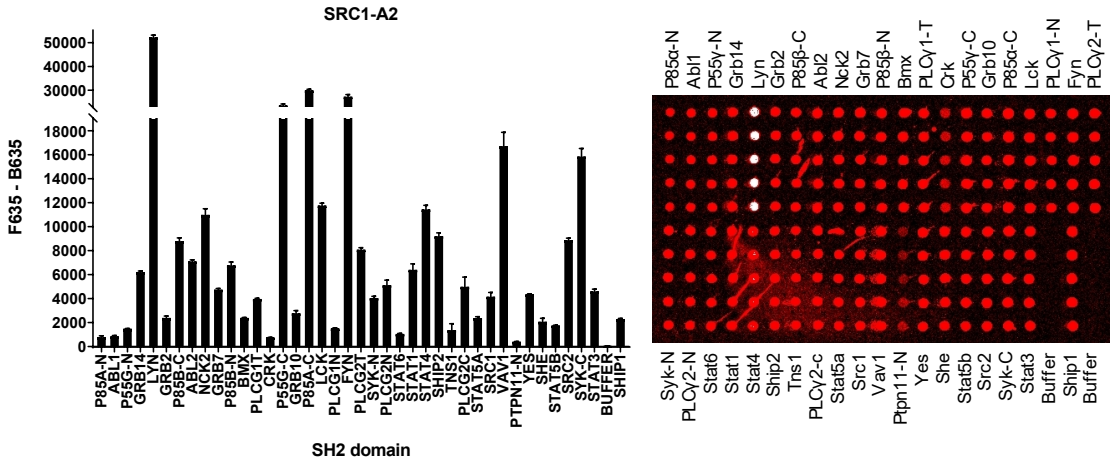

Figure 5.12. A Src1 SH2 Affimer reagent showed binding to all 40 SH2 domains in the protein microarray. *Result from the SH2 microarray for Affimer binder Src1-A2 revealed binding to all 40 SH2 domain protein spots, but not to the buffer-only controls. White spots indicate signal saturation. Graph shows the mean background-corrected fluorescent signal at 635 nm for each SH2 domain, quantified from the image on the right using GenePix® Pro 7 software. Data is displayed as mean ± SD from one experimental repeat (five replicates per SH2).*

of the SH2s; such as the BAP-tag or His-tag, or the linker region between these tags and the SH2 domain. Alternatively, this binder could be non-specifically binding the targets in the phosphotyrosine pocket, which is highly conserved between domains. To help determine this, an array containing chemically biotinylated SH2 domains without the BAP-tag, as well as un-related proteins both with and without His-tags could be used.

In comparison to the specificity phage ELISAs performed on Grb2 SH2 binders (Chapter 3, section 3.6), the microarrays did not show similar specificity profiles for many of the Affimer clones tested. Firstly, binders Grb2-8, Grb2-12, Grb2-A6 and Grb2-D2 were all counted as non-binding in accordance with the microarray criteria. This did not correlate to other *in vitro* assays (Chapter 3), which showed binding of these clones to the Grb2 SH2 via ELISA; fluorescence polarisation; and pull-down from lysate. In addition, SPR showed Grb2-8 to have an estimate binding affinity in the nanomolar range. In the microarray, these clones did show some binding to the target; however signals were often weak and binding was inconsistent across the repeats. The mean signals for these clones ranged between ca. 16-fold and 29-fold that of the buffer-only control.

Both Grb2-A4 and Grb2-H1 were identified as specific in accordance with ELISAs (see Figure 5.13A for example). Grb2-F1, Grb2-F5 and Grb2-D6 were also identified as specific, even though these had shown cross-binding to SH2s Crk, Abl2 and Yes in the ELISAs. Grb2-F1 did show binding to Abl2 in the third experimental repeat (Figure 5.13B) but this cross-reaction was not detected consistently. In accordance with ELISA results Grb2-F5 also bound to the Crk SH2, displaying a mean signal ca. 50-fold that of the buffer control; however this was only 2.5% of the on-target Grb2 signal, causing it to be classified as specific. This was also true for Grb2-D6, which showed low binding to Abl2 and Crk which only equated to 6.3% and 1.5% of the on-target signal. It is worth noting that the specificity phage ELISAs had been performed only once and therefore a reliable comparison cannot be drawn without repeats of this assay. Binder Grb2-D5, although passing the criteria for a positive hit in the microarray, showed only weak binding to the Grb2 SH2 (Figure 5.13C). Binding was also inconsistent over experimental repeats. This could imply that a lack of dimerisation resulted in weaker binding of the Grb2 SH2 by this clone; however, other Grb2 SH2 binders that had been validated by previous *in vitro* assays had also displayed weak binding in the microarray.

For the previously isolated p85α-N SH2 binders (Tiede et al. 2017), specificity profiles correlated with phage ELISAs that had tested cross-reactivity to all PI3K domains. A combination of binders that were specific to p85α-N, cross-reactive with either p85β-N or p55γ-N, or both, were tested. Microarrays successfully detected all cross-reactions previously observed in the ELISAs.

In general, a low background signal and uniform spot morphology was seen in the microarrays. However, as shown in the Abl1-C2 and Src2-A2 images (Figure 5.10 and 5.12), occasionally some spot smearing was observed; this was particularly prevalent with high affinity binders displaying high target signals. These smears were not visualised in the post-print analyses of slides at 532 nm, indicating that this occurred during slide processing. This could be a result of overloading the surface with SH2 protein, as has been observed previously with antibody microarrays (Balboni et al., 2008). The GenePix® Pro 7 software was set to identify irregularly shaped objects as protein spots. As a consequence, spot smears were usually correctly identified and included in the spot area by the software. These artefacts were therefore unlikely to have a major impact on

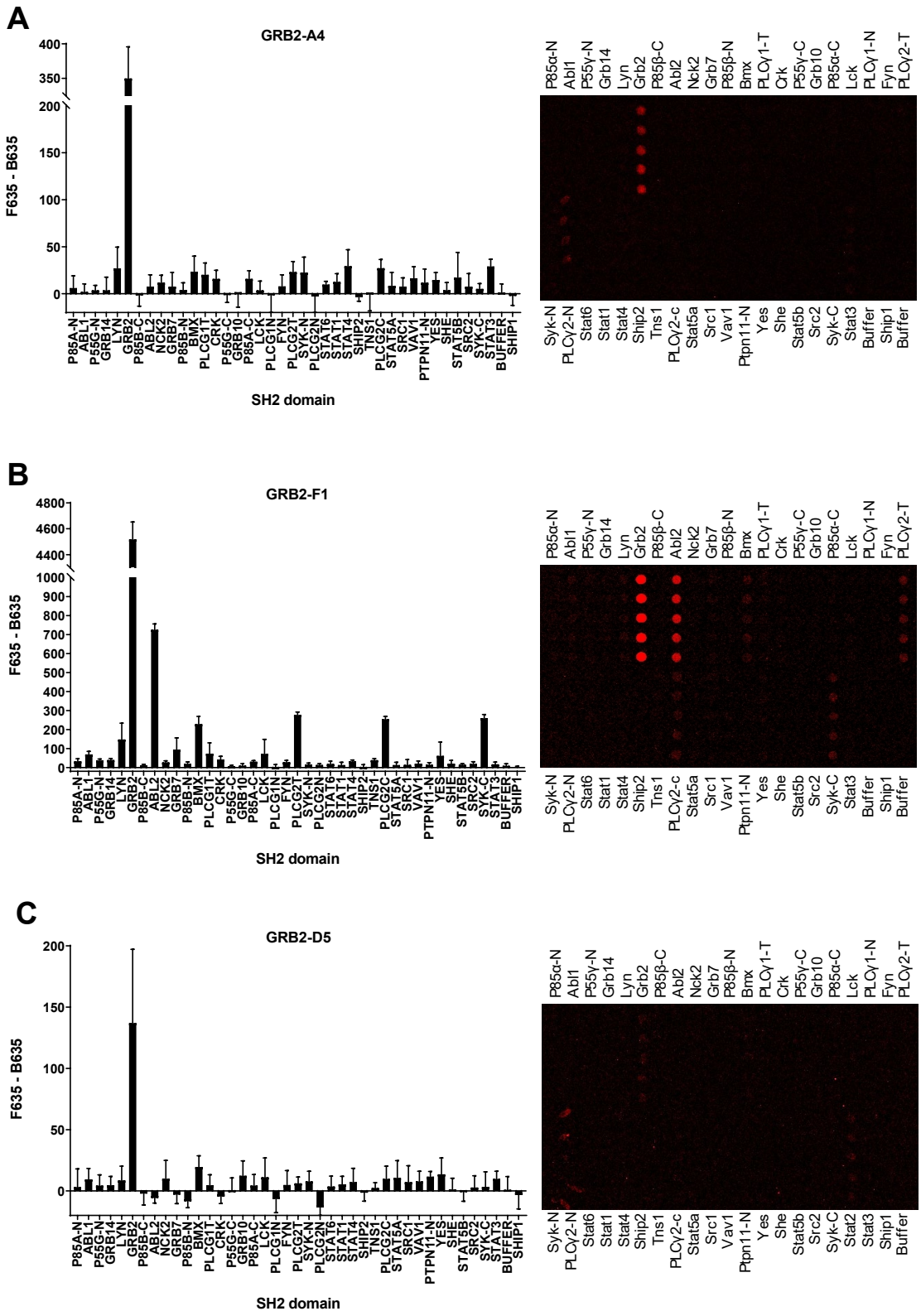

Figure 5.13. Grb2 SH2-binding Affimer specificities in the SH2 protein microarray. *Results from SH2 microarrays for Grb2 SH2 Affimer binders.* ***(A)*** *Grb2-A4 as an example of a specific binder.* ***(B)*** *Cross-binding of Affimer F1, mainly to the Abl2 SH2, was detected in one experimental repeat.* ***(C)*** *Binder Grb2-D5 showed little to no binding to the Grb2 SH2 in the microarray. Graphs show mean background-corrected fluorescence at 635 nm (± SD) for each SH2 from one experimental repeat, quantified using GenePix® Pro 7.*

binding analysis over the three experimental repeats. A list of target-specific binders identified by microarray for each target is displayed in Table 5.1. Significant cross-reactions for each Affimer are more extensively detailed in Appendix D.

5.5 ELISAs testing Affimer clones that showed little binding by microarray

Following the protein microarrays, purified protein ELISAs were then performed on non-binding or weakly binding clones against their target, to confirm the microarray results. This was due to the observation that certain SH2 targets showed no positive hits in the array work; it was thought that the drying of protein solutions onto the slide surface could have resulted in denaturation of these targets, accounting for the lack of binding by their Affimer reagents. The ELISA was used to determine this, as SH2 domain proteins are kept in solution during this assay and are therefore less likely to become denatured. The assay was also similar in format to the original phage ELISAs that were used to confirm binding of Affimer clones to their target after the phage display screening.

HA-tagged Affimer reagents used in microarrays were incubated with biotinylated BAP-tagged SH2 domains immobilised in streptavidin-coated wells. Bound Affimer was detected using a non-conjugated HA-tag antibody and a HRP-conjugated secondary antibody. Each clone was also tested against a streptavidin-only well. Grb2-F5 tested against Grb2 SH2 was used as a positive control. Results showed that only 14 out of 56 binders tested showed significant binding to their target (Figure 5.14). This included clone Grb10-D9, which was a positive hit in the microarray but had shown inconsistent binding between repeats, and three clones against p55γ-N which had also qualified as positive hits but had shown weak signals. All other hits in the ELISA had been classified as non-binding in the microarray. All three p85α-C binders showed binding to their target, indicating this target could have become unfolded when immobilised and dried onto the microarray slide surface.

This method showed matching results from both methods for 82% of the binders tested in ELISA, confirming that the microarray was a relatively accurate method for selecting Affimer clones to take forward based on target-binding and specificity. It is worth noting that a similar ELISA format using HRP-conjugated

Table 5.1. Target-specific Affimer clones as determined by SH2 protein microarray. *Table summarising specific Affimer clones for SH2 targets, identified by the protein microarray. Clones were deemed specific if off-target interactions showed a signal < 10% of that for the intended target.*

Target	Specific clones	Number of specific clones
Abl1	C2	1
Abl2	E1 B3 D4 A2 A1	5
Bmx	G1 A1 D1 A4	4
Crk	A1 F3 H3	3
Fyn	D2 A2 D3 A4	4
Grb2	A4 D6 F1 F5 H1	5
Grb10	D9	1
Grb14	F3 C3	2
Lyn	A2 C2 B2	3
P55γ-C	C1 B5 G1 E5 E3	5
P85α-N	H2 H1 (old screen)	2
P85β-N	E6	1
P55γ-N	F2	1
PLCγ1-N	B7	1
PLCγ2-T	A1	1
PLCγ2-N	A8	1
Ship1	C8	1
Ship2	G5	1
Stat3	H2 H6 B1	3
Stat4	F3 H3 H2	3
Stat6	C3	1
Syk-N	D2 F2	2

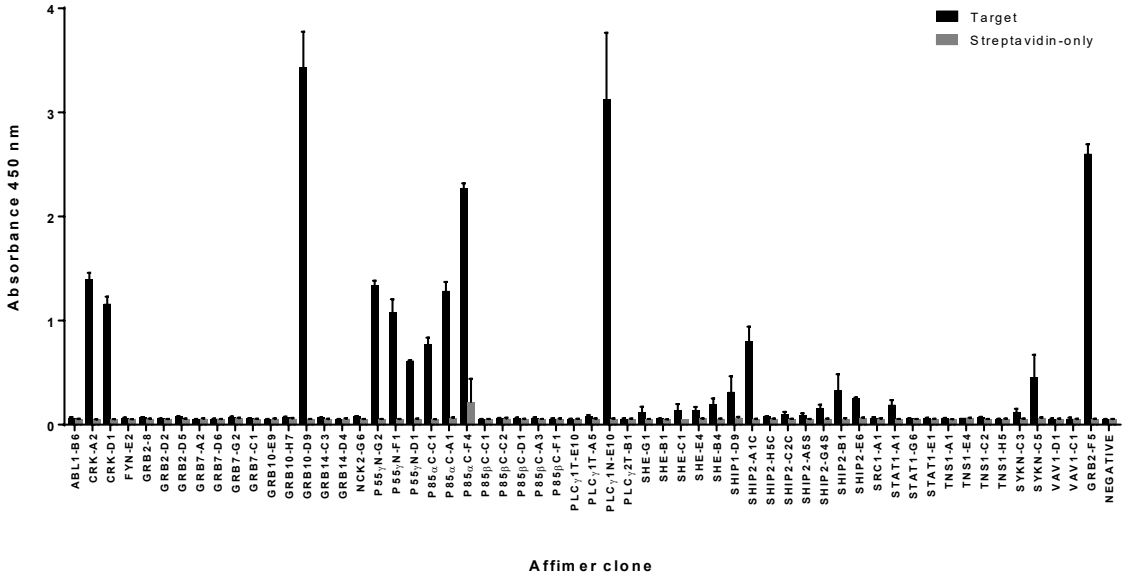

Figure 5.14. Purified protein ELISA testing Affimer clones against their targets. *BAP-tagged SH2 targets were bound to streptavidin-coated wells and incubated with HA-tagged Affimer reagents used in microarrays, for 1 h at room temp. Bound Affimer was detected with a non-conjugated HA-tag antibody (1:20,000) followed by a HRP-conjugated anti-mouse secondary antibody (1;10,000). After washing, HRP substrate TMB was added to each well. After 10 min, the reaction was stopped with 1M H_2SO_4 and absorbance read at 450 nm. Each clone was also tested against a streptavidin-only well. Grb2-F5 incubated with Grb2 SH2 was used as a positive control.*

antibody detection has been shown to be less sensitive than a fluorescence protein microarray using the same reagents (Zhong et al., 2010). This supports the theory that the negative results seen for some clones in microarrays was not due to a lack of sensitivity of that assay, but could be due to the folding of the target protein.

5.6 Discussion

In this work, a high-throughput method for effectively testing the specificity of Affimer reagents to target proteins was established. The microarray was much less laborious and required less purified protein than ELISAs; which is a benefit when working with protein families such as SH2 domains that are difficult to produce. Additionally, this work demonstrated that Affimer clones could be isolated that were specific to one target in a set of 41 highly homologous proteins.

Of 162 Affimer clones tested, 108 showed binding to their intended target (Figure 5.9). Including Affimer clones that were cross-reactive between different SH2 domains of the PI3K protein, 62 Affimer clones that were protein-specific were identified from 162 tested. Not including cross-reactive PI3K binders, this number was 51 (Table 5.1). This showed an overall hit rate of 67% and a specificity hit rate of 32%. As 33 of the 35 SH2 targets displayed positive hits (including p85α-C in the purified protein ELISA) and 22 of these were bound specifically, a target hit rate of 94% was achieved with a specificity hit rate of 63%.

Previous work testing the specificity of SH2 domain-binding antibody fragments reported a specificity ELISA hit rate of 55%, with 379 of the scFvs showing specific binding to their target out of 695 tested (Pershad et al., 2010). This rate is higher than demonstrated by the Affimer reagents; however DNA analysis revealed these hits only equated to 148 unique antibody clones (21% of the total tested). Therefore, the Affimer screen showed a higher rate of specific binding compared to this study. Additionally the panel of SH2s tested against the scFvs was considerably smaller, consisting of just 20 domains. In another related study, the number of SH2 domains bound specifically by scFvs and hybridomas in a microarray ranged from 10 – 13 out of the 20 targets depending on the antibody library used (Colwill et al., 2011). This gave specificity hit rates of 50 – 65% of targets; comparable to the Affimer screen.

Monobodies raised against the SH2 domains of the Src family kinases (SFKs) were shown to be selective for either the SrcA (Yes, Src1, Src2) or SrcB subgroup (Hck, Lck, Lyn, Blk) in a yeast binding assay testing specificity (Kukenshoner et al., 2017). However, only two binders out of the 11 tested showed high specificity for their target alone, with all others cross-reacting with at least one of the seven other SH2 domains. In the Affimer microarray, binders specific for Lyn that did not show binding to Lck were successfully isolated, which was not achieved in the monobody work. Another monobody raised against the Abl SH2 domain, termed HA4, was also tested for specificity in a protein microarray against 84 SH2 domains (Wojcik et al., 2010). This binder could not discriminate between the Abl1 and Abl2 SH2s, unlike some Affimer clones. HA4 additionally cross-reacted significantly with three other SH2s and weakly with 15 others in this microarray, although estimated K_d values indicated selectivity for the Abl domains over these other interactions.

It is worth noting that in the work detailed in this chapter, seven of the specific Affimer binders isolated were against three of the Stat proteins. As the Stat constructs encode more of the protein than just the SH2 domain, it cannot be said that these clones bind in the SH2 domain region and therefore they are not necessarily specific SH2 domain binders.

Disparities in the specificity profiles of Grb2 SH2 binders were seen between phage ELISAs (Chapter 3, Figure 3.11) and the microarray (Figure 5.13). The microarray may be a more stringent method of selecting binders for further characterisation than the phage ELISA, as not all Grb2 SH2 binders showed significant binding in the microarray method. As binding of these clones to the Grb2 SH2 has been evidenced by several other *in vitro* methods, the lack of target binding could be the due to the accessibility or orientation of the Grb2 SH2 on the microarray surface. Equally, the criteria for positive hits in the microarray could be viewed as too rigorous; if this was lowered to a signal ≥ 20-fold that of the buffer-only control, rather than ≥ 50-fold, all but one Affimer would have been positive hits in the array. Comparison of the two methods is limited however, as the specificity phage ELISAs were performed only once.

The results from purified protein ELISAs revealed that the microarray was a suitable method for correctly identifying most target-binding Affimer clones, having shown comparable results to the ELISA for 82% of clones tested (Figure 5.14). However, for some SH2 domains the microarray did not appear to successfully detect interactions with their binders, as clones against targets such as p85α-C displayed binding in the ELISA and not the array. For these Affimer clones, the next step could be to test their specificity against all the SH2s in the ELISA format.

The SH2 protein microarray in this work deduced the specificities of 162 Affimer reagents in an efficient way and demonstrated that the level of specificity in the Affimer population was comparable to, or surpassed, previously isolated SH2 domain binding proteins. Specificity is of great importance for reagents targeting highly homologous protein families such as SH2s. The Affimer reagents in this work were able to discriminate against domains of up to 90% sequence identity with high specificity. With a total number of 22 SH2s for which specific reagents were identified, this work details the largest number of successfully targeted SH2 domains by any antibody or non-antibody binding protein. The microarray also

proved to be a method which could effectively and stringently select Affimer binders for use in functional cell-based assays.

5.6.1 Grb2-D5 dimerisation

As discussed in Chapter 3, the Grb2 SH2 Affimer D5 had shown the formation of a stable dimer in SDS-PAGE analysis when produced from pET11a for *in vitro* characterisation. However, when produced from the pET-lectra vector in this work, the Grb2-D5 Affimer protein was observed as a monomer (Figure 5.3A). The DNA chromatogram from sequencing analysis of Grb2-D5 in pET11a was studied, to determine whether a cloning error had resulted in duplication of the Affimer sequence within the vector, which could cause the expression of a fused dimer. As seen in Figure 5.15A, no such duplication of the sequence was observed; however, the chromatogram signal dramatically decreased after base pair ca. 310 (Figure 5.15B). This was in the region encoding the C-terminus of the Affimer, before the His-tag sequence. This sudden reduction in signal could indicate DNA secondary structure, such as a hairpin loop. Secondary structure in the DNA template can impede the progress of the DNA polymerase used during sequencing, causing an early termination or dramatic decrease in the chromatogram signal.

This vector was re-sequenced using a protocol recommended by Genewiz for difficult templates with secondary structure. Analysis of the chromatogram revealed no significant decrease in signal on this occasion, although a small region of high background at base pairs ca. 330 – 334 can be seen instead (Figure 5.15C). This region encodes the last alanine residue of the Affimer scaffold and the first histidine residue of the His-tag. The high background was observed immediately after a G-C rich region, which are prone to forming secondary structures. However, this portion of sequence is present in all Affimer clones; the secondary structure formation in Grb2-D5 alone must have therefore occurred during the subcloning of this clone from the pBSTG to the pET11a vector. Additional analysis could have included use of a sequence analysis tool to predict regions prone to secondary structure formation, however this was not conducted.

The difference between the Affimer sequences encoded in the pET11a vector and the pET-lectra vector was the insertion of the HA-tag sequence between the

A

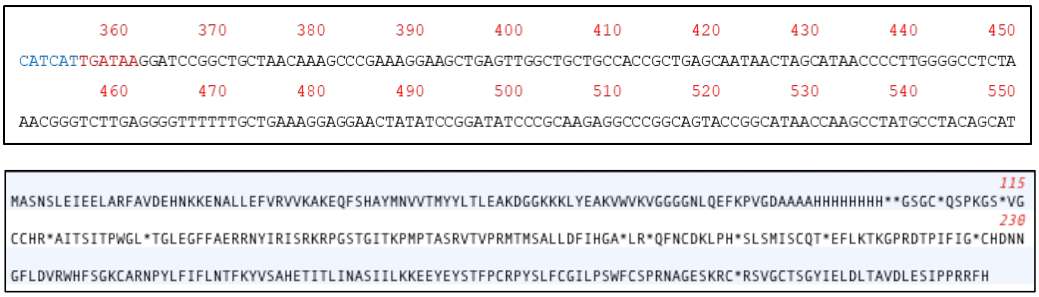

B

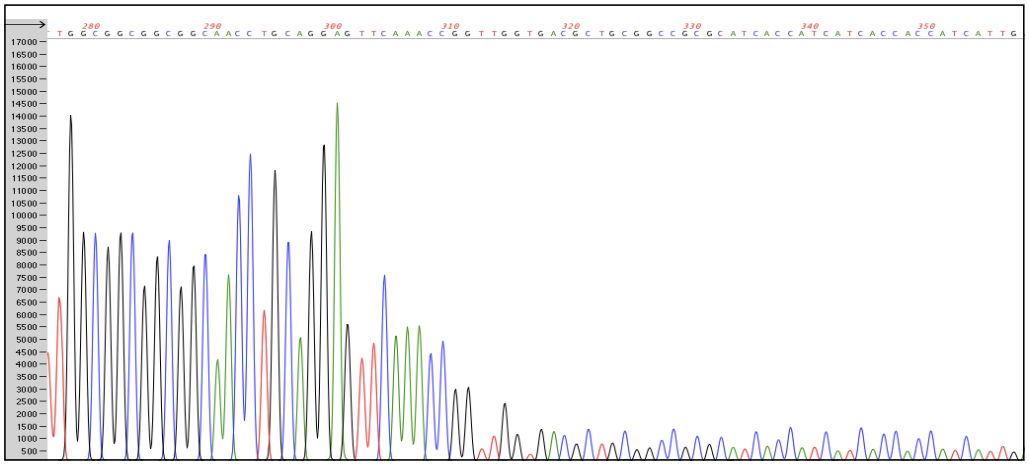

C

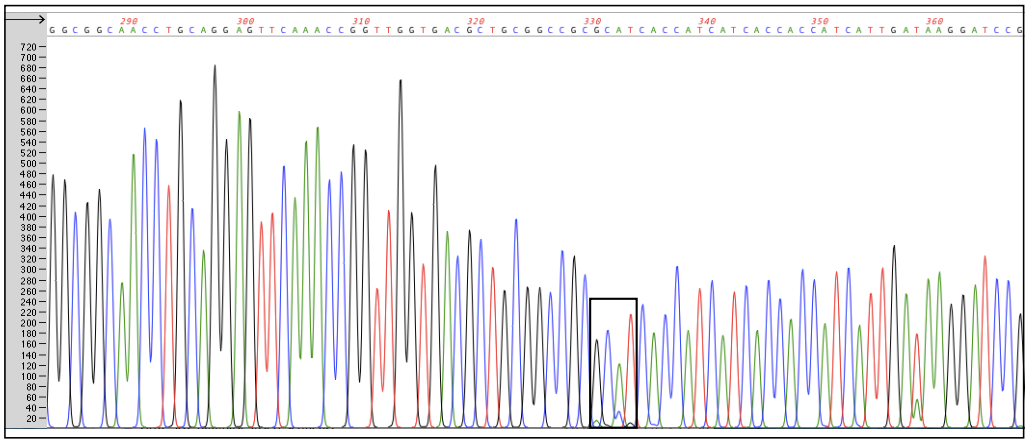

Figure 5.15. Analysis of Grb2-D5 pET11a DNA. ***(A)*** *Top box shows the Grb2-D5 pET11a DNA region encoding the end of the Affimer (blue) and two stop codons (red). The sequence after this shows no duplication of the Affimer sequence. Translation of the entire Grb2-D5 Affimer-encoding region in the pET11a vector and the following sequence. Numbers in red indicate base pair or amino acid position.* ***(B)*** *DNA sequence chromatogram showing the drop in signal at base pair ca. 310.* ***(C)*** *Repeat analysis of the sequence using a specialised protocol for templates with secondary structure showed a minimal drop in signal, but a region of slightly overlapping peaks is outlined at base pair ca. 330. Translation and chromatogram analysis were performed using MacVector 13.5.2.*

C-terminus of the Affimer and the His-tag sequence; the region of possible secondary structure in pET11a. When subcloning into the pET-lectra vector, the Affimer sequence amplified from the pBSTG phagemid vector did not include the base pairs encoding the last four C-terminal alanine residues of the Affimer scaffold, or the His-tag. Therefore, the portion of DNA possibly forming secondary structure in the Grb2-D5 pET11a vector is not present in the Grb2-D5 pET-lectra vector and any consequent effects on the translated protein are no longer seen. Alternatively, it could be the presence of the HA-tag in the translated protein itself which inhibits the interaction between monomers responsible for dimerisation.

The production of monomeric Grb2-D5 protein for microarrays nevertheless provided an interesting opportunity to determine whether dimerisation of binder D5 conferred its ability to bind the Grb2 SH2. As discussed previously, the monomeric binder demonstrated weak and inconsistent binding to its target in microarray analysis, suggesting that dimerisation could be necessary for high binding affinity of this clone.

Chapter 6

Validating SH2-binding Affimer reagents for use in cell-based assays

Chapter 6
Validating SH2-binding Affimer reagents for use in cell-based assays

6.1 Introduction

Studying the function of individual SH2 domains allows dissection of many intracellular pathways and a better understanding of how they become aberrant in disease. It is critical to study these and other signalling domains in a native environment, within the context of the whole cell. This is why SH2 domain reagents are most valuable when they perform well in functional cell-based assays. Reagents that inhibit SH2 function at the protein level are a valuable discovery tool for mapping protein–protein interactions (PPIs), simulating drug–target interactions, and validating novel drug targets in cancer (Lawrence, 2005). Antibodies and their fragments have often been used for targeting PPIs, but this has been mainly limited to extracellular targets (Bakail and Ochsenbein, 2016). This is due to their dependence on disulphide bonds for stability, which often results in failure to fold correctly or bind their intended target in the reducing environment of the cytoplasm (Amstutz et al., 2005; Helma et al., 2015).

Even though there have been advances in developing antibodies, known as ‘intrabodies’, that function in the cytoplasmic milieu, there often remains a requirement for complex selection strategies during library screening or conjugation to localisation motifs for full effectiveness (Marschall et al., 2015; Stocks, 2004). This is one of the key benefits of using non-antibody binding scaffolds (nABPs) for studying SH2 domain interactions; their ability to retain their function in cell-based assays is superior to antibodies and antibody fragments, due to the lack of disulphide bonds.

There are several recent examples of nABPs used to study intracellular signalling by disrupting PPIs and leading to better understanding of the targeted pathways (Martin et al., 2018). For instance, monobodies have been used to perturb PPIs within the Wnt signalling pathway, which is dysregulated in many cancers (Clevers et al. 2012). These monobodies bound the β-catenin and Dishevelled proteins, showing inhibition in a TOPflash reporter assay in HEK293 and DLD1 (colorectal cancer) cells (Yeh et al., 2013). To further investigate

crosstalk between this pathway and the Notch signalling pathway, binders were also isolated against the Notch Ankyrin region and used in cellular assays. The monobodies demonstrated that inhibition of the Notch Ankyrin domain increases the inhibitory activity of Notch towards Wnt signalling. This elucidated a novel function of the Notch Ankyrin domain, which had never before been described as a regulatory region for Wnt pathway crosstalk (Yeh et al., 2013).

Another monobody, termed NS1, was shown to bind H-Ras and K-Ras in both their GDP- and GTP-bound states (Spencer-Smith et al., 2017). NS1 disrupted Ras dimerisation, leading to a blocking of c-Raf and b-Raf heterodimerisation and activation. As NS1 bound the α4-β6-α5 region of Ras, this work demonstrated the importance of the α4-β6-α5 interface in Ras signalling and highlighted a novel site to target for inhibition of Ras. These studies have shown the use of nABPs in dissecting intracellular signalling networks and determining the function of individual domains in disease.

As mentioned in Chapter 1, Affimer reagents have been previously used to target SH2 domain signalling in intracellular assays, showing successful signalling inhibition. Prior to the work detailed in this thesis, binders were isolated against the SH2 domains of the p85 subunit of PI3K. The PI3K/Akt pathway, like the MAPK pathway, is also activated by receptor tyrosine kinases and Ras, and mediated by Grb2 (Liu et al., 2009). This pathway regulates cell proliferation and survival. These Affimer reagents were shown to block p85 SH2 domain function in transiently transfected NIH3T3 (murine fibroblast) cells, indicated by an increase in phosphorylation of downstream target Akt, but did not disrupt the formation of the p85:p110 subunit complex (Tiede et al., 2017).

To further validate Affimer reagents for use in cell-based assays for studying SH2 domain function, the Grb2 SH2 domain binders were once again utilised. The extensive knowledge of Grb2 SH2-mediated pathways, such as the MAPK cascade, allowed specific endpoints to be measured in functional cell-based assays. The Grb2 SH2 Affimer reagents had shown high affinity for their target, competition for the active site of the domain and binding to endogenous Grb2 (Chapter 3). We therefore reasoned that these reagents could potentially be used in mammalian cells to inhibit Grb2-mediated signalling and reduce the phosphorylation of downstream targets Erk1 and 2 (see Chapter 3, Figure 3.1) (Honma et al., 2006; Rojas et al., 1996). Five Grb2 SH2 Affimer clones were

selected based on results of previous *in vitro* assays. Clones 8, A4, D5, F1 and H1 were chosen for their high specificity for Grb2; their ability to capture endogenous Grb2 from lysate; their capacity to competitively inhibit the SH2; or a combination of these qualities.

6.2 Transiently expressed Grb2 SH2 Affimer reagents reduce Erk phosphorylation in HEK293 cells

To test intracellular disruption of Grb2 SH2 signalling by Affimer proteins, it was decided to transiently transfect the Affimer-encoding DNA into mammalian cells and observe levels of Erk phosphorylation after stimulation of the Grb2-regulated MAPK pathway. If the Affimer reagents were successfully inhibiting Grb2 SH2 domain interactions, a decrease in growth factor-induced Erk phosphorylation would be expected. Transient transfection of DNA was chosen as a suitable method due to its ease and rapidity; transient transfection is much less laborious than creating stable cell lines (Durocher et al., 2002). Additionally, a high copy number of the transfected material leads to high levels of protein expression (Jäger et al., 2015; Geisse and Voedisch, 2012), which may be needed to effectively block Grb2 SH2 function.

Sequences for Grb2-8, -A4, -D5, -F1, -H1 and a ySUMO Affimer control, YS-10, were subcloned from the pBSTG phagemid into the mammalian expression vector pcDNA5. These expression plasmids encoded the Affimer proteins with a C-terminal 8xHis-tag; the same as for proteins encoded by pET11a for use in *in vitro* assays. The transient transfection protocol, described in outline below and in detail in Chapter 2 (section 2.2.14), had been optimised in HEK293 (human embryonic kidney) cells using a pcDNA5 plasmid encoding a GFP-tagged protein. As determined by immunofluorescence microscopy, the transfection efficiencies achieved using this protocol ranged from ca. 50 – 60%.

HEK293 cells were seeded in 6-well plates and left for 24 h (ca. 60% confluent). Cells were then transiently transfected with Affimer pcDNA5 plasmids using Lipofectamine® 2000, a cationic lipid. Forty-eight hours after transfection, cells were serum-starved for 90 min and stimulated with 25 ng/ml human epidermal growth factor (EGF) for 10 min, to initiate the MAPK pathway via the epidermal growth factor receptor (EGFR). Lysates were subject to western blot analysis to detect and quantify phospho-Erk1/2 (p-Erk), total Erk, Grb2, His-tagged Affimer

proteins, and tubulin as a loading control. Mock-transfected cells, incubated with transfection reagents only, were used as controls.

As seen in Figure 6.1 (n = 3), all Grb2 SH2 Affimer-expressing cell lines except F1 showed a significant decrease in levels of p-Erk when compared with the EGF-stimulated mock transfection control (p <0.05). However, the reduction seen was not large for any Grb2 Affimer tested, with A4 showing the biggest decrease of just 26.7 ± 5 %. Successful EGF stimulation of cells was signified by the difference in p-Erk between stimulated and non-stimulated controls (p = 0.007).

Fixed-cell staining was then also performed on transfected HEK293 cells, to visualise the transfection efficiency of Affimer pcDNA5 plasmids (Chapter 2, section 2.2.20). Cells were stained for His-tagged Affimer proteins, as well as Grb2. Grb2 siRNA knockdown (72 h) was used as a control for Grb2 staining. Immunofluorescent imaging was performed on stained cells and images were analysed using NIS-Elements software (Nikon). Even though the HEK293 transfection protocol with pcDNA5 had previously been tested and showed a transfected cell population of ca. 50 – 60% (data not shown), the calculated transfection efficiencies for these six Affimer constructs ranged between 32 – 39% (see Figure 6.2, n = 3). Grb2 and His-tagged Affimer reagents showed similar staining patterns in transfected cells.

Although the number of transfected cells was low, the level of expressed protein in some of the transfected cells appeared to be high, as indicated by signal intensity in fixed-cell staining. This did vary from cell to cell however, which could clearly have affected the results. The level of expressed protein was expected to be high, as HEK293s stably express the adenovirus 13 S E1a protein, which significantly increases transcription from the CMV promoter (Gorman et al., 1989) which is responsible for Affimer production in the pcDNA5 vector.

As the transfection efficiency of the Affimer DNA was 32 – 29% and the reduction in p-Erk levels were 20 - 27% in Grb2 SH2 Affimer-expressing cells (except for binder F1), this suggested that the Affimer proteins were in fact causing almost a complete abolition of Erk phosphorylation in the successfully transfected cells. However, the low transfection efficiency was affecting global p-Erk levels in western blot analysis. Expression of Affimer proteins did not appear to affect

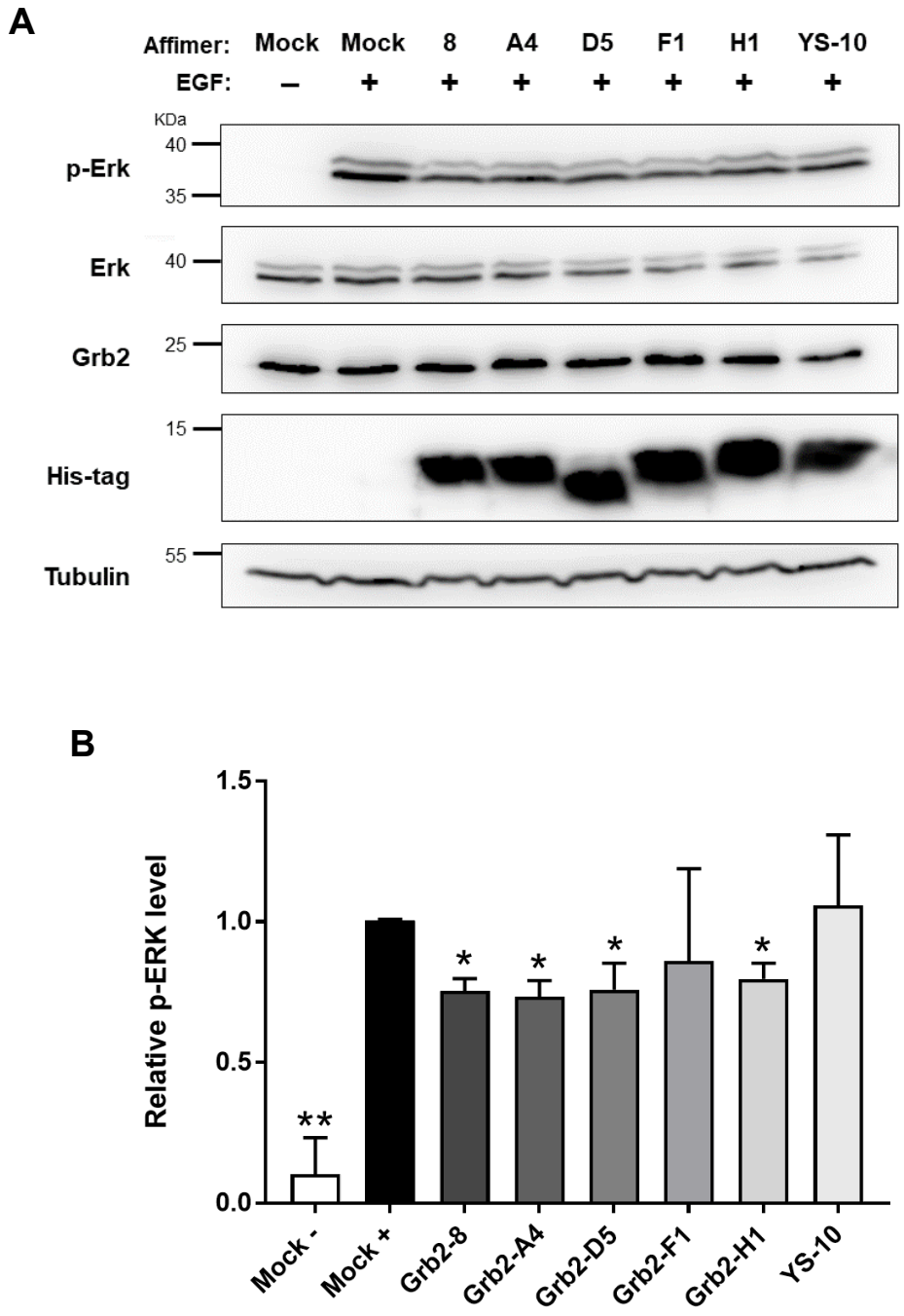

Figure 6.1. Transiently expressed Grb2 SH2 Affimer reagents reduce EGF-induced Erk phosphorylation in HEK293 cells. ***(A)*** *Western blot analysis to detect levels of phospho-Erk1/2 (p-Erk), total Erk, Grb2, and His-tagged Affimer in whole cell lysate from HEK293 cells transfected with 2.4 µg Affimer-pcDNA5 vector, or incubated with transfection reagents only (Mock). 48 h post-transfection, cells were serum starved for 90 min and stimulated with EGF for 10 min (25 ng/ml). Tubulin was used as a loading control. HRP-conjugated antibodies detected with Luminata Forte. Blot is representative of 3 independent experiments.* ***(B)*** *Quantification of p-Erk from western blots shown in (A). Levels of p-Erk1 and 2 were quantified together. Quantities were standardised to tubulin for each condition, then normalised to the EGF-stimulated Mock control. Data is presented as mean ± SD (n = 3), paired t-tests conducted using GraphPad Prism 7. p <0.01**, p <0.05*.*

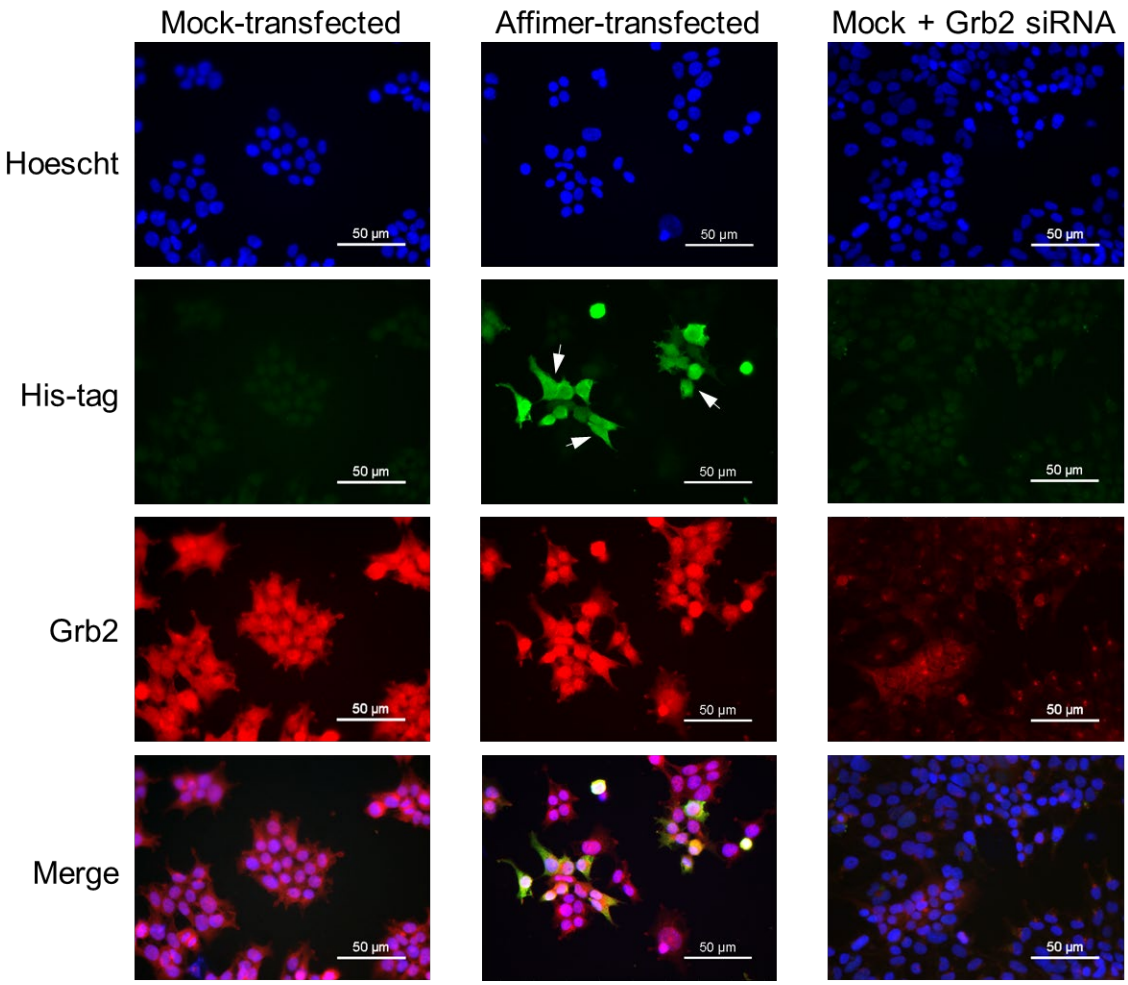

Figure 6.2. Grb2 SH2 Affimer-pcDNA5 plasmids show low transfection efficiencies in HEK293 cells. *HEK293 cells transiently transfected with Affimer-pcDNA5 vectors for 48 h were fixed in 4% PFA and immunofluorescence microscopy was performed. Antibodies against His-tagged Affimer proteins (green) and Grb2 (red) were used, followed by fluorescent species-specific secondary antibodies. Nuclei were stained with Hoechst 33342. Arrows indicate examples of cells successfully transfected with Affimer DNA. Grb2 siRNA knockdown was used as a negative control for Grb2 staining. Scale bar = 50µm, images are representative of three independent experiments.*

growth or phenotype of the transfected cells, although this was not quantified in an assay.

6.3 Transiently expressed Grb2 SH2 Affimer reagents bind Grb2 in HEK293 cells

To confirm that Grb2 SH2 Affimer reagents were binding to their target in the transiently transfected HEK293 cells, a co-immunoprecipitation assay was performed on whole cell lysates from both EGF-stimulated (25 ng/ml human EGF for 10 min) and non-stimulated cells. His-tag Dynabeads™ were used to capture His-tagged Affimer proteins from the lysate; after washing, bound proteins were eluted from beads and subject to immunoblotting to determine the presence of an Affimer-Grb2 complex. As visualised by western blot, all His-tagged Affimer proteins were successfully captured from lysate (Figure 6.3, n = 3). All Grb2 SH2 binders, but not the YS-10 Affimer control, also co-precipitated Grb2 in both stimulated and non-stimulated cells. Bands were seen at the expected MW of ca. 12 kDa and ca. 25 kDa for Affimer proteins and Grb2, respectively.

6.4 Stably expressed Grb2 SH2 Affimer reagents with a DD-tag do not affect Erk phosphorylation in U-2 OS cells

It was then decided to test stable transduction of Affimer DNA to observe the effect of Affimer proteins on Erk phosphorylation. This was due to the indication that Affimer proteins were binding and inhibiting Grb2 in transiently transfected cells, but results from western blot analysis were being effected by a low transfection efficiency. The transient transfection efficiency appeared to not be high enough to see a large global difference in p-Erk levels. Stable transduction and selection overcomes this issue as it ensures a transduced cell population of 100%.

The ProteoTuner™ system (ClonTech) was chosen for stable transduction and inducible expression of Affimer proteins in target cell lines. By cloning into the pRetroX-PTuner vector (Figure 6.4A), a protein of interest is expressed conjugated to a destabilisation domain (DD). This DD tag is based on a 12 kDa mutant form of the FK506 binding protein and targets the expressed fusion

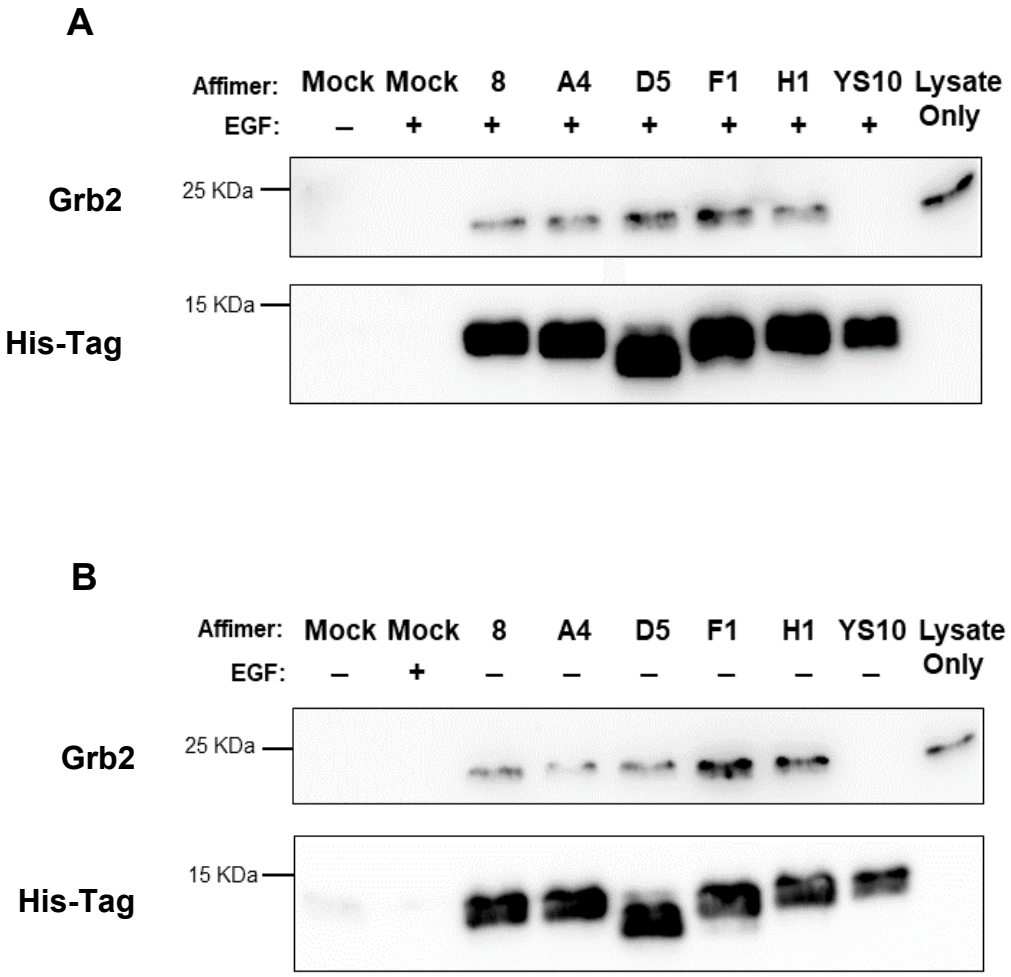

Figure 6.3. Transiently expressed Grb2 SH2 Affimer proteins show binding of endogenous Grb2 in HEK293 cell lysate. *Western blots showing co-immunoprecipitation of endogenous Grb2 from HEK293 cell lysate, by transiently expressed Grb2 SH2 Affimer proteins. HEK293s were transfected with 2.4 µg Affimer-pcDNA5 vectors, or incubated with transfection reagents only (Mock). After 48 h cells were* ***(A)*** *serum starved for 90 min and stimulated with 25 ng/ml EGF for 10 min or* ***(B)*** *harvested without starvation. His-tagged Affimer proteins were captured from lysate using His-Tag Dynabeads™. Eluted proteins were subject to western blotting to detect Grb2 (ca. 25 kDa) and His-tagged Affimer proteins (ca. 12 kDa). Mock = mock-transfected cells (no Affimer). YS-10 = ySUMO-binding Affimer negative control. Lysate only = Mock + EGF lysate not incubated with beads as a positive control for Grb2. HRP-conjugated antibodies detected with Luminata Forte. Blots are representative of three experimental repeats.*

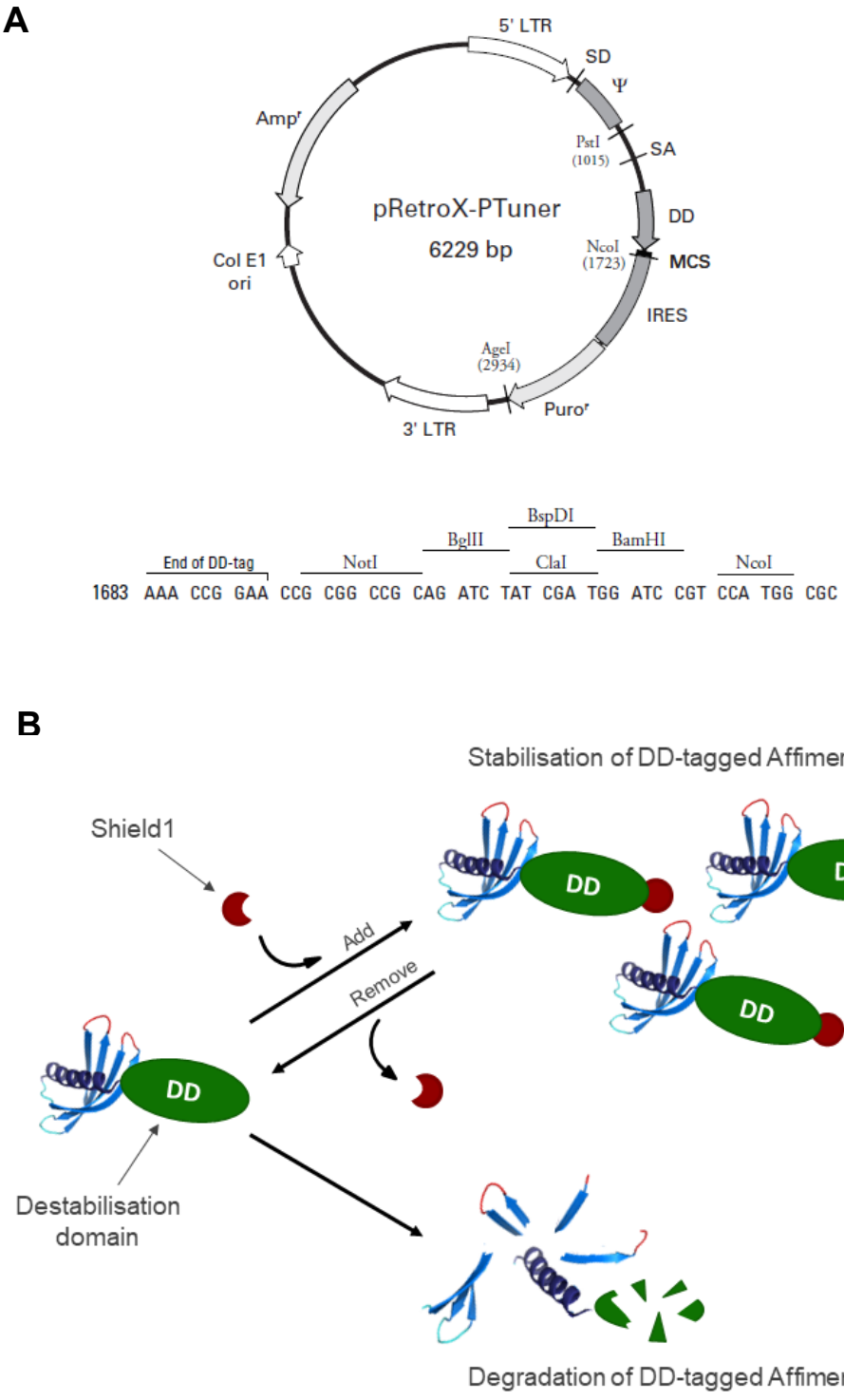

Figure 6.4. The pRetro-X ProteoTuner system. ***(A)*** *Vector map of the pRetroX-PTuner vector, used for stable transduction of DNA encoding your protein of interest into target cell lines. The multiple cloning site (MCS) sequence has been enlarged at the bottom (Clontech cat no. 632171).* ***(B)*** *A schematic of the ProteoTuner-Shield1™ system, allowing stabilisation of DD-tagged Affimer proteins in the cell; 'switching on' any effects of the Affimer in a dose-dependent manner. Addition of Shield1™ into culture medium prevents the targeted degradation of the Affimer and causes accumulation of the protein within the cell. Omission of Shield™ from medium results in rapid degradation of the Affimer.*

protein for rapid proteasomal degradation (Banaszynski et al. 2012). When the membrane-permeable ligand Shield1™ is added to the culture medium, it binds to the DD and inhibits degradation, resulting in accumulation of the fusion protein (see Figure 6.4B). This stabilisation of the DD-tagged protein occurs in a Shield1TM-dose dependent manner, which would allow direct control of Affimer protein levels within the cell. This would should enable dose-dependent studies on the effects of Affimer reagents in target cell lines, and would also ensure the healthy growth of transduced cells until Affimer expression was 'switched on' by Shield1™; useful if the binders caused an increase in cell death, for example. Induction of proteins using this system had no detectable off-target effects on gene expression in Shield1™-treated NIH3T3 cells, as determined by gene microarray (Maynard-Smith et al., 2007), however gene expression levels may not be reflective of the effect of Shield1™ at the protein level.

Affimer coding sequences were subcloned from the pBSTG plasmid into the pRetroX-PTuner retroviral vector. The resulting plasmids encoded the Affimer proteins with an N-terminal DD, and no His-tag. U-2 OS (human osteosarcoma) cells were stably transduced with Affimer-pRetroX plasmids using retroviral transduction (Chapter 2, section 2.2.15). U-2 OS cells were chosen due to their ease of handling for assays and because they were a cancer cell line, which was therapeutically relevant for Grb2 SH2 domain reagents. Additionally, there was evidence in the literature for the role of the MAPK pathway in tumour proliferation, migration and metastasis in osteosarcoma (Noh et al., 2011, Yu et al., 2011, Chandhanayingyong et al., 2012).

Transduced U-2 OS cells were subject to puromycin selection to ensure a transduced cell population of 100%. After selection, cells were exposed to Shield1™ concentrations ranging from 50 nM – 1 µM for 4 h and western blot analysis was performed on lysates to detect the DD. A Shield1™ dose-dependent increase in DD-tagged Affimer expression was seen for all constructs tested (Grb2-8, -A4, -H1 and YS-10), as indicated by a ca. 24 kDa band which corresponded to the ca. 12 – 13 kDa Affimer proteins fused with the ca. 12 kDa DD (Figure 6.5A). Signals for the DD tag in 500 nM and 1 µM Shield1™ samples were similar for most clones, so it was decided to use 500 nM Shield1™ in further assays to reduce use of the Shield1 ™ reagent.

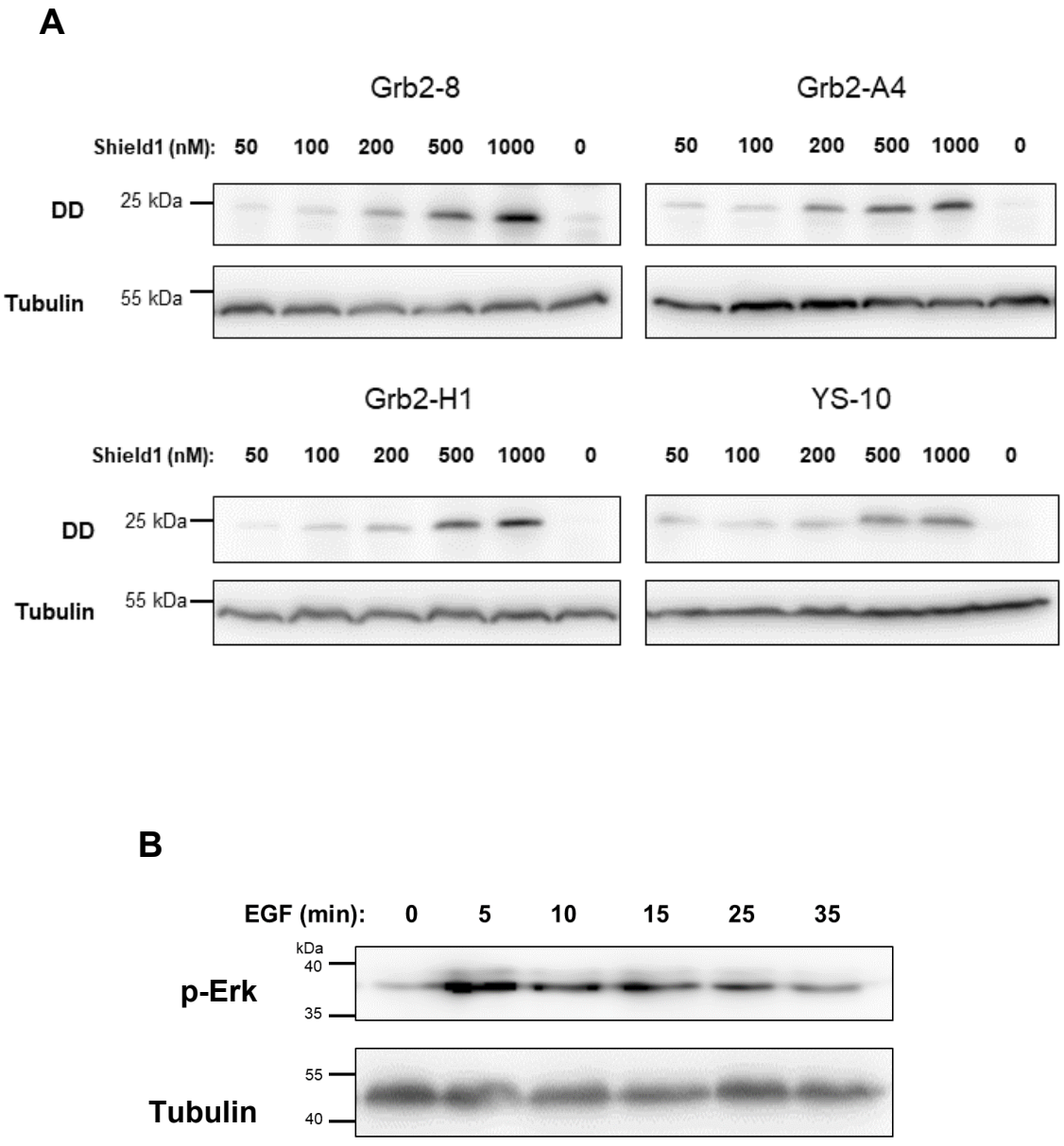

Figure 6.5. Inducible expression of DD-tagged Affimer proteins in stably transfected U-2 OS cells and EGF-induced Erk phosphorylation in wild type U-2 OS. ***(A)*** *Shield1-induced dose-dependent expression of DD-tagged Affimer proteins in stably transfected U-2 OS cells. U-2 OS cells were incubated with media containing different concentrations of Shield1 for 4 h. Lysates were harvested and immunoblotted for the DD-tag. HRP-conjugated secondary antibodies were detected using Luminata Forte. Tubulin was detected as a loading control.* ***(B)*** *Western blot to detect levels of phospho-Erk1/2 (p-Erk) in whole cell lysate from U-2 OS cells, after serum starvation and stimulation with 25 ng/ml EGF for 0 – 35 min. Tubulin was used as a loading control. HRP-conjugated secondary antibodies detected with Luminata Forte. Blot is representative of two independent experiments.*

Before commencing Grb2 SH2 signalling inhibition assays on transduced U-2 OS cells, a time-course of EGF stimulation (25 ng/ml) was performed on wild type U-2 OS cells to determine the optimum timepoint for harvesting lysates (Figure 6.5B). A peak in p-Erk was seen after 5 min EGF stimulation, so it was decided to harvest cells at this time as any decrease in p-Erk would be more easily quantified.

Affimer-expressing U-2 OS cell lines were seeded in 6-well plates and grown for 24 h (ca. 60 – 70% confluency). Shield1™ concentrations ranging from 0 – 500 nM in serum-free media were added for 4 h and cells were stimulated with 25 ng/ml EGF for 5 min. Lysates were subject to western blot analysis to detect and quantify p-Erk, Grb2, DD-tagged Affimer proteins and tubulin. No effect on p-Erk levels was seen with Grb2 SH2 Affimer expression (data not shown). Incubation with Shield1™ was then extended to 16 h overnight, followed by serum starvation for 90 min in serum-free media containing Shield1™, before performing the same assay. This increase in incubation time was implemented because stabilisation and expression of DD-tagged proteins has been shown to steadily increase up to 24 h after Shield1™ addition, although this is protein-dependent (Banaszynski et al., 2006; Schoeber et al., 2009).

Again, no significant difference in p-Erk levels were seen in Affimer-expressing cells compared with non-expressing cells (Figure 6.6, n = 3). This was also true for the YS-10 control, as expected. Western blot analysis detected expression of all Affimer-DD fusion proteins, although the exposure times for anti-DD blots were prolonged. This could suggest the level of expressed Affimer proteins, even at higher concentrations of Shield1™, were low; however quantification with a DD-tagged protein standard would be required in order to determine if this were the case. No DD-tagged Affimer reagents were detected in non-induced samples, indicating these were true controls. It was therefore next decided to test whether the DD-tagged Affimer reagents were even binding to Grb2. As the DD tag was positioned at the N-terminus of the Affimer, close to the variable regions, it was thought this could be inhibiting the binding of the reagents.

A limitation of these experiments to note is the lack of a Shield1™ wild-type cell control, which would be important in determining if Shield1™ itself has any effect on the phosphorylation of Erk.

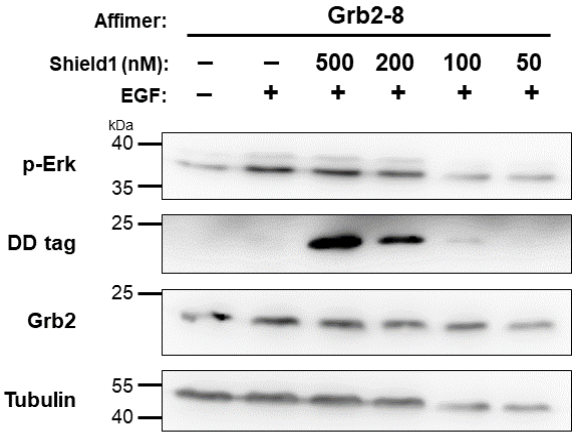
Affimer:
Grb2-8
Shield1 (nM): – – 500 200 100 50
EGF: – + + + + +
kDa
p-Erk
40
35
DD tag
25
Grb2
25
Tubulin
55
40

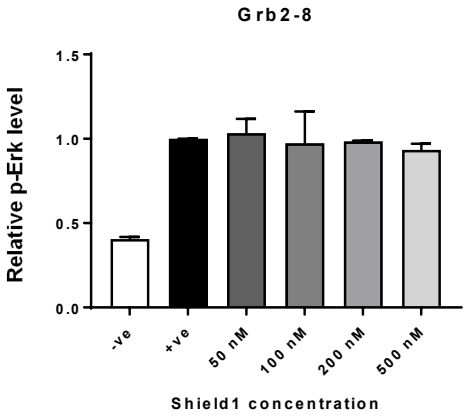
Grb2-8
Relative p-Erk level
1.5
1.0
0.5
0.0
-ve
+ve
50 nM
100 nM
200 nM
500 nM
Shield1 concentration

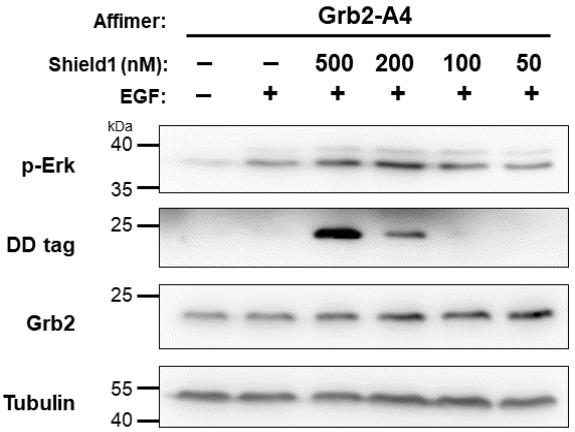
Affimer:
Grb2-A4
Shield1 (nM): – – 500 200 100 50
EGF: – + + + + +
kDa
p-Erk
40
35
DD tag
25
Grb2
25
Tubulin
55
40

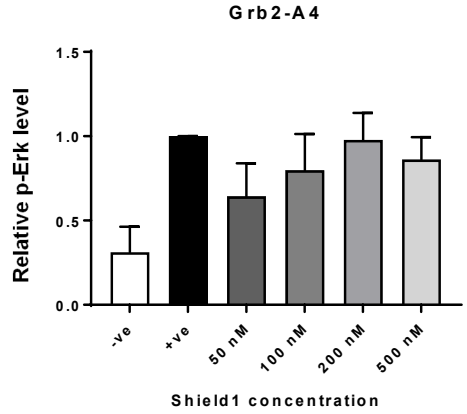
Grb2-A4
Relative p-Erk level
1.5
1.0
0.5
0.0
-ve
+ve
50 nM
100 nM
200 nM
500 nM
Shield1 concentration

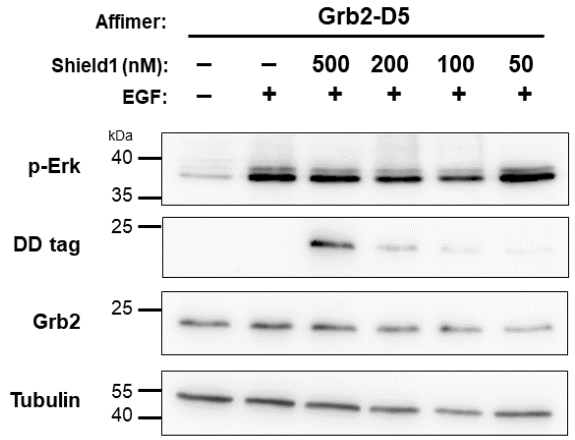
Affimer:
Grb2-D5
Shield1 (nM): – – 500 200 100 50
EGF: – + + + + +
kDa
p-Erk
40
35
DD tag
25
Grb2
25
Tubulin
55
40

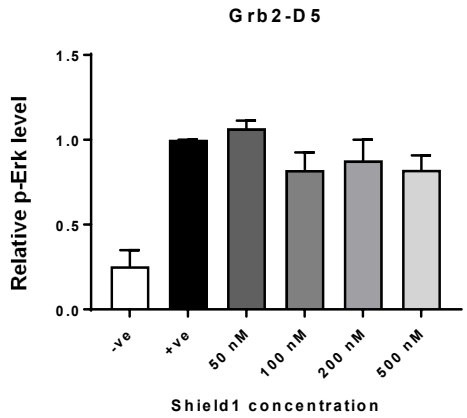
Grb2-D5
Relative p-Erk level
1.5
1.0
0.5
0.0
-ve
+ve
50 nM
100 nM
200 nM
500 nM
Shield1 concentration

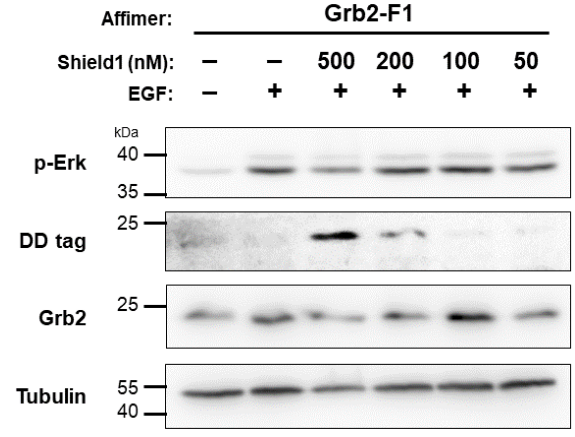
Affimer:
Grb2-F1
Shield1 (nM): – – 500 200 100 50
EGF: – + + + + +
kDa
p-Erk
40
35
DD tag
25
Grb2
25
Tubulin
55
40

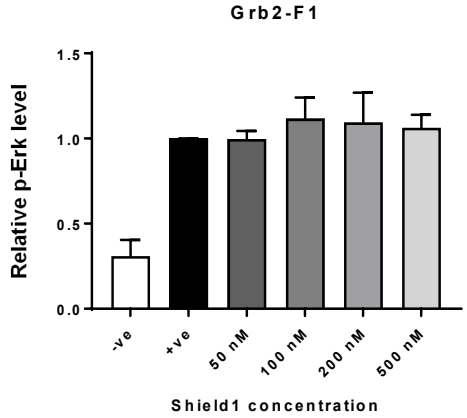
Grb2-F1
Relative p-Erk level
1.5
1.0
0.5
0.0
-ve
+ve
50 nM
100 nM
200 nM
500 nM
Shield1 concentration

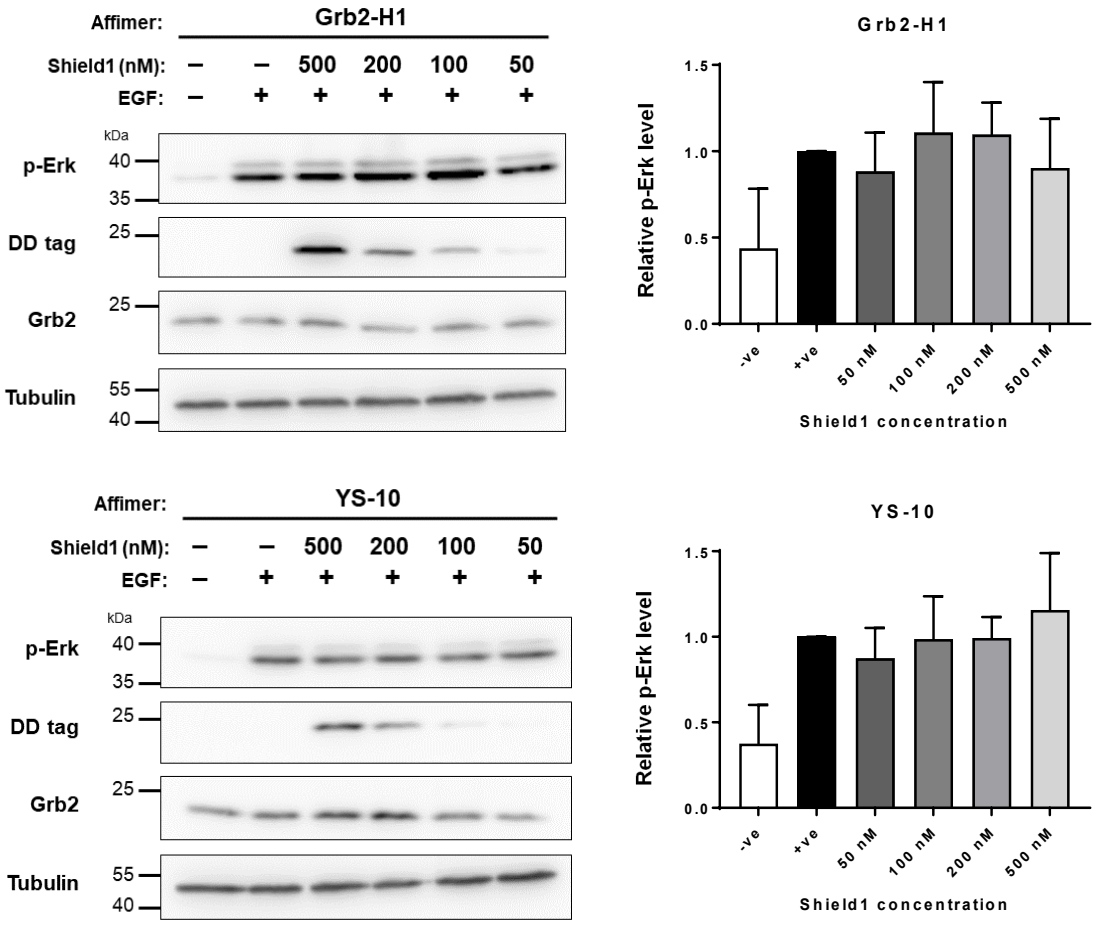

Figure 6.6. DD-tagged Grb2 SH2 Affimer reagents do not reduce EGF-induced Erk phosphorylation in stably transfected U-2 OS cells. *Western blots to detect levels of phospho-Erk1/2 (p-Erk), DD-tagged Affimer, and Grb2 in whole cell lysates from U-2 OS cells stably transfected with Affimer-pRetroX vectors. Shield1 concentrations were added to culture medium overnight to stabilise Affimer levels. Cells were then serum starved in media containing the same Shield1 concentration and stimulated with EGF for 5 min (25 ng/ml). Tubulin was used as a loading control. HRP-conjugated antibodies detected with Luminata Forte. Blot is representative of 3 independent experiments. Quantification of p-Erk from western blots is shown to the left of corresponding blot. Levels of p-Erk were standardised to tubulin for each condition, then normalised to the EGF-stimulated control. Data is presented as mean ± SD (n = 3).*

6.5 Stably expressed DD-tagged Grb2 SH2 Affimer reagents do not bind Grb2 in U-2 OS cells

To determine whether DD-tagged Affimer reagents were able to bind Grb2 in stably transfected U-2 OS cells, a co-immunoprecipitation assay was performed on lysate from both EGF-stimulated (25 ng/ml EGF for 5 mins) and non-stimulated cells for clones Grb2-A4, Grb2-D5 and YS-10. Grb2 was captured from lysate using a recombinantly expressed Affimer which binds the N-terminal SH3 domain, conjugated to His-tag Dynabeads™. After washing, bound proteins were eluted from beads and subject to western blot analysis to determine the presence of the Affimer-Grb2 complex.

As shown in Figure 6.7 (n = 1), Grb2 was successfully captured from lysate for all samples (MW ca. 25 kDa). However, Grb2 SH2 binders and the YS-10 Affimer

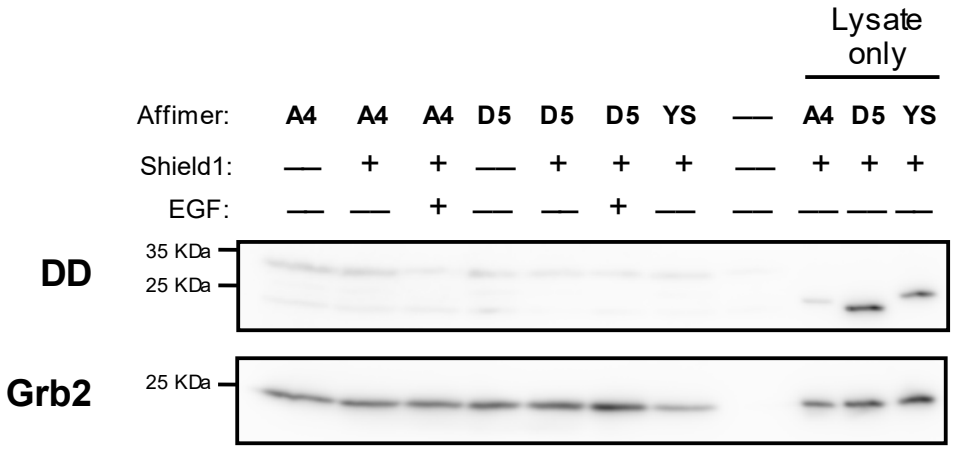

Figure 6.7. Stably expressed Grb2 SH2 Affimer proteins do not show binding of endogenous Grb2 in U-2 OS cell lysate. *Western blots showing results of a co-immunoprecipitation assay performed on whole cell lysates from U-2 OS cells stably transfected with Affimer-pRetroX vectors. Grb2 was captured from lysate using a recombinantly-expressed Grb2 SH3 domain Affimer, conjugated to His-Tag Dynabeads™. After washing, proteins were eluted from beads and subject to western blotting to detect Grb2 (ca. 25 kDa) and DD-tagged Affimer proteins (ca. 24 kDa). Shield1 positive = cells incubated with 500 nM Shield1 overnight to induce Affimer expression. EGF positive = cells serum starved for 90 min and stimulated with 25 ng/ml EGF for 5 min. Cells not induced with Shield1 were used as negative controls, as well as YS; a ySUMO-binding Affimer. Lysate only = lysate not incubated with beads as a positive control. HRP-conjugated antibodies were detected with Luminata Forte.*

control were not co-precipitated with Grb2, shown by detection of the DD. The DD was detected in Affimer-expressing lysate not incubated with beads (lysate only samples, ca. 24 kDa), demonstrating successful expression of DD-tagged fusion proteins. Although two faint protein bands can be seen in some immunoprecipitation samples in the DD blot, when overexposed these bands were present in all samples, including the negative controls and buffer-only control. Additionally, they did not correspond exactly to MW of the DD bands in the lysate only samples. This indicated that Grb2 SH2 Affimer proteins were not binding the Grb2 SH2 in the stably transfected U-2 OS cells. However, it is worth noting that this experiment was conducted only once, and could have been optimised.

In addition, a different co-immunoprecipitation method was used here, compared to that used with the transiently expressed His-tagged Affimer constructs. This involved capturing the target Grb2 from lysate instead of the Affimer as there was no His-tag on the Affimer-DD proteins preventing their capture. A better strategy would have been to include a His-tag coding region when cloning into the pRetroX-PTuner vector, to make the co-immunoprecipitation assay results comparable to the transiently expressed Affimer proteins.

6.6 Addition of a helical linker region between Affimer proteins and the DD-tag has no effect on Erk phosphorylation

As the DD tag is relatively large (ca. 12 kDa) and was positioned on the N-terminus of the Affimer, close to the variable regions, it was considered possible that the DD could be blocking the binding of Grb2 SH2 Affimer proteins to their target. This would account for the lack of Grb2 SH2 inhibition and binding seen for these constructs.

To test this theory, a helical linker sequence was introduced into three of the Affimer-pRetroX plasmids (A4, D5 and H1), to separate the DD from the Affimer (Arai et al., 2001; Marqusee and Baldwin, 1987). These helix-forming peptide linkers have been shown to reduce interference between the domains of bifunctional fusion proteins. The linker sequence encoded a 20 amino acid peptide containing three helix-forming repeats (EAAAK) and providing a separation distance of ca. 53.5Å (Arai et al., 2001). This sequence was

introduced into the Affimer-pRetroX vectors between the DD and Affimer using a Quikchange-style reaction (Chapter 2, section 2.2.15).

DNA sequencing showed successful addition of the linker encoding sequence for binders A4 and H1, but the sequence in D5 contained an additional five repeats of the helix-forming motif (see Figure 6.8A). It was decided to continue with all three constructs. These were stably transduced into U-2 OS cells as before, and after completing puromycin selection, Shield1^{TM}-induced Affimer expression was confirmed by western blot analysis (data not shown). The same Erk phosphorylation assay was then performed as with the previous Affimer-DD constructs (section 6.5). This assay yielded similar results as before, with no decrease in p-Erk seen in Affimer expressing cells compared with controls, for any of the binders (Figure 6.8B).

6.7 Grb2 is essential in EGF-induced Erk phosphorylation in U-2 OS cells

Before attempting to use the Grb2 SH2 Affimer reagents in a different stable transfection system, a test was performed to check the importance of Grb2 in downstream Erk phosphorylation in U-2 OS cells. This was to confirm that inhibition of Grb2 signalling would indeed result in a detectable change in p-Erk levels. To achieve this, siRNA knockdown of Grb2 was performed in U-2 OS cells (Chapter 2, section 2.2.17). Seventy-two hours post-transfection, cells were stimulated with 25 ng/ml EGF for 5 min (as with previous assays) and the levels of p-Erk were observed by western blot analysis. U-2 OS cells treated only with transfection reagents and with non-targeting (NT) siRNA pools were used as controls. siRNA knockdown of PLCγ1 was also tested to determine whether this could be compensating for Grb2 inhibition in Erk phosphorylation. PLCγ1 is activated by the EGFR (Meisenhelder et al. 1989; Kwon et al. 2003) and has been shown to mediate Erk phosphorylation upon growth factor stimulation (Kwon et al., 2003; Kim, M.J. et al., 2000), including EGF-induced Erk phosphorylation (Choi et al., 2004).

It is also known to compete with Grb2 for other RTKs, such as FGFR2. For example, Grb2 knockdown resulted in constitutive binding of PLCγ1 to the FGFR2 via its SH3 domain (Timsah et al., 2014). This recruitment of PLCγ1 to

A

```
Affimer   Amino acid sequence
          ....110.........120.........130.........140.........150.........160
          DD Helical linker
A4        KPELAEAAAKEAAAKEAAAKAAAPRPQISASNSLEIEELARFAVDEHNKKENALL
H1        KPELAEAAAKEAAAKEAAAKAAAPRPQISASNSLEIEELARFAVDEHNKKENALL
D5        KPELAEAAAKEAAAKEAAAKEAAAKEAAAKAAAKEAAAKEAAAKAAAPRPQISAS
```

B

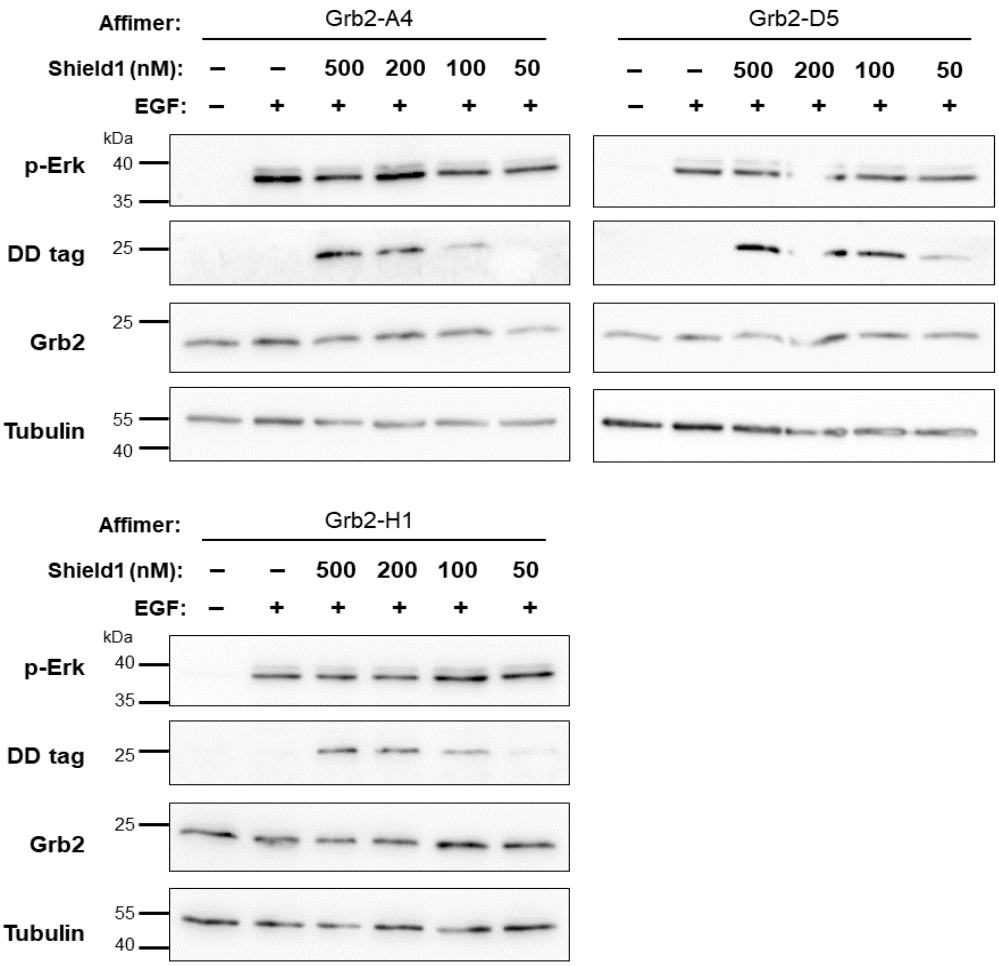

Figure 6.8. Insertion of a helical linker between the DD tag and Affimer has no effect on EGF-induced Erk phosphorylation in U-2 OS cells. ***(A)*** *Amino acid alignment of DD-Affimer DNA in pRetroX-PTuner plasmids, after insertion of a helical linker sequence (blue) between the DD and Affimer (red) sequences. DNA sequences were translated using MacVector 13.5.2.* ***(B)*** *Western blot detecting phospho-Erk1/2 (p-Erk), Grb2 and DD-tagged Affimer in lysate from stably transfected U-2 OS cells expressing DD-tagged Affimer proteins with helical linkers. Cells incubated with Shield1 overnight, serum starved and stimulated with 25 ng/ml EGF for 5 min. Tubulin used as loading control. HRP-conjugated antibodies detected with Luminata Forte. For H1 n = 3, for A4 and D5 n = 1.*

the FGFR2 upon Grb2 knockdown resulted in upregulated phospholipase activity. Although this was in non-stimulated cells, and was mediated by the SH3 domains of both proteins, we were interested to see whether a similar competitive relationship between Grb2 and PLCγ1 was apparent in the EGF-stimulated U-2 OS cells. The effect on phosphorylation of Akt was also measured to observe the consequence of Grb2 inhibition on the PI3K/Akt pathway, and potentially identify another measurable end-point for our target phosphorylation assay.

The non-targeting siRNA pool initially used as a control (NT2, Dharmacon™, GE Healthcare) consistently showed a significant reduction in p-Erk in comparison to the mock control, so it was decided that this was not a suitable control for the experiment. A different non-targeting pool (NT1, Dharmacon™, GE Healthcare), was used in the final experimental repeat instead. As seen in Figure 6.9 ($n = 3$ for all but NT1), Grb2 siRNA knockdown resulted in a significant reduction in EGF-induced Erk phosphorylation compared with the mock-transfected U-2 OS control ($p < 0.0001$) and showed a large reduction compared with the NT1 siRNA control in the final repeat, although statistics could not be performed for this comparison ($n = 1$).

Phospho-Erk levels in Grb2 siRNA treated cells were reduced by 81 ± 10% compared with the mock control ($p < 0.0001$) and by 77 ± 13% compared with NT1. The p-Erk levels in the EGF-stimulated mock and NT1 samples were similar, indicating that NT1 was a more suitable control than NT2, which showed a significant decrease from the mock ($p < 0.0001$).

Grb2 knockdown also caused a significant reduction in p-Akt compared with the mock control (64 ± 34%, $n = 3$). The NT1 pool also showed a reduction in p-Akt of 42% from the mock control, however. PLCγ1 knockdown caused a decrease in p-Erk which was not as marked as Grb2, but was a significant reduction from the mock-transfected control (32 ± 3%; $n = 3$, $p < 0.002$).

Interestingly, p-Akt levels were increased by almost 2.4-fold with PLCγ1 knockdown; this result was not in accordance with previous studies, which have reported a decrease in Akt phosphorylation with knockdown or inhibition of PLCγ1 in various cell lines; such as c-Myc-overexpressing mammary epithelial cells (Myc83), rat aortic smooth muscle cells (RASMCs) and human lung epithelial cells (A549) (Deb et al., 2004; Jiang et al., 2017; Zhu et al., 2014).

A

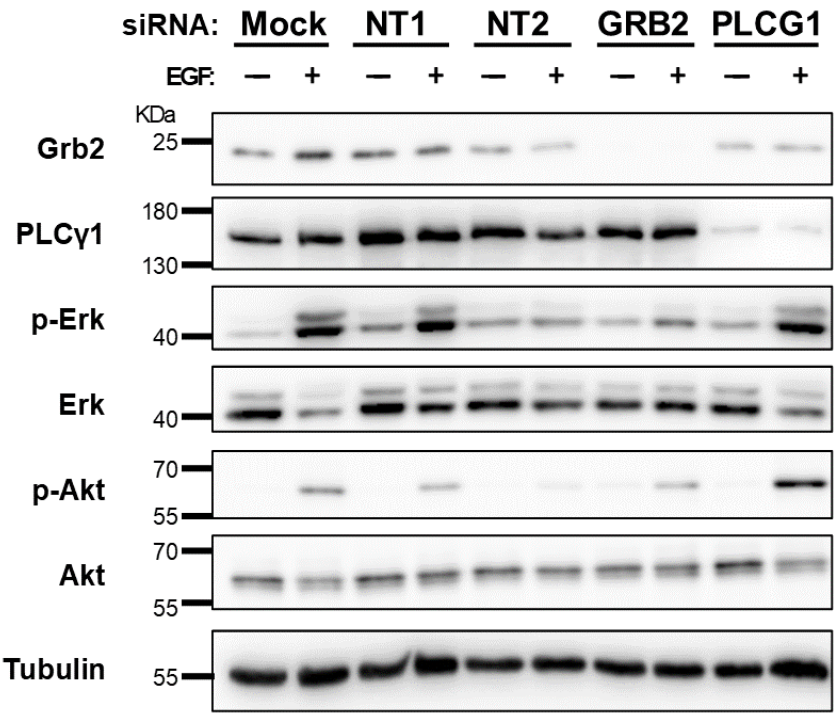
siRNA: Mock NT1 NT2 GRB2 PLCG1
EGF: — + — + — + — + — +
KDa
Grb2
25
PLCγ1
180
130
p-Erk
40
Erk
40
p-Akt
70
55
Akt
70
55
Tubulin
55

B

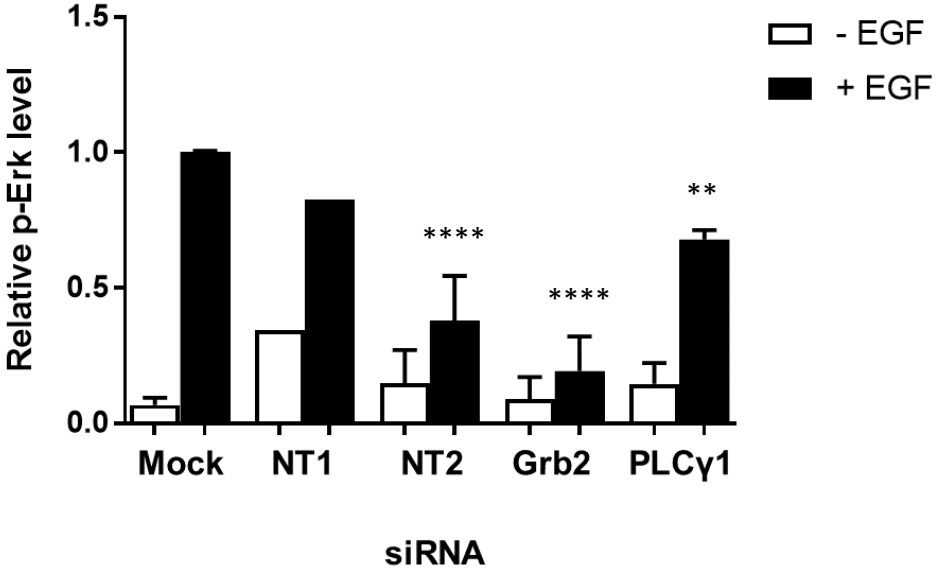
Relative p-Erk level
1.5
1.0
0.5
0.0
- EGF
+ EGF
****
****
**
Mock
NT1
NT2
Grb2
PLCγ1
siRNA

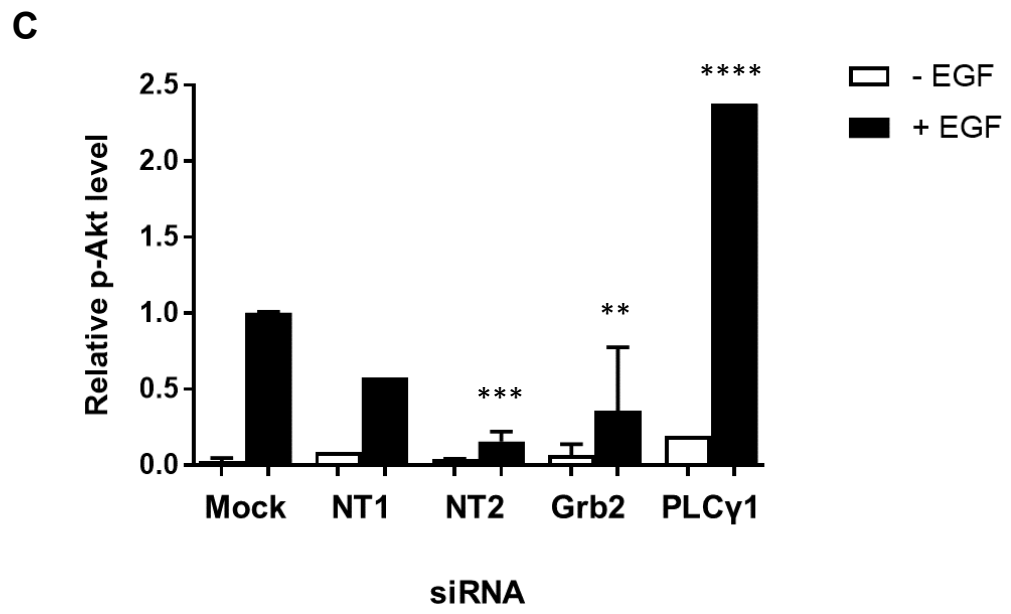

Figure 6.9. Effect of siRNA knockdown of Grb2 and PLCγ1 in U-2 OS cells. *(A) Western blots to detect levels of Grb2, PLCγ1, phospho-Erk1/2 (p-Erk), total Erk, phospho-Akt (p-Akt) and total Akt in whole cell lysate from U-2 OS cells, after siRNA knockdown of Grb2 and PLCγ1. U-2 OS cells were serum-starved and (for + EGF samples) stimulated with 25 ng/ml EGF for 5 min, 72 h post-transfection with Grb2, PLCγ1, or non-targeting siRNA pools (NT1 and NT2), or transfection reagents only (Mock). Tubulin used as a loading control. HRP-conjugated antibodies detected with Luminata Forte. Blot is representative of three independent experiments. Quantification of p-Erk* ***(B)*** *and p-Akt* ***(C)*** *from the western blots shown in* ***(A)****. Levels of p-Erk/p-Akt were standardised to tubulin for each condition, then normalised to the EGF-stimulated mock control. Data presented as mean ± SD (n = 3), for all but NT1 (n =1). Black asterixis signify significance compared to mock. ****p <0.0001, ***p <0.0002, **p <0.002.*

PLCγ1 and PI3K, which is an activator of Akt, both use the same substrate (phosphatidylinositol 4,5-bisphosphate; PIP_2) to form second messengers and propagate signalling pathways. It is therefore possible that knockdown of PLCγ1 results in more availability of PIP_2 to be bound by PI3K, and consequently more phosphorylation and activation of Akt. Competition for PIP_2 by PLCγ1 and PI3K has not previously been observed in the literature however.

These results confirmed that Grb2 was essential in the phosphorylation of Erk, and that inhibition of Grb2 signalling should show a substantial reduction in p-Erk as expected. This also indicated that PLCγ1 was not compensating for Grb2 in Erk phosphorylation in this cell line. Additionally, measurement of p-Akt was

highlighted as an alternative endpoint if no results with p-Erk were seen, although the reduction in Akt phosphorylation was not as great as Erk phosphorylation with Grb2 knockdown.

6.8 His-tagged Grb2 SH2 Affimer reagents A4 and D5 reduce Erk phosphorylation when stably expressed in U-2 OS cells

The Grb2 SH2 Affimer reagents were then tested in a different stable expression system, without the use of a DD-tag or inducible expression. This was to eliminate the possibility that the DD-tag was inhibiting the Grb2 SH2-Affimer interaction, whilst still keeping the benefit of a 100% transduced cell population. The sequences for binders Grb2-8, -A4, -D5, -F1, -H1 and YS-10 were subcloned from the pET11a vector into the mammalian expression vector pBABE. This is a retroviral vector that allows stable, constitutive expression of the protein of interest. The Affimer constructs in this plasmid contained a C-terminal HA tag and 6xHis-tag (Chapter 2, section 2.2.16).

MCF-7 (human breast cancer) cells were also tested using this system. MCF-7 cells overexpress Grb2, leading to an increase in Grb2-Sos1 complex formation and upregulation of Ras signalling in this cell line (Daly et al., 1994). Grb2 SH2 peptidic antagonists have shown a reduction in cell viability in MCF-7 cells (Hsiao et al., 2013) and KGF-induced motility in MCF-7s is dependent upon Grb2 and its activation of Erk (Zang et al., 2004), demonstrating the importance of Grb2-mediated pathways in this cell line. MCF-7 also expresses EGFR so can be stimulated via this receptor (Subik et al., 2010; Nunes-Xavier et al., 2012).

Both U-2 OS and MCF-7 cells were transduced with pBABE-Affimer DNA using retroviral transduction, and subject to puromycin selection to ensure a population of 100% successfully transduced cells. Both cell lines that were transduced with retrovirus containing the Affimer F1 plasmid did not survive selection. This is likely due to failed retroviral production or transduction of target cells, but could potentially be a potent pro-apoptotic effect of binder F1 in these cells. Due to time constraints, retroviral transduction was not repeated for this construct, however this should be re-attempted in the continuation of the project.

Experiments were therefore continued with the remaining four Grb2 SH2 binders and YS-10 control. After puromycin selection, successful expression of Affimer proteins was confirmed via western blot analysis of lysates to detect the His-tag

(Figure 6.10). Affimer-expressing cell lines and wild-type controls were then seeded in 6-well plates and left to grow for 48 h (ca. 60% confluency). Cells were serum-starved for 90 min and stimulated with EGF (25 ng/ml) for 5 and 30 min, or were not stimulated at all. Lysates were used in western blot analysis to detect p-Erk, total Erk, Grb2, His-tagged Affimer proteins and tubulin.

As seen in Figure 6.11A (n = 3), in comparison with the wild-type controls, U-2 OS cells expressing clones Grb2-A4 and -D5 showed a significant decrease in Erk phosphorylation after 5 min EGF stimulation. Affimer A4 showed a reduction of 36 ± 6% ($p < 0.001$) in p-Erk levels, and Affimer D5 a 38 ± 8% reduction ($p < 0.001$), as quantified by western blot densitometry (Figure 6.11B). D5 also showed a significant decrease in p-Erk at 30 min post-stimulation (36 ± 13%, $p < 0.01$). The decrease in p-Erk at 30 min for A4 (38% ± 11%) was not significant, due to the larger standard deviation in the control 30 minute timepoint of ± 0.15 (40%). These results signified a disruption of Grb2 SH2-mediated signalling in U-2 OS cells by Affimer reagents A4 and D5. Clones Grb2-8 and -H1, as well as the YS-10 control, did not show a significant change in p-Erk levels for any time points. However, there was large variation in p-Erk levels for H1-expressing cells at 5 min post-EGF stimulation, showing a reduction of 27 ± 21%, so the assay could be repeated for this clone to confirm these results.

Affimer-expressing MCF-7 cell lines were also tested in the same assay, but no significant decrease in p-Erk was seen for any Grb2 Affimer (Figure 6.12, n = 1). This was the case for all timepoints tested. This assay was not repeated due to time constraints.

6.9 His-tagged Grb2 SH2 Affimer reagents 8, A4 and D5 bind Grb2 in stably transfected U-2 OS cells

To confirm binding of Grb2 SH2 Affimer reagents to Grb2 in the stably transfected U-2 OS cells, the co-immunoprecipitation assay used for transiently expressed Affimer proteins in HEK293 cells was repeated (section 6.3). Whole cell lysates from both EGF-stimulated (25 ng/ml, 10 min) and non-stimulated U-2 OS cells were used. His-tag Dynabeads^{TM} were used to capture His-tagged Affimer proteins from the lysate and after washing, bound proteins were eluted from beads and subject to immunoblotting to determine the presence of an Affimer-Grb2 complex.

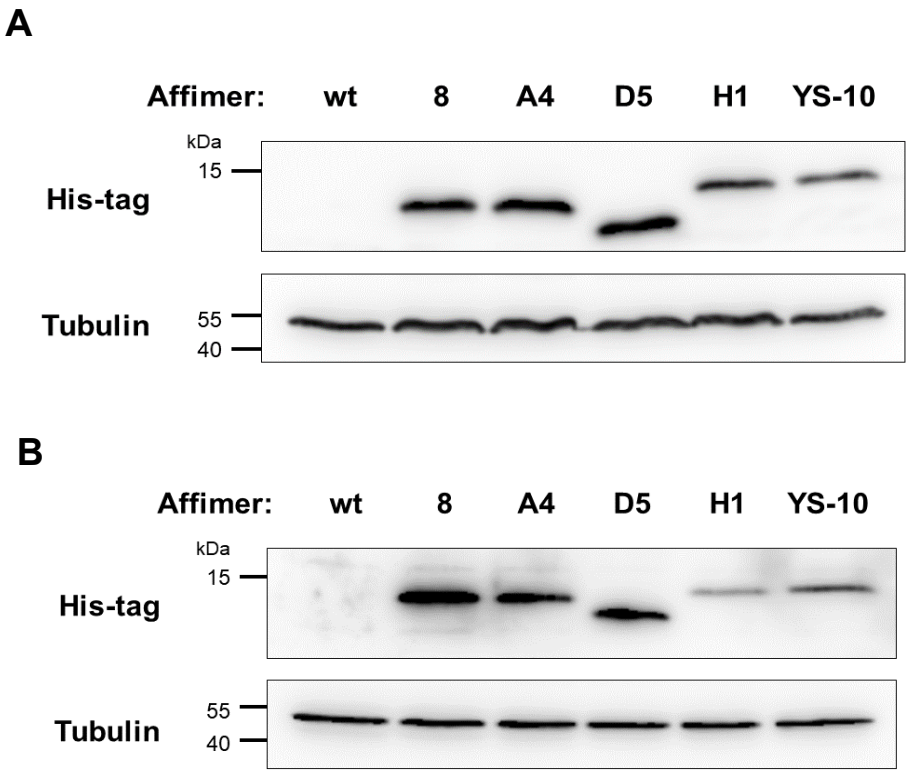

Figure 6.10. Stable expression of His-tagged Affimer proteins in U-2 OS cells. *Western blot to detect levels of His-tagged Affimer proteins (ca. 12 – 13 kDa) expressed from pBABE vectors in* ***(A)*** *stably transduced U-2 OS cells and* ***(B)*** *stably transduced MCF-7 cells. Tubulin was used as a loading control. HRP-conjugated antibodies detected with Luminata Forte. MW marker = PageRuler Prestained.*

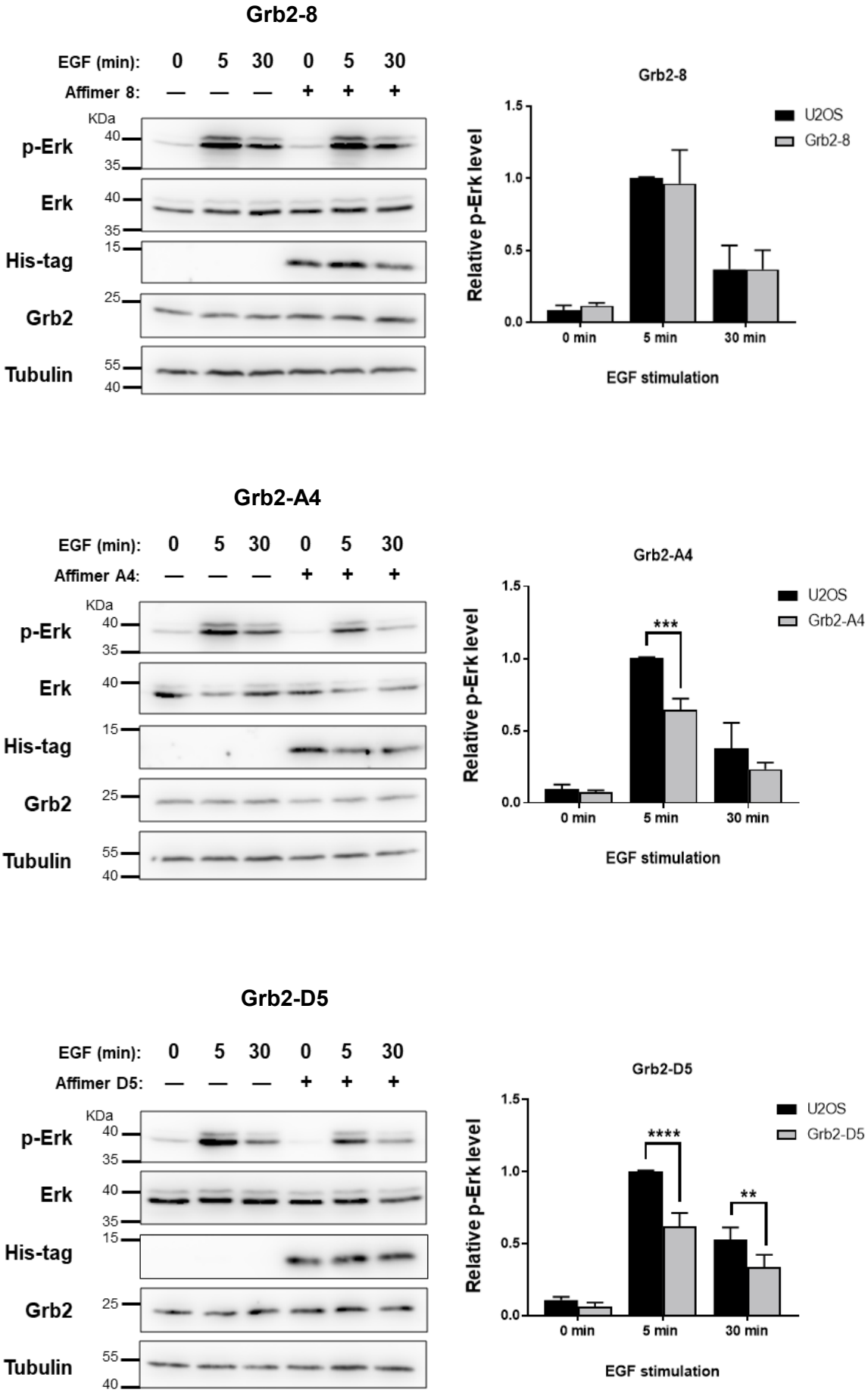
Grb2-8
EGF (min): 0 5 30 0 5 30
Affimer 8: — — — + + +
KDa
p-Erk
Erk
His-tag
Grb2
Tubulin
40
35
15
25
55
Grb2-8
U2OS
Grb2-8
Relative p-Erk level
1.5
1.0
0.5
0.0
0 min
5 min
30 min
EGF stimulation
Grb2-A4
EGF (min): 0 5 30 0 5 30
Affimer A4: — — — + + +
***
Grb2-A4
U2OS
Grb2-A4
Grb2-D5
EGF (min): 0 5 30 0 5 30
Affimer D5: — — — + + +
****
**
Grb2-D5
U2OS
Grb2-D5

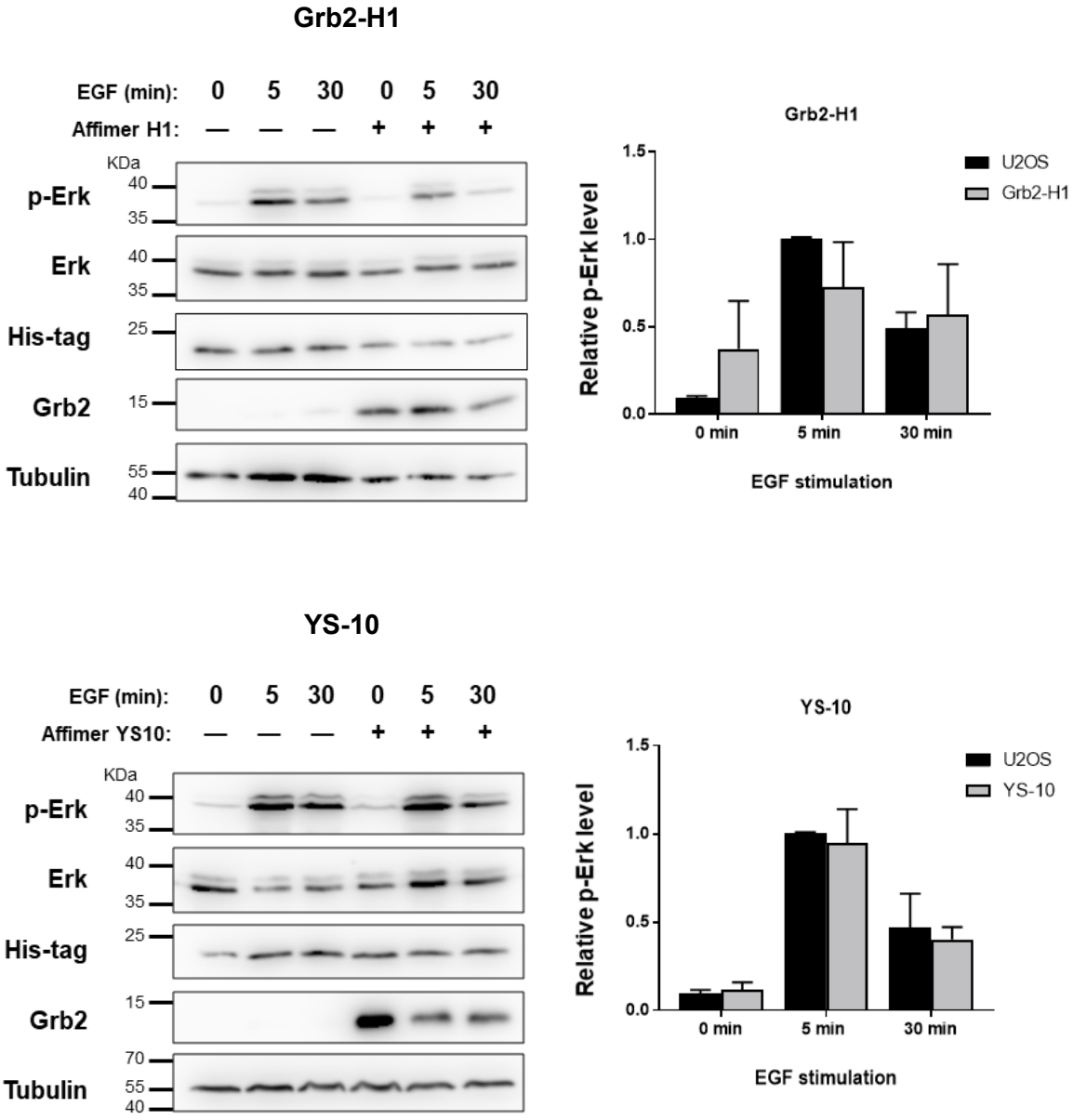

Figure 6.11. His-tagged Grb2 SH2 Affimer reagents reduce EGF-induced Erk phosphorylation in stably transfected U-2 OS cells. *Western blots to detect levels of phospho-Erk1/2 (p-Erk), total Erk, His-tagged Affimer and Grb2 in whole cell lysates from U-2 OS cells stably transfected with Affimer-pcDNA5 vectors. Cells were serum starved for 90 min and stimulated with EGF for 5 min (25 ng/ml). Tubulin was used as a loading control, HRP-conjugated antibodies detected with Luminata Forte. Blot is representative of three independent experiments. Quantification of p-Erk from western blots is shown to the left of corresponding blot. Levels of p-Erk were standardised to tubulin for each condition, then normalised to the EGF-stimulated control. Data is presented as mean ± SD (n = 3). Paired t-tests conducted using GraphPad Prism 7. ** p <0.01, *** p <0.0005, **** p <0.0001.*

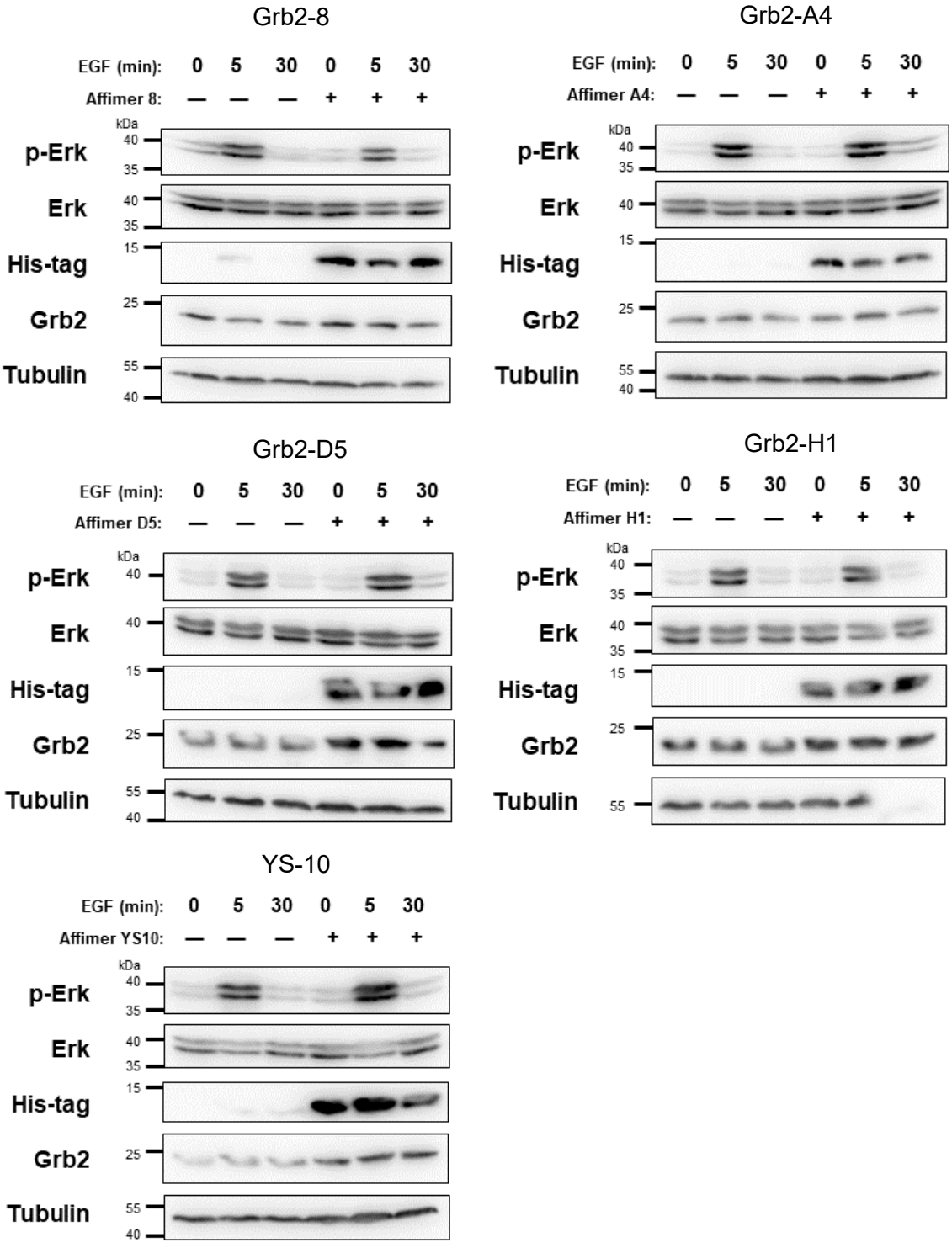

Figure 6.12. His-tagged Grb2 SH2 Affimer reagents do not reduce EGF-induced Erk phosphorylation in stably transfected MCF-7 cells. *Western blots to detect levels of phospho-Erk1/2 (p-Erk), total Erk, His-tagged Affimer and Grb2 in whole cell lysates from MCF-7 cells stably transfected with Affimer-pcDNA5 vectors. Cells were serum starved for 90 min and stimulated with EGF for 5 min (100 ng/ml). Tubulin was used as a loading control, HRP-conjugated antibodies detected with Luminata Forte. Blot is representative of three independent experiments.*

As visualised by western blot analysis, all His-tagged Affimer proteins were successfully captured from lysate. Grb2 SH2 binders 8, A4 and D5, but not H1 or the YS-10 Affimer control, co-precipitated Grb2 in both stimulated and non-stimulated cells (Figure 6.13, n = 3). Affimer D5 co-precipitated the highest level of Grb2 consistently over all repeats, with 8 and A4 showing weaker protein bands. In some experimental repeats, a very faint Grb2 protein band could be visualised in Affimer H1 when the blot was overexposed, but this was not consistent. The lack of Grb2 present in H1 samples could be attributed to the lower level of this Affimer protein captured from lysate, compared with other clones bands were seen at the expected MW of ca. 12 kDa and ca. 25 kDa for Affimer proteins and Grb2, respectively.

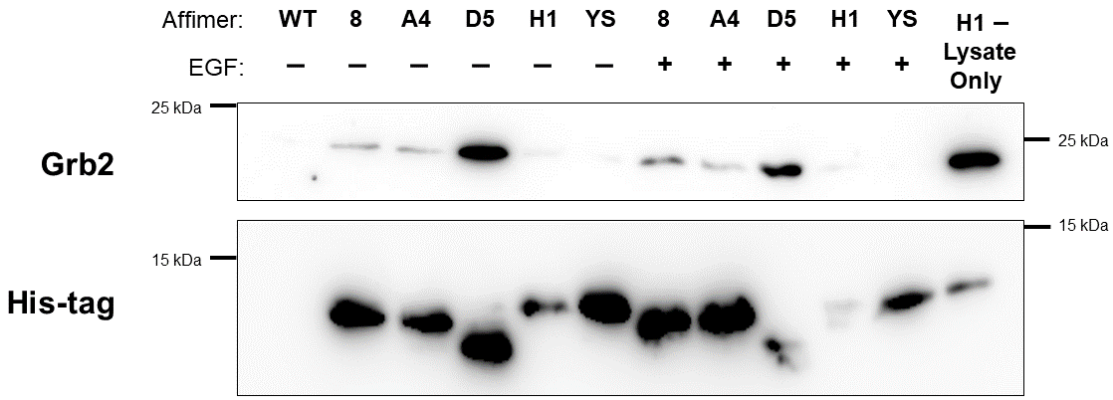

Figure 6.13. Stably expressed His-tagged Grb2 SH2 Affimer proteins show binding of endogenous Grb2 in U-2 OS cell lysate. *Western blots showing co-immunoprecipitation of endogenous Grb2 from U-2 OS cell lysate, by stably expressed Grb2-8, -A4 and -D5 Affimer proteins. Stably transduced U-2 OS cell lines were seeded in 6-well plates and 48 h later were serum starved for 90 min and stimulated with 25 ng/ml EGF for 10 min (+ EGF), or not serum starved or EGF stimulated (- EGF). Cells were lysed and His-tagged Affimer proteins were captured from lysate using His-Tag Dynabeads™. After washing, proteins were eluted from beads and subject to western blotting to detect Grb2 (ca. 25 kDa) and His-tagged Affimer proteins (ca. 12 kDa). WT = wildtype U-2 OS cells (no Affimer DNA). YS = ySUMO-binding Affimer control. H1- lysate only = lysate from non-stimulated Grb2-H1 Affimer cells not incubated with beads, as a positive control for Grb2 and Affimer. HRP-conjugated antibodies were detected with Luminata Forte. Blots are representative of three experimental repeats.*

6.10 His-tagged Grb2 SH2 Affimer reagents show a similar staining pattern to Grb2 in stably transfected U-2 OS cells

Fixed-cell staining was performed on stable Affimer-expressing U-2 OS cell lines, to visualise expression levels of Affimer proteins and their cellular localisation. Both non-stimulated and EGF-stimulated (25 ng/ml, 5 min) cells were stained for His-tagged Affimer proteins, as well as Grb2. Immunofluorescent imaging was performed on stained cells and images were analysed using NIS-Elements software (Nikon). Grb2 siRNA knockdown was performed on wild-type U-2 OS cells as a Grb2 staining control, and showed greatly reduced staining with the Grb2 antibody compared to mock-transfected cells (Figure 6.14).

His-tagged Affimer proteins showed similar staining patterns to Grb2 in transfected cells, in both non-stimulated and stimulated cells (Figure 6.15A – D, n = 2). Interestingly, both Grb2 and the Affimer proteins displayed predominantly nuclear over cytoplasmic staining. Nuclear staining of Grb2 and Affimer proteins was also seen in the transiently transfected HEK293 cells (Figure 6.2), but not as intensely as it appeared in the pBABE-transduced U-2 OS cells. Although Grb2 is thought of as a cytoplasmic protein, there is evidence for Grb2 nuclear localisation in numerous cell lines (Yamazaki et al. 2002; Verbeek et al. 1997; Fortian and Sorkin, 2014; Chen et al. 2012). This indicates that an alternative cell line to U-2 OS could have been more appropriate for this study, and demonstrates the importance in choosing the correct cell line for cell-based assays.

The YS-10 control did not show a similar a staining pattern to Grb2; instead displaying exclusively nuclear staining. The nucleus is a major site for SUMOylation in the cell (Hughes et al., 2017) and SUMOylation often results in translocation of proteins to the nucleus (Hang and Dasso, 2002; Matunis et al., 1998), indicating binding of YS-10 to a human homologue of its target. Indeed, Affimer reagents raised against human SUMO-1, -2 and -3 have been shown to co-localise with SUMO proteins in the nuclei of HEK293 cells (Hughes et al., 2017). The YS-10 Affimer had previously shown high specificity for yeast SUMO over human SUMO-1 and -2 in ELISA and western blot analysis, although human SUMO-3 and -4 were not tested (Tiede et al., 2014).

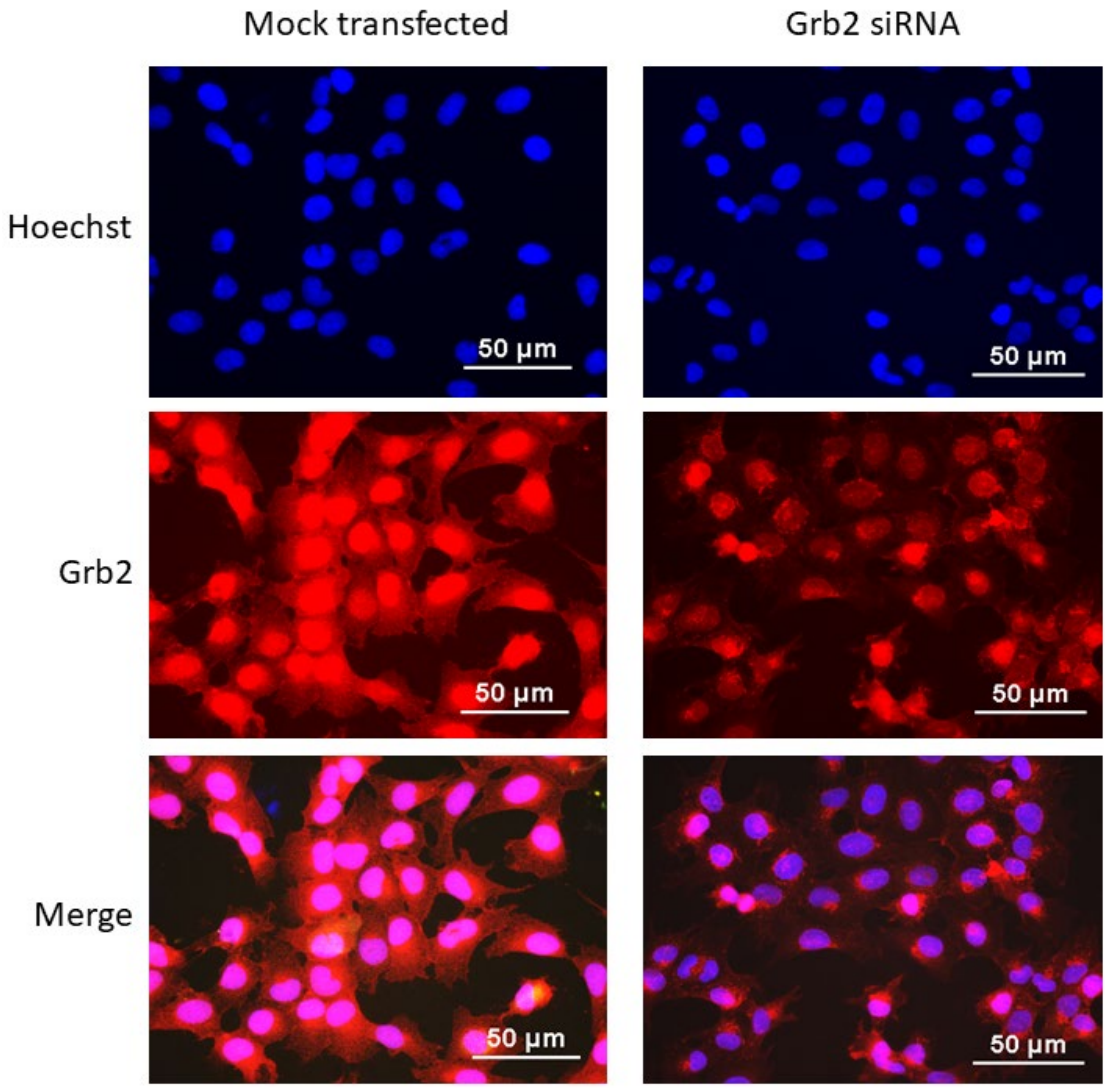

Figure 6.14. Grb2 siRNA knockdown staining control in U-2 OS cells. *U-2 OS cells were transfected with 50 nM Grb2 siRNA and incubated for 72 h. Cells were fixed in 4% PFA and immunofluorescence microscopy was performed using an antibody against Grb2 (red), followed by a fluorescent species-specific secondary antibody. Nuclei were stained with Hoechst 33342. Scale bar = 50µm, images are from one independent experiment.*

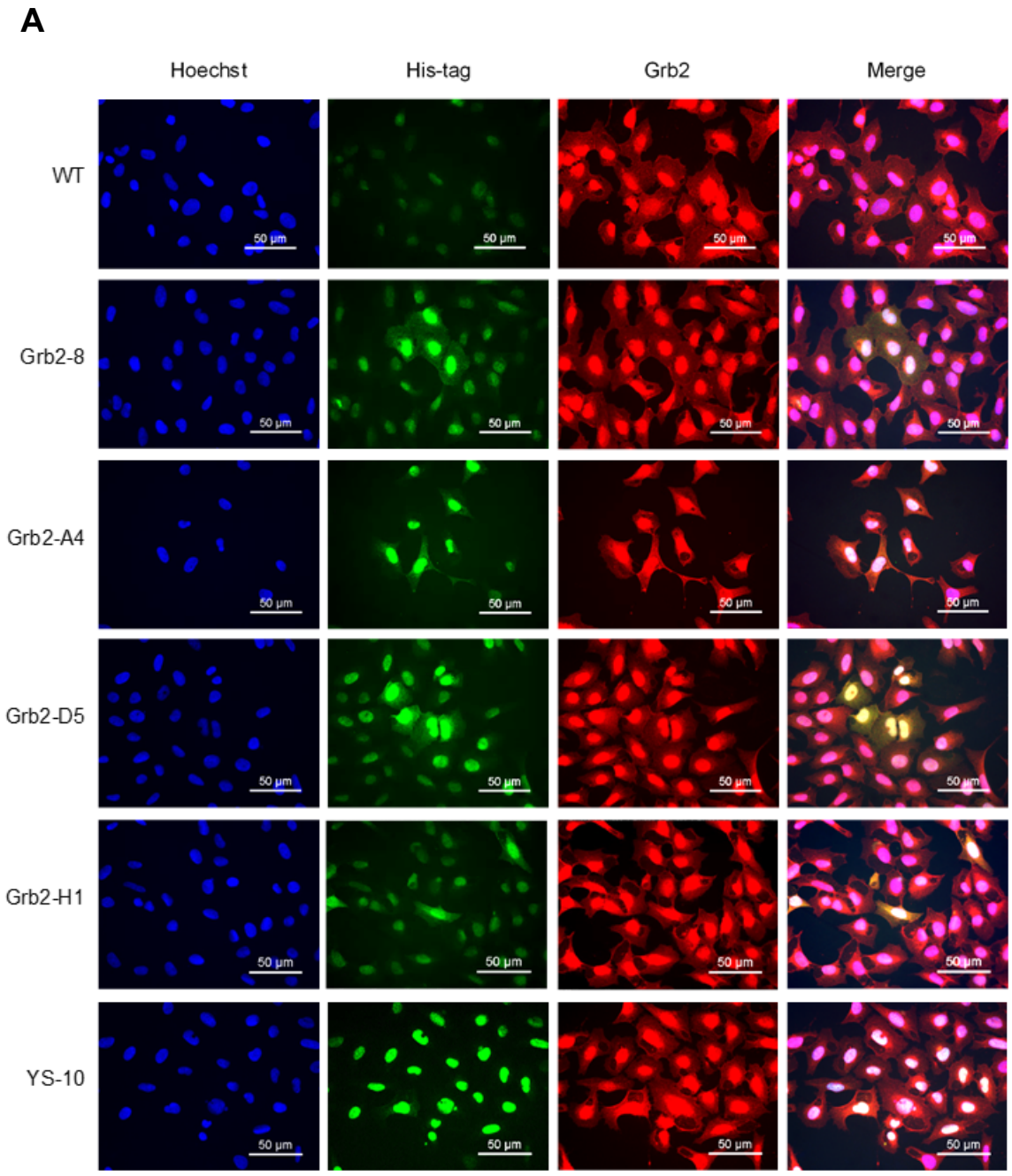
A
Hoechst
His-tag
Grb2
Merge
WT
Grb2-8
Grb2-A4
Grb2-D5
Grb2-H1
YS-10
50 μm

B

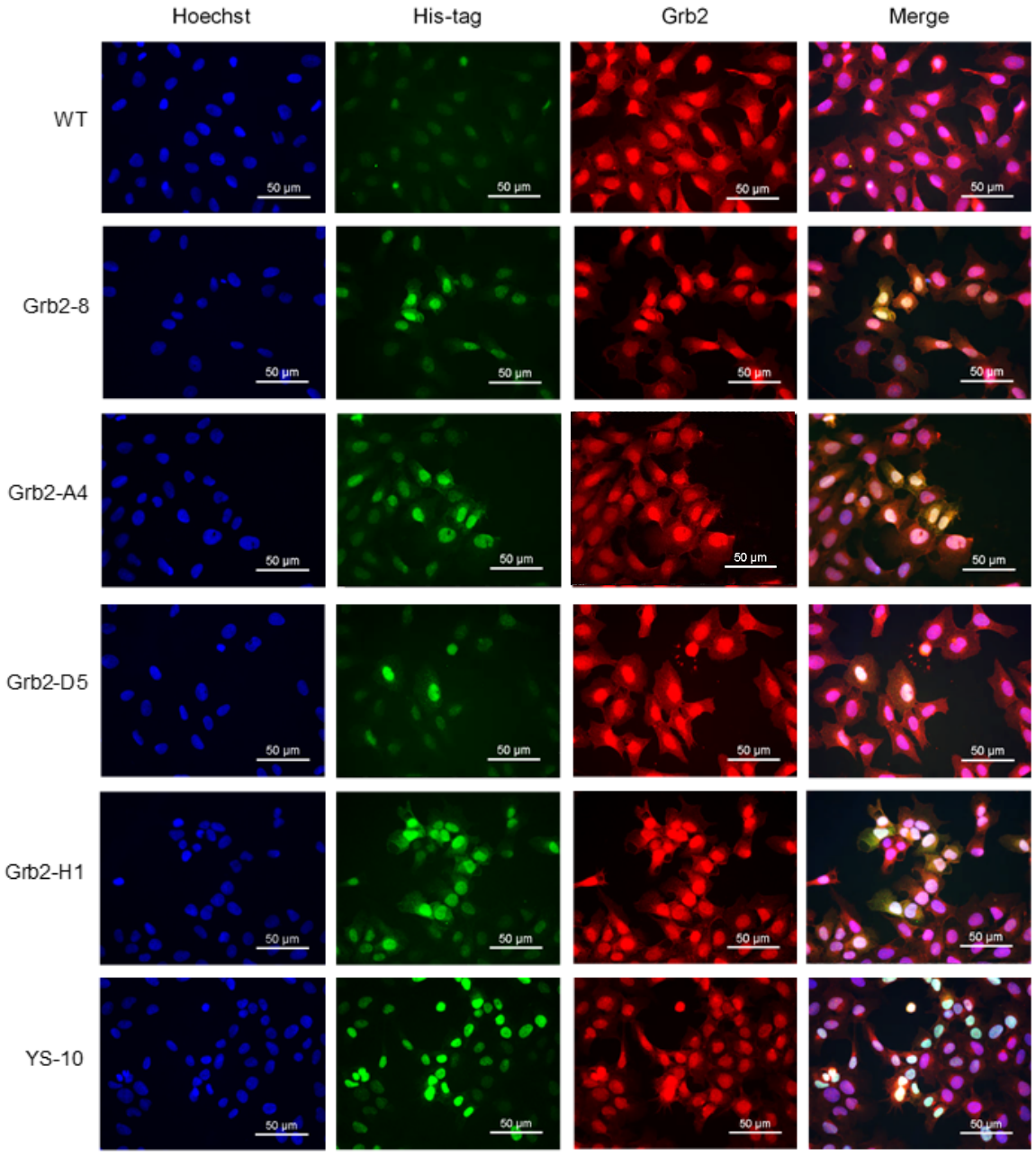
Hoechst
His-tag
Grb2
Merge
WT
Grb2-8
Grb2-A4
Grb2-D5
Grb2-H1
YS-10
50 μm

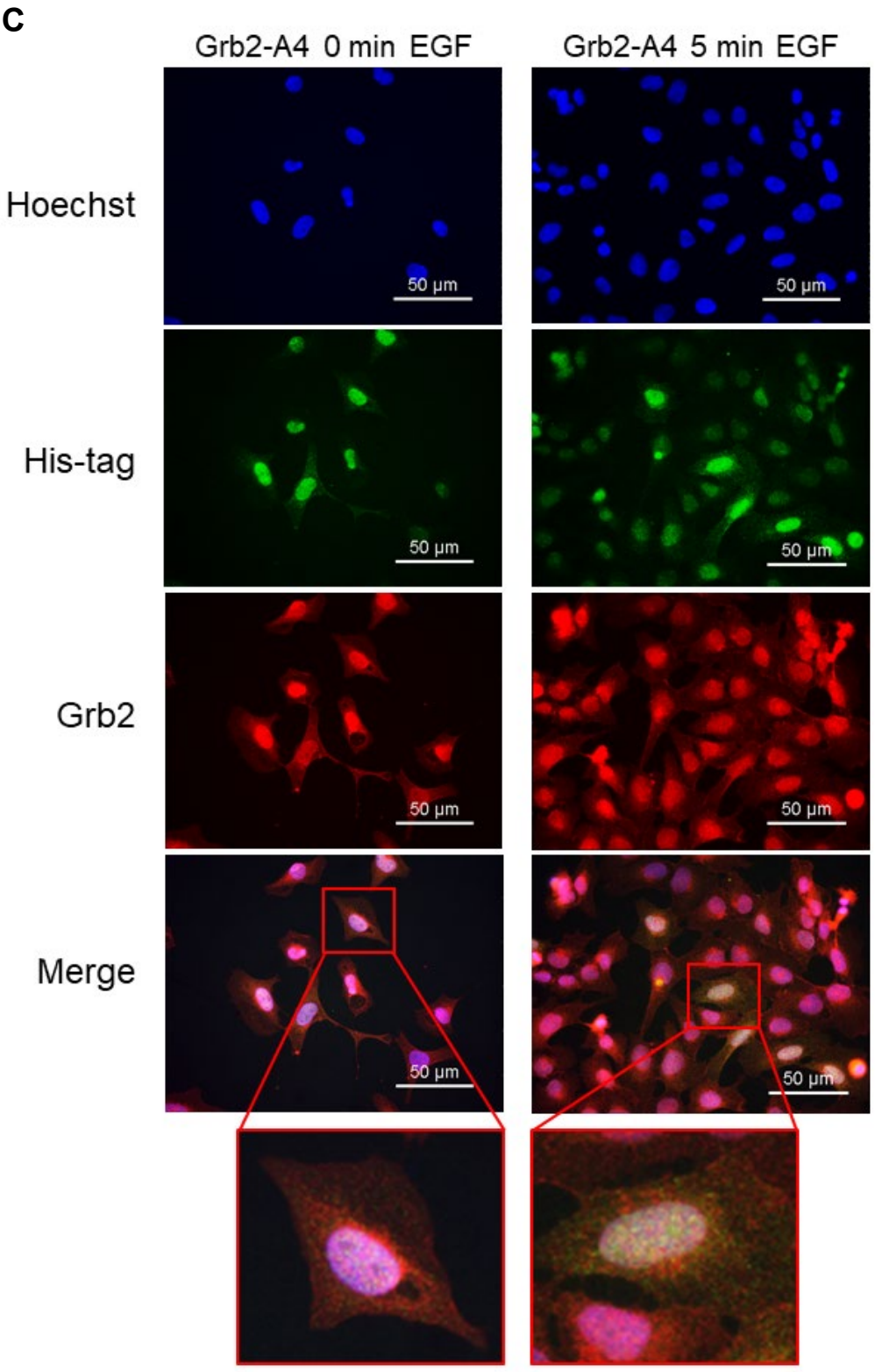
C
Grb2-A4 0 min EGF
Grb2-A4 5 min EGF
Hoechst
His-tag
Grb2
Merge
50 μm

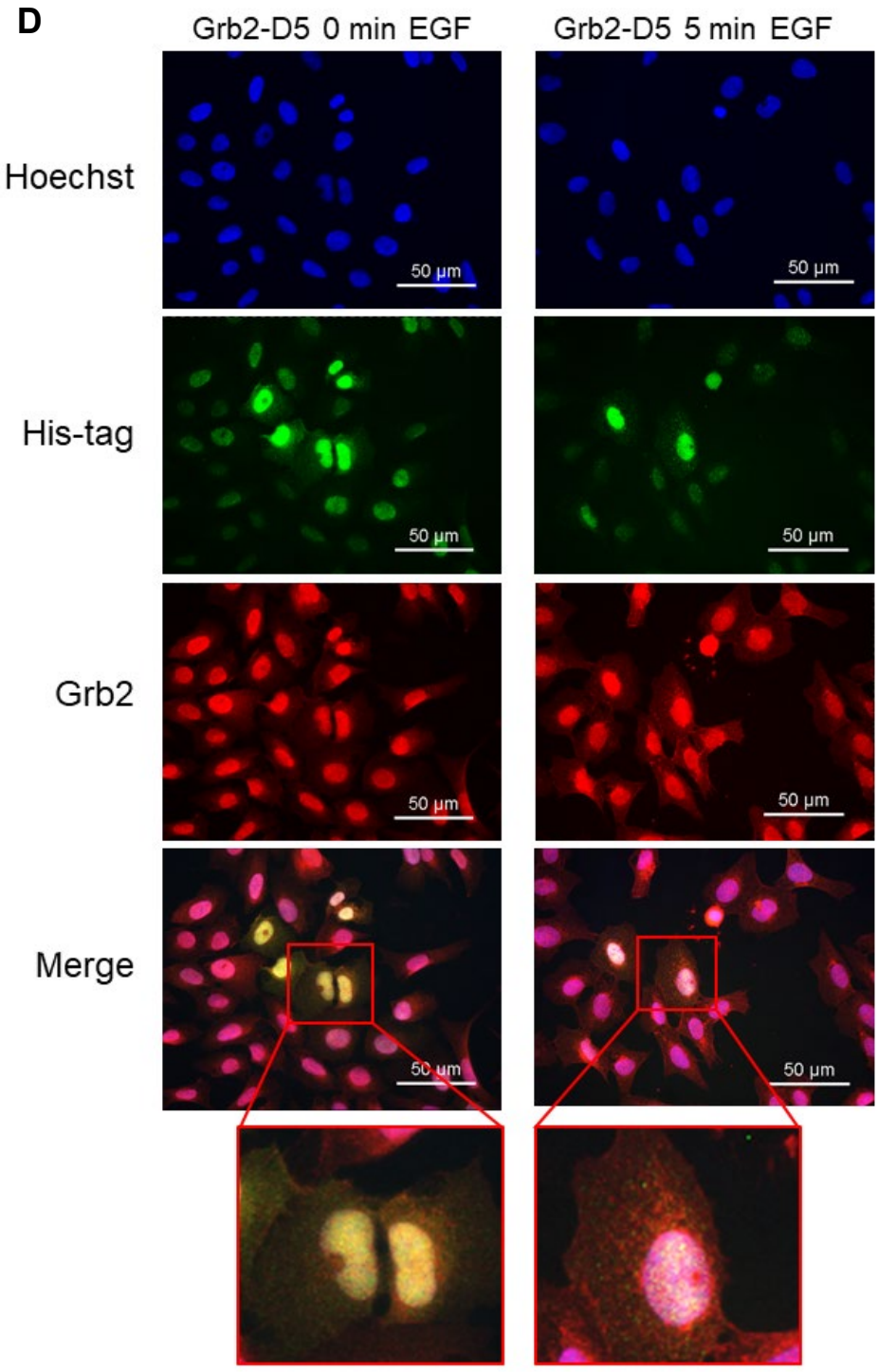

Figure 6.15. Stably expressed His-tagged Grb2 SH2 Affimer proteins show similar staining patterns to Grb2 in U-2 OS cells. *U-2 OS cells stably transduced with Affimer-pBABE vectors were* ***(A)*** *serum-starved or* ***(B)*** *serum-starved and stimulated with 25 ng/ml EGF (5 min). Cells were fixed in 4% PFA and immunofluorescence microscopy was performed. Antibodies against His-tagged Affimer proteins (green) and Grb2 (red) were used, followed by fluorescent species-specific secondary antibodies. Nuclei were stained with Hoechst 33342.* ***(C)*** *and* ***(D)*** *show Grb2-A4 and -D5 expressing cells in closer detail. Cells enlarged in boxes show possible redistribution of Grb2 and Affimer after EGF stimulation. Scale bar = 50µm, images are representative of two independent experiments.*

The levels of expressed Affimer appeared low in comparison to transiently transfected HEK293 stained using the same antibodies and staining protocol (Figure 6.2). Exposure time for detecting the His-tag antibody was greatly increased for the U-2 OS cells and many cells showed a low level of antibody staining, despite continued growth in puromycin-containing media to ensure a transduced cell population. This suggests lower expression levels of the Affimer proteins in these cell lines.

After EGF stimulation, it seemed there could be re-distribution of Grb2 and the Affimer proteins to the cytoplasm, as staining appeared more intense in the nucleus of non-stimulated cells (Figure 6.15A) compared with stimulated cells (Figure 6.15B). However, when examined in greater detail in cells expressing the two Affimer clones that affected signalling, Grb2-A4 and Grb2-D5 (Figure 6.15C and D), it is difficult to determine whether this is indeed the case. Further experiments could include immunofluorescence confocal microscopy using these two Affimer clones, to better observe any re-localisation of Grb2 and the Affimer proteins upon EGF stimulation.

6.11 Discussion

Grb2 SH2-binding Affimer proteins were used in this work to test the potential of the Affimer as a reagent for studying SH2 domain-mediated signalling pathways in intracellular assays. Both transient expression and an inducible stable expression system failed to elicit any substantial effect on the measured endpoint of Grb2 signalling, namely downstream Erk phosphorylation.

Transient transfection of DNA was the technique first used to deliver Grb2 SH2 Affimer proteins into mammalian cells, because it would be a useful tool for other researchers using the Affimer as a SH2 reagent due to its rapidity and compatibility with high-throughput screens (Geisse and Voedisch, 2012; Durocher et al., 2002). Most Grb2 SH2 Affimer-expressing cells did show a statistically significant decrease in p-Erk compared with the control, however this reduction was not very large (Figure 6.1). This was most likely due to the low transfection efficiency of the Affimer-pcDNA5 plasmids, which would have affected western blot results measuring p-Erk levels from the entire cell population. This observed transfection efficiency was lower than expected (Figure 6.2), even though HEK293 cells were chosen for their amenability to

transfection and often high efficiencies (Thomas and Smart, 2005; Molinas et al., 2014). As mentioned previously, the transfection efficiency (ca. 30 – 40%) and the reduction in p-Erk levels in Affimer-expressing cells (ca. 20 – 30%) were similar; suggesting that the Affimer proteins were having a marked effect on Erk phosphorylation in the cells that were successfully transfected.

The transfection protocol could therefore have been further optimised to yield a higher efficiency and this could be a future line of work in the SH2 domain Affimer project. Additionally, staining of p-Erk in immunofluorescence microscopy of transiently transfected cells could be used instead of western blot analysis. This would allow identification of successfully transfected cells by staining for the Affimer His-tag, and any changes in p-Erk levels in these individual cells could be observed and compared to control cells. If a plasmid encoding the Affimer proteins with a fluorescent tag was produced, successfully transduced cells could then even be sorted by fluorescent activated cell sorting (FACS) using flow cytometry to separate cells expressing the tagged Affimer from non-expressing cells (Basu et al., 2010). A limitation of this method is cell viability after sorting however, and FACS can induce oxidative stress in cells which alters cell metabolism (Llufrio et al., 2018).

It was decided instead to use stable expression of DD-tagged Grb2 SH2 Affimer reagents using the pRetroX PTuner system, as this had the benefits of a 100% transduced population and controlled inducible expression for dose-dependent studies. These stably expressed reagents failed to effect Erk phosphorylation (Figure 6.6), perhaps due to the DD tag blocking Affimer-Grb2 SH2 interactions after a co-immunoprecipitation assay showed no evidence of a Grb2:Affimer complex in the lysate (Figure 6.7). It has been noted in a ProteoTuner/Shield1™ protocol that some proteins will not function with a DD fusion to a certain terminus (Hagan et al., 2009). It was suggested in this protocol to either try a fusion to the C-terminus or add a linker sequence to help the protein fold properly. A helical linker peptide sequence was chosen, which had been designed and tested in comparison with other linkers (Arai et al., 2001). In this study, the helical linker peptides showed better separation of two fused GFP variants in a FRET assay than flexible linkers of the same length. The addition of the helical linker between the DD and Affimer sequences still made no difference to p-Erk levels in Affimer-expressing cell lines compared with controls (Figure 6.8). This could be due to

the separation distance of the two proteins not being sufficient to restore binding of the Affimer proteins to their target, although this does seem unlikely. Indeed, the presence of 5 more EAAAK repeats in Affimer D5 conflicts with this theory since the addition of more EAAAK repeats in the linkers results in further separation of the two fused proteins (Arai et al., 2001).

The Grb2 SH2 Affimer constructs in the pBABE vector showed more promising results than the previously tested mammalian expression systems, with two of the four Grb2 SH2 Affimer-expressing cell lines showing a significant reduction in EGF-stimulated Erk phosphorylation (Figure 6.11). Upon 5 minute EGF stimulation, Grb2-A4 and Grb2-D5 U-2 OS cell lines showed an average decrease in p-Erk of 36% and 38%, respectively. Although this reduction in p-Erk was statistically significant, other Grb2 SH2-inhibiting methods described below have shown a larger decrease.

Limited work has been done to quantify the contribution of the SH2 domain alone to Erk phosphorylation and activation, but one such study used dominant negative mutations in the Grb2 SH2 domain to achieve this (Tanaka et al., 1995). In this work, the conserved arginine in the FLVRES binding sequence of the SH2 domain was changed to a lysine residue, rendering the SH2 inactive. This mutant Grb2 sequence was transiently co-transfected with GST-tagged Erk into HEK293T cells. After 48 h, transfected cells were stimulated with 100 ng/ml EGF for 15 min and an *in vitro* kinase assay was performed on lysates to measure Erk activity, using myelin basic protein as the Erk substrate. Quantifying myelin basic protein via SDS-PAGE analysis of samples, they showed a 75 – 94% reduction in Erk activity in the SH2 domain mutant sample compared with the control.

Another Grb2 SH2 domain inhibitor, actinomycin D, showed a dose-dependent decrease in EGF-induced Erk phosphorylation in a NIH3T3-derived cell line (B104-1-1) treated with the compound for 24 h (Kim et al., 1999). The top actinomycin D concentration of 50 nM showed a ca. 50% reduction in p-Erk as quantified by western blot analysis of whole cell lysates.

Although these inhibitors showed a greater effect on downstream Erk phosphorylation than the Grb2 SH2 Affimer reagents, the methods used are not directly comparable, due to the different techniques and systems used. The method used by Tanaka et al. (1995) to determine Grb2 activation of Erk measured a different endpoint than the level of p-Erk; namely the formation of

myelin basic protein in a kinase assay. Additionally, Erk DNA was co-transfected into cells along with the mutant Grb2 DNA, whereas the Affimer-expressing cell lines contained only endogenous Erk.

In fact, recent work in our lab has shown that co-transfection of Affimer DNA in a pCMV6 vector with FLAG-tagged Erk in pCMV6 yields much better inhibition of Erk phosphorylation, when targeting other signalling proteins in the MAPK pathway (data not published). In the study by Kim et al. (1999), the Actinomycin D concentration of 50 nM would have been much higher than the expressed concentration of Affimer. It is possible that the inhibition of Erk phosphorylation seen with the Affimer reagents is concentration dependent, and therefore would be comparable if the reagents were delivered into cells at similar levels to Actinomycin D.

Conversely, previously developed Grb2 SH2 domain inhibitors have been shown to decrease Erk phosphorylation at a comparable level to the Affimer reagents, or have shown no effect on this downstream target at all. A Grb2 SH2 binder has been reported that constituted two clones isolated from a phage-displayed naïve library of a Ubiquitin variant scaffold, fused together in tandem (Leung et al., 2017). This tandem binder was termed Ubv.G2.2-1c and displayed an IC_{50} of 6 nM for the SH2 in a competitive ELISA, as well as pull-down of endogenous Grb2. Transient expression of Ubv.G2.2-1c in HEK293T cells overexpressing the EGFR showed only a 27% decrease in p-Erk upon EGF stimulation, compared with mock-transfected cells. Another Grb2 SH2 antagonist, C90, that showed inhibition of hepatocyte growth factor (HGF)-stimulated migration of PC3M cells did not block HGF-induced phosphorylation of Erk or Akt in the same cell line over the same concentration range (30 – 300 nmol/L), although this work targeted a different RTK than the EGFR (Giubellino et al., 2007).

The Grb2 SH2 Affimer binders in this work have demonstrated that Affimer proteins can be used to disrupt SH2 domain signalling in an intracellular environment. The reduction of Grb2 SH2 signalling, although not a complete abolition, was comparable to some other previously generated Grb2 SH2 inhibitors. The expression system or delivery of the Affimer needs to be optimised to achieve better inhibition of future targeted SH2s; in particular for the Grb2 SH2 studies, the effect of Grb2 and Affimer nuclear localisation needs to be further explored and expression patterns observed in alternative cell lines.

However, this work has demonstrated the potential of Affimer proteins as SH2 domain reagents. If used in phenotypic assays of specific cancer cell lines, these could help elucidate the role of less-studied SH2 domains in different cancer pathways.

Chapter 7

Discussion and future perspectives

Chapter 7

Discussion and future perspectives

This work investigated the suitability of a non-antibody binding protein, the Affimer, as a SH2 domain-binding reagent for use in research. There is a need for novel SH2-binding research tools, as there is still a lack of protein-specific reagents available; particularly for use in intracellular functional assays (Gay et al., 1999, Sjoberg et al., 2012). Development of new SH2 domain binders would further our understanding of SH2-mediated interactions and their role in disease. Affimer reagents were successfully raised against 38 of the 43 SH2s utilised in this project. Using the Grb2 SH2 as a target for proof-of-principle studies, it has been demonstrated that Affimer reagents can bind and inhibit the phosphotyrosine-binding site of their target SH2 in *in vitro* applications. They are also able to disrupt signalling of the domain in mammalian cell-based assays. Additionally, it was revealed that highly specific Affimer clones can be isolated against SH2 domains, which is essential for the success of an SH2-binding reagent. Of the set of 43 SH2 domains, specific Affimer binders were identified against 22 of these targets. The sequence analysis of the Affimer variable regions (Chapter 4) coupled with the specificity microarray results (Chapter 5) will provide interesting insights into which peptide sequences could confer specificity for certain SH2 domains.

7.1 SH2 domain production & preparation

An important observation from the present work was the effect of SH2 domain production quality on various Affimer validation assays. Many other studies aiming to isolate SH2 domain binders have stressed the importance of high quality target proteins (Colwill et al., 2011, Pershad et al., 2010). The repeated phage display screens for Lck, Nck2, Src1 and Syk-N demonstrated this, as the single difference from the original screens was the production of fresh target proteins; indicating the failure of previous screens was due to SH2 sample preparation.

The work in Chapter 5 also highlighted that SH2 domain target preparation was critical for successful microarray analysis. There was some variability in results

between microarray repeats for a selection of Affimer reagents (such as Grb10-D9). This was most likely due to SH2 target preparation and immobilisation rather than Affimer protein preparation, because any disparities in results tended to occur for all Affimer reagents against a particular target.

For example, no binding of any PLCγ2-N reagents was observed in experimental repeat 2, whilst binding occurred in other experimental repeats. As discussed, whilst most clones deemed 'non-binding' in the microarray also exhibited similar results in a purified protein ELISA, a few binders revealed discrepancies between the two methods. In particular, all 3 p85α-C Affimer reagents showed binding to their target in ELISA, when no detectable binding was measured in the microarray. This indicates that the microarray format is not compatible with all targets. Therefore, although the microarray is a useful tool for rapid, high through-put screening of large numbers of Affimers, it is recommended to validate results by testing a number of negative hits via an alternative format such as ELISA.

7.2 Grb2-D5 dimerisation

The dimerisation of Affimer Grb2-D5 was an interesting result throughout the project. Stable dimerisation appeared to be observed when D5 was produced from the pET11a vector, but from no other vectors used in the project. However, these other vectors either produced different Affimer constructs containing varying C-terminal tags, or the proteins were produced in the intracellular environment which is not a comparable system to recombinant production in *E. coli*.

As discussed in Chapter 5, possible secondary structure in the Grb2-D5 pET11a vector was observed in the region encoding the C-terminus of the Affimer scaffold and the C-terminal His-tag, but no duplication of the Affimer sequence was seen. Dimerisation has been previously observed in ubiquitin-binding Affimer reagents (Michel et al., 2017) through a strand swap of the last β strand in the 2nd VR; a region that differed greatly in Grb2-D5 compared with other Affimer binders, due to a truncated VR and scaffold sequence. The presence of the C-terminal HA tag in the protein produced from pET-lectra was therefore thought to disrupt monomer interactions via this region, preventing dimerisation.

The dimerised ubiquitin Affimer proteins displayed superior binding properties to their monomeric counterparts (Michel et al., 2017). This is largely in accordance with results for Grb2-D5. The monomeric Grb2-D5 used in microarrays displayed only weak or no binding to the Grb2 SH2. This conflicted results from other *in vitro* assays utilising dimeric Grb2-D5; such as immunoprecipitation where this clone consistently captured higher levels of Grb2 than other binders, or in fluorescence polarisation where it displaced a high affinity phosphopeptide from the Grb2 SH2.

When produced from mammalian expression vectors pcDNA, pRetroX-PTuner and pBABE, Grb2-D5 also appeared monomeric. However, the Grb2-D5 protein produced from pBABE did show a significant reduction in Grb2-mediated Erk phosphorylation in U-2 OS cells, suggesting this protein was still able to bind to the Grb2 SH2 potently enough to hinder its signalling. This construct contained a HA-tag, as in the microarray, although the intracellular milieu is a vastly different environment to *in vitro* assays and therefore the performances of Grb2-D5 between the two cannot be directly compared.

In order to determine whether dimerisation of Grb2-D5 affects its ability to bind to its target, binding affinities for both the monomeric and dimeric Grb2-D5 need to be measured and compared. In addition, structural data on the Grb2-D5 dimer would provide intriguing insights into the mode of dimerisation.

7.3 Comparison to other SH2 binding reagent studies

7.3.1 SH2-binding antibody fragments

There has been great interest in the scientific community of generating protein-specific renewable binding reagents against the entire human proteome (Taussig et al., 2007, Berglund et al., 2008, Uhlen et al., 2008, Stoevesandt and Taussig, 2012). High-throughput methods to generate and validate these affinity reagents are imperative to achieving this task and are still in need of significant development. As discussed in Chapters 4 and 5, a comparable study to the work in this thesis was the multicentre effort to raise and validate antibody binders against SH2 domains (Colwill et al., 2011, Pershad et al., 2010, Sjoberg et al., 2012). This was initiated as a pilot study to assess whether systematic coverage of the human proteome using antibodies and their fragments could be achieved.

This was by far the largest project on SH2 domain binders in the literature in terms of the number of reagents generated, although the set of targets consisted of only 20 domains.

The project isolated binders with exceptional specificity and low nanomolar affinities (Colwill et al., 2011, Pershad et al., 2010). Successful use immunofluorescence was also demonstrated with a Shc1 SH2-targeting scFv. Additionally, the ability of scFvs to recognise their denatured targets in immunoblotting, as both purified domains and within the full-length protein, was shown (Pershad et al., 2010, Mersmann et al., 2010). This attribute was not tested in the Affimer reagents. Although the recognition of native folded domains by Affimer binders was more important for their eventual use in functional cell-based assays, detection of denatured target is still a useful property as it enables their application in immunoblotting. Many of the SH2-binding antibody fragments tested in immunoprecipitation assays failed to capture endogenous target, however; including binders against the Grb2 SH2 domain (Colwill et al., 2011). The Affimer reagents proved superior in this area, as 14 of 16 binders tested consistently pulled out endogenous Grb2 from cell lysate.

The collaborative effort described by Colwill et al. (2011) identified 340 unique antibody fragments, although this was the result of 4 laboratories working together to screen 6,972 clones which yielded 1,788 hits in ELISA. The phage display screening detailed in this thesis was the work of 2 individuals and yielded 622 unique clones from screening 2,136 and sequencing 1,393 hits in ELISA. Both of these studies exemplify the need to screen large quantities of reagents in a high-throughput manner in order to successfully generate SH2 binders, but the results from the Affimer library demonstrated a higher hit rate in initial ELISA validation. This increased efficiency shows that use of the Affimer library reduces the quantity of screened clones needed to achieve the same end result.

In addition, the screening process of the Affimer library was extremely rapid, with completion achieved in less than 2 weeks including phage ELISA validation. In this work, 32 targets were screened simultaneously; demonstrating the potential for the high-throughput isolation of Affimer binders. The Affimer could therefore be a valuable addition to any proteome-wide effort for generating affinity reagents, and could be used in conjunction with antibody fragments and other non-antibody scaffolds to accomplish this goal.

7.3.2 SH2-targeting monobodies

The only other non-antibody scaffold tested as SH2 domain reagents has been the monobody (Sha et al., 2013, Wojcik et al., 2010, Kukenshoner et al., 2017). Monobodies against Abl, SHP2 and Src family kinase SH2s have been reported; 8 SH2 domains in total. These binders have shown successful capture of endogenous target from cell lysates, displacement of phosphopeptides in fluorescence polarisation and high levels of selectivity in SH2 protein microarrays. However, the Abl monobody HA4 could not distinguish between the Abl1 or Abl2 domains and exhibited detectable interactions with at least 15 other SH2s (Wojcik et al., 2010). Furthermore, the binders against Src family SH2s were not protein-specific, showing only selectivity between SrcA and SrcB subgroups (Kukenshoner et al., 2017). Certain Affimer reagents against the same targets exceeded the specificity of these monobodies.

One area in which monobodies have arguably surpassed Affimer reagents when targeting SH2 domains has been their efficacy in cell-based assays, with some studies resulting in the discovery of novel sites for target inhibition (Spencer-Smith et al., 2017). Monobodies against both SHP2 SH2 domains demonstrated almost complete abolition of downstream ERK phosphorylation in a lung cancer cell line (Sha et al., 2013); a feat not yet accomplished by Grb2 SH2 Affimer reagents in U-2 OS cells. Monobodies targeting the Abl SH2 domain at both the phosphotyrosine-binding site and the SH2-kinase interface have also both shown potent inhibition of Bcr-Abl activation in cells, as well as induction of apoptosis in a chronic myelogenous leukaemia cell line (Grebien et al., 2011, Wojcik et al., 2010).

However, it is worth noting that disruption of the SH2-kinase interface with monobody 7c12 was originally accomplished only after fusion to another monobody, as 7c12 was not potent enough alone (Grebien et al., 2011). Disruption of this interaction in cells was finally achieved with single reagents, after the screening of a newly designed monobody library (Koide et al., 2012, Wojcik et al., 2016). As discussed in Chapter 6, two Grb2 SH2 Affimer reagents did show a reduction of ca. 36 – 38% in Grb2-mediated ERK phosphorylation, but the expression system or delivery of the Affimer requires optimisation to achieve more potent inhibition of SH2s. Optimisation of transient transfection in particular would be particularly valuable; a robust transient expression system

for SH2-targeting Affimer reagents would be useful tool for researchers, with the potential for high-throughput screening of cancer cell lines (Geisse and Voedisch, 2012, Durocher et al., 2002).

It is notable that the results in the present work were achieved without 1) negative selection against related SH2 domains during phage display screening or 2) affinity maturation of binders. Affinity maturation is a process used to improve the binding affinity of protein binders, through additional cycles of mutagenesis and selection (Colwill et al., 2011). This strategy was utilised for some of the Fab and scFv fragments against SH2 domains, as well as the monobody binders (Colwill et al., 2011, Wojcik et al., 2016, Sha et al., 2013). None of these studies used negative selection during screening however; and similar to the Affimer reagents, antibody fragments were still able to distinguish between highly homologous family members such as the Abl1 and Abl2 domains (Pershad et al., 2010).

7.4 Continuation of the project & future applications

7.4.1 Structural characterisation of SH2-Affimer interactions

The data gathered in this thesis could be expanded and improved upon in several ways. Firstly, there is a lack of structural characterisation data in this project which has been present in other studies on SH2 domain binding reagents; namely all the SH2-targeting monobodies (Wojcik et al., 2010, Sha et al., 2013, Kukenshoner et al., 2017). Determining the mode of binding of the Grb2 SH2 Affimer reagents via crystallisation of the Affimer-SH2 complex would have added important structural information to this project. Co-crystallisation of the SH2 with several Affimer reagents was attempted by the Oxford Protein Production Facility; however, this has been unsuccessful to date.

The continuation of the SH2 domain Affimer project is focusing on this goal, and crystallisation trials of Grb2 SH2-Affimer complexes are currently underway. It will be very interesting to gain such insight into the binding of these Affimer reagents, for comparison to previously isolated Grb2 SH2 inhibitors and identification of any residues that could have conferred specificity of clones in the microarray. In several other Affimer projects, reagents have successfully co-crystallised with their target; such as FcγRIIIa, SUMO-1, SUMO-2 and ubiquitin

binding Affimer reagents (Robinson et al., 2017, Hughes et al., 2018, Michel et al., 2017). As exhibited by these and by monobody studies, unexpected or unusual binding modes of reagents can be revealed by determining the crystal structures of binder-target complexes.

For example, the SHP2 SH2 Monobodies were shown to bind occupy the phosphotyrosine-binding pockets of their targets, making contacts with residues that differed between SHP1 and SHP2 which explained their specificity for SHP2. Surprisingly however, the segments of the reagents that bound within the phosphopeptide-binding site ran in the opposite direction to that of phosphopeptides and other SH2 monobodies, revealing a novel binding mechanism of inhibitors (Sha et al., 2013). Affimer reagents have previously been co-crystallised with various targets, which has also revealed allosteric modes of inhibition and provided explanations for binding specificity (Robinson et al., 2018, Michel et al., 2017).

Another method for gathering information on Affimer-SH2 interactions would be site-directed mutagenesis of the variable regions, through techniques such as alanine-scanning (Weiss et al., 2000). Mutagenesis of specific residues within binding peptides has proven invaluable in probing the contributions individual amino acid sidechains in an interaction. Alanine-scanning mutagenesis is a method of systematic alanine substitution of residues; replacement of a residue with alanine removes all sidechain atoms past the β-carbon. This allows the role of sidechain groups at specific positions to be deduced (Morrison and Weiss, 2001). Alanine lacks unusual backbone dihedral angle preferences; unlike glycine for example, which would also nullify the sidechain, but can introduce conformational flexibility into the backbone of the protein (Morrison and Weiss, 2001).

The alanine-scanning method has been utilised in other Affimer projects to establish the importance of each variable region in a reagent to the binding of a target, as well as the contribution of individual residues within the regions (data not published). Testing the alanine mutants of the Grb2 SH2 Affimer binders in the fluorescent polarisation assay would determine which residues are important in binding of the phosphotyrosine binding site and consequent Grb2 SH2 inhibition.

Once structural data of a protein-peptide complex has been obtained, inhibitory binders may also act as lead structures for drug development. Structural data helps to refine the existing binding reagent, or design novel binding peptides (Helmer and Schmitz, 2016). The information from structural studies can give a more detailed understanding of the interaction surface, identifying novel binding motifs and binding interfaces that can be exploited in future inhibitor design (Kyle et al., 2015). This concept has been explored using Affimer reagents targeting the HIF-1α/p300 interface (Kyle et al., 2015). Hypoxia-inducible factor 1 (HIF-1) is a transcription factor associated with poor prognosis in cancer patients. Complex formation with its transcriptional coactivator protein, p300, leads to activation of several processes including cell proliferation and survival.

A p300-binding Affimer (Ad34) was crystallised, and the binding mode investigated by *in silico* docking against the NMR structure of p300. This was used in conjunction with protein NMR spectroscopy of p300 in complex with a high affinity peptide to provide detailed information on the p300 binding interface. This work identified novel binding motifs and binding surface regions of p300, which could be used to inform the design of future inhibitors.

In this way, mimicking the variable regions of highly specific SH2 Affimer reagents in a small molecule or peptide could result in the development of inhibitors that specifically and potently target SH2 domains.

7.4.2 Use of Affimer reagents in functional cell-based assays

The chief intended use for SH2 Affimer reagents was the specific inhibition of SH2 interactions in cells and investigation of the biological consequences, to discover novel functions of SH2 domains. Grb2-A4 and D5 showed promise of the reagents in this area; but the system for intracellular Affimer expression needs to be improved. As discussed in Chapter 6, recent work in our group has shown improved results in cell-based assays when using co-transfection of Affimer DNA in pCMV6 vectors with FLAG-tagged Erk in a pCMV6 vector, compared with the pBABE expression system tested in this work (data not published). This strategy has been utilised for Affimer reagents targeting other signalling proteins within the MAPK pathway and thus holds much promise for Grb2 SH2 binders. Future work on the SH2 domain Affimer project could therefore adopt this expression system for intracellular assays.

Once a robust mammalian expression system for Affimer reagents has been established, a potential application for them would be a screening tool to determine the importance of each SH2 domain in different cancers. SH2-targeting Affimer DNA could be transfected in various cancer cell lines in a high-throughput manner, much like siRNA screens are used to study protein function and the contribution of individual proteins to cancer phenotypes (Williams et al., 2017, Krausz, 2007, Mohr et al., 2014). These siRNA screens have become a powerful tool to systematically explore the effects of genome-wide gene silencing on phenotypes, resulting in the discovery of new cellular pathways and potential drug targets (Sharma and Rao, 2009, Mohr et al., 2014). Affimer reagents could likewise be used to systematically knock down function of specific domains of protein families such as the SH2-domain containing proteins.

In addition to highly specific SH2 Affimer reagents, cross-reactive clones could also be valuable tools in this use. Observing the cumulative effect of inhibiting two, three, or even more SH2 domains could also lead to the discovery of SH2s that need to be targeted simultaneously to modulate disease phenotypes. Targeting multiple proteins is emerging as a potentially beneficial cancer therapy, as drug resistance is more likely to develop with specific targeting of a single protein or signalling pathway (Petrelli and Giordano, 2008).

Another strategy currently being employed in the continuation of this project is not direct cellular inhibition of SH2 domains, but their targeted degradation. A technique to rapidly degrade endogenous proteins in mammalian cells without modification of the genome has recently been described (Clift et al., 2017). Titled Trim-Away, this method utilises the endogenous cellular degradation machinery to selectively remove unmodified proteins. TRIM21 is an E3 ubiquitin ligase that binds with high affinity to the Fc-domain of antibodies (James et al., 2007). TRIM21 recruits the ubiquitin-proteasome system to antibody-bound targets during infection, leading to their degradation. Trim-away uses a 3-step process; the introduction of exogenous TRIM21, the introduction of an antibody against the protein of interest, and finally TRIM21-mediated ubiquitination and degradation of the antibody-bound protein.

The rapidity of this application also minimises the activation of compensatory mechanisms that may mask a phenotype. This method requires only the specific binding of the target protein, not necessarily in the active site which is required

for inhibition. Fusion of a nanobody to the Fc-domain has already been performed and utilised in this system. An anti-GFP nanobody fused to the Fc showed degradation of GFP-tagged Histone H2B in the nucleus (Clift et al., 2017).

Affimer-Fc fusions could therefore also be used to rapidly degrade SH2 domain-containing proteins; although the major drawback with this approach is that it would not allow study of SH2 domain-specific interactions, but rather the domain-containing protein as a whole. This is still a potentially very useful tool for the study of cancer signalling pathways. As with other cell-based assays, the specificity of the Affimer is key; to avoid any off-target effects caused by degradation of other proteins, only binders which showed protein-specific binding in the microarray should be utilised in this system.

7.4.3 SH2-binding Affimer reagents in protein expression profiling of cancer cells

An exciting potential application for the SH2 Affimer reagents is their use in a microarray for screening of SH2-containing proteins in both normal and diseased tissue samples. This array technique has been reported with antibody binders, and has allowed better understanding of changes in protein expression associated with diseases including cancer (Haab, 2005, Hoheisel et al., 2013, Alhamdani et al., 2012).

In this method, antibodies (or other binding reagents) are arrayed on a solid support such as a glass slide. The relevant protein mix is then isolated and labelled, usually with a fluorescent dye, and incubated with the array. Captured antigens are then detected using the fluorescent label and the signal intensities provide information on the level of expressed protein within the sample. Simultaneous incubation of samples labelled with different dyes is also possible; although the quality of results produced with this approach is under contention (Hoheisel et al., 2013). Use of antibody arrays on several sample types have been reported in cancer research, including serum; plasma; cell culture supernatants; tissue culture lysates; and resected tumour specimens (Haab, 2005).

A microarray containing 810 spotted antibodies targeting 741 cancer-related proteins has been successfully used to analyse the cellular proteomes of 24

pancreatic cancer cell lines and 2 controls (Alhamdani et al., 2012). This analysis detected 72 disease markers that had not been previously described, as well as allowing the identification of the tumour source (primary tumour, liver metastases, or ascites). In addition, comparison of cells with different degrees of differentiation (well, moderately, or poorly differentiated) resulted in unique marker sets for each differentiation category.

In another study, microarrays displaying 83 different antibodies were used on proteins extracted from resected tumour tissue (Tannapfel et al., 2003). Proteins from 30 hepatocellular carcinoma tumours and 15 normal liver samples were analysed. Thirty-two of the isolated proteins showed differential expression between the tumour and control groups, with expression level results confirmed by western blot analysis. Two proteins, cyclin D1 and suppressor of cytokine signalling 1, showed an association with tumour prognosis. This work resulted in the identification of new proteins associated with carcinogenesis or prognosis in hepatocellular carcinoma.

SH2 domain Affimer reagents could be used in this same application; they have already shown their ability to function in a protein microarray, and can be easily labelled or tagged for immobilisation on an array surface. This application would provide researchers studying SH2 signalling in cancer with information about their expression profiles in cancer subtypes. It could also help to identify which cancers may be more responsive to SH2 domain inhibition as a treatment strategy. However, if this utility of the reagents was pursued, it would be beneficial to isolate specific Affimer reagents to all known SH2 domains, in order to establish a more comprehensive array.

Although the number of SH2 domains successfully targeted in the current work exceeds that of other renewable binding reagent studies, it has still only encompassed roughly one third of known SH2 domains. Therefore, the continuation of this project could also focus on the isolation of Affimer reagents to the rest of the SH2 domain family, and testing their specificity.

7.4.4 SH2 Affimer reagents themselves as therapeutics

Affimer reagents being utilised as therapeutics themselves is also a future possibility; other biologics such as monoclonal antibodies have already been developed as cancer therapeutics and are a rapidly growing class of drugs (Sliwkowski and Mellman, 2013). The high specificity of antibodies in particular

is a favourable quality for the selective targeting of cancer cells (Wold et al., 2016). There are currently over 17 FDA-approved monoclonal antibodies for the treatment of cancer (Wold et al., 2016).

These antibodies are mostly directed to cell-surface antigens and operate by recruiting the immune system to attack the cells they bind. Many additionally function through specific inhibition of targets; such as growth factor receptors. By targeting these receptors, potent inhibition of growth signalling is achieved (Wold et al., 2016). Another approach is to use antibodies to deliver drugs directly to tumours. The antibody is conjugated to a cytotoxic compound, so after it binds the cancer cell and is internalised, the drug is released and causes cell death (Sliwkowski and Mellman, 2013).

If SH2-targeting Affimer reagents were also to be used as therapeutics in this way, an efficient system for their intracellular delivery would need to be developed however. Biologics face several challenges not encountered by small molecule drugs; chiefly, efficient delivery. Due to their size, macromolecules such as peptides and proteins are unable to cross the cell membrane (Walker et al., 2017). Several strategies have been developed to overcome this problem; including the use of biodegradable polymersomes, liposomes, and cell-penetrating peptides (Anajafi and Mallik, 2015, Lönn et al., 2016).

Polymersomes are stable vesicles prepared from amphiphilic polymers, which can be used for drug encapsulation. Polymersome functionalisation can be carried out using proteins or peptides that bind cell-surface targets, to direct them to tumours for biologic release (Pourtau et al., 2013). To enhance the drug's bioavailability, polymersomes can also be engineered to become stimuli-responsive; enabling the controlled release of a drug only upon stimulation (Anajafi and Mallik, 2015).

Conjugation to a cell-penetrating peptide promotes the uptake of a biologic by endocytosis (Ziegler et al., 2005). The discovery of a cationic delivery peptide derived from the human immunodeficiency virus (HIV-1) protein, trans-activator of transcription (TAT), led to the use of this and other cell-penetrating peptides in drug delivery. Covalent linking of these peptides allows the conjugated macromolecule to traverse the cell membrane (Ziegler et al., 2005).

Despite these advances in intracellular delivery of proteins, it remains a challenging task for any new biologic therapy. In addition, the immunogenicity of

biologics is also a hurdle to overcome (Garcês and Demengeot, 2018). Both Type I and Type II Affimer scaffolds have shown low immunogenicity in an industry standard study, using an *in vitro* immune cell assay (Avacta® Life Sciences, 2017). Peripheral blood mononuclear cell samples were collected from 50 human donors, and incubated with 50 µg/ml Affimer samples for 7 days. Activation and proliferation of these cells was then measured to assess immune cell stimulation by the reagents. Both Type I and Type II scaffolds elicited a low immunogenic response, comparable to that of the therapeutic antibody Avastin®, which was tested alongside as a negative control (Avacta® Life Sciences, 2017). Although this study indicates there are no fundamental immunogenicity issues with the scaffold, and the addition of a cell-penetrating peptide or encapsulation in polymersomes are potential methods for the intracellular delivery of Affimer reagents, their use as therapies themselves in SH2-mediated diseases is still a distant prospect.

7.5 Conclusions

Affimer binders have shown great promise for use as SH2 domain research reagents. Grb2 SH2 Affimers displayed good potential in proof-of-principle studies, with preliminary characterisation data indicating low nanomolar binding affinities, the ability to capture endogenous full-length protein from mammalian cell lysate, and competition for the SH2 active site with phosphorylated substrates. The rapid process of screening the Affimer library combined with the ease of screening multiple targets at once, results in a cost-effective method of generating research tools to large protein families such as SH2 domains.

Arguably the most important feature of a successful SH2 domain reagent is high specificity; a quality difficult to achieve due to the structural and sequence homology of the domains. Some of the reagents raised in this work were highly specific, discriminating between proteins with pairwise sequence identities of up to 90%. Specific clones were isolated for over 50% of the SH2 targets used in this study. Although the subset of SH2s in this study totalled only one third of the SH2 domain family, this is still the largest number successfully targeted by a singular reagent.

The variable region sequencing analysis combined with the specificity microarray data can now provide insight into which motifs confer binding specificity for

individual SH2s. With the addition of structural data, this will inform the design of future specific reagents and inhibitors. Next, successful inhibition of the SH2 domain targets need to be tested in functional cell-based assays. Although a more robust expression or delivery system is desirable for these reagents, their specificity holds great potential for their use in functional cell-based assays to discover new roles of SH2 domain signalling in disease.

In most of the areas tested, SH2-binding Affimer reagents have shown comparable or superior qualities to other SH2-targeting binding reagents. The use of the Affimer in conjunction with antibody fragments and other non-immunoglobulin scaffolds could result in the generation of specific renewable affinity reagents against the complete SH2 domain family; and eventually the entire human proteome.

References

References

Ahmed, Z., Timsah, Z., Suen, K.M., Cook, N.P., Lee, G.R.t., Lin, C.C., Gagea, M., Marti, A.A. and Ladbury, J.E. 2015. Grb2 monomer-dimer equilibrium determines normal versus oncogenic function. *Nature Communications.* **6**, p7354.

Alhamdani, M.S., Youns, M., Buchholz, M., Gress, T.M., Beckers, M.C., Marechal, D., Bauer, A., Schroder, C. and Hoheisel, J.D. 2012. Immunoassay-based proteome profiling of 24 pancreatic cancer cell lines. *Journal of Proteomics.* **75**(12), pp.3747-3759.

Ali, K., Southwell, A.L., Bugg, C.W., Ko, J.C. and Patterson, P.H. 2011. Recombinant Intrabodies as Molecular Tools and Potential Therapeutics for Huntington's Disease. In: Lo, D.C. and Hughes, R.E. eds *Frontiers in Neuroscience.* Boca Raton (FL): CRC Press/Taylor & Francis Llc.

Amstutz, P., Binz, H.K., Parizek, P., Stumpp, M.T., Kohl, A., Grutter, M.G., Forrer, P. and Pluckthun, A. 2005. Intracellular kinase inhibitors selected from combinatorial libraries of designed ankyrin repeat proteins. *Journal of Biological Chemistry.* **280**(26), pp.24715-24722.

Anajafi, T. and Mallik, S. 2015. Polymersome-based drug-delivery strategies for cancer therapeutics. *Therapeutic Delivery.* **6**(4), pp.521-534.

Angenendt, P. 2005. Progress in protein and antibody microarray technology. *Drug Discovery Today.* **10**(7), pp.503-511.

Arai, R., Ueda, H., Kitayama, A., Kamiya, N. and Nagamune, T. 2001. Design of the linkers which effectively separate domains of a bifunctional fusion protein. *Protein Engineering.* **14**(8), pp.529-532.

Arkin, M.R., Glicksman, M.A., Fu, H., Havel, J.J. and Du, Y. 2004. Inhibition of Protein-Protein Interactions: Non-Cellular Assay Formats. In: Sittampalam, G.S., et al. eds. *Assay Guidance Manual.* Bethesda MD.

Bakail, M. and Ochsenbein, F. 2016. Targeting protein–protein interactions, a wide open field for drug design. *Comptes Rendus Chimie.* **19**(1-2), pp.19-27.

Balboni, I., Limb, C., Tenenbaum, J.D. and Utz, P.J. 2008. Evaluation of microarray surfaces and arraying parameters for autoantibody profiling. *Proteomics.* **8**(17), pp.3443-3449.

Banaszynski, L.A., Chen, L.C., Maynard-Smith, L.A., Ooi, A.G. and Wandless,

T.J. 2006. A rapid, reversible, and tunable method to regulate protein function in living cells using synthetic small molecules. *Cell.* **126**(5), pp.995-1004.

Barbulovic-Nad, I., Lucente, M., Sun, Y., Zhang, M., Wheeler, A.R. and Bussmann, M. 2006. Bio-microarray fabrication techniques--a review. *Critical Reviews in Biotechnology.* **26**(4), pp.237-259.

Barendt, P.A. and Sarkar, C.A. 2009. Cell-free display systems for protein engineering. In: Park, S.J. and Cochran, J.R. eds. *Protein Engineering and Design.* CRC Press, pp.51 - 83.

Bazan, J., Calkosinski, I. and Gamian, A. 2012. Phage display--a powerful technique for immunotherapy: 1. Introduction and potential of therapeutic applications. *Human Vaccines & Immunotherapeutics.* **8**(12), pp.1817-1828.

Beckett, D., Kovaleva, E. and Schatz, P.J. 1999. A minimal peptide substrate in biotin holoenzyme synthetase-catalyzed biotinylation. *Protein Science.* **8**(4), pp.921-929.

Benfield, A.P., Whiddon, B.B., Clements, J.H. and Martin, S.F. 2007. Structural and energetic aspects of Grb2-SH2 domain-swapping. *Archives of Biochemistry and Biophysics.* **462**(1), pp.47-53.

Belov, A.A., and Mohammadi, M. 2012. Grb2, a Double-Edged Sword of Receptor Tyrosine Kinase Signaling. *Science Signaling*. **5**(249): pe49.

Berglund, L., Bjorling, E., Oksvold, P., Fagerberg, L., Asplund, A., Szigyarto, C.A., Persson, A., Ottosson, J., Wernerus, H., Nilsson, P., Lundberg, E., Sivertsson, A., Navani, S., Wester, K., Kampf, C., Hober, S., Ponten, F. and Uhlen, M. 2008. A genecentric Human Protein Atlas for expression profiles based on antibodies. *Molecular Cell Proteomics.* **7**(10), pp.2019-2027.

Binz, H.K., Amstutz, P. and Pluckthun, A. 2005. Engineering novel binding proteins from nonimmunoglobulin domains. *Nature Biotechnology.* **23**(10), pp.1257-1268.

Binz, H.K. and Pluckthun, A. 2005. Engineered proteins as specific binding reagents. *Current Opinion in Biotechnology.* **16**, pp.459-469.

Bradshaw, J.M. and Waksman, G. 1999. Calorimetric examination of high-affinity Src SH2 domain-tyrosyl phosphopeptide binding: dissection of the phosphopeptide sequence specificity and coupling energetics. *Biochemistry.* **38**(16), pp.5147-5154.

Bruhns, P., Vely, F., Malbec, O., Fridman, W.H., Vivier, E. and Daeron, M. 2000.

Molecular basis of the recruitment of the SH2 domain-containing inositol 5-phosphatases SHIP1 and SHIP2 by fcgamma RIIB. *Journal of Biological Chemistry.* **275**(48), pp.37357-37364.

Buettner, R., Mora, L.B. and Jove, R. 2002. Activated STAT signaling in human tumors provides novel molecular targets for therapeutic intervention. *Clinical Cancer Research.* **8**(4), pp.945-954.

Bukowska, M.A. and Grutter, M.G. 2013. New concepts and aids to facilitate crystallization. *Current Opinion in Structural Biology.* **23**(3), pp.409-416.

Campbell, S.J. and Jackson, R.M. 2003. Diversity in the SH2 domain family phosphotyrosyl peptide binding site. *Protein Engineering.* **16**(3), pp.217-227.

Cao, T. and Heng, B.C. 2005. Intracellular antibodies (intrabodies) versus RNA interference for therapeutic applications. *Annals of Clinical & Laboratory Science.* **35**(3), pp.227-229.

Carter, P.J. 2011. Introduction to current and future protein therapeutics: a protein engineering perspective. *Experimental Cell Research.* **317**(9), pp.1261-1269.

Chandhanayingyong, C., Kim, Y., Staples, J.R., Hahn, C., and Youngin Lee, F. 2012. *Sarcoma.* **2012**, 404810.

Chang Ming Li, Hua Dong, Qin Zhou and H.Goh, K. 2008. Biochips – fundamentals and applications. In: Xueji Zhang, et al. eds. *Electrochemical Sensors, Biosensors and their Biomedical Applications.* Elsevier, pp.307-383.

Chen, C.H., Martin, V.A., Gorenstein, N.M., Geahlen, R.L. and Post, C.B. 2011. Two closely spaced tyrosines regulate NFAT signaling in B cells via Syk association with Vav. *Molecular Cell Biology.* **31**(14), pp.2984-2996.

Chen, J., Bai, L., Bernard, D., Nikolovska-Coleska, Z., Gomez, C., Zhang, J., Yi, H. and Wang, S. 2010. Structure-Based Design of Conformationally Constrained, Cell-Permeable STAT3 Inhibitors. *ACS Medicinal Chemistry Letters.* **1**(2), pp.85-89.

Chen, J., Nikolovska-Coleska, Z., Yang, C.Y., Gomez, C., Gao, W., Krajewski, K., Jiang, S., Roller, P. and Wang, S. 2007. Design and synthesis of a new, conformationally constrained, macrocyclic small-molecule inhibitor of STAT3 via 'click chemistry'. *Bioorganic & Medicinal Chemistry Letters.* **17**(14), pp.3939-3942.

Choi, J.H., Park, J.B., Bae, S.S., Yun, S., Kim, H.S., Hong, W.P., Kim, I.S., Kim,

J.H., Han, M.Y., Ryu, S.H., Patterson, R.L., Snyder, S.H. and Suh, P.G. 2004. Phospholipase C-gamma1 is a guanine nucleotide exchange factor for dynamin-1 and enhances dynamin-1-dependent epidermal growth factor receptor endocytosis. *Journal of Cell Science.* **117**(Pt 17), pp.3785-3795.

Clift, D., McEwan, W.A., Labzin, L.I., Konieczny, V., Mogessie, B., James, L.C. and Schuh, M. 2017. A Method for the Acute and Rapid Degradation of Endogenous Proteins. *Cell.* **171**(7), pp.1692-1706.e1618.

Cobb, B.S., Schaller, M.D., Leu, T.H. and Parsons, J.T. 1994. Stable association of pp60src and pp59fyn with the focal adhesion-associated protein tyrosine kinase, pp125FAK. *Molecular Cell Biology.* **14**(1), pp.147-155.

Coffey, A.J., Brooksbank, R.A., Brandau, O., Oohashi, T., Howell, G.R., Bye, J.M., Cahn, A.P., Durham, J., Heath, P., Wray, P., Pavitt, R., Wilkinson, J., Leversha, M., Huckle, E., Shaw-Smith, C.J., Dunham, A., Rhodes, S., Schuster, V., Porta, G., Yin, L., Serafini, P., Sylla, B., Zollo, M., Franco, B., Bolino, A., Seri, M., Lanyi, A., Davis, J.R., Webster, D., Harris, A., Lenoir, G., de St Basile, G., Jones, A., Behloradsky, B.H., Achatz, H., Murken, J., Fassler, R., Sumegi, J., Romeo, G., Vaudin, M., Ross, M.T., Meindl, A. and Bentley, D.R. 1998. Host response to EBV infection in X-linked lymphoproliferative disease results from mutations in an SH2-domain encoding gene. *Nature Genetics.* **20**(2), pp.129-135.

Coffey, G., Betz, A., Graf, J., Stephens, G., Hua Lin, P., Imboden, J. and Sinha, U. 2013. Methotrexate and a spleen tyrosine kinase inhibitor cooperate to inhibit responses to peripheral blood B cells in rheumatoid arthritis. *Pharmacology Research & Perspectives.* **1**(2), pe00016.

Coleman, D.R.t., Ren, Z., Mandal, P.K., Cameron, A.G., Dyer, G.A., Muranjan, S., Campbell, M., Chen, X. and McMurray, J.S. 2005. Investigation of the binding determinants of phosphopeptides targeted to the SRC homology 2 domain of the signal transducer and activator of transcription 3. Development of a high-affinity peptide inhibitor. *Journal of Medicinal Chemistry.* **48**(21), pp.6661-6670.

Colicelli, J. 2010. ABL tyrosine kinases: evolution of function, regulation, and specificity. *Science Signaling.* **3**(139), pre6.

Colwill, K., Renewable Protein Binder Working Group and Graslund, S. 2011. A roadmap to generate renewable protein binders to the human proteome. *Nature Methods.* **8**(7), pp.551-558.

Daly, R.J., Binder, M.D. and Sutherland, R.L. 1994. Overexpression of the Grb2 gene in human breast cancer cell lines. *Oncogene.* **9**(9), pp.2723-2727.

De Las Rivas, J., and Fontanillo, C. 2010. Protein–protein interactions essentials: key concepts to building and analyzing interactome networks. *PLoS Computational Biology.* **6**(6), e1000807.

Deb, T.B., Coticchia, C.M. and Dickson, R.B. 2004. Calmodulin-mediated activation of Akt regulates survival of c-Myc-overexpressing mouse mammary carcinoma cells. *Journal of Biological Chemistry .* **279**(37), pp.38903-38911.

Dekker, F.J., de Mol, N.J., Bultinck, P., Kemmink, J., Hilbers, H.W. and Liskamp, R.M. 2003. Role of solution conformation and flexibility of short peptide ligands that bind to the p56(lck) SH2 domain. *Bioorganic & Medicinal Chemistry.* **11**(6), pp.941-949.

Dekker, F.J., de Mol, N.J., Fischer, M.J. and Liskamp, R.M. 2003. Amino propynyl benzoic acid building block in rigid spacers of divalent ligands binding to the Syk SH2 domains with equally high affinity as the natural ligand. *Bioorganic & Medicinal Chemistry Letters.* **13**(7), pp.1241-1244.

Dennis, M.S. and Lazarus, R.A. 1994. Kunitz domain inhibitors of tissue factor-factor VIIa. I. Potent inhibitors selected from libraries by phage display. *Journal of Biological Chemistry .* **269**(35), pp.22129-22136.

Dharmawardana, P.G., Peruzzi, B., Giubellino, A., Burke, T.R., Jr. and Bottaro, D.P. 2006. Molecular targeting of growth factor receptor-bound 2 (Grb2) as an anti-cancer strategy. *Anticancer Drugs.* **17**(1), pp.13-20.

Durocher, Y., Perret, S. and Kamen, A. 2002. High-level and high-throughput recombinant protein production by transient transfection of suspension-growing human 293-EBNA1 cells. *Nucleic Acids Research.* **30**(2), pE9.

Dutartre, H., Harris, M., Olive, D. and Collette, Y. 1998. The human immunodeficiency virus type 1 Nef protein binds the Src-related tyrosine kinase Lck SH2 domain through a novel phosphotyrosine independent mechanism. *Virology.* **247**(2), pp.200-211.

Eck, M.J., Shoelson, S.E. and Harrison, S.C. 1993. Recognition of a high-affinity phosphotyrosyl peptide by the Src homology-2 domain of p56lck. *Nature.* **362**(6415), pp.87-91.

Edwards, P.R., Gill, A., Pollard-Knight, D.V., Hoare, M., Buckle, P.E., Lowe, P.A. and Leatherbarrow, R.J. 1995. Kinetics of protein-protein interactions at the

surface of an optical biosensor. *Analytical Biochemistry.* **231**(1), pp.210-217.

Feller, S.M. 2001. Crk family adaptors-signalling complex formation and biological roles. *Oncogene.* **20**(44), pp.6348-6371.

Filippakopoulos, P., Muller, S. and Knapp, S. 2009. SH2 domains: modulators of nonreceptor tyrosine kinase activity. *Current Opinion in Structural Biology.* **19**, pp.643-649.

Fortian, A. and Sorkin, A. 2014. Live-cell fluorescence imaging reveals high stoichiometry of Grb2 binding to the EGF receptor sustained during endocytosis. *Journal of Cell Science.* **127**(Pt 2), pp.432-444.

Frei, J.C., and Lai, J.R. +2016. Protein and Antibody Engineering by Phage Display. *Methods in Enzymology*. **580**, pp. 45-87.

Furet, P., Gay, B., Caravatti, G., Garcia-Echeverria, C., Rahuel, J., Schoepfer, J. and Fretz, H. 1998. Structure-based design and synthesis of high affinity tripeptide ligands of the Grb2-SH2 domain. *Journal of Medicinal Chemistry.* **41**(18), pp.3442-3449.

Gan, W. and Roux, B. 2009. Binding specificity of SH2 domains: insight from free energy simulations. *Proteins.* **74**(4), pp.996-1007.

Gao, Y., Luo, J., Yao, Z.J., Guo, R., Zou, H., Kelley, J., Voigt, J.H., Yang, D. and Burke, T.R., Jr. 2000. Inhibition of Grb2 SH2 domain binding by non-phosphate-containing ligands. 2. 4-(2-Malonyl)phenylalanine as a potent phosphotyrosyl mimetic. *Journal of Medicinal Chemistry.* **43**(5), pp.911-920.

Garces, S. and Demengeot, J. 2018. The Immunogenicity of Biologic Therapies. *Current Problems in Dermatology.* **53**, pp.37-48.

Garcia-Garcia, J., Bonet, J., Guney, E., Fornes, O., Planas, J., Oliva, B. 2012. Networks of Protein-Protein Interactions: From Uncertainty to Molecular Details. *Molecular Informatics.* **31**(5), pp.342-362.

Gay, B., Suarez, S., Weber, C., Rahuel, J., Fabbro, D., Furet, P., Caravatti, G. and Schoepfer, J. 1999. Effect of potent and selective inhibitors of the Grb2 SH2 domain on cell motility. *The Journal of Biological Chemistry.* **274**(33), pp.23311-23315.

Gebauer, M., Schiefner, A., Matschiner, G. and Skerra, A. 2013. Combinatorial design of an Anticalin directed against the extra-domain b for the specific targeting of oncofetal fibronectin. *Journal of Molecular Biology.* **425**(4), pp.780-802.

Gebauer, M. and Skerra, A. 2009. Engineered protein scaffolds as next-generation antibody therapeutics
Current Opinion in Chemical Biology **13**(1), pp.245-255.

Geisse, S. and Voedisch, B. 2012. Transient expression technologies: past, present, and future. *Methods in Molecular Biology.* **899**, pp.203-219.

Genini, D., Brambilla, L., Laurini, E., Merulla, J., Civenni, G., Pandit, S., D'Antuono, R., Perez, L., Levy, D.E., Pricl, S., Carbone, G.M., Catapano, C.V. 2017. Mitochondrial dysfunction induced by a SH2 domain-targeting STAT3 inhibitor leads to metabolic synthetic lethality in cancer cells. *Proceedings of the National Academy of Sciences*. **114**(25), E4924-E4933.

Gilbreth, R.N., Truong, K., Madu, I., Koide, A., Wojcik, J.B., Li, N.S., Piccirilli, J.A., Chen, Y. and Koide, S. 2011. Isoform-specific monobody inhibitors of small ubiquitin-related modifiers engineered using structure-guided library design. *Proceedings of the National Academy of Sciences.* **108**(19), pp.7751-7756.

Giubellino, A., Burke, T.R. and Bottaro, D.P. 2008 Grb2 Signaling in Cell Motility and Cancer. *Expert Opinion on Therapeutic Targets.* **12**(8), pp.1021-1033.

Giubellino, A., Gao, Y., Lee, S., Lee, M.J., Vasselli, J.R., Medepalli, S., Trepel, J.B., Burke, T.R., Jr. and Bottaro, D.P. 2007. Inhibition of tumor metastasis by a growth factor receptor bound protein 2 Src homology 2 domain-binding antagonist. *Cancer Research.* **67**(13), pp.6012-6016.

Glaser, R.W. 1993. Antigen-antibody binding and mass transport by convection and diffusion to a surface: a two-dimensional computer model of binding and dissociation kinetics. *Analytical Biochemistry.* **213**(1), pp.152-161.

Goldman, R.D. 2000. Antibodies: indispensable tools for biomedical research. *Trends in Biochemical Science.* **25**(12), pp.593-595.

Gomez, C., Bai, L., Zhang, J., Nikolovska-Coleska, Z., Chen, J., Yi, H. and Wang, S. 2009. Design, synthesis, and evaluation of peptidomimetics containing Freidinger lactams as STAT3 inhibitor++++s. *Bioorganic & Medicinal Chemistry Lett.* **19**(6), pp.1733-1736.

Gorman, C.M., Gies, D., McCray, G. and Huang, M. 1989. The human cytomegalovirus Major Immediate Early Promoter can be trans-activated by Adenovirus early proteins. *Virology.* **171**(2), pp.377-385.

Govindarajan, R., Duraiyan, J., Kaliyappan, K. and Palanisamy, M. 2012. Microarray and its applications. *Journal of Pharmacy & Bioallied Sciences.*

4(Suppl 2), pp.S310-312.

Gram, H., Schmitz, R., Zuber, J.F. and Baumann, G. 1997. Identification of phosphopeptide ligands for the Src-homology 2 (SH2) domain of Grb2 by phage display. *European Journal of Biochemistry.* **246**(3), pp.633-637.

Grebien, F., Hantschel, O., Wojcik, J., Kaupe, I., Kovacic, B., Wyrzucki, A.M., Gish, G.D., Cerny-Reiterer, S., Koide, A., Beug, H., Pawson, T., Valent, P., Koide, S. and Superti-Furga, G. 2011. Targeting the SH2-Kinase Interface in Bcr-Abl Inhibits Leukemogenesis. *Cell* **147**(2), pp.306-319.

Gronwall, C., Sjoberg, A., Ramstrom, M., Hoiden-Guthenberg, I., Hober, S., Jonasson, P. and Stahl, S. 2007. Affibody-mediated transferrin depletion for proteomics applications. *Biotechnology Journal.* **2**(11), pp.1389-1398.

Gupta, A., Xu, J., Lee, S., Tsai, S.T., Zhou, B., Kurosawa, K., Werner, M.S., Koide, A., Ruthenburg, A.J., Dou, Y. and Koide, S. 2018. Facile target validation in an animal model with intracellularly expressed monobodies. *Nat Chemistry & Biology.* **14**(9), pp.895-900.

Haab, B.B. 2005. Antibody arrays in cancer research. *Mol Cell Proteomics.* **4**(4), pp.377-383.

Hagan, E.L., Banaszynski, L.A., Chen, L.C., Maynard-Smith, L.A. and Wandless, T.J. 2009. Regulating protein stability in mammalian cells using small molecules. *Cold Spring Harbor Protocols.* **2009**(3).

Han, J.D., Bertin, N., Hao, T., Goldberg, D.S., Berriz, G.F., Zhang, L.V., Dupuy, D., Walhout, A.J., Cusick, M.E., Roth, F.P., and Vidal, M. 2004. Evidence for dynamically organized modularity in the yeast protein–protein interaction network. *Nature*. **430**(6995), pp.88-93.

Hang, J. and Dasso, M. 2002. Association of the human SUMO-1 protease SENP2 with the nuclear pore. *Journal of Biological Chemistry.* **277**(22), pp.19961-19966.

Helma, J., Cardoso, M.C., Muyldermans, S. and Leonhardt, H. 2015. Nanobodies and recombinant binders in cell biology. *The Journal of Cell Biology.* **209**(5), pp.633-644.

Hemminki, A., Niemi, S., Hoffren, A.M., Hakalahti, L., Soderlund, H. and Takkinen, K. 1998. Specificity improvement of a recombinant anti-testosterone Fab fragment by CDRIII mutagenesis and phage display selection. *Protein Engineering.* **11**(4), pp.311-319.

Hey, T., Fiedler, E., Rudolph, R. and Fiedler, M. 2005. Artificial, non-antibody binding proteins for pharmaceutical and industrial applications. *Trends in Biotechnology.* **23**(10), pp.514-522.

Hoheisel, J.D., Alhamdani, M.S. and Schroder, C. 2013. Affinity-based microarrays for proteomic analysis of cancer tissues. *Proteomics Clinical Applications.* **7**(1-2), pp.8-15.

Honma, M., Higuchi, O., Shirakata, M., Yasuda, T., Shibuya, H., Iemura, S., Natsume, T. and Yamanashi, Y. 2006. Dok-3 sequesters Grb2 and inhibits the Ras-Erk pathway downstream of protein-tyrosine kinases. *Genes Cells.* **11**(2), pp.143-151.

Hsiao, Y.-C., Lee, C.-Y., Lin, Y.-J., Tsai, S.-H., Jeng, K.-C.G., Chao, W.-T. and Lung, F.-D.T. 2013. Design, synthesis, and evaluation of fluorescent cell-penetrating peptidic antagonists of Grb2-SH2 for targeting MCF-7 breast cancer cells. *Medicinal Chemistry Research.* **22**, pp.5337-5343.

Hu, S., Li, Y., Liu, G., Song, Q., Wang, L., Han, Y., Zhang, Y., Song, Y., Yao, X., Tao, Y., Zeng, H., Yang, H., Wang, J., Zhu, H., Chen, Z.N. and Wu, L. 2007. A protein chip approach for high-throughput antigen identification and characterization. *Proteomics.* **7**(13), pp.2151-2161.

Hughes, D.J., Tiede, C., Penswick, N., Tang, A.A., Trinh, C.H., Mandal, U., Zajac, K.Z., Gaule, T., Howell, G., Edwards, T.A., Duan, J., Feyfant, E., McPherson, M.J., Tomlinson, D.C. and Whitehouse, A. 2017. Generation of specific inhibitors of SUMO-1- and SUMO-2/3-mediated protein-protein interactions using Affimer (Adhiron) technology. *Science Signaling.* **10**(505).

Ingley, E. 2012. Functions of the Lyn tyrosine kinase in health and disease. *Cell Communication and Signaling.* **10**(1), p21.

Ijaz, M., Wang, F., Shahbaz, M., Jiang, W., Fathy, A.H., and Nesa, E.U. 2018. The Role of Grb2 in Cancer and Peptides as Grb2 Antagonists. *Protein & Peptide Letters*. **24**(12), pp.1084-1095.

Jacobs, S.A., Diem, M.D., Luo, J., Teplyakov, A., Obmolova, G., Malia, T., Gilliland, G.L. and O'Neil, K.T. 2012. Design of novel FN3 domains with high stability by a consensus sequence approach. *Protein Engineering, Design and Selection.* **25**(3), pp.107-117.

Jäger, V., Büssow, K. and Schirrmann, T. 2015. Transient Recombinant Protein Expression in Mammalian Cells. **9**, pp.27-64.

James, L.C., Keeble, A.H., Khan, Z., Rhodes, D.A. and Trowsdale, J. 2007. Structural basis for PRYSPRY-mediated tripartite motif (TRIM) protein function. *Proceedings of the National Academy of Sciences.* **104**(15), pp.6200-6205.

Jenko, S., Dolenc, I., Guncar, G., Dobersek, A., Podobnik, M. and Turk, D. 2003. Crystal structure of Stefin A in complex with cathepsin H: N-terminal residues of inhibitors can adapt to the active sites of endo- and exopeptidases. *Journal of Molecular Biology.* **326**(3), pp.875-885.

Jeong, J.S., Jiang, L., Albino, E., Marrero, J., Rho, H.S., Hu, J., Hu, S., Vera, C., Bayron-Poueymiroy, D., Rivera-Pacheco, Z.A., Ramos, L., Torres-Castro, C., Qian, J., Bonaventura, J., Boeke, J.D., Yap, W.Y., Pino, I., Eichinger, D.J., Zhu, H. and Blackshaw, S. 2012. Rapid identification of monospecific monoclonal antibodies using a human proteome microarray. *Molecular Cell Proteomics.* **11**(6).

Jiang, D., Zhuang, J., Peng, W., Lu, Y., Liu, H., Zhao, Q., Chi, C., Li, X., Zhu, G., Xu, X., Yan, C., Xu, Y., Ge, J. and Pang, J. 2017. Phospholipase Cγ1 Mediates Intima Formation Through Akt-Notch1 Signaling Independent of the Phospholipase Activity. *Journal of the American Heart Association.* **6**(7).

Jones, R.B., Gordus, A., Krall, J.A. and MacBeath, G. 2006. A quantitative protein interaction network for the ErbB receptors using protein microarrays. *Nature* **439**(7073), pp. 168-174.

Kadrmas, J.L., Beckerle, M.C. 2004. The LIM domain: from the cytoskeleton to the nucleus. *Nature Reviews Molecular Cell Biology*. **5**(11), pp.920-31.

Kanai, M., Goke, M., Tsunekawa, S. and Podolsky, D.K. 1997. Signal transduction pathway of human fibroblast growth factor receptor 3. Identification of a novel 66-kDa phosphoprotein. *Journal of Biological Chemistry.* **272**(10), pp.6621-6628.

Kasembeli, M.M., Xu, X. and Tweardy, D.J. 2009. SH2 domain binding to phosphopeptide ligands: potential for drug targeting. *Frontiers in Bioscience (Landmark Edition).* **14**, pp.1010-1022.

Kehoe, J.W. and Kay, B.K. 2005. Filamentous phage display in the new millennium. *Chemical Reviews.* **105**(11), pp.4056-4072.

Kim, Nam, J.-Y., Han, M.Y., Lee, E.K., Choi, J.-D., Bok, S.H. and Kwon, B.-M. 1999. Actinomycin D as a novel SH2 domain ligand inhibits Shc/Grb2 interaction in B104-1-1 (neu*-transformed NIH3T3) and SAA (hEGFR-overexpressed

NIH3T3) cells. *FEBS Letters.* **453**(1-2), pp.174-178.

Kim, M.J., Chang, J.S., Park, S.K., Hwang, J.I., Ryu, S.H. and Suh, P.G. 2000. Direct interaction of SOS1 Ras exchange protein with the SH3 domain of phospholipase C-gamma1. *Biochemistry.* **39**(29), pp.8674-8682.

Kofler, N.M. and Simons, M. 2015. Angiogenesis versus arteriogenesis: neuropilin 1 modulation of VEGF signaling. *F1000Prime Rep.* **7**, p26.

Koide, A., Abbatiello, S., Rothgery, L. and Koide, S. 2002. Probing protein conformational changes in living cells by using designer binding proteins: application to the estrogen receptor. *Proceedings of the National Academy of Sciences.* **99**(3), pp.1253-1258.

Koide, A., Wojcik, J., Gilbreth, R.N., Hoey, R.J. and Koide, S. 2012. Teaching an old scaffold new tricks: monobodies constructed using alternative surfaces of the FN3 scaffold. *Journal of Molecular Biology.* **415**(2), pp.393-405.

Kraskouskaya, D., Duodu, E., Arpin, C.C. and Gunning, P.T. 2013. Progress towards the development of SH2 domain inhibitors. *Chemical Society Reviews.* **42**(8), pp.3337-3370.

Krausz, E. 2007. High-content siRNA screening. *Molecular Biosystems.* **3**(4), pp.232-240.

Kuil, J., Branderhorst, H.M., Pieters, R.J., de Mol, N.J. and Liskamp, R.M. 2009. ITAM-derived phosphopeptide-containing dendrimers as multivalent ligands for Syk tandem SH2 domain. *Organic & Biomolecular Chemistry.* **7**(19), pp.4088-4094.

Kukenshoner, T., Schmit, N.E., Bouda, E., Sha, F., Pojer, F., Koide, A., Seeliger, M., Koide, S. and Hantschel, O. 2017. Selective Targeting of SH2 Domain-Phosphotyrosine Interactions of Src Family Tyrosine Kinases with Monobodies. *Journal of Molecular Biology.* **429**(9), pp.1364-1380.

Kummer, L., Hsu, C.W., Dagliyan, O., MacNevin, C., Kaufholz, M., Zimmermann, B., Dokholyan, N.V., Hahn, K.M. and Pluckthun, A. 2013. Knowledge-based design of a biosensor to quantify localized ERK activation in living cells. *Chemistry & Biology.* **20**(6), pp.847-856.

Kummer, L., Parizek, P., Rube, P., Millgramm, B., Prinz, A., Mittl, P.R., Kaufholz, M., Zimmermann, B., Herberg, F.W. and Pluckthun, A. 2012. Structural and functional analysis of phosphorylation-specific binders of the kinase ERK from designed ankyrin repeat protein libraries. *Proceedings of the National Academy*

of Sciences. **109**(34), pp.2248-2257.

Kwon, Y.K., Jang, H.J., Kole, S., He, H.J. and Bernier, M. 2003. Role of the pleckstrin homology domain of PLCgamma1 in its interaction with the insulin receptor. *Journal of Cell Biology.* **163**(2), pp.375-384.

Kyle, H.F., Wickson, K.F., Stott, J., Burslem, G.M., Breeze, A.L., Tiede, C., Tomlinson, D.C., Warriner, S.L., Nelson, A., Wilson, A.J. and Edwards, T.A. 2015. Exploration of the HIF-1alpha/p300 interface using peptide and Adhiron phage display technologies. *Molecular Biosystems.* **11**(10), pp.2738-2749.

Ladner, R.C. 1995. Constrained peptides as binding entities. *Trends in Biotechnology.* **13**(10), pp.426-430.

Laviola, L., Giorgino, F., Chow, J.C., Baquero, J.A., Hansen, H., Ooi, J., Zhu, J., Riedel, H. and Smith, R.J. 1997. The adapter protein Grb10 associates preferentially with the insulin receptor as compared with the IGF-I receptor in mouse fibroblasts. *Journal of Clinical Investigations.* **99**(5), pp.830-837.

Lawrence, D.S. 2005. Signaling protein inhibitors via the combinatorial modification of peptide scaffolds. *Biochimica et Biophysica Acta.* **1754**(1-2), pp.50-57.

Lee, S.C., Park, K., Han, J., Lee, J.J., Kim, H.J., Hong, S., Heu, W., Kim, Y.J., Ha, J.S., Lee, S.G., Cheong, H.K., Jeon, Y.H., Kim, D. and Kim, H.S. 2012. Design of a binding scaffold based on variable lymphocyte receptors of jawless vertebrates by module engineering. *Proceedings of the National Academy of Sciences.* **109**(9), pp.3299-3304.

Leung, I., Jarvik, N. and Sidhu, S.S. 2017. A Highly Diverse and Functional Naive Ubiquitin Variant Library for Generation of Intracellular Affinity Reagents. *Journal of Molecular Biology.* **429**(1), pp.115-127.

Li, W. and Caberoy, N.B. 2010. New perspective for phage display as an efficient and versatile technology of functional proteomics. *Applied Microbiology & Biotechnology.* **85**(4), pp.909-919.

Liotta, L.A., Espina, V., Mehta, A.I., Calvert, V., Rosenblatt, K., Geho, D., Munson, P.J., Young, L., Wulfkuhle, J. and Petricoin, E.F., 3rd. 2003. Protein microarrays: meeting analytical challenges for clinical applications. *Cancer Cell.* **3**(4), pp.317-325.

Liu, B.A., Engelmann, B.W. and Nash, P.D. 2012. The language of SH2 domain interactions defines phosphotyrosine-mediated signal transduction. *FEBS*

Letters. **586**(17), pp.2597-2605.

Liu, B.A., Jablonowski, K., Raina, M., Arce, M., Pawson, T. and Nash, P.D. 2006. The Human and Mouse Complement of SH2 Domain Proteins—Establishing the Boundaries of Phosphotyrosine Signaling. *Molecular Cell.* **22**(6), pp.851-868.

Liu, B.A. and Nash, P.D. 2012. Evolution of SH2 domains and phosphotyrosine signalling networks. *Philosophical Transactions of the Royal Society B.* **367**(1602), pp.2556-2573.

Liu, P., Cheng, H., Roberts, T.M. and Zhao, J.J. 2009. Targeting the phosphoinositide 3-kinase pathway in cancer. *Nature Reviews Drug Discovery.* **8**(8), pp.627-644.

Lo, A.S., Zhu, Q. and Marasco, W.A. 2008. Intracellular antibodies (intrabodies) and their therapeutic potential. *Handbook of Experimental Pharmacology.* (181), pp.343-373.

Lofblom, J., Feldwisch, J., Tolmachev, V., Carlsson, J., Stahl, S. and Frejd, F.Y. 2010. Affibody molecules: engineered proteins for therapeutic, diagnostic and biotechnological applications. *FEBS Letters.* **584**(12), pp.2670-2680.

Lonn, P., Kacsinta, A.D., Cui, X.S., Hamil, A.S., Kaulich, M., Gogoi, K. and Dowdy, S.F. 2016. Enhancing Endosomal Escape for Intracellular Delivery of Macromolecular Biologic Therapeutics. *Scientific Reports.* **6**, p32301.

Lowenstein, E.J., Daly, R.J., Batzer, A.G., Li, W., Margolis, B., Lammers, R., Ullrich, A., Skolnik, E.Y., Bar-Sagi, D. and Schlessinger, J. 1992. The SH2 and SH3 domain-containing protein GRB2 links receptor tyrosine kinases to ras signaling. *Cell.* **70**(3), pp.431-442.

Machida, K. and Mayer, B.J. 2005. The SH2 domain: versatile signaling module and pharmaceutical target. *Biochimica et Biophysica Acta* **1747**(1), pp.1 - 25.

Mandal, P.K., Liao, W.S. and McMurray, J.S. 2009. Synthesis of phosphatase-stable, cell-permeable peptidomimetic prodrugs that target the SH2 domain of Stat3. *Organic Letters.* **11**(15), pp.3394-3397.

Mandal, P.K., Limbrick, D., Coleman, D.R., Dyer, G.A., Ren, Z., Birtwistle, J.S., Xiong, C., Chen, X., Briggs, J.M. and McMurray, J.S. 2009. Conformationally constrained peptidomimetic inhibitors of signal transducer and activator of transcription. 3: Evaluation and molecular modeling. *Journal of Medicinal Chemistry.* **52**(8), pp.2429-2442.

Marqusee, S. and Baldwin, R.L. 1987. Helix stabilization by Glu-...Lys+ salt

bridges in short peptides of de novo design. *Proceedings of the National Academy of Sciences.* **84**(24), pp.8898-8902.

Marschall, A.L., Dubel, S. and Boldicke, T. 2015. Specific in vivo knockdown of protein function by intrabodies. *MAbs.* **7**(6), pp.1010-1035.

Martin, H.L., Bedford, R., Heseltine, S.J., Tang, A.A., Haza, K.Z., Rao, A., McPherson, M.J. and Tomlinson, D.C. 2018. Non-immunoglobulin scaffold proteins: Precision tools for studying protein-protein interactions in cancer. *New Biotechnology.*

Matunis, M.J., Wu, J. and Blobel, G. 1998. SUMO-1 Modification and Its Role in Targeting the Ran GTPase-activating Protein, RanGAP1, to the Nuclear Pore Complex. *The Journal of Cell Biology.* **140**(3), pp.499-509.

Mayer, B.J. 2015. The discovery of modular binding domains: building blocks of cell signalling. *Nature Reviews Molecular Cell Biology.* **16**(11), pp.691-698.

Maynard-Smith, L.A., Chen, L.C., Banaszynski, L.A., Ooi, A.G. and Wandless, T.J. 2007. A directed approach for engineering conditional protein stability using biologically silent small molecules. *Journal of Biological Chemistry .* **282**(34), pp.24866-24872.

McAllister, T., Horner, K. and Webb, M. 2014. Evaluation of the interaction between phosphohistidine analogues and phosphotyrosine binding domains. *Chembiochem.* **15**(8), pp.1088-1091.

McDonald, C.B., Seldeen, K.L., Deegan, B.J., Lewis, M.S. and Farooq, A. 2008. Grb2 adaptor undergoes conformational change upon dimerization. *Archives of Biochemistry & Biophysics.* **475**(1), pp.25-35.

Mersmann, M., Meier, D., Mersmann, J., Helmsing, S., Nilsson, P., Graslund, S., Consortium, S.G., Colwill, K., Hust, M. and Dubel, S. 2010. Towards proteome scale antibody selections using phage display. *New Biotechnology.* **27**(2), pp.118-128.

Meyer, G.D., Morán-Mirabal, J.M., Branch, D.W. and Craighead, H.G. 2006. Nonspecific binding removal from protein microarrays using thickness shear mode resonators. *IEEE Sensors journal.* **6**(2), pp.254-261.

Michel, M.A., Swatek, K.N., Hospenthal, M.K. and Komander, D. 2017. Ubiquitin Linkage-Specific Affimers Reveal Insights into K6-Linked Ubiquitin Signaling. *Molecular Cell.* **68**(1), pp.233-246 e235.

Moghaddam, A., Borgen, T., Stacy, J., Kausmally, L., Simonsen, B., Marvik, O.J.,

Brekke, O.H. and Braunagel, M. 2003. Identification of scFv antibody fragments that specifically recognise the heroin metabolite 6-monoacetylmorphine but not morphine. *Journal of Immunological Methods.* **280**(1-2), pp.139-155.

Mohr, S.E., Smith, J.A., Shamu, C.E., Neumuller, R.A. and Perrimon, N. 2014. RNAi screening comes of age: improved techniques and complementary approaches. *Nature Reviews Molecular Cell Biology.* **15**(9), pp.591-600.

Molinas, M., Beer, C., Hesse, F., Wirth, M. and Wagner, R. 2014. Optimizing the transient transfection process of HEK-293 suspension cells for protein production by nucleotide ratio monitoring. *Cytotechnology.* **66**(3), pp.493-514.

Moran, M.F., Koch, C.A., Anderson, D., Ellis, C., England, L., Martin, G.S. and Pawson, T. 1990. Src homology region 2 domains direct protein-protein interactions in signal transduction. *Proceedings of the National Academy of Sciences.* **87**(21), pp.8622-8626.

Morlacchi, P., Robertson, F.M., Klostergaard, J. and McMurray, J.S. 2014. Targeting SH2 domains in breast cancer. *Future Medicinal Chemistry.* **6**(17), pp.1909-1926.

Morrison, K.L. and Weiss, G.A. 2001. Combinatorial alanine-scanning. *Current Opinion in Chemistry & Biology.* **5**(3), pp.302-307.

Nam, N.H., Pitts, R.L., Sun, G., Sardari, S., Tiemo, A., Xie, M., Yan, B. and Parang, K. 2004. Design of tetrapeptide ligands as inhibitors of the Src SH2 domain. *Bioorganic & Medicinal Chemistry.* **12**(4), pp.779-787.

Nguyen, H.H., Park, J., Kang, S. and Kim, M. 2015. Surface plasmon resonance: a versatile technique for biosensor applications. *Sensors (Basel).* **15**(5), pp.10481-10510.

Nichols, K.E., Harkin, D.P., Levitz, S., Krainer, M., Kolquist, K.A., Genovese, C., Bernard, A., Ferguson, M., Zuo, L., Snyder, E., Buckler, A.J., Wise, C., Ashley, J., Lovett, M., Valentine, M.B., Look, A.T., Gerald, W., Housman, D.E. and Haber, D.A. 1998. Inactivating mutations in an SH2 domain-encoding gene in X-linked lymphoproliferative syndrome. *Proceedings of the National Academy of Sciences.* **95**(23), pp.13765-13770.

Nioche, P., Liu, W.Q., Broutin, I., Charbonnier, F., Latreille, M.T., Vidal, M., Roques, B., Garbay, C. and Ducruix, A. 2002. Crystal structures of the SH2 domain of Grb2: highlight on the binding of a new high-affinity inhibitor. *Journal of Molecular Biology.* **315**(5), pp.1167-1177.

Noh, K., Kim, K.O., Patel, N.R., Staples, J.R., Minematsu, H., Nair, K., and Lee, F.Y. 2011. Targeting inflammatory kinase as an adjuvant treatment for osteosarcomas. *Journal of Bone and Joint Surgery*. **93**(8), pp.723–732.

Nord, K., Gunneriusson, E., Uhlen, M. and Nygren, P.A. 2000. Ligands selected from combinatorial libraries of protein A for use in affinity capture of apolipoprotein A-1M and taq DNA polymerase. *J Biotechnol.* **80**(1), pp.45-54.

Nunes-Xavier, C.E., Elson, A. and Pulido, R. 2012. Epidermal growth factor receptor (EGFR)-mediated positive feedback of protein-tyrosine phosphatase epsilon (PTPepsilon) on ERK1/2 and AKT protein pathways is required for survival of human breast cancer cells. *Journal of Biological Chemistry .* **287**(5), pp.3433-3444.

Olle, E.W., Messamore, J., Deogracias, M.P., McClintock, S.D., Anderson, T.D. and Johnson, K.J. 2005. Comparison of antibody array substrates and the use of glycerol to normalize spot morphology. *Experimental Molecular Pathology.* **79**(3), pp.206-209.

Papaioannou, D., Geibel, S., Kunze, M.B., Kay, C.W. and Waksman, G. 2016. Structural and biophysical investigation of the interaction of a mutant Grb2 SH2 domain (W121G) with its cognate phosphopeptide. *Protein Science.* **25**(3), pp.627-637.

Pascal, S.M., Singer, A.U., Gish, G., Yamazaki, T., Shoelson, S.E., Pawson, T., Kay, L.E. and Forman-Kay, J.D. 1994. Nuclear magnetic resonance structure of an SH2 domain of phospholipase C-gamma 1 complexed with a high affinity binding peptide. *Cell.* **77**(3), pp.461-472.

Paschke, M. 2006. Phage display systems and their applications. *Applied Microbiology & Biotechnology.* **70**(1), pp.2-11.

Pawson, T. and Gish, G.D. 1992. SH2 and SH3 domains: from structure to function. *Cell.* **71**(3), pp.359-362.

Pawson, T., Gish, G.D. and Nash, P. 2001. SH2 domains, interaction modules and cellular wiring. *Trends in Cellular Biology.* **11**(12), pp.504-511.

Pawson, T., Raina. M., and Nash, P. 2002. Interaction domains: from simple binding events to complex cellular behavior. *FEBS Letters*. **513**(1), pp.2-10.

Peluso, P., Wilson, D.S., Do, D., Tran, H., Venkatasubbaiah, M., Quincy, D., Heidecker, B., Poindexter, K., Tolani, N., Phelan, M., Witte, K., Jung, L.S., Wagner, P. and Nock, S. 2003. Optimizing antibody immobilization strategies for

the construction of protein microarrays. *Analytical Biochemistry.* **312**(2), pp.113-124.

Pero, S.C., Oligino, L., Daly, R.J., Soden, A.L., Liu, C., Roller, P.P., Li, P. and Krag, D.N. 2002. Identification of novel non-phosphorylated ligands, which bind selectively to the SH2 domain of Grb7. *Journal of Biological Chemistry .* **277**(14), pp.11918-11926.

Pershad, K., Pavlovic, J.D., Graslund, S., Nilsson, P., Colwill, K., Karatt-Vellatt, A., Schofield, D.J., Dyson, M.R., Pawson, T., Kay, B.K. and McCafferty, J. 2010. Generating a panel of highly specific antibodies to 20 human SH2 domains by phage display. *Protein Engineering, Design & Selection.* **23**(4), pp.279-288.

Petrelli, A. and Giordano, S. 2008. From single- to multi-target drugs in cancer therapy: when aspecificity becomes an advantage. *Current Medicinal Chemistry.* **15**(5), pp.422-432.

Plummer, M.S., Holland, D.R., Shahripour, A., Lunney, E.A., Fergus, J.H., Marks, J.S., McConnell, P., Mueller, W.T. and Sawyer, T.K. 1997. Design, synthesis, and cocrystal structure of a nonpeptide Src SH2 domain ligand. *Journal of Medicinal Chemistry.* **40**(23), pp.3719-3725.

Pourtau, L., Oliveira, H., Thevenot, J., Wan, Y., Brisson, A.R., Sandre, O., Miraux, S., Thiaudiere, E. and Lecommandoux, S. 2013. Antibody-Functionalized Magnetic Polymersomes: In vivo Targeting and Imaging of Bone Metastases using High Resolution MRI. In: Ueda, E. and Levkin, P.A. eds. *Advanced Healthcare materials.*

Quartararo, J.S., Wu, P. and Kritzer, J.A. 2012. Peptide bicycles that inhibit the Grb2 SH2 domain. *Chembiochem.* **13**(10), pp.1490-1496.

Raina, M., Sharma, R., Deacon, S.E., Tiede, C., Tomlinson, D., Davies, A.G., McPherson, M.J. and Walti, C. 2014. Antibody mimetic receptor proteins for label-free biosensors. *Analyst.*

Ramani, S.R., Tom, I., Lewin-Koh, N., Wranik, B., Depalatis, L., Zhang, J., Eaton, D. and Gonzalez, L.C. 2012. A secreted protein microarray platform for extracellular protein interaction discovery. *Analytical Biochemistry.* **420**(2), pp.127-138.

Richter, A., Eggenstein, E. and Skerra, A. 2014. Anticalins: exploiting a non-Ig scaffold with hypervariable loops for the engineering of binding proteins. *FEBS Letters.* **588**(2), pp.213-218.

Robinson, J.I., Baxter, E.W., Owen, R.L., Thomsen, M. and Tomlinson, D.C. 2018. Affimer proteins inhibit immune complex binding to FcgammaRIIIa with high specificity through competitive and allosteric modes of action. *Proceedings of the National Academy of Sciences.* **115**(1), pp.72-81.

Rojas, M., Yao, S. and Lin, Y.Z. 1996. Controlling epidermal growth factor (EGF)-stimulated Ras activation in intact cells by a cell-permeable peptide mimicking phosphorylated EGF receptor. *Journal of Biological Chemistry .* **271**(44), pp.27456-27461.

Russell, R.B., Breed, J. and Barton, G.J. 1992. Conservation analysis and structure prediction of the SH2 family of phosphotyrosine binding domains. *FEBS Letters.* **304**(1), pp.15-20.

Sadowski, I., Stone, J.C. and Pawson, T. 1986. A noncatalytic domain conserved among cytoplasmic protein-tyrosine kinases modifies the kinase function and transforming activity of Fujinami sarcoma virus P130gag-fps. *Molecular Cell Biology.* **6**(12), pp.4396-4408.

Saffran, D.C., Parolini, O., Fitch-Hilgenberg, M.E., Rawlings, D.J., Afar, D.E., Witte, O.N. and Conley, M.E. 1994. Brief report: a point mutation in the SH2 domain of Bruton's tyrosine kinase in atypical X-linked agammaglobulinemia. *New England Journal of Medicine.* **330**(21), pp.1488-1491.

Salameh, A., Galvagni, F., Bardelli, M., Bussolino, F. and Oliviero, S. 2005. Direct recruitment of CRK and GRB2 to VEGFR-3 induces proliferation, migration, and survival of endothelial cells through the activation of ERK, AKT, and JNK pathways. *Blood.* **106**(10), pp.3423-3431.

Salema, V. and Fernandez, L.A. 2017. Escherichia coli surface display for the selection of nanobodies. *Microbial biotechnology*. **10**(6), pp.1468-1484.

Sayos, J., Wu, C., Morra, M., Wang, N., Zhang, X., Allen, D., van Schaik, S., Notarangelo, L., Geha, R., Roncarolo, M.G., Oettgen, H., De Vries, J.E., Aversa, G. and Terhorst, C. 1998. The X-linked lymphoproliferative-disease gene product SAP regulates signals induced through the co-receptor SLAM. *Nature.* **395**(6701), pp.462-469.

Schoeber, J.P., van de Graaf, S.F., Lee, K.P., Wittgen, H.G., Hoenderop, J.G. and Bindels, R.J. 2009. Conditional fast expression and function of multimeric TRPV5 channels using Shield-1. *American journal of physiology. Renal physiology.* **296**(1), pp.204-211.

Schweizer, A., Roschitzki-Voser, H., Amstutz, P., Briand, C., Gulotti-Georgieva, M., Prenosil, E., Binz, H.K., Capitani, G., Baici, A., Pluckthun, A. and Grutter, M.G. 2007. Inhibition of caspase-2 by a designed ankyrin repeat protein: specificity, structure, and inhibition mechanism. *Structure.* **15**(5), pp.625-636.

Avacta Life Sciences. 2017. *Affimer Technology: Results of PBMC Immunogenicity Testing.* [Online]. [Accessed 4 August]. Available from: https://www.avacta.com/resources/affimer-technology-results-pbmc-immunogenicity-testing.

Sela-Culang, I., Kunik, V. and Ofran, Y. 2013. The structural basis of antibody-antigen recognition. *Frontiers in Immunology.* **4**, p302.

Sennhauser, G., Amstutz, P., Briand, C., Storchenegger, O. and Grutter, M.G. 2007. Drug export pathway of multidrug exporter AcrB revealed by DARPin inhibitors. *PLoS Biology.* **5**(1), pe7.

Sha, F., Basak, E., Gencer, Georgeon, S., Koide, A., Yasui, N., Koide, S. and Hantschel, O. 2013. Dissection of the BCR-ABL signaling network using highly specific monobody inhibitors to the SHP2 SH2 domains. *Proceedings of the National Academy of Sciences.* **110**(37), pp.14924-14929.

Sha, F., Salzman, G., Gupta, A. and Koide, S. 2017. Monobodies and other synthetic binding proteins for expanding protein science. *Protein Science.* **26**(5), pp.910-924.

Sharma, S. and Rao, A. 2009. RNAi screening: tips and techniques. *Nature Immunology.* **10**(8), pp.799-804.

Sjoberg, R., Sundberg, M., Gundberg, A., Sivertsson, A., Schwenk, J.M., Uhlen, M. and Nilsson, P. 2012. Validation of affinity reagents using antigen microarrays. *New Biotechnology.* **29**(5), pp.555-563.

Skerra, A. 2007. Alternative non-antibody scaffolds for molecular recognition. *Current Opinion in Biotechnology.* **18**(4), pp.295-304.

Skrlec, K., Strukelj, B. and Berlec, A. 2015. Non-immunoglobulin scaffolds: a focus on their targets. *Trends in Biotechnology.* **33**(7), pp.408-418.

Sliwkowski, M.X. and Mellman, I. 2013. Antibody therapeutics in cancer. *Science.* **341**(6151), pp.1192-1198.

Smith, G.P. 1985. Filamentous fusion phage: novel expression vectors that display cloned antigens on the virion surface. *Science.* **228**(4705), pp.1315-1317.

Songyang, Z., Shoelson, S.E., Chaudhuri, M., Gish, G., Pawson, T., Haser, W.G., King, F., Roberts, T., Ratnofsky, S., Lechleider, R.J. and et al. 1993. SH2 domains recognize specific phosphopeptide sequences. *Cell.* **72**(5), pp.767-778.

Songyang, Z., Shoelson, S.E., McGlade, J., Olivier, P., Pawson, T., Bustelo, X.R., Barbacid, M., Sabe, H., Hanafusa, H., Yi, T. and et al. 1994. Specific motifs recognized by the SH2 domains of Csk, 3BP2, fps/fes, GRB-2, HCP, SHC, Syk, and Vav. *Molecular Cell Biology.* **14**(4), pp.2777-2785.

Soriano, J.V., Liu, N., Gao, Y., Yao, Z.J., Ishibashi, T., Underhill, C., Burke, T.R., Jr. and Bottaro, D.P. 2004. Inhibition of angiogenesis by growth factor receptor bound protein 2-Src homology 2 domain bound antagonists. *Molecular Cancer Therapeutics.* **3**(10), pp.1289-1299.

Sorkin, A., McClure, M., Huang, F. and Carter, R. 2000. Interaction of EGF receptor and grb2 in living cells visualized by fluorescence resonance energy transfer (FRET) microscopy. *Current Biology.* **10**(21), pp.1395-1398.

Spencer-Smith, R., Koide, A., Zhou, Y., Eguchi, R.R., Sha, F., Gajwani, P., Santana, D., Gupta, A., Jacobs, M., Herrero-Garcia, E., Cobbert, J., Lavoie, H., Smith, M., Rajakulendran, T., Dowdell, E., Okur, M.N., Dementieva, I., Sicheri, F., Therrien, M., Hancock, J.F., Ikura, M., Koide, S. and O'Bryan, J.P. 2017. Inhibition of RAS function through targeting an allosteric regulatory site. *Nature Chemistry & Biology.* **13**(1), pp.62-68.

Stadler, L.K., Hoffmann, T., Tomlinson, D.C., Song, Q., Lee, T., Busby, M., Nyathi, Y., Gendra, E., Tiede, C., Flanagan, K., Cockell, S.J., Wipat, A., Harwood, C., Wagner, S.D., Knowles, M.A., Davis, J.J., Keegan, N. and Ferrigno, P.K. 2011. Structure-function studies of an engineered scaffold protein derived from Stefin A. II: Development and applications of the SQT variant. *Protein Engineering, Design and Selection.* **24**(9), pp.751-763.

Stocks, M.R. 2004. Intrabodies: production and promise. *Drug Discovery Today.* **9**(22), pp.960-966.

Stoevesandt, O. and Taussig, M.J. 2012. European and international collaboration in affinity proteomics. *New Biotechnology.* **29**(5), pp.511-514.

Subik, K., Lee, J.F., Baxter, L., Strzepek, T., Costello, D., Crowley, P., Xing, L., Hung, M.C., Bonfiglio, T., Hicks, D.G. and Tang, P. 2010. The Expression Patterns of ER, PR, HER2, CK5/6, EGFR, Ki-67 and AR by Immunohistochemical Analysis in Breast Cancer Cell Lines. *Breast Cancer*

(Auckl). **4**, pp.35-41.

Sutandy, F.X., Qian, J., Chen, C.S. and Zhu, H. 2013. Overview of protein microarrays. *Curr Protoc Protein Science.* **Chapter 27**, pUnit 27.21.

Takayanagi, H. 2007. Osteoimmunology: shared mechanisms and crosstalk between the immune and bone systems. *Nature Reviews Immunology.* **7**(4), pp.292-304.

Tanaka, M., Gupta, R. and Mayer, B.J. 1995. Differential inhibition of signaling pathways by dominant-negative SH2/SH3 adapter proteins. *Molecular Cell Biology.* **15**(12), pp.6829-6837.

Tang, A.A., Tiede, C., Hughes, D.J., McPherson, M.J. and Tomlinson, D.C. 2017. Isolation of isoform-specific binding proteins (Affimers) by phage display using negative selection. *Science Signaling.* **10**(505).

Tannapfel, A., Anhalt, K., Hausermann, P., Sommerer, F., Benicke, M., Uhlmann, D., Witzigmann, H., Hauss, J. and Wittekind, C. 2003. Identification of novel proteins associated with hepatocellular carcinomas using protein microarrays. *Journal of Pathology.* **201**(2), pp.238-249.

Tari, A.M. and Lopez-Berestein, G. 2001. GRB2: a pivotal protein in signal transduction. *Seminars in Oncology.* **28**(5 Suppl 16), pp.142-147.

Tartaglia, M., Mehler, E.L., Goldberg, R., Zampino, G., Brunner, H.G., Kremer, H., van der Burgt, I., Crosby, A.H., Ion, A., Jeffery, S., Kalidas, K., Patton, M.A., Kucherlapati, R.S. and Gelb, B.D. 2001. Mutations in PTPN11, encoding the protein tyrosine phosphatase SHP-2, cause Noonan syndrome. *Nature Genetics.* **29**(4), pp.465-468.

Taussig, M.J., Stoevesandt, O., Borrebaeck, C.A., Bradbury, A.R., Cahill, D., Cambillau, C., de Daruvar, A., Dubel, S., Eichler, J., Frank, R., Gibson, T.J., Gloriam, D., Gold, L., Herberg, F.W., Hermjakob, H., Hoheisel, J.D., Joos, T.O., Kallioniemi, O., Koegl, M., Konthur, Z., Korn, B., Kremmer, E., Krobitsch, S., Landegren, U., van der Maarel, S., McCafferty, J., Muyldermans, S., Nygren, P.A., Palcy, S., Pluckthun, A., Polic, B., Przybylski, M., Saviranta, P., Sawyer, A., Sherman, D.J., Skerra, A., Templin, M., Ueffing, M. and Uhlen, M. 2007. ProteomeBinders: planning a European resource of affinity reagents for analysis of the human proteome. *Nature Methods.* **4**(1), pp.13-17.

Thomas, P. and Smart, T.G. 2005. HEK293 cell line: a vehicle for the expression of recombinant proteins. *Journal of Pharmacology Toxicology Methods.* **51**(3),

pp.187-200.

Tiede, C., Bedford, R., Heseltine, S.J., Smith, G., Wijetunga, I., Ross, R., AlQallaf, D., Roberts, A.P., Balls, A., Curd, A., Hughes, R.E., Martin, H., Needham, S.R., Zanetti-Domingues, L.C., Sadigh, Y., Peacock, T.P., Tang, A.A., Gibson, N., Kyle, H., Platt, G.W., Ingram, N., Taylor, T., Coletta, L.P., Manfield, I., Knowles, M., Bell, S., Esteves, F., Maqbool, A., Prasad, R.K., Drinkhill, M., Bon, R.S., Patel, V., Goodchild, S.A., Martin-Fernandez, M., Owens, R.J., Nettleship, J.E., Webb, M.E., Harrison, M., Lippiat, J.D., Ponnambalam, S., Peckham, M., Smith, A., Ferrigno, P.K., Johnson, M., McPherson, M.J. and Tomlinson, D.C. 2017. Affimer proteins are versatile and renewable affinity reagents. *Elife.* **6**.

Tiede, C., Tang, A.A.S., Deacon, S.E., Mandal, U., Nettleship, J.E., Owen, R.L., George, S.E., Harrison, D.J., Owens, R.J., Tomlinson, D.C. and McPherson, M.J. 2014. Adhiron: a stable and versatile peptide display scaffold for molecular recognition applications. *Protein Engineering, Design & Selection* **27** (5), pp.145-155.

Tinti, M., Kiemer, L., Costa, S., Miller, M.L., Sacco, F., Olsen, J.V., Carducci, M., Paoluzi, S., Langone, F., Workman, C.T., Blom, N., Machida, K., Thompson, C.M., Schutkowski, M., Brunak, S., Mann, M., Mayer, B.J., Castagnoli, L. and Cesareni, G. 2013. The SH2 domain interaction landscape. *Cell Reports.* **3**(4), pp.1293-1305.

Uhlen, M., Bjorling, E., Agaton, C., Szigyarto, C.A., Amini, B., Andersen, E., Andersson, A.C., Angelidou, P., Asplund, A., Asplund, C., Berglund, L., Bergstrom, K., Brumer, H., Cerjan, D., Ekstrom, M., Elobeid, A., Eriksson, C., Fagerberg, L., Falk, R., Fall, J., Forsberg, M., Bjorklund, M.G., Gumbel, K., Halimi, A., Hallin, I., Hamsten, C., Hansson, M., Hedhammar, M., Hercules, G., Kampf, C., Larsson, K., Lindskog, M., Lodewyckx, W., Lund, J., Lundeberg, J., Magnusson, K., Malm, E., Nilsson, P., Odling, J., Oksvold, P., Olsson, I., Oster, E., Ottosson, J., Paavilainen, L., Persson, A., Rimini, R., Rockberg, J., Runeson, M., Sivertsson, A., Skollermo, A., Steen, J., Stenvall, M., Sterky, F., Stromberg, S., Sundberg, M., Tegel, H., Tourle, S., Wahlund, E., Walden, A., Wan, J., Wernerus, H., Westberg, J., Wester, K., Wrethagen, U., Xu, L.L., Hober, S. and Ponten, F. 2005. A human protein atlas for normal and cancer tissues based on antibody proteomics. *Molecular Cell Proteomics.* **4**(12), pp.1920-1932.

Uhlen, M., Graslund, S. and Sundstrom, M. 2008. A pilot project to generate affinity reagents to human proteins. *Nature Methods.* **5**(10), pp.854-855.

Verbeek, B.S., Adriaansen-Slot, S.S., Rijksen, G. and Vroom, T.M. 1997. Grb2 overexpression in nuclei and cytoplasm of human breast cells: a histochemical and biochemical study of normal and neoplastic mammary tissue specimens. *Journal of Pathology.* **183**(2), pp.195-203.

Waksman, G., Kumaran, S. and Lubman, O. 2004. SH2 domains: role, structure and implications for molecular medicine. *Expert Reviews in Molecular Medicine.* **6**(3), pp.1-18.

Waksman, G., Shoelson, S.E., Pant, N., Cowburn, D. and Kuriyan, J. 1993. Binding of a high affinity phosphotyrosyl peptide to the Src SH2 domain: crystal structures of the complexed and peptide-free forms. *Cell.* **72**(5), pp.779-790.

Walker, B.J., Stan, G.V. and Polizzi, K.M. 2017. Intracellular delivery of biologic therapeutics by bacterial secretion systems. *Expert Reviews in Molecular Medicine.* **19**, pe6.

Wei, C.Q., Gao, Y., Lee, K., Guo, R., Li, B., Zhang, M., Yang, D. and Burke, T.R., Jr. 2003. Macrocyclization in the design of Grb2 SH2 domain-binding ligands exhibiting high potency in whole-cell systems. *Journal of Medicinal Chemistry.* **46**(2), pp.244-254.

Weiss, G.A., Watanabe, C.K., Zhong, A., Goddard, A. and Sidhu, S.S. 2000. Rapid mapping of protein functional epitopes by combinatorial alanine scanning. *Proceedings of the National Academy of Sciences.* **97**(16), pp.8950-8954.

Williams, S.P., Barthorpe, A.S., Lightfoot, H., Garnett, M.J. and McDermott, U. 2017. High-throughput RNAi screen for essential genes and drug synergistic combinations in colorectal cancer. *Scientific Data*. **4**, p170139.

Wojcik, J., Hantschel, O., Grebien, F., Kaupe, I., Bennett, K.L., Barkinge, J., Jones, R.B., Koide, A., Superti-Furga, G. and Koide, S. 2010. A potent and highly specific FN3 monobody inhibitor of the Abl SH2 domain. *Nature Structural & Molecular Biology.* **17**(4), pp.519-527.

Wojcik, J., Lamontanara, A.J., Grabe, G., Koide, A., Akin, L., Gerig, B., Hantschel, O. and Koide, S. 2016. Allosteric Inhibition of Bcr-Abl Kinase by High Affinity Monobody Inhibitors Directed to the Src Homology 2 (SH2)-Kinase Interface. *Journal of Biological Chemistry* . **291**(16), pp.8836-8847.

Wold, E.D., Smider, V.V. and Felding, B.H. 2016. Antibody Therapeutics in

Oncology. *Immunotherapy.* **2**(1).

Wong, L., Deb, T.B., Thompson, S.A., Wells, A. and Johnson, G.R. 1999. A differential requirement for the COOH-terminal region of the epidermal growth factor (EGF) receptor in amphiregulin and EGF mitogenic signaling. *Journal of Biological Chemistry .* **274**(13), pp.8900-8909.

Wu, C., Sun, M., Liu, L. and Zhou, G.W. 2003. The function of the protein tyrosine phosphatase SHP-1 in cancer. *Gene.* **306**, pp.1-12.

Wu, C.H., Liu, I.J., Lu, R.M. and Wu, H.C. 2016. Advancement and applications of peptide phage display technology in biomedical science. *Journal of Biomedical Science.* **23**, p8.

Y.J.Wang, J. 2010. Nuclear and Cytoplasmic Functions of Abl Tyrosine Kinase. In: Bradshaw, R.A. and Dennis, E.A. eds. *Handbook of Cell Signaling* 2ed. Elsevier Inc, pp.2217-2223.

Yamazaki, T., Zaal, K., Hailey, D., Presley, J., Lippincott-Schwartz, J. and Samelson, L.E. 2002. Role of Grb2 in EGF-stimulated EGFR internalization. *Journal of Cell Science.* **115**(9), pp.1791-1802.

Yeh, J.T.H., Binari, R., Gocha, T., Dasgupta, R. and Perrimon, N. 2013. PAPTi: A Peptide Aptamer Interference Toolkit for Perturbation of Protein-Protein Interaction Networks. *Scientific Reports.* **3**(1), p1156.

Yodmongkol, S., Sutapun, B., Praphanphoj, V., Srikhirin, T., Brandstetter, T. and Rühe, J. 2016. Fabrication of protein microarrays for alpha fetoprotein detection by using a rapid photo-immobilization process. *Sensing and Bio-Sensing Research.* **7**, pp.95-99.

Young, R.M., Hardy, I.R., Clarke, R.L., Lundy, N., Pine, P., Turner, B.C., Potter, T.A. and Refaeli, Y. 2009. Mouse models of non-Hodgkin lymphoma reveal Syk as an important therapeutic target. *Blood.* **113**(11), pp.2508-2516.

Yu, Y., Luk, F., Yang, J.L. and Walsh, W.R. 2011. Ras/Raf/MEK/ERK pathway is associated with lung metastasis of osteosarcoma in an orthotopic mouse model. *Anticancer Research*. **31**(4), pp.1147–1152.

Yue, P. and Turkson, J. 2009. Targeting STAT3 in cancer: how successful are we? *Expert Opinion on Investigational Drugs.* **18**(1), pp.45-56.

Zang, X.P., Siwak, D.R., Nguyen, T.X., Tari, A.M. and Pento, J.T. 2004. KGF-induced motility of breast cancer cells is dependent on Grb2 and Erk1,2. *Clinical & Experimental Metastasis.* **21**(5), pp.437-443.

Zanotti, R., Frattini, F., Ghia, P., Visco, C., Zamo, A., Perbellini, O., Stella, S., Facco, M., Giaretta, I., Chilosi, M., Pizzolo, G. and Ambrosetti, A. 2010. ZAP-70 expression is associated with increased risk of autoimmune cytopenias in CLL patients. *American Journal of Hematology.* **85**(7), pp.494-498.

Zhu, L., Ly, H. and Liang, Y. 2014. PLC-γ1 signaling plays a subtype-specific role in postbinding cell entry of influenza A virus. *Journal of Virology.* **88**(1), pp.417-424.

Ziegler, A., Nervi, P., Durrenberger, M. and Seelig, J. 2005. The cationic cell-penetrating peptide CPP(TAT) derived from the HIV-1 protein TAT is rapidly transported into living fibroblasts: optical, biophysical, and metabolic evidence. *Biochemistry.* **44**(1), pp.138-148.

Appendix A
Vector Maps

Figure 1. *Vector map of the pBSTG phagemid vector (Tiede et al., 2014).*

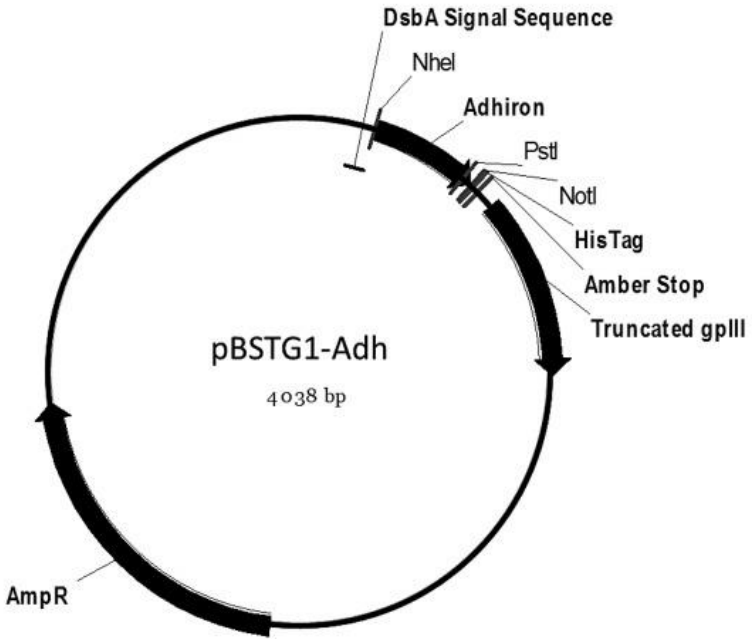

Figure 2. *Vector map of the pET11a Affimer-containing expression vector (Tiede et al., 2014).*

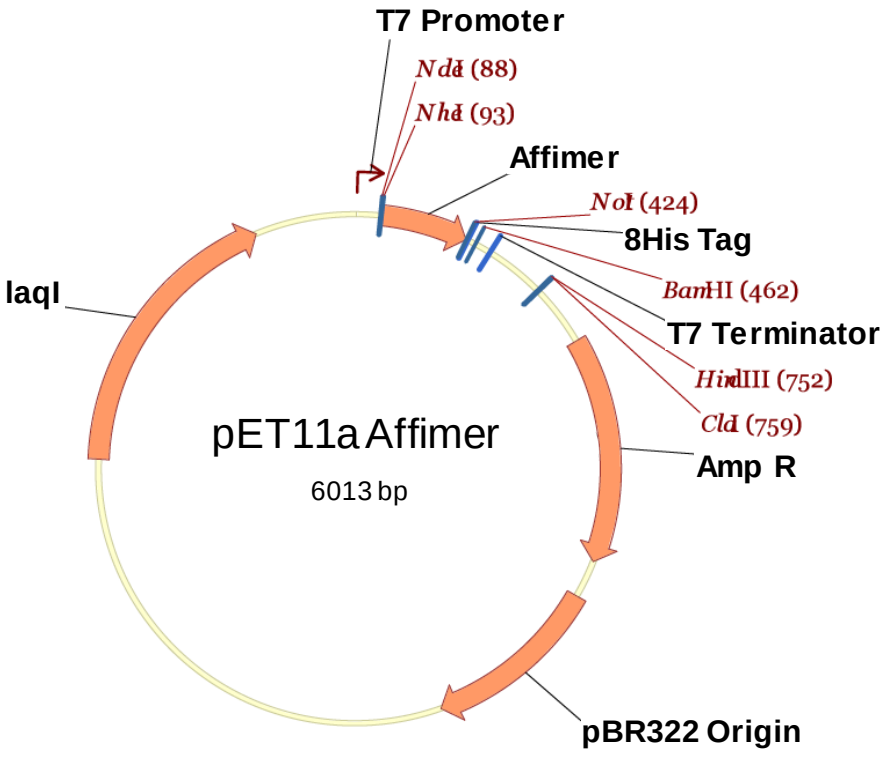

Figure 3. *Vector map of the pET-lectra expression vector, showing the multiple cloning site in which the Affimer was subcloned between the two SapI sites.*

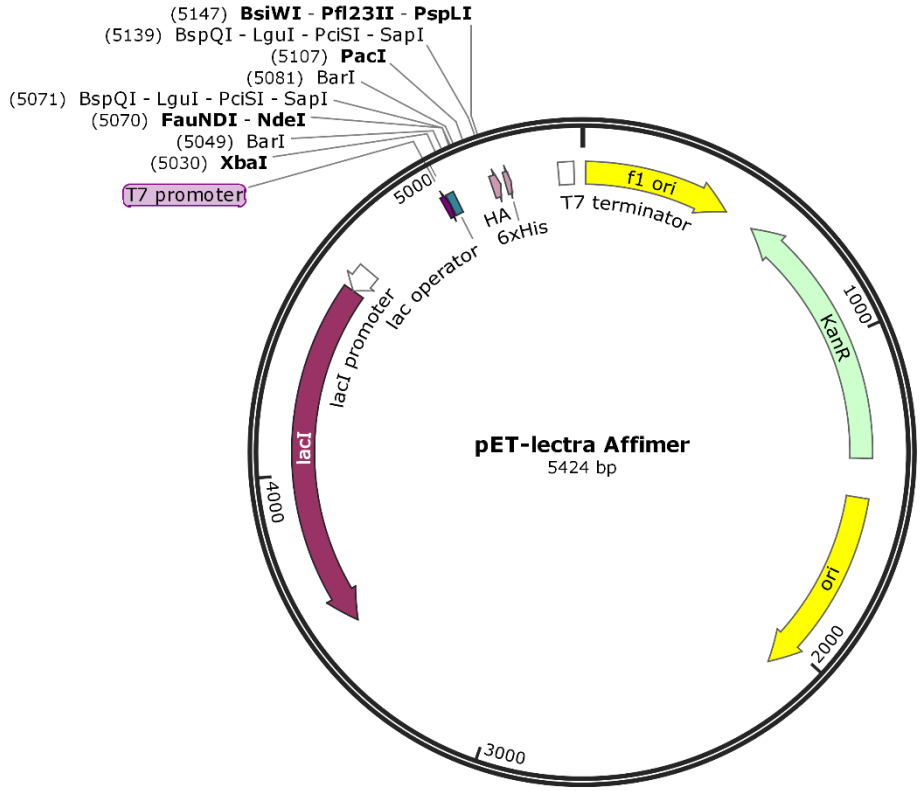

Figure 4. *Vector map of the pET28 SacB AP expression vector, in which the SH2 domains were encoded between the 6XHis-tag and TEV site sequences (Samuel Lunenfeld Research Institute, Canada).*

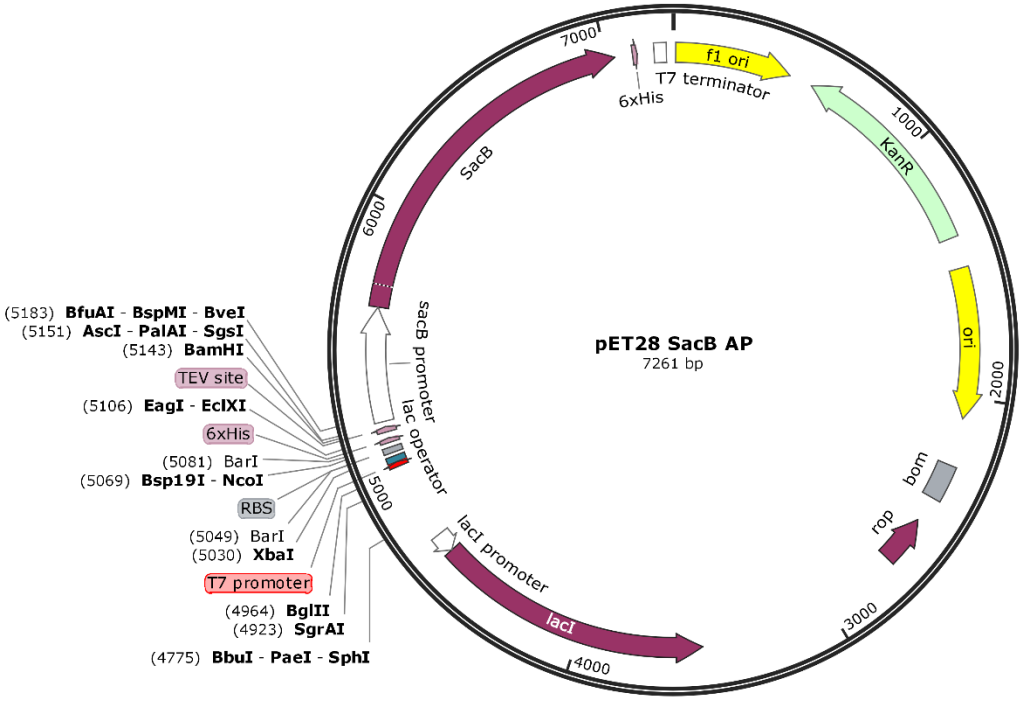

Figure 5. *Vector map of the pcDNA5 mammalian expression vector (Invitrogen™ catalogue number V601020).*

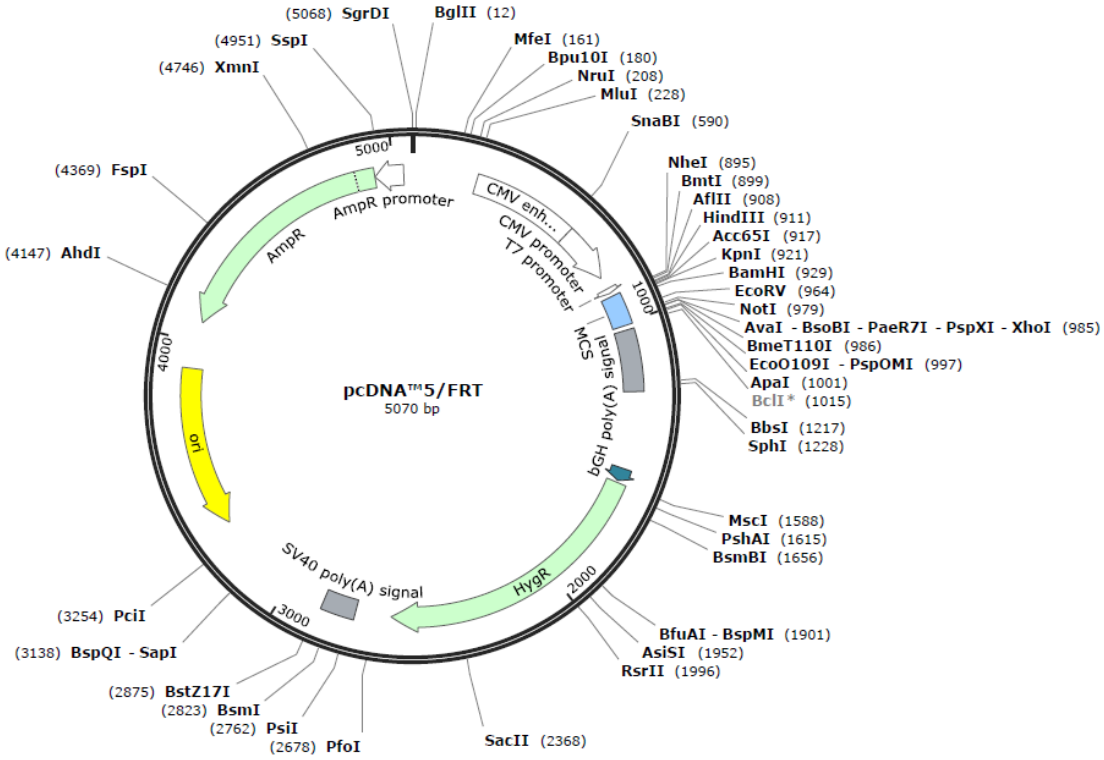

Figure 6. *Vector map of the pRetroX-PTuner retroviral vector (Clontech™ catalogue number 632171).*

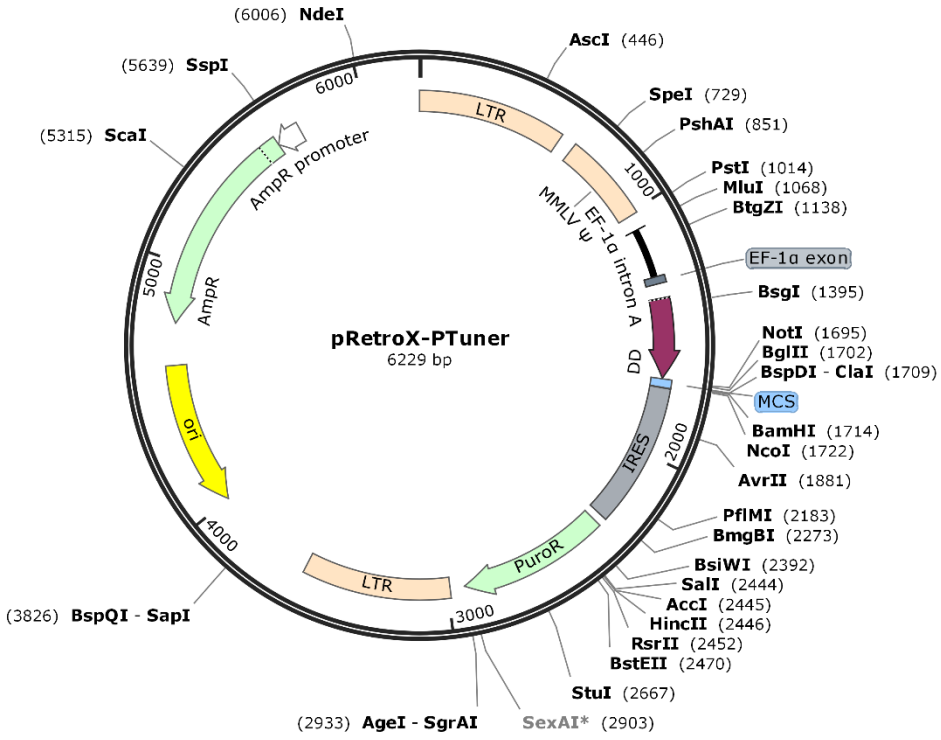

Figure 7. *Vector map of the pBABE-puro retroviral vector (AddGene catalogue number 1794).*

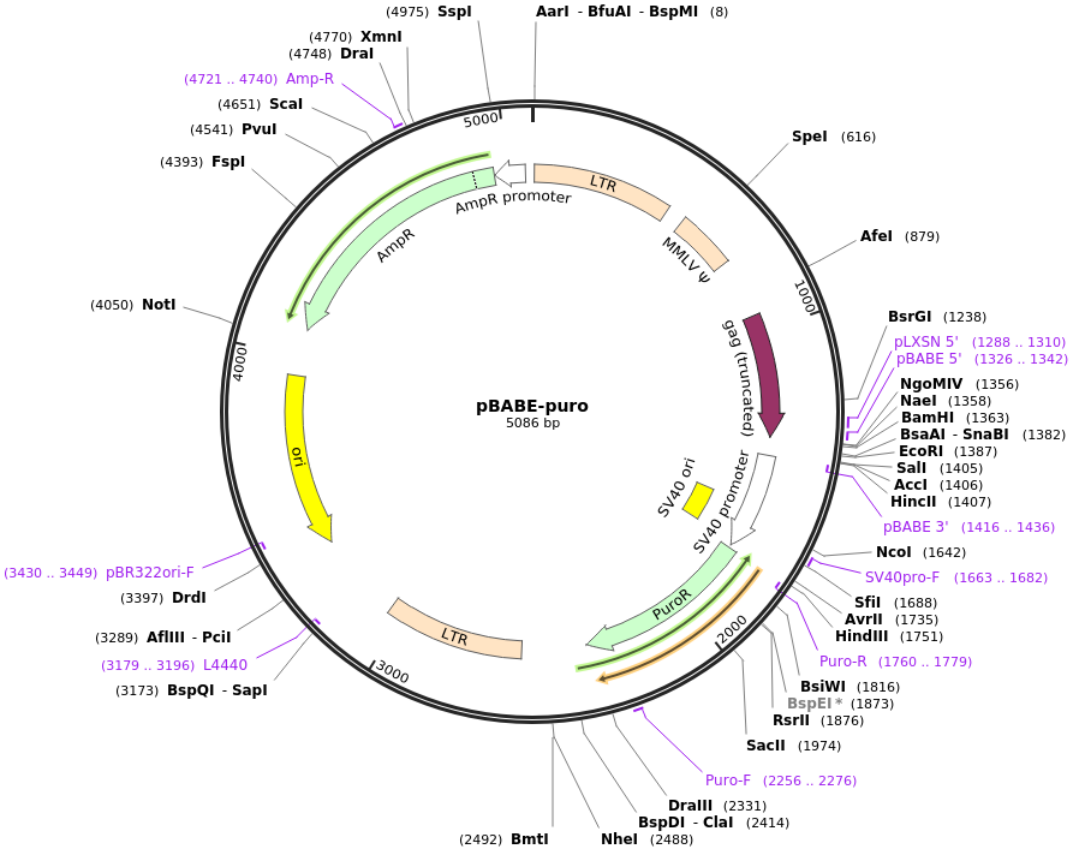

Appendix B
SH2 domain targets

The following table lists the SH2 domain targets used in this study, showing the abbreviation used in the text, as well as the full name of their parent protein.

SH2 Target Name	Description / Parent Protein
Abl1	Abelson tyrosine-protein kinase 1
Abl2	Abelson tyrosine-protein kinase 2, also known as Abelson-related gene protein (Arg)
Bmx	Cytoplasmic tyrosine-protein kinase Bmx (Bone marrow tyrosine kinase gene in chromosome X)
Crk	Adapter molecule Crk, also known as proto-oncogene c-Crk, p38
Fyn	Tyrosine-protein kinase Fyn, also known as proto-oncogene Syn
Grb2	Growth factor receptor-bound protein 2, also known as Ash
Grb7	Growth factor receptor-bound protein 7
Grb10	Growth factor receptor-bound protein 10
Grb14	Growth factor receptor-bound protein 14
Lck	Tyrosine-protein kinase Lck, also known as leukocyte C-terminal Src kinase
Lyn	Tyrosine-protein kinase Lyn (Lck/Yes novel tyrosine kinase)
Nck1	Cytoplasmic protein Nck1 (non-catalytic region of tyrosine kinase adaptor protein 1)
Nck2	Cytoplasmic protein Nck2 (non-catalytic region of tyrosine kinase adaptor protein 2), also known as Grb4
P85α-C	C-terminal SH2 domain of phosphatidylinositol 3-kinase (PI3K) regulatory subunit alpha
P85α-N	N-terminal SH2 domain of phosphatidylinositol 3-kinase (PI3K) regulatory subunit alpha
P85β-C	C-terminal SH2 domain of phosphatidylinositol 3-kinase (PI3K) regulatory subunit beta
P85β-N	N-terminal SH2 domain of phosphatidylinositol 3-kinase (PI3K) regulatory subunit beta
P55γ-C	C-terminal SH2 domain of phosphatidylinositol 3-kinase (PI3K) regulatory subunit gamma
P55γ-N	N-terminal SH2 domain of phosphatidylinositol 3-kinase (PI3K) regulatory subunit gamma
PLCγ1-T	Both SH2 domains of phospholipase C-gamma-1, also known as 1-phosphatidylinositol 4,5-bisphosphate phosphodiesterase gamma-1, in tandem
PLCγ1-N	N-terminal SH2 domain of phospholipase C-gamma-1
PLCγ2-T	Both SH2 domains of phospholipase C-gamma-2, 1-phosphatidylinositol 4,5-bisphosphate phosphodiesterase gamma-2, in tandem
PLCγ2-N	N-terminal SH2 domain of phospholipase C-gamma-2
PLCγ2-C	C-terminal SH2 domain of phospholipase C-gamma-2

Continued overleaf

SH2 Target Name	Description / Parent Protein
Ptpn11-N	N-terminal SH2 domain of tyrosine-protein phosphatase non-receptor type 11, also known as SHP-2
She	SH2 domain-containing adapter protein E
Ship1	Phosphatidylinositol 3,4,5-trisphosphate 5-phosphatase 1, also known as SH2 domain-containing inositol 5'-phosphatase 1
Ship2	Phosphatidylinositol 3,4,5-trisphosphate 5-phosphatase 2, also known as SH2 domain-containing inositol 5'-phosphatase 2
Src1	Proto-oncogene tyrosine-protein kinase Src, also known as c-Src
Src2	c-Src 2, also known as tyrosine-protein kinase Fgr
Stat1	Signal transducer and activator of transcription 1
Stat2	Signal transducer and activator of transcription 2
Stat3	Signal transducer and activator of transcription 3
Stat4	Signal transducer and activator of transcription 4
Stat5a	Signal transducer and activator of transcription 5A
Stat5b	Signal transducer and activator of transcription 5B
Stat6	Signal transducer and activator of transcription 6
Syk-C	C-terminal SH2 domain of tyrosine-protein kinase Syk, also known as spleen tyrosine kinase
Syk-N	N-terminal SH2 domain of tyrosine-protein kinase Syk, also known as spleen tyrosine kinase
Tec	Tyrosine-protein kinase Tec
Tns1	Tensin-1
Vav1	Proto-oncogene vav
Yes	Tyrosine-protein kinase Yes, also known as proto-oncogene c-Yes

Appendix C
SH2 domain Affimer reagents for use in protein microarrays

The following pages list all SH2 domain Affimer clones chosen to take forward in protein microarrays. Clones highlighted in pink were not successfully subcloned into the relevant expression vectors, and therefore emitted from the experiment.

SH2 Target	Affimer Clones	Scaffold Type	VR1	VR2
Abl1	A1	II	LINWGEYMD	EEDHYTQMH
	B6	II	YFQIEGYPQ	YYYRFIHMD
	B3	II	GMLYYWPPD	AAE
	C2	II	NVVYVDAGF	EDEHIAIWF
	G2	II	EHLMDEYSD	EEYSYQKHS
Abl2	E1	II	QPLEWLELP	AAE
	B3	II	MPLDWLPMP	AAE
	D4	II	PPLPWLKVP	AAE
	A2	II	KALYYWPPD	NMGPDPMHH
	A1	II	APLDWLDLP	EDHNAGNFS
Bmx	G1	II	IRYSSFATQ	RSMPMIKLH
	A1	II	FKYFSSHKI	RYQSIIHLK
	D1	II	GNIVQQWYH	DTPGMWHWN
	A4	II	YHEYQNGAF	WYPYNLWLK
	A3	I	MPAYFEKWY	FSDEEFNPW
Crk	A2	II	TVDYTNQQH	KDRLTWGFW
	A1	II	FYDWPGNEYQSI	VAWMKNNVN
	D1	II	QSAWTGEQH	EVHYPFSFS
	F3	II	YDMPYPTVG	LWLKQYKGM
	H3	II	DWWNFPVFN	AAE
Fyn	D2	II	QYLNSYWHG	KIMIEEDVY
	A2	II	DQKMDEYQD	YIFFDPWWV
	D3	II	YRNQSGDQD	YIYFSPWWV
	A4	II	IGEFAQKWA	EVWMDPWKV
	E2	II	EMVWMWQLG	HIKHTDYDF
Grb2	8	II	QWSWQNAVD	VRPRGLFWD
	12	II	FQPIYINIV	PDEPRYVLG
	A4	II	HVLWENAGP	HTRYEYFVY
	A6	II	HEYPMHQHN	PLFMNVPLP
	B4	II	KWYQNVMFP	ESIDYPDHE
	B5	II	NKEQRHWSE	FQYVNWPVP
	C1	II	RHWVNVPFP	GDGFDNALH
	C2	II	QWYVNTMSP	EVYHIKNKR
	D1	II	KWYMNTMFP	EPGRFNEML
	D2	II	DPKKYVNV	NPVDKFDKI
	D5	II	FSHAYMNVV	VGGGGN
	D6	II	PWYQNVPYP	REERNMNAM
	F1	II	RWYVNVSLP	DNMDNMNKI
	F5	II	DWWEAGVFM	WNEINYMFD
	H1	II	RKLWENYKE	AMRMYYPEW
	H4	II	RWYVNIKFP	NWTEFNSKT
Grb7	D6 (standard)	II	MWYEAKYDH	YPFGYYYNN
	G2 (competitive)	II	WQENNFGMQ	SGWYSNPQF
	C1 (competitive)	II	QASDRYWHS	DSEYANPIY
	A2 (competitive)	II	PYGQSVTPG	FYFTNWYAN
	E2 (competitive)	II	PDAHLHESV	FPYGRYYSN
	G3 (competitive)	II	QLSWGYPAT	YIYGPEYSN
Grb10	D7 (competitive)	II	RQESPMIRD	WWYFPSAIM
	H7 (competitive)	II	MMWTEWEPELYVFG	KWPPMSQLM
	D9 (competitive)	II	SVTQPTRLQ	QWYFPMATM

SH2 Target	Affimer Clones	Scaffold Type	VR1	VR2
Grb14	F3 (competitive)	II	ARPEEPHWW	YKDNVYYFL
	A1 (competitive)	II	EPKLYENQQ	PMVIPARWT
	D4 (competitive)	II	PHPYISRE	FFYENNNTH
Lck	A1	II	ITHELFMD	QKAYILRYG
	A7	II	VWHVRDPRS	QWIFNHADL
	A9	II	QHTSPSEQW	KLFEKIITL
	B2	II	VVGRDWQVA	KLVMPSFNY
	B9	II	QWNDRTPIA	RWIGPTFIM
Lyn	A4	II	EWQKKGYVS	ERSVKWVLP
	A2	II	AEEFMTFMG	QFLMPRMNL
	C2	II	PEGSGITVA	RWNMPKRFV
	B2	II	PEMMNVFWV	TYIMPPGRI
Nck1	A1	II	KFVYDPVAH	TNIYNRYSF
	F1	II	PQEHGWWHH	FPAPAYPEI
	F2	II	QVNVDPIVL	QNYYNQHMF
Nck2	C3	II	YIYAPGWGL	WYFQERNVF
	E1	II	YESVSSDES	NFHMIFTHW
	G1	II	NKAYADSP	NVFEFKISH
	G6	II	KRKKLRIRN	AAE
P85α-C	C1	II	DIWAIQHVI	DDLNFNMRD
	A1	II	WMWGFMDEE	IVWSTPAEE
	F4	II	WFFEQAYEV	VSWDFSPVF
P85α-N	D1	II	YYWSHFQQS	TDINDPYER
	B1	II	ISMARFDGT	KYIQVELDG
	A1	II	IMEEDYYWL	PWMMPILLI
	C6	II	WDPEYQFIG	HWMRPEKLI
	H2	II	FEFNYNGQF	WIMLFDDGD
	D2 (old screen)	II	WEWQAWGSQ	HNKEFMPNW
	D6 (old screen)	II	WAYGADYHM	PWMIPVLLF
	E5 (old screen)	II	SYFIAMYEY	NENYFMPLV
	G6 (old screen)	II	WTDRGPYDH	PFMNPLNLL
	H1 (old screen)	II	WFTEVGPDH	QWLLPIHLM
	H6 (old screen)	II	TYYIAHYEY	YEQGMMLWD
P85β-C	C1	II	HAFDDPDQD	AAE
	C2	II	HAFDDHSQD	AAE
	D1	II	HAFEQYDID	AAE
	A3	II	YAFDDPSQD	AAE
	F1	II	HAFEDWQQD	AAE
	H4	I	AVFPAE	AAQATRLLADLE
P85β-N	A1	II	PQSDHMNAE	YGTNWLADL
	H2	II	DWQALPIDQ	ENNAWARIT
	C1	II	SYFIAMYEY	NENYFMPLV
	E6	II	AAVVAYITS	QEHWQHYMI
	A3	I	LTKHYY	YHIKHLLIAPSL
P55γ-C	C1	II	LESQETVEF	LPQRLMTIW
	B5	II	PPGRAGIEW	LPHYLLTIW
	G1	II	PKYGEVSPH	IPHLILRIW
	E5	II	NMMHARRQW	EPHRLFVVW
	E3	II	YNSVDPHYD	MPHRLLTIW
P55γ-N	F2	II	WTDRGPYDH	PFMNPLNLL
	G2	I	WEEYHE	MSRTEYRDMSDR
	F1	I	WEEYHE	SGQHMEPSWPII
	D1	I	WEEYHE	YAVIYNPAASMS
PLCγ1-T	E10 (pan 3)	II	VRFLFKTIP	HAPNHQGIT
	B8 (pan 3)	II	YKLLMPAFP	NFDRHAIGR
	E9 (pan 3)	II	FRILMSGFP	QGPNAYEKF
	A5	I	TKSGPFTFH	REIGKSRDV
	B10 (pan 3)	II	YRFMITAMP	NGHKPIV
PLCγ1-N	B7	II	WMDNFWRRM	QVHGNPWMD
	E10	II	HENTTFYSN	KYPHTWNIS

SH2 Target	Affimer Clones	Scaffold Type	VR1	VR2
PLCγ2-T	A1	II	HRWWYDNFV	LAGHYAPSV
	B1	II	VIMLTWSPE	DQHMYEGWD
	G4	II	QYMSITADD	YNYSRKRHN
PLCγ2-N	B3 (– BAP)	II	KQTVVEPTQ	SYWFLPMKQ
	B8 (– BAP)	II	AQYMPHWR	YNWLDEGYS
	C2 (– BAP)	II	MSKHEISEV	RYYAWAGWA
	A7	II	PWERIDISD	YQYYNNLKM
	A8	II	HTFTWKWWY	NEDIESYEL
She	G1	II	MYANYTDWA	RSRPKWKEI
	B1	II	EQYDLQFT	TWAPEEGLE
	C1	II	YYANYDVTA	YFRLGQTR
	E4	II	AWSWYNMDE	TFVQVFPRF
	B4	II	MHLIMYERP	TFDNIWIPD
Ship1	D9 (standard)	II	VEYYDMTEL	WENRNFKSA
	C8 (standard)	II	AHGPPDYHM	SIYFPMNYW
	A11 (standard)	II	KEEWYPYQK	YLKAAFIEF
Ship2	G5 (standard)	II	KYHDGYGPEPE	GLWWTPAHF
	A1 (competitive)	I	NTHWDHQNY	IYKNWKLIG
	H5 (competitive)	I	AGMYMD	QYKITTEGVKWD
	C2 (competitive)	I	QGVYVD	NYMFTAAGWQHT
	A5 (standard)	I	PTQPIM	LWEFTPNSTIVH
	G4 (standard)	I	RMFYGT	MMTWQDQVFDVT
	B1 (competitive)	I	RMFYGT	MMTWQDQVFDVT
	E6 (competitive)	I	KGVFMH	SYQISQGHVAVF
Src1	A1	II	IEKRAVISS	RERRLHLTP
	A2	II	QMFGQSPSY	RKYWLG
	A4	II	IRFLFFWVG	AAE
	D1	II	SSWFFTRNE	DMMLGSGNY
Stat1	A1	II	PPDYIYQRF	WAFGMMMGP
	D5	II	LPEQWAKRFRIIM	AAE
	G6	I	PVYHKKVFF	YRVEAEGMW
	E1	I	NNYRKLRVT	HVFNMSSLQ
Stat3	H2	II	HGPVRVPWQ	DYGANLPLL
	D6	II	FQYMDMWIE	VFQSSTHPF
	E1	II	EWDPGHPWR	ELLINMHYE
	H6	II	SPEEETPWA	SFQVNLQWI
	B1	II	EHDPTNPWT	RIQFHQQWH
Stat4	F3	II	FQNMWHSHS	QDLMLYQAP
	H3	II	TIHFRTFNS	EYIGNVFPM
	H2	II	HTFDYPAIH	PRIGKPKPK
	E2	II	YQWNYPKIE	RVRAPTSDA
	F4	II	YRYEYPLIH	QQMHHKGSN
Stat5a	D4	II	IVQRPPQQA	NYIWNWNIS
	A2	II	KQQFPQSQQ	TNFNIKLIK
Stat5b	E6	II	KTVRGVFQD	AYRWEHNFG
	G6	II	MTSMVDGTE	FKMWHWNVM
	H6	II	EPKNKGAHE	IYIYGWNVG
	B6	II	MFERPHQYH	VNIYHMSIS
Stat6	C3	II	HPLEMYEDE	VIYAWGGLM
Syk-N	C3	II	RTYFHGYPE	HFFRHMTHP
	C5	II	PYVVNSGWF	GLLLKRHWA
	D2	II	NWQPLLSYW	PKTGAQELY
	F2	II	RTYPPFVFY	KNQNIFALY
Tec	E3	II	FPDNMVWRQ	IFLPIFTLL
	F3	II	DVSLIADET	EIFRAVWNL
	G2	II	VFSIKHTQK	ELYKYTYSL
	A3	II	VELEHNPDS	TYYTYILTA
	B2	II	HEASKYEW	EPHMLYIMW

Tns1	A1	II	AEEDEEYTG	FWIYENMP
	E4	II	DMRDWEFTN	HDLPKLWEP
	C2	II	THHMSGYFN	PDYPFLWHS
	H5	II	WKHDYGMND	QYYWANQVV
Vav1	F1	II	QYWVNIQDE	TLWQKEPFM
	D1	II	QYWVNDPTE	YMEFDEFEQ
	F4	II	VAFPTNLSE	PNIRLNYHL
	C1	II	NYWVNVDNE	VPKWWQPNM
	F2	II	LYWVNVQDE	YYMDPGMRA

Appendix D
SH2 domain Affimer reagent specificities

The following pages list all SH2 domain Affimer reagents tested in protein microarrays, and their binding specificities. Cross-reactions to targets other than the intended SH2 are detailed (signal ≥10% of the target signal in microarrays). Reagents binding between 0 – 4 other targets have been highlighted (green = specific, blue = +1 other, yellow = +2, orange = +3 and pink = +4).

Affimer Clone	Number of cross-reactions	Additional targets bound
Abl1-A1	1	Abl2
Abl1-B6	Non-binding	
Abl1-B3	4	Abl2, Lyn, PLCγ2-C, Src1
Abl1-C2	0	
Abl1-G2	1	Abl2
Abl2-E1	0	
Abl2-B3	0	
Abl2-D4	0	
Abl2-A2	0	
Abl2-A1	0	
Bmx-G1	0	
Bmx-A1	0	
Bmx-D1	0	
Bmx-A4	0	
Bmx-A3	14	Lck, Lyn, P55γN, P85α-C, P85α-N, PLCγ1T, PLCγ2C, PLCγ2T, Nck2, Src1, Syk-C, Tns1, Vav1, Yes
Crk-A2	Non-binding	
Crk-A1	0	
Crk-D1	Non-binding	
Crk-F3	0	
Crk-H3	0	
Fyn-D2	0	
Fyn-A2	0	
Fyn-D3	0	
Fyn-A4	0	
Fyn-E2	Non-binding	
Grb2-8	Non-binding	
Grb2-12	Non-binding	
Grb2-A4	0	
Grb2-A6	Non-binding	
Grb2-B5	3	Lyn, PLCγ2C, Syk-C
Grb2-C1	6	Abl2, Bmx, Ship1, Syk-C, PLCγ2C, PLCγ2T
Grb2-C2	5	Abl2, Bmx, Ship1, PLCγ2C, P55γN
Grb2-D1	1	Abl2
Grb2-D2	Non-binding	
Grb2-D5	11	Abl1, Bmx, Fyn, Lck, Lyn, Src1, Syk-N, Yes, PLCγ2C, PLCγ2T, P85β-N

Affimer Clone	Number of cross-reactions	Additional targets bound
Grb2-D6	0	
Grb2-F1	0	
Grb2-F5	0	
Grb2-H1	0	
Grb2-H4	8	Abl1, Abl2, Bmx, Crk, Grb14, Src1, PLCγ2T, PLCγ2C
Grb7-D6	Non-binding	
Grb7-G2	10	Bmx, Lyn, P85α-C, PLCγ1T, PLCγ2C, PLCγ2T, Src1, Stat6, Tns1, Vav1
Grb7-C1	9	Bmx, Lyn, Nck2, Stat6, Syk-N, Src1, P55γN, PLCγ2C, PLCγ2T
Grb7-A2	Non-binding	
Grb7-E2	15	Bmx, Fyn, Grb2, Lck, P85α-N, P85β-N, P55γ-N, PLCγ1T, PLCγ2T, PLCγ2C, Ship2, Src1, Syk-C, Tns1, Yes
Grb7-G3	10	Bmx, Fyn, Lck, Lyn, P85α-N, P85β-N, PLCγ2T, PLCγ2C, Src2, Yes
Grb10-D7	Non-binding	
Grb10-H7	12	Abl1, Bmx, Grb14, Lck, Lyn, P55γN, P85α-C, P85α-N, P85β-N, PLCγ2C, PLCγ2T, Syk-C
Grb10-D9	0	
Grb14-F3	0	
Grb14-C3	0	
Grb14-D4	Non-binding	
Lck-A1	3	Fyn, Lyn, Yes
Lck-A7	2	Lyn, P85β-N
Lck-A9	6	Fyn, Lyn, Src1, Src1, Yes, PLCγ2N
Lck-B2	1	Lyn
Lck-B9	1	Lyn
Lyn-A4	1	Lck
Lyn-A2	0	
Lyn-C2	0	
Lyn-B2	0	
Nck2-C3	20	Abl1, Bmx, Fyn, Lck, Lyn, P85α-C, P85α-N, P55γ-N, PLCγ1T, PLCγ2T, PLCγ2C, PLCγ2N, Src1, Stat3, Stat4, Syk-C, Syk-N, Tns1, Vav1, Yes
Nck2-E1	22	Abl1, Bmx, Fyn, Grb10, Grb2, Grb7, Lck, Lyn, P85α-C, P85α-N, P55γ-N, P85β-N, PLCγ1T, PLCγ2T, PLCγ2C, She, Src1, Src2, Syk-C, Tns1, Vav1, Yes
Nck2-G1	13	Abl1, Grb2, Lck, Lyn, P85α-N, P55γ-N, P85β-N, PLCγ1T, PLCγ2T, PLCγ2C, She, Src1, Src2, Syk-C, Tns1, Vav1, Yes
Nck2-G6	Non-binding	
P55γC-C1	0	
P55γC-B5	0	
P55γC-G1	0	
P55γC-E5	0	
P55γC-E3	0	
P55γN-F2	0	

Affimer Clone	Number of cross-reactions	Additional targets bound
P55γN-G2	29	Abl2, Bmx, Fyn, Grb10, Grb7, Lck, Lyn, Nck2, P85α-C, P85α-N, P85β-C, P85β-N, PLCγ1T, PLCγ2C, PLCγ2T, Ptpn11-N, She, Src1, Src2, Stat1, Stat3, Stat4, Stat5a, Stat5b, Syk-C, Syk-N, Tns1, Vav1, Yes
P55γN-F1	15	Bmx, Grb2, Lck, Lyn, P85α-C, P85β-N, PLCγ1T, PLCγ2C, PLCγ2T, Src1, Stat6, Syk-C, Tns1, Yes
P55γN-D1	30	Abl1, Abl2, Bmx, Crk, Fyn, Grb10, Grb14, Grb2, Grb7, Lck, Lyn, Nck2, P85α-C, P85α-N, P85β-C, P85β-N, PLCγ1T, PLCγ2C, PLCγ2T, Ptpn11-N, She, Src1, Src2, Stat3, Stat4, Stat6, Syk-C, Tns1, Vav1, Yes
P55γN-D1	30	Abl1, Abl2, Bmx, Crk, Fyn, Grb10, Grb14, Grb2, Grb7, Lck, Lyn, Nck2, P85α-C, P85α-N, P85β-C, P85β-N, PLCγ1T, PLCγ2C, PLCγ2T, Ptpn11-N, She, Src1, Src2, Stat3, Stat4, Stat6, Syk-C, Tns1, Vav1, Yes
P85αC-C1	Non-binding	
P85αC-A1	Non-binding	
P85αC-F4	Non-binding	
P85αC-C1	Non-binding	
P85αN-D2 (old)	5	Bmx, Lck, Lyn, PLCγ2C, Yes
P85αN-D6 (old)	2	P85β-N, P55γ-N
P85αN-E5 (old)	1	P85β-N
P85αN-G6 (old)	9	P85α-C, P85β-N, P55γ-N, PLCγ1T, Grb14, Grb2, Src1, Tns1, Yes
P85αN-H1 (old)	0	
P85αN-H6 (old)	1	P85β-N
P85αN-D1	4	Crk, P85α-C, P85β-N, Stat6
P85αN-B1	2	P85β-N, P55γ-N
P85αN-A1	1	P55γ-N
P85αN-C6	1	P55γ-N
P85αN-H2	0	
P85βC-C2	Non-binding	
P85βC-D1	Non-binding	
P85βC-A3	Non-binding	
P85βC-F1	Non-binding	
P85βN-A1	2	P55γ-N, P85α-N
P85βN-H2	1	P85α-N
P85βN-C1	1	P85α-N
P85βN-E6	0	
PLCγ1T-E10	Non-binding	
PLCγ1T-B8	7	Bmx, Lyn, P85α-C, PLCγ2T, PLCγ1N, PLCγ2C, PLCγ2N
PLCγ1T-E9	5	PLCγ2T, PLCγ1N, PLCγ2N, Stat5a, Stat6
PLCγ1T-A5	9	PLCγ2C, PLCγ2T, Src1, Stat3, Stat4, Stat5a, Stat5b, Stat6, Tns1
PLCγ1N-B7	0	
PLCγ1N-E10	Non-binding	
PLCγ2T-A1	0	

Affimer Clone	Number of cross-reactions	Additional targets bound
PLCγ2T-B1	10	PLCγ2C, PLCγ2N, Bmx, Grb14, Grb2, Lyn, Src1, Syk-C, Tns1, Yes
PLCγ2T-G4	2	PLCγ2N, PLCγ1N
PLCγ2N-B3	Non-binding	
PLCγ2N-B8	7	Bmx, Lck, Lyn, Src1, Syk-C, PLCγ2C, PLCγ2T
PLCγ2N-C2	16	PLCγ1N, PLCγ1T, PLCγ2C, PLCγ2T, P85α-C, P55γ-C, P85β-N, Bmx, Fyn, Grb10, Grb2, Lck, Lyn, She, Syk-C, Vav1
PLCγ2N-A7	3	Lck, PLCγ1N, PLCγ2T
PLCγ2N-A8	0	
She-G1	Non-binding	
She-B1	Non-binding	
She-C1	Non-binding	
She-E4	Non-binding	
She-B4	Non-binding	
Ship1-D9	Non-binding	
Ship1-C8	0	
Ship2-A1	Non-binding	
Ship2-H5	Non-binding	
Ship2-C2	Non-binding	
Ship2-A5	Non-binding	
Ship2-G4	Non-binding	
Ship2-B1C	Non-binding	
Ship2-E6C	Non-binding	
Ship2-G5S	0	
Src1-A1	Non-binding	
Src1-A2	38	Abl1, Abl2, Bmx, Crk, Fyn, Grb2, Grb7, Grb10, Grb14, Lck, Lyn, Nck2, P85α-C, P85α-N, P85β-C, P85β-N, P55γ-C, P55γ-N, PLCγ1-T, PLCγ1-N, PLCγ2-T, PLCγ2-N, PLCγ2-C, She, Ship1, Ship2, Src2, Stat1, Stat3, Stat4, Stat5a, Stat5b, Stat6, Syk-C, Syk-N, Tns1, Vav1, Yes
Src1-A4	19	Abl2, Bmx, Fyn, Lck, Lyn, Nck2, P85α-C, P85α-N, P85β-N, P55γ-N, PLCγ1-T, PLCγ2-T, PLCγ2-C, She, Src2, Syk-C, Tns1, Vav1, Yes
Src1-D1	30	Abl1, Abl2, Bmx, Crk, Fyn, Grb10, Grb14, Grb2, Grb7, Lck, Lyn, Nck2, P85α-C, P85α-N, P85β-C, P85β-N, P55γ-C, P55γ-N, PLCγ1-T, PLCγ2-N, PLCγ2-T, PLCγ2-C, She, Stat3, Stat4, Stat5a, Syk-C, Tns1, Vav1, Yes
Stat1-A1	Non-binding	
Stat1-G6	Non-binding	
Stat1-E1	Non-binding	
Stat1-D5	32	Abl1, Abl2, Bmx, Crk, Fyn, Grb10, Grb14, Grb2, Lck, Lyn, Nck2, P85α-C, P85α-N, P85β-C, P85β-N, P55γ-C, P55γ-N, PLCγ1-T, PLCγ2-N, PLCγ2-T, PLCγ2-C, Ptpn11-N, She, Src1, Src2, Stat3, Stat4, Stat5a, Stat5b, Syk-C, Tns1, Vav1, Yes
Stat3-H2	0	
Stat3-D6	1	Stat4

Affimer Clone	Number of cross-reactions	Additional targets bound
Stat3-E1	1	Stat4
Stat3-H6	0	
Stat3-B1	0	
Stat4-F3	0	
Stat4-H3	0	
Stat4-H2	0	
Stat5a-D4	1	Stat5b
Stat5a-A2	Non-binding	
Stat5b-E6	Non-binding	
Stat5b-G6	Non-binding	
Stat5b-H6	5	Stat5a, Bmx, Grb2, Lyn, PLCγ2C
Stat5b-B6	3	Stat5a, Stat6, PLCγ2C
Stat6-C3	0	
SykN-C3	Non-binding	
SykN-C5	Non-binding	
SykN-D2	0	
SykN-F2	0	
Tns1-A1	Non-binding	
Tns1-E4	Non-binding	
Tns1-C2	Non-binding	
Tns1-H5	Non-binding	
Vav1-F1	Non-binding	
Vav1-D1	Non-binding	
Vav1-F4	Non-binding	
Vav1-C1	Non-binding	
Vav1-F2	5	Lyn, P55γ-N, P85α-N, PLCγ2T, Stat1